PB98-149248

CENTER
FOR
TRANSPORTATION
ENGINEERING
STUDIES

A COMPARATIVE STUDY OF PERFORMANCE OF DIFFERENT DESIGNS FOR FLEXIBLE PAVEMENTS

Volume II of II

by

N. Paul Khosla, Satish Sankaran,
Nakseok Kim, and Y. Richard Kim

DEPARTMENT OF CIVIL ENGINEERING

A COMPARATIVE STUDY OF PERFORMANCE OF DIFFERENT DESIGNS FOR FLEXIBLE PAVEMENTS

Volume II of II

by

N. Paul Khosla, Satish Sankaran,
Nakseok Kim, and Y. Richard Kim

A COMPARATIVE STUDY OF PERFORMANCE OF DIFFERENT DESIGNS FOR FLEXIBLE PAVEMENTS

by

N. Paul Khosla
Principal Investigator

Satish Sankaran
Graduate Research Assistant

Nakseok Kim
Graduate Research Assistant

Y. Richard Kim
Associate Professor

Research Project 23241-87-1

Final Report

in cooperation with the

North Carolina Department of Transportation

and

Federal Highway Administration
The United States Department of Transportation

CENTER FOR TRANSPORTATION ENGINEERING STUDIES
Department of Civil Engineering
North Carolina State University
Raleigh, NC 27695-7908

July 1996

Technical Report Documentation Page

1. Report No.	2. Government Accession No.	3. Recipient's Catalog No.
FHWA/NC/97-004		

4. Title and Subtitle	5. Report Date
A Comparative Study of Performance of Different Designs for Flexible Pavements	July 1996
	6. Performing Organization Code
	8. Performing Organization Report No.
7. Author(s) Dr. N. Paul Khosla, Satish Sankaran Nakseok Kim, and Dr. Y. Richard Kim	
9. Performing Organization Name and Address Center for Transportation Engineering Studies North Carolina State University Box 7908 Raleigh, NC 27695-7908	10. Work Unit No. (TRAIS) 11. Contract or Grant No. 23241-87-1
12. Sponsoring Agency Name and Address North Carolina Department of Transportation Raleigh, NC 27611 The Federal Highway Administration Raleigh, NC 27611	13. Type of Report and Period Covered Final Report 7/1/86 - 6/30/96 14. Sponsoring Agency Code

15. Supplementary Notes

16. Abstract

The objective of this research was to conduct a comparative study of performance of different designs for flexible pavements. This objecive was approached through extensive field and laboratory testing of test pavements. Also, a comprehensive computer-based design procedure for flexible pavements was developed based on results from the field and laboratory tests. Testing was carried out at a test facility constructed on US 421 Bypass near Siler City, North Carolina. The experimental stretch was about seven and one-half miles long and was composed of 12 pavement section types, two of each type in two directions of traffic (having different expected traffic loads), for a total of 48 sections. Of these, only 24 sections on the south-bound lane were instrumented. Response parameters were measured in the field using stress and strain gages embedded in the pavement structure, and an assembly of LVDT's were used to measure deflections at various layer interfaces. In addition, traffic volume and pavement distresses were monitored during the pavement life. Traffic measurements were made using a weigh-in-motion device.

Based on the nondestructive testing procedures, layer moduli for the various pavement layers were backcalculated. A comparison of predicted and measured responses were carried out based on measurements obtained from field instrumentation. Distress survey data, along with the measured responses, were used to compare the various designs employed in the study. In the laboratory testing, the mechanical properties of pavement layer materials were determined by subjecting specimens of the given materials to a series of dynamic load tests under environmental conditions representative of those experienced in the field. Performance prediction models for predicting fatigue cracking and rutting of the asphaltic concrete layers were developed. A study of the variability observed in the field data was performed. A reliability-based methodology to deal with the variability in pavement layer properties was developed. The application of the reliability-based methodology in pavement design computations has been demonstrated. Calibration factors for fatigue and rutting based on field and laboratory results were developed. In addition, a methodology for a calibrated mechanistic design, based on fatigue and rutting criteria, was developed. Also, based on the mechanistic principles developed, a computer program (NCFLEX) was created that could be used to analyze and design flexible pavement systems based on fatigue and rutting criteria. A comparative study of the various existing pavement design methods like AASHTO, VESYS, and the Asphalt Institute was carried out with respect to the US 421 field observed distress data.

17. Key Words	18. Distribution Statement
flexible pavements, field study, base and subgrade stabilization, fatigue, rutting, distress survey, computer based design procedure	No Restrictions - 175 copies of this document were printed at a cost of $4.53

19. Security Classif. (of this report)	20. Security Classif. (of this page)	21. No. of Pages	22. Price
		151	

Form DOT F 1700.7 (8-72) Reproduction of completed page authorized

DISCLAIMER

The contents of this report reflect the views of the author who is responsible for the facts and the accuracy of the data presented herein. The contents do not necessarily reflect the official views or policies of the North Carolina Department of Transportation or the Federal Highway Administration. This report does not constitute a standard, specification, or regulation.

ACKNOWLEDGMENTS

The authors express their sincere appreciation to the authorities of the North Carolina Department of Transportation and the Federal Highway Administration for making available the funds needed for this research.

Sincere thanks go to Mr. W.K. Creech, Chairman, Technical Advisory Committee, for his interest and helpful suggestions through the course of this study. Equally, the appreciation is extended to other members of the committee, Dr. J. Corley-Lay, Mr. W. R. Brown, Dr. S. S. Wu, Mr. M. P. Strong, and Dr. M. Biswas of the North Carolina Department of Transportation and Mr. R.C. Shelton of the Federal Highway Administration for their continuous support of this study.

Sincere appreciation is also due to Dr. J. Corley-Lay and other members of the Pavement Management Unit of the North Carolina Department of Transportation for their cooperation and support during the field testing phase of this study.

Additional thanks are extended to Mr. J. H. Trogdon for his help and assistance during the field instrumentation phase of the study and Mr. B. G. Jenkins for his invaluable support and encouragement during the conduct of this study.

ABSTRACT

The objective of this research was to conduct a comparative study of performance of different designs for flexible pavements. This objecive was approached through extensive field and laboratory testing of test pavements. Also, a comprehensive computer-based design procedure for flexible pavements was developed based on results from the field and laboratory tests. Testing was carried out at a test facility constructed on US 421 Bypass near Siler City, North Carolina. The experimental stretch was about seven and one-half miles long and was composed of 12 pavement section types, two of each type in two directions of traffic (having different expected traffic loads), for a total of 48 sections. Of these, only 24 sections on the south-bound lane were instrumented. Response parameters were measured in the field using stress and strain gages embedded in the pavement structure, and an assembly of LVDT's were used to measure deflections at various layer interfaces. In addition, traffic volume and pavement distresses were monitored during the pavement life. Traffic measurements were made using a weigh-in-motion device.

Based on the nondestructive testing procedures, layer moduli for the various pavement layers were backcalculated. A comparison of predicted and measured responses were carried out based on measurements obtained from field instrumentation. Distress survey data, along with the measured responses, were used to compare the various designs employed in the study. In the laboratory testing, the mechanical properties of pavement layer materials were determined by subjecting specimens of the given materials to a series of dynamic load tests under environmental conditions representative of those experienced in the field. Performance prediction models for predicting fatigue cracking and rutting of the asphaltic concrete layers were developed. A study of the variability observed in the field data was performed. A reliability-based methodology to deal with the variability in pavement layer properties was developed. The application of the reliability-based methodology in pavement design computations has been demonstrated. Calibration factors for fatigue and rutting based on field and laboratory results were developed. In addition, a methodology

for a calibrated mechanistic design, based on fatigue and rutting criteria, was developed. Also, based on the mechanistic principles developed, a computer program (NCFLEX) was created that could be used to analyze and design flexible pavement systems based on fatigue and rutting criteria. A comparative study of the various existing pavement design methods like AASHTO, VESYS, and the Asphalt Institute was carried out with respect to the US 421 field observed distress data.

TABLE OF CONTENTS

LIST OF TABLES

LIST OF FIGURES

CHAPTER 6
PERFORMANCE PREDICTION MODEL FOR FATIGUE CRACKING

6.1 Fatigue Cracking - Definition

Fatigue cracking of the asphalt concrete surface layer of a flexible pavement is generally considered one of the most significant and common forms of distresses. Many researchers (Yoder et al., 1975; Khosla et al., 1988) define fatigue as a phenomenon of repetitive load-induced cracking caused by a repeated stress or strain level, below the ultimate strength of a material. As a result of this phenomenon, repeated load applications of traffic and the variation of the traffic load intensity will result in cracking at the bottom of the surface layer of asphalt concrete pavements. The pavement is considered to have failed from fatigue when the surface layer can no longer perform in a satisfactory condition.

6.2 Literature Survey

6.2.1 Laboratory Testing Methods

Fatigue tests may be conducted under different testing conditions and specimen configurations. These are the diametral indirect tensile test (Hadley et al., 1983; Kennedy, 1977; Quintus et al, 1982; Tangella et al., 1990; Yoder et al., 1975), flexural (beam) test (Hadley et al., 1983; Quintus et al., 1982; Tangella et al., 1990), trapezoidal test (Bazin et al., 1967; Bonnaure et al., 1977; Tangella et al., 1990), torsion test (Tangella et al., 1990), direct tension test (Raithby et al., 1970; Tangella et al., 1990), and wheel tracking test (WTT) (Bohn et al., 1977; Tangella et al., 1990). The tests can be carried out either in controlled stress or controlled strain mode.

In general, to obtain a fatigue life that is comparable to that in the field, the test method should simulate, as closely as possible, the conditions of loading, support, and the stress state to which the material is subjected to, in the pavement. Many investigators (Raithby et al., 1970; Sausa et al., 1990; Tangella et al., 1990) have found from laboratory

tests that the testing condition variables can significantly affect fatigue lives. Therefore, to obtain fatigue lives that are comparable to those that occur in the field, a realistic loading time, loading configuration, loading level, testing temperature, and rest period duration should be used in the test method.

Diametral Indirect Tensile Test

The diametral indirect tensile test was developed simultaneously, but independently, in Brazil and in Japan (Kennedy et al., 1968). The test is a type of tensile strength test used for stabilized materials. The loading configuration develops a relatively uniform tensile stress perpendicular to the direction of the applied load and along the vertical diametral plane, which ultimately causes the specimen to fail by splitting along the vertical diameter. Figure 6.1 shows the loading configuration and failure caused in a diametral indirect tensile test.

Before 1965, the diametral indirect tensile test had been used primarily to measure the tensile strength of concrete (Kennedy, 1977). Since 1965, a series of research results at the University of Texas have suggested the use of diametral indirect tensile test as the most practical test for determining the tensile characteristics of pavement materials.

In 1972, Schmidt reported that the resilient modulus of asphalt-treated mixes could be measured using a repeated load, diametral indirect tensile test. He concluded that the test was relatively inexpensive and more rapid than any other routine stability tests.

In 1977, Kennedy suggested that the repeated load diametral indirect tensile fatigue test could be used to characterize fatigue cracking of asphalt pavement materials. Ruth and Olson (1977) conducted diametral indirect tensile tests in the same year to predict fatigue life of an asphalt concrete pavement. Since then, many researchers (Hadley et al., 1983; Khosla, 1984; Khosla et al., 1985) have conducted diametral indirect tensile tests for the evaluation of the tensile properties of stabilized materials.

Review of literature concerning diametral indirect tensile tests, yielded many advantages and disadvantages. The test has the following advantages (Kennedy et al., 1968; Khosla et al., 1985; Tangella et al., 1990):

(1) The test is relatively simple to conduct.

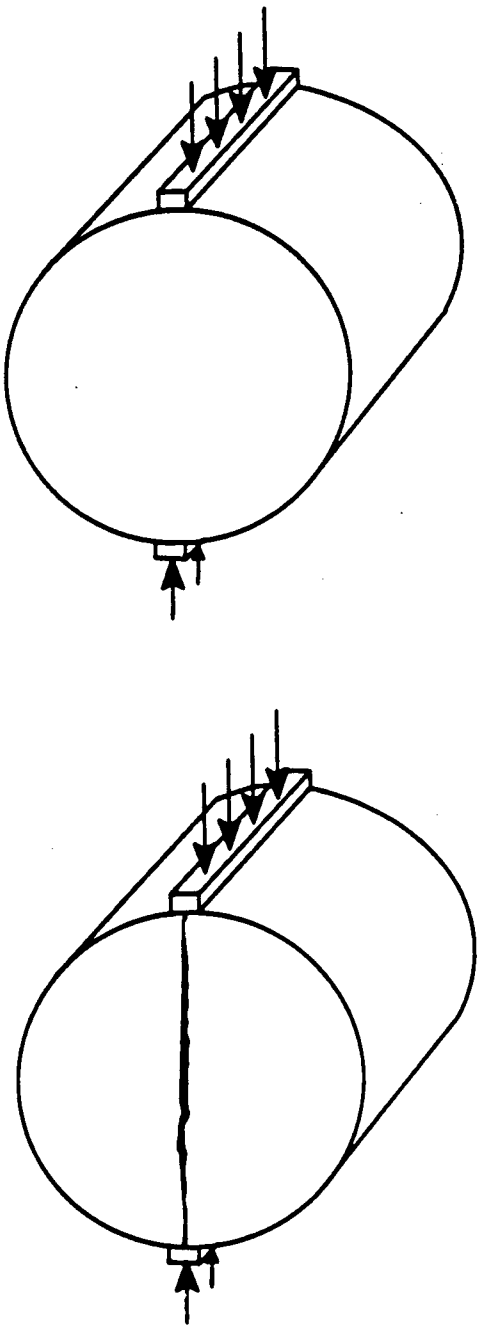

Figure 6.1 Load configuration and failure of diametral test.

(2) The type of specimen and the equipment are the same as those used for the resilient modulus test and indirect tensile strength test.

(3) Failure is not seriously affected by surface conditions.

(4) Failure is initiated in a region of relatively uniform tensile stress.

(5) The coefficient of variation of test results is low compared to other test methods.

(6) A biaxial state of stress induced in the test can represent the field conditions better, when compared to simple flexural (beam) test.

(7)Tests can be performed not only on laboratory specimens but on field cores as well.

In addition, the test provides information on:

(1) The tensile strength, modulus of elasticity, and Poisson's ratio for both static and repeated loads.

(2) Fatigue characteristics.

(3) Permanent deformation characteristics of pavement materials.

On the other hand, the test has the following disadvantages (Kennedy, 1977; Sousa et al., 1991; Tangella et al., 1990):

(1) The test loading conditions do not simulate those existing in the field.

(2) The theory is more complicated than that for direct tension and flexural (beam) tests.

(3) There is a possible concern about the absence of stress reversal and the accumulation of permanent deformation.

(4) The determination of Poisson's ratio or moduli based on the vertical deformation is subject to significant inaccuracies.

(5) The theory of elasticity has to be assumed to calculate modulus and strains.

Based on the literature review, it is considered that the diametral indirect tensile test has the greatest potential for evaluation of the tensile properties of highway materials (Kennedy et al., 1968). The main disadvantage attributed to the test is its failure to simulate loading conditions in practice. Although such conditions may be desirable, they are not decisive and are more than offset by the many advantages of the test. The diametral indirect tensile test is therefore considered to be a common test for evaluating the tensile properties of stabilized paving materials.

Flexural (Beam) Test

The flexural beam test involves the application of a repeated load that results in the bending of a beam specimen. Figure 6.2 shows the schematic drawing of a repeated flexural apparatus that is commonly used. There are two standard methods for applying loads to a simply supported beam. The load may be applied as two equal concentrated loads at the third points of the beam or as a simple concentrated load at the mid point of the beam.

In general, the flexural formula is used to estimate tensile stresses in a beam. Various forms of the bending deflection formula exist, that use the applied loads and the resulting center or third point beam deflections, to estimate modulus and tensile strains. It should be noted, however, that the resulting deflected shape of the beam is a function of both flexural (or bending) effect and shear force effect. If the deflection of a beam under a given load is used in estimating modulus and tensile strains, both effects should be considered (Hadley et al., 1983).

From the literature review many advantages and disadvantages of the simple flexural (beam) test was found. The test has the following advantages (Hadley et al., 1983):

(1) The test is relatively well known and widely used.

(2) Results of controlled-stress testing and controlled-strain testing can be used for the design of thick and thin asphalt pavements, respectively.

(3) In third-point loading, failure of the specimen is initiated in a region of relatively uniform stress.

On the other hand, the test has the following disadvantages (Hadley et al., 1983; Tangella et al., 1990):

(1) The test is expensive and time consuming.

(2) The state of stress is uniaxial; therefore, it is difficult to simulate the state of stress within the pavement structure.

(3) Elastic theory must be assumed to compute the tensile strain or stress.

Trapezoidal Test

Shell researchers have conducted bending tests on trapezoidal specimens (Tangella

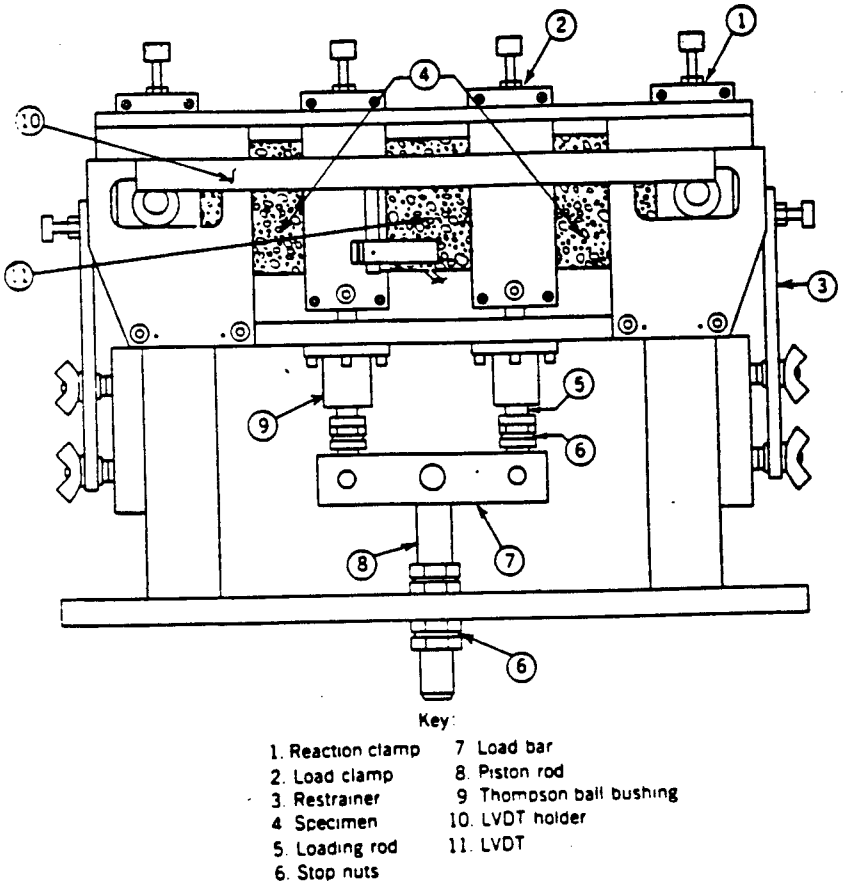

Figure 6.2 Repeated flexural apparatus.

et al.,1990). The larger dimension of the specimen is fixed and the smaller end is subjected to either a sinusoidal stress or strain. By carefully selecting the dimensions of the sample, the maximum stress can be obtained near its mid height (Bonnaure et al.,1977). For example, specimen dimensions tested by van Dijk (1975) had a base cross section of 2.17"x0.79" (5.5x2.0 cm), a top cross section of 0.79"x0.79" (2.0x2.0 cm), and a length of 9.84 in. (25 cm). In 1967, Bazin and Saunier used the trapezoidal specimen to characterize the complex modulus and fatigue behavior of asphalt pavement. The advantages and disadvantages are similar to those observed with the flexural (beam) test.

Wheel Tracking Test (WTT)

Several researchers (Quintus et al., 1982, Terrel et al., 1972) have carried out triaxial tests which undoubtedly correlate better with stress conditions in practice than the simple bending tests. However, the effect of a rolling wheel is still difficult to simulate in these laboratory tests, where the pattern of crack initiation and propagation is often quite different from observations made in practice. Therefore, in order to better simulate the effects of a rolling wheel on the pavement and to better understand the pattern of crack initiation and propagation, a wheel tracking machine has been developed to study fatigue characteristics of an asphalt slab (Tangella et al., 1990).

The wheel tracking machine is a test apparatus in which a loaded wheel with a pneumatic tire is rolled back and forth on a slab of asphalt concrete. The wheel has a diameter of 0.82 ft. (0.25 m) and its path is 1.97 ft. (0.60 m) long with a width in the range of 0.16 to 0.23 ft. (0.05 to 0.07 m). The slab is supported by a rubber mat. A schematic drawing of the apparatus is given in Figure 6.3.

The primary advantages of the wheel tracking test are as follows (Bohn et al., 1977; Tangella et al., 1990; Van Dijk, 1975):

(1) The test can simulate the actual state of stress of field conditions.

(2) The information on crack initiation and propagation can be monitored from strain gauges attached at the bottom of the asphalt concrete slab.

The disadvantages of the test are as follows (Bohn et al., 1977; Tangella et al., 1990; van

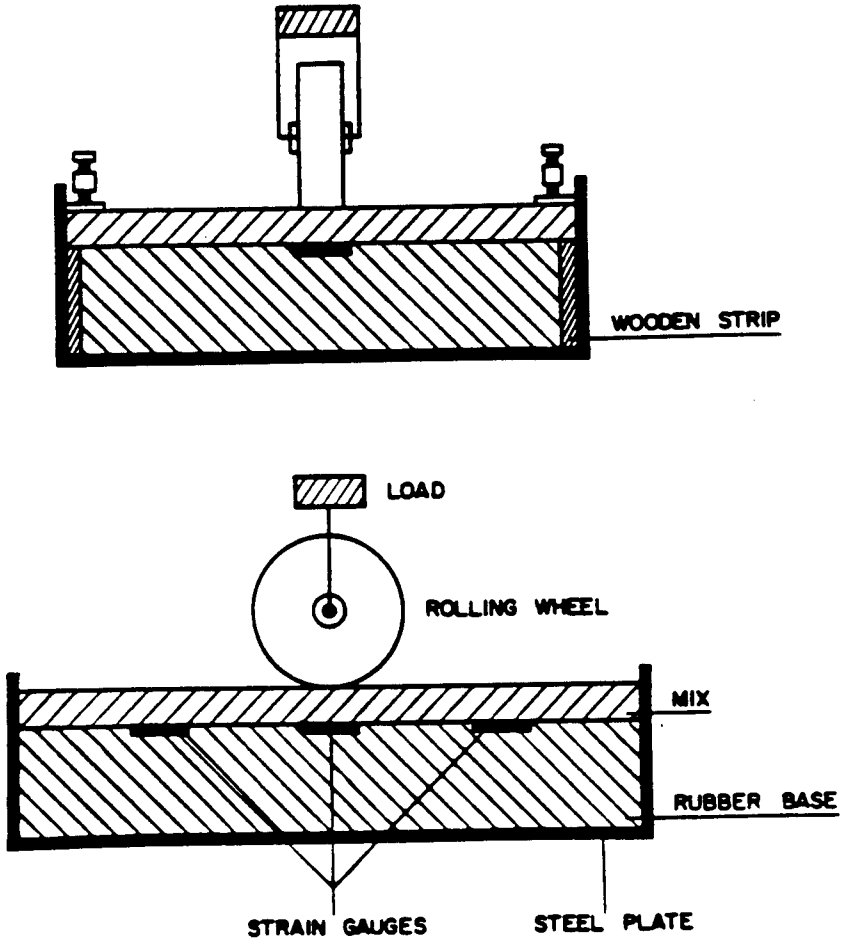

Figure 6.3 Schematic representation of wheel tracking machine.

Dijk, 1975):

(1) The test is too elaborate and time consuming.

(2) The rolling wheel has some limitations pertaining to speed..

6.2.2 Performance Prediction Models

The fatigue characteristics of asphalt mixtures have been described traditionally as a relationship between the number of load repetitions to failure and some significant engineering parameter. Various efforts have been made to find out the most significant engineering parameter that explains the general fatigue performance of asphalt concrete pavements. These efforts have produced many phenomenological or mathematical fatigue models.

Perhaps one of the most commonly used conventional approaches to describe the fatigue life of a given mixture is through a relationship between the initial tensile stress or strain and the number of load repetitions to failure. The initial tensile stress or strain during the test is plotted against the number of cycles to failure on a log-log scale. A linear relationship between logarithms of the initial tensile stress or strain and the fatigue life confirmed the following phenomenological fatigue models:

$$N_f = K_1(\frac{1}{\varepsilon_i})^{K_2} \qquad (6.1.1)$$

or

$$N_f = K_1(\frac{1}{\sigma_i})^{K_2} \qquad (6.1.2)$$

where N_f = fatigue life,

ε_i = initial tensile strain,

σ_i = initial tensile stress, and

K_1, K_2 = experimentally determined regression constants.

Some investigators (Kim et al., 1991) have recommended that for asphalt mixtures the "recoverable strain" be considered as the significant engineering parameter instead of the "total initial tensile strain." The same approach is followed using the recoverable tensile strain at the 200th cycle instead of using initial tensile stress or strain corresponding to the ordinate of the plots. The linear behavior between the recoverable tensile strain and the fatigue life on a log-log scale generated the following power form of the fatigue model:

$$N_f = K_3(\frac{1}{\varepsilon_r})^{K_4} \qquad (6.2)$$

where N_f = fatigue life,

ε_r = recoverable tensile strain, and

K_3, K_4 = experimentally determined regression constants.

In 1985, Monismith et al. suggested the following mathematical relationship that is more applicable to asphalt-aggregate mixtures in general:

$$N_f = A(\frac{1}{\varepsilon_i})^b(\frac{1}{S_i})^c \qquad (6.3)$$

where N_f = fatigue life,

ε_i = initial tensile strain,

S_i = initial mixture stiffness, and

A, b, c = experimentally determined regression constants.

Many researchers (Chomton et al., 1972; Pronk et al., 1990; Tayebali et al., 1992) have performed the flexural beam fatigue test to characterize a given asphalt mixture using energy concepts. They used an energy based approach for explaining fatigue behavior of the asphalt mixture, and have shown that the total cumulative dissipated energy and fatigue life have the following relationship:

$$W_t = A(N_f)^b \qquad (6.4)$$

where W_t = total cumulative dissipated energy,

N_f = fatigue life, and

A, b = experimentally determined regression constants.

It is noted that in Equations (6.1) through (6.3) the fatigue life is described with the initial elastic material responses whereas in Equation (6.4) the fatigue life is related with the overall viscoelastic material behaviors during the test. That is, the total cumulative dissipated energy is estimated from the fundamental stress and strain relationships along with phase shifts from beginning to the end. It is considered that the phase shifts between stress and strain are an important engineering parameter in explaining the fatigue behavior of the time-dependent and temperature-dependent viscoelastic asphalt mixtures. However, neither approach directly recognizes how damage to the mixture actually develops as loading accumulates during the fatigue test (Tayebali et al., 1992).

6.3 Selection of Test Method

As discussed earlier in the literature review, the diametral fatigue test has many advantages compared with other test methods. The greatest advantages are that it is relatively inexpensive, simple, and efficient. In addition to these, one of the main objectives in this research was to select the most simple and realistic performance testing method that can be adopted by the NCDOT materials and testing laboratory.

With these objectives in mind, the repeated load diametral fatigue test was selected and used to characterize fatigue properties of asphalt concrete due to its relative advantages. Also, test mode, type of specimen, and equipment are almost the same as those used in conventional resilient modulus tests and indirect tensile strength tests.

A haversine load with 0.05-second load duration and 0.45-second rest period was repeated until the sample "failed". The stress amplitude was kept constant throughout testing, and vertical loads and the corresponding horizontal deformations were recorded at a specified number of load repetitions. Three load levels, low, intermediate, and high, were used which induced the specimen to fail under a specific condition at about 10,000, 30,000, and 100,000 cycles, respectively.

6.3.1 Test Fixture and Measurement

The MTS fixture used in the resilient modulus testing was used for the diametral (indirect tensile) fatigue test. Vertical loads and the corresponding horizontal displacements were measured by the load cell and extensometers, respectively. Test data for each channel were collected at the speed of 400 readings per second (0.0025 second per reading) over approximately five continuous cycles. This data acquisition was repeated (in a logarithmic scale) over many repetitions throughout the test until failure.

The load cell was used to measure the load at two ranges (2 kip and 20 kip (8.90 KN and 88.96 KN)) depending upon the vertical load level applied. The extensometers were used to measure the horizontal deformations at two ranges (0.015 inch (0.38 mm) and 0.15 inch (3.81 mm)). Ranging the transducers to 10 % of full scale calibrates the output to a finer scale and allows higher resolution from small deformations.

6.3.2 Experimental Design for Fatigue Characterization

The second experiment design studied the effects of the three asphalt mixtures and three temperature levels on the fatigue life of test specimens. Table 6.1 presents the experimental design.

Independent (Controlled) Variables

Tests were performed with three asphalt mixture types (HDS, HDB,and HB) at three temperature levels (32, 50, and 68°F (0, 10, and 20°C)). The mixes are typical of those used by the NC Department of Transportation. The temperatures (0, 10, and 20°C), represent temperatures at which fatigue cracking may be a cause for concern. With the present experimental test set-up, testing at higher temperatures would cause the specimen to deform before the appearance of any cracks.

Dependent (Response) Variables

The response variables evaluated were engineering parameters, which represent the fatigue damage growth of asphalt mixtures. These parameters were used to predict the

Table 6.1 Experimental design for fatigue characterization.

Temperature	Mix Type		
(°F)	HDS	HDB	HB
32	x	x	x
50	x	x	x
68	x	x	x

Note: Three replications at least in each cell.

pavement fatigue life from the number of repetitions of applied loads.

6.3.3 Test Procedure

The repeated indirect tensile (diametral) fatigue test was conducted as follows:

(1) The load amplitudes, which cause fatigue failure around 10,000 and 100,000 cycles, were determined by preliminary testing.

(2) Test specimens were brought to the specified test temperature. The specimens were maintained in the temperature controlled chamber at a specified test temperature for 15 hours prior to testing.

(3) A specimen was placed in the loading apparatus, and the loading strips were positioned to be parallel to and centered on the vertical diametral plane. The electronic measuring systems were adjusted and balanced as necessary.

(4) A repeated haversine waveform load (0.05-second of loading time and 0.45-second of rest period) was applied to the specimen. The transient vertical loads and the corresponding horizontal deformations were measured using a data acquisition system at a specified number of repetitions regularly based on a logarithmic scale including a 200th cycle.

(5) The number of load applications to failure was recorded.

(6) Steps 2 through 5 were repeated with varying stress levels on a number of test specimens.

(7) The initial total horizontal strain, initial recoverable horizontal strain at 200th cycle, and the dissipated energy from the stress-strain hysteresis loops were estimated at a specified number of load repetitions. The dissipated energy was computed from the average value of five continuous stress-strain hysterisis loops.

To determine the initial total horizontal strain and initial recoverable horizontal strain in the middle plane, the following derivations were made. Also, a more detailed theoretical background of diametral line loading in indirect tensile tests is described in (Kim,1994)

Horizontal tensile strain, ε_x, in the indirect tensile specimen under the line loading can be determined from the following (Frocht, 1957):

$$\varepsilon_x = \frac{2P}{E\pi td}\left[\frac{(1+3\mu)d^4-8x^2d^2(1+\mu)+16x^4(1-\mu)}{(d^2+4x^2)^2}\right] \qquad (6.5)$$

where P = load amplitude applied,

E = elastic modulus of the specimen,

t = thickness of the specimen,

d = diameter of the specimen,

μ = Poisson's ratio of the specimen, and

x = the distance from the center line of the specimen.

Integrating Equation (6.5) along the diameter of the specimen, one can obtain the following equation for the horizontal deformation, δ_H:

$$\delta_H = \frac{P}{tE}\left(\frac{4}{\pi}-1+\mu\right) \qquad (6.6)$$

Since we are interested in the largest horizontal strain, which occurs in the middle plane, we replace x in Equation (6.5) with zero and get:

$$\varepsilon_o = \frac{2P(1+3\mu)}{E\pi td} \qquad (6.7)$$

where ε_o = horizontal strain in the middle plane.

Equating Equations (6.6) and (6.7), and assuming that Poisson's ratio of the material is 0.35, one can get:

$$\varepsilon_o = 0.5235\delta_H \qquad (6.8)$$

Therefore, the recoverable horizontal strain, $\Delta\varepsilon_0$, in the middle plane can be determined from:

$$\Delta\varepsilon_o = 0.5235\Delta\delta_H \qquad (6.9)$$

6.3.4 Failure Criteria

The fatigue life of the specimen predicted from the laboratory tests may be significantly influenced by the definition of "failure." According to an earlier study by Scholz (1989), the failure in diametral fatigue testing occurs when the permanent horizontal deformation reaches between 0.28 inch (0.71 cm) and 0.36 inch (0.91 cm). It was recommended that the lead-based foil tape attached on the specimen and the fatigue shut-off wiring for the MTS be used to automatically stop the testing when the permanent horizontal deformation reached the failure criteria.

Some preliminary testing was performed under various conditions to determine the appropriate failure criteria for the controlled-stress diametral fatigue tests conducted in this study. Throughout the preliminary testing, horizontal deformation was monitored and plotted against the number of cycles (Figures 6.4(a) through 6.4(c)). Irrespective of the mixture type and the applied load, it was found that the horizontal deformation increased dramatically on reaching values of 0.01, 0.02, and 0.10 inch (0.25, 0.51, and 2.54 mm) of horizontal deformation at temperatures of 32, 50, and 68°F (0, 10, and 20°C), respectively.

It should be noted that the horizontal deformation increased dramatically on reaching the value of 0.01 inch of total horizontal deformation at 32°F (0°C) and resulted in "specimen explosion" due to the typical brittle behavior of the bituminous materials at low temperatures. It was considered that the abrupt specimen explosion might cause damage to the measuring devices such as the horizontal extensometers, which measure the fine changes in horizontal deformations. To avoid possible damage to the measuring devices, 0.01, 0.02, and 0.10 inch (0.25, 0.51, and 2.54 mm) of the total horizontal deformations were used as failure criteria at three temperatures of 32, 50, and 68°F (0, 10, and 20°C), respectively.

The primary advantage of having failure criteria is that the fatigue test can be automatically stopped using the limit detectors on the MTS without any additional devices or mechanisms. That is, the limit detector automatically turns off the hydraulic pressure when the horizontal extensometer reading becomes larger than the preset limit, i.e., a

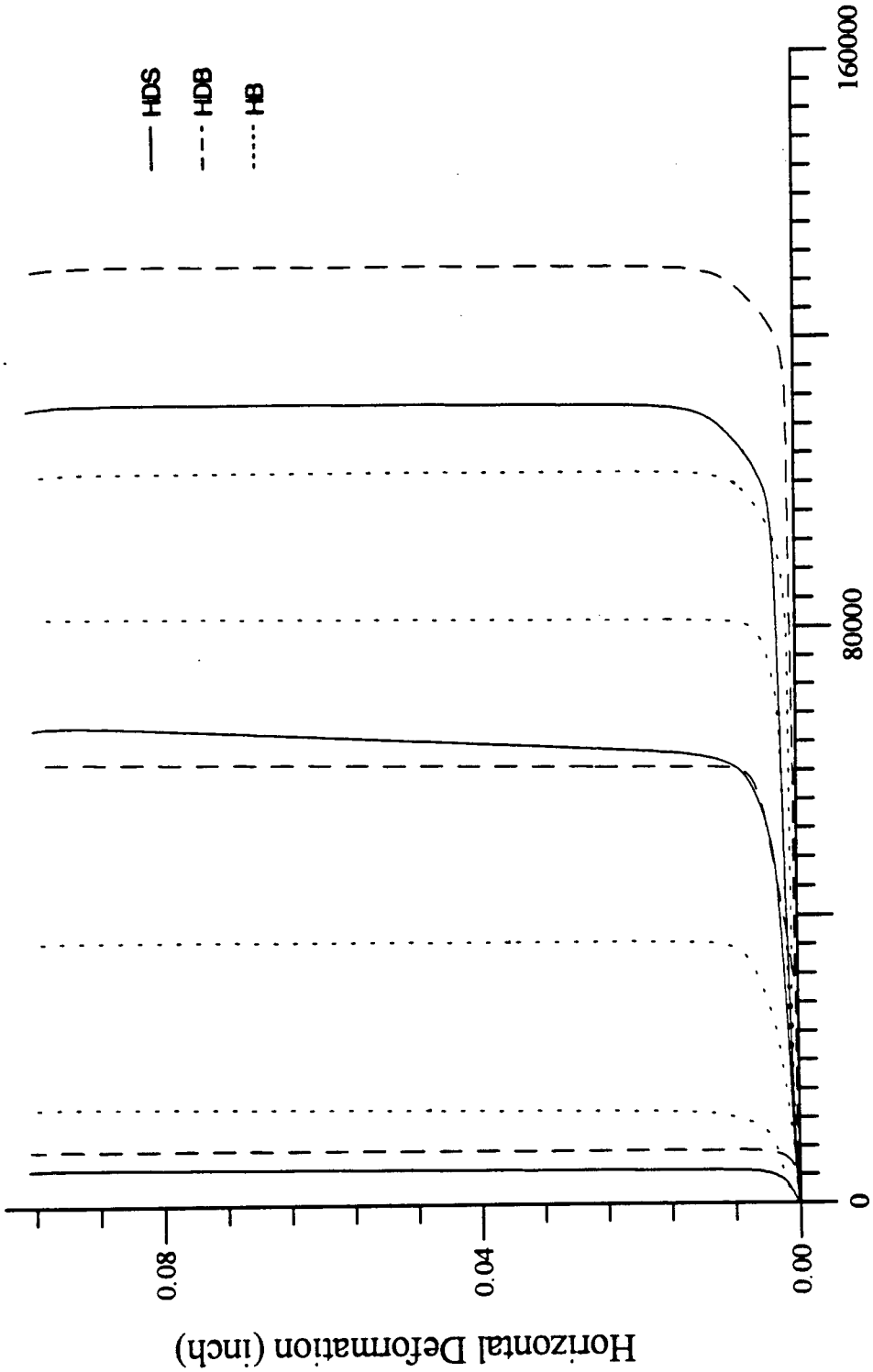

Figure 6.4(a) Growth of horizontal deformations at 32°F (0°C).

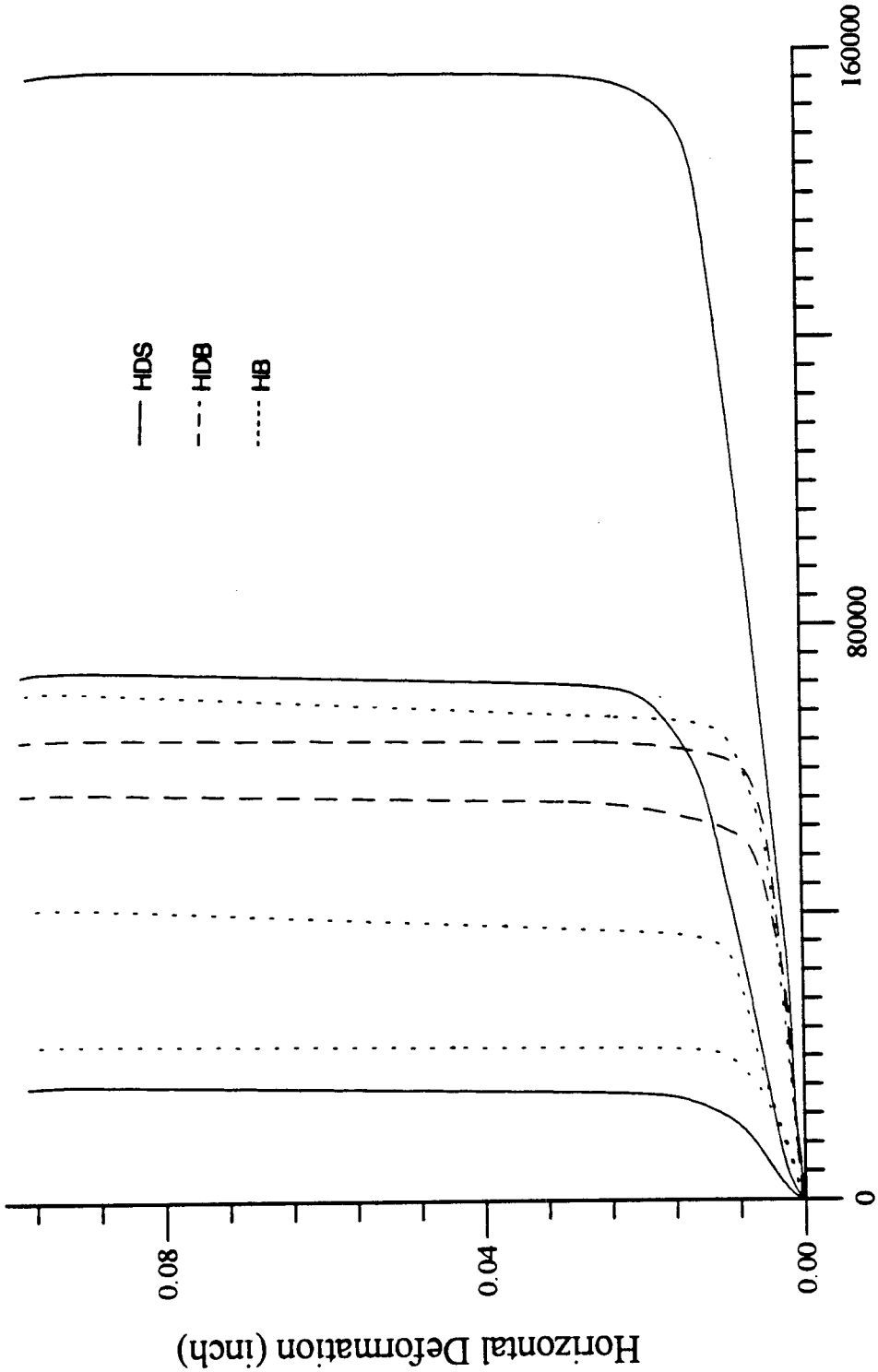

Figure 6.4(b) Growth of horizontal deformations at 50°F (10°C).

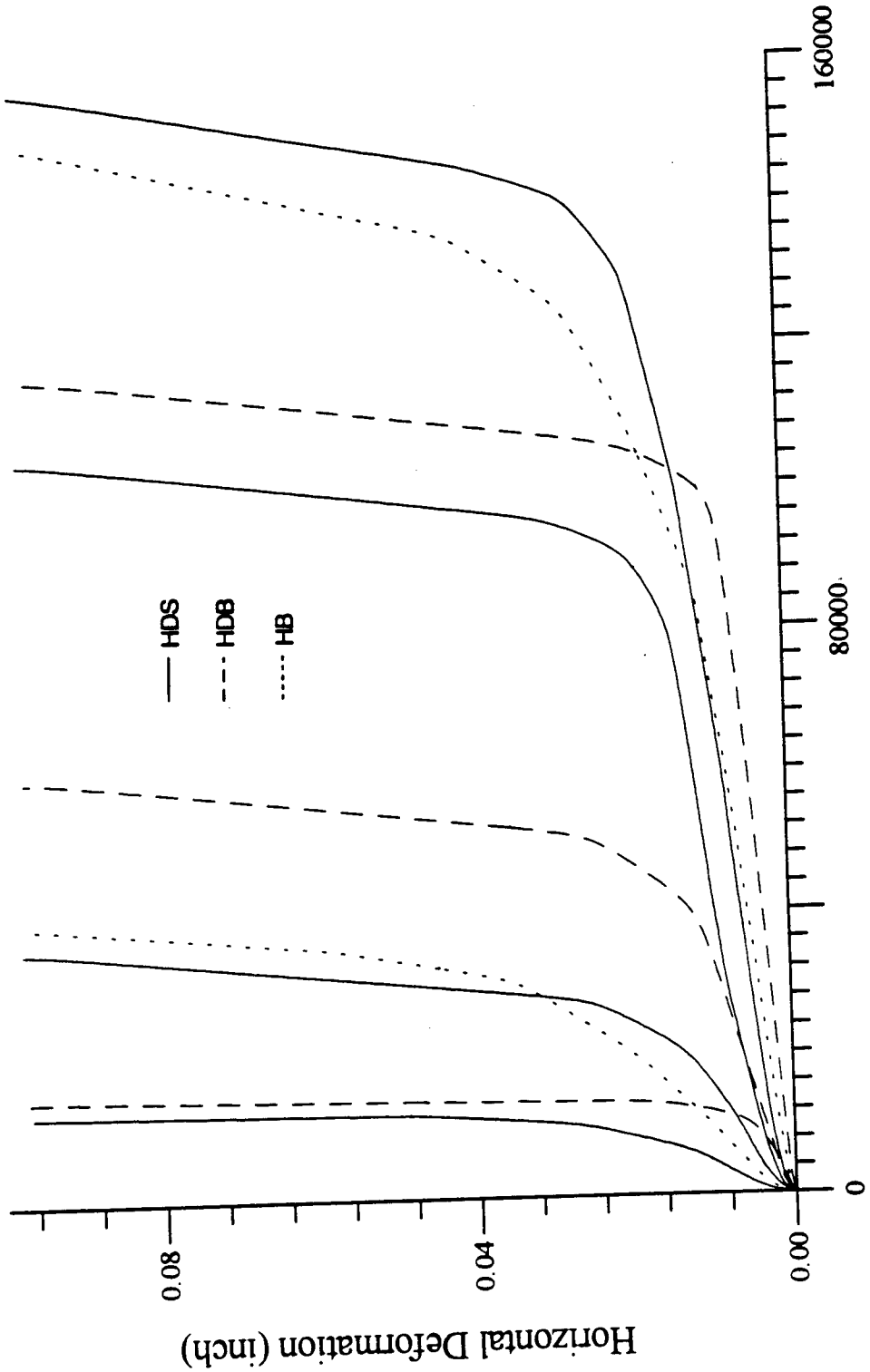

Figure 6.4(c) Growth of horizontal deformations at 68°F (20°C).

horizontal deformations of 0.01, 0.02, or 0.10 inch (0.25, 0.51, or 2.54 mm).

6.4 Development of Fatigue Prediction Models

The advantages of the dissipated energy approach over other concepts are well documented by the SHRP A-003A study. As of this date, however, the energy considerations have been applied only to the flexural beam and trapezoidal fatigue tests. One of the objective of this research was to apply the energy considerations to the diametral fatigue test and to identify the critical engineering parameter(s) which govern the damage (fatigue cracking) growth in asphaltic mixtures.

Traditionally, the fatigue performance of flexible pavements has been correlated to simple engineering parameters such as induced maximum tensile stress, strain, or recoverable strain. One of the biggest problems of this phenomenological fatigue characterization has been their time consumption. Many researchers (Huang, 1993; Robert et al., 1991; Yoder et al., 1975) have reported that the conventional fatigue test takes a significant amount of time, since approximately ten samples or more have to be tested to produce enough data to develop required relationships.

To demonstrate the superiority of the dissipated energy in representing the fatigue performance over the induced strain, the comparison of R-square values between the fatigue life (N_f) and the various engineering parameters is presented in Figure 6.5. In this comparison, the various engineering parameters include, the total cumulative dissipated energy (TCDE), initial dissipated energy (IDE), recoverable horizontal strain (RHS), and the initial total horizontal strain (ITHS). Figure 6.5 shows that the R-square values between the energy-based parameters and the fatigue life are higher than those between the induced strains and the fatigue life.

One of the biggest advantages of the dissipated energy approach is that a stronger correlation can be found between the dissipated energy and the number of cycles to failure as compared to the relationships between other conventional engineering parameters and the number of repetitions to failure. The primary reason for the stronger correlation is due to the fact that the dissipated energy includes not only the induced strain but also the stress and the

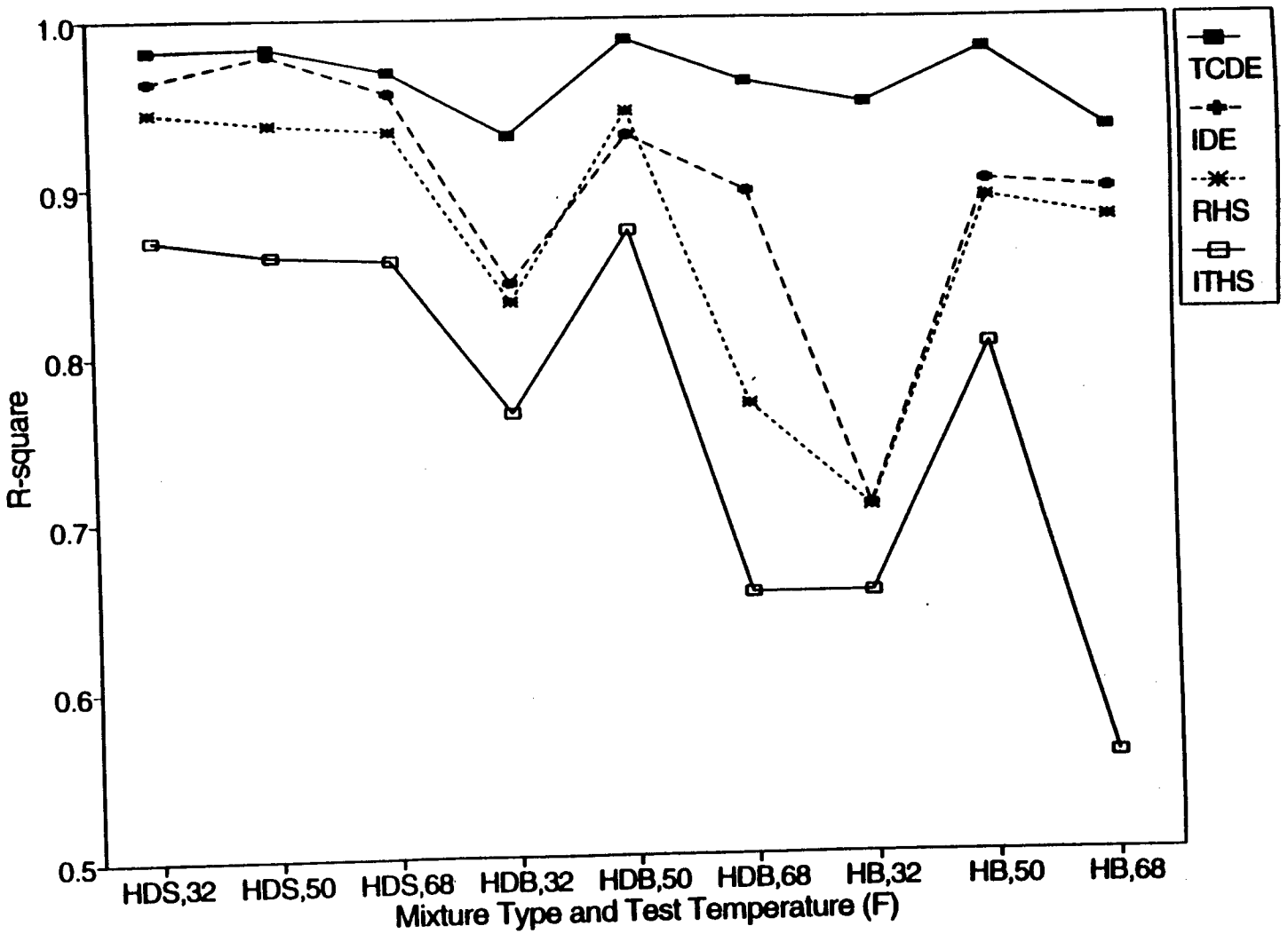

Figure 6.5 Comparison of R-square values between number of repetitions to failure and different engineering parameters.

time-dependent relationship between the stress and strain. That is, the dissipated energy is computed from the history based stress-strain relationship of materials.

In addition, Figure 6.5 presents a stronger correlation between the total cumulative dissipated energy and the fatigue life, than that obtained from a relationship between the initial dissipated energy and the fatigue life. The main reason for the stronger correlation is that the total cumulative dissipated energy includes comprehensive material behavior, ie., it includes material behavior from the initial stage to the final stage of the specimen life.

Based on these findings and within the limitations of this research, it was confirmed that the dissipated energy which results from time dependent behavior between the applied stress and the induced strain can be a better engineering parameter to characterize the fatigue behavior of asphalt mixtures than those obtained using conventional engineering parameters. In spite of this advantage, it is difficult as of this date to directly apply this energy approach to practical pavement design as it necessitates the use of a complex viscoelastic structural analysis method.

Figure 6.6 demonstrates a typical hysteresis loop from a diametral fatigue test in the controlled-stress mode. The dissipated energy is defined as the area inside the hysteretic stress-strain loop; that is,

$$w = \int \sigma \, d\varepsilon \qquad (6.10)$$

where w = dissipated energy at a certain load cycles,

σ = applied stress, and

$d\varepsilon$ = corresponding infinitesimal strain changes.

It must be noted that the dissipated energy is due not only to damage growth in the system but also to the history-dependence of the material. In fact, it can be easily shown using theory of viscoelasticity that most of the dissipated energy in earlier cycles is due to the history-dependent nature of the material. Figure 6.7 presents the variations of dissipated energy with increasing number of load applications in a controlled-stress mode test. This figure shows that the dissipated energy remains relatively constant until the dramatic increase near failure.

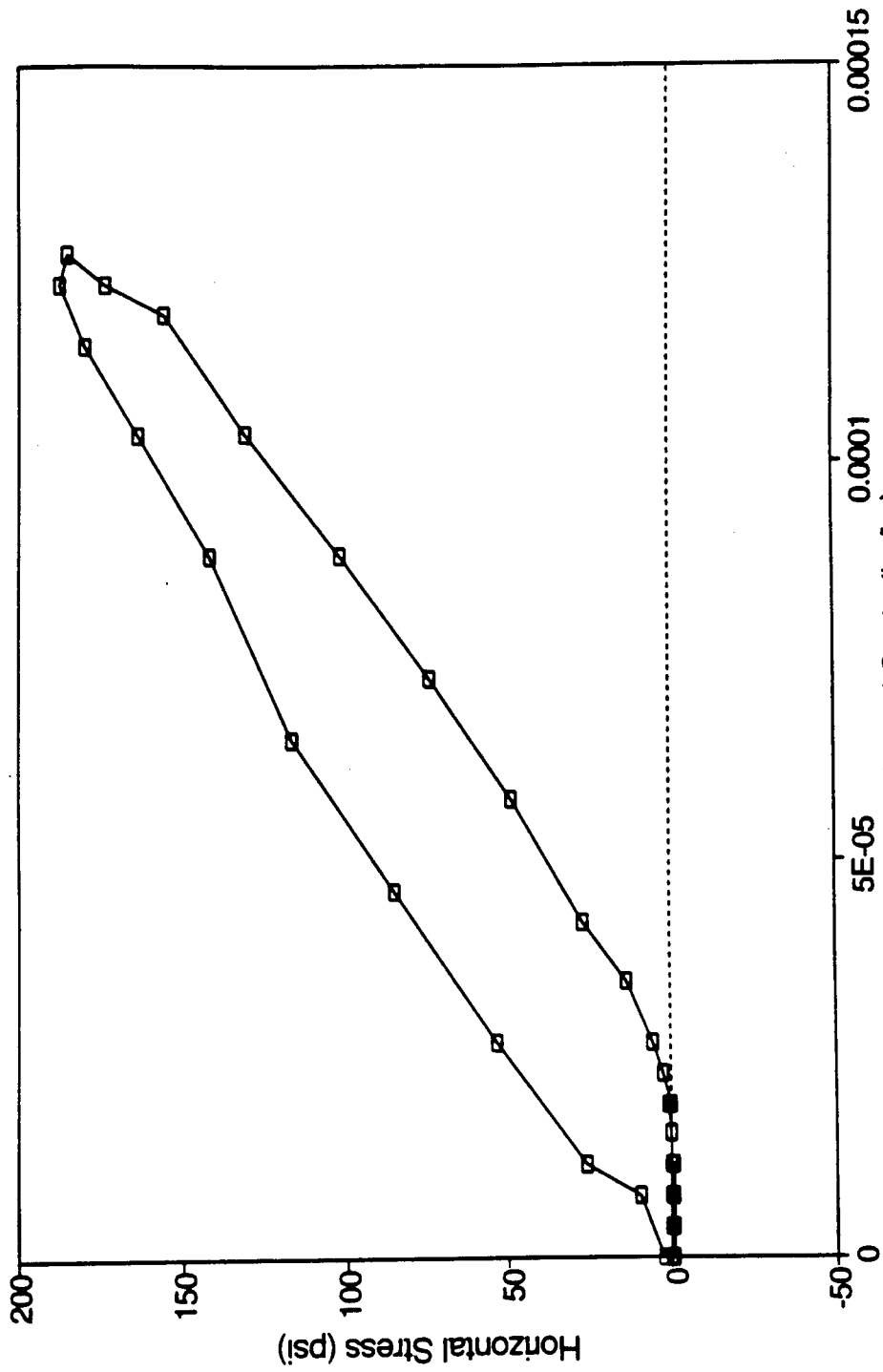

Figure 6.6 Typical stress-strain hysteresis loop at 32 °F (0 °C).

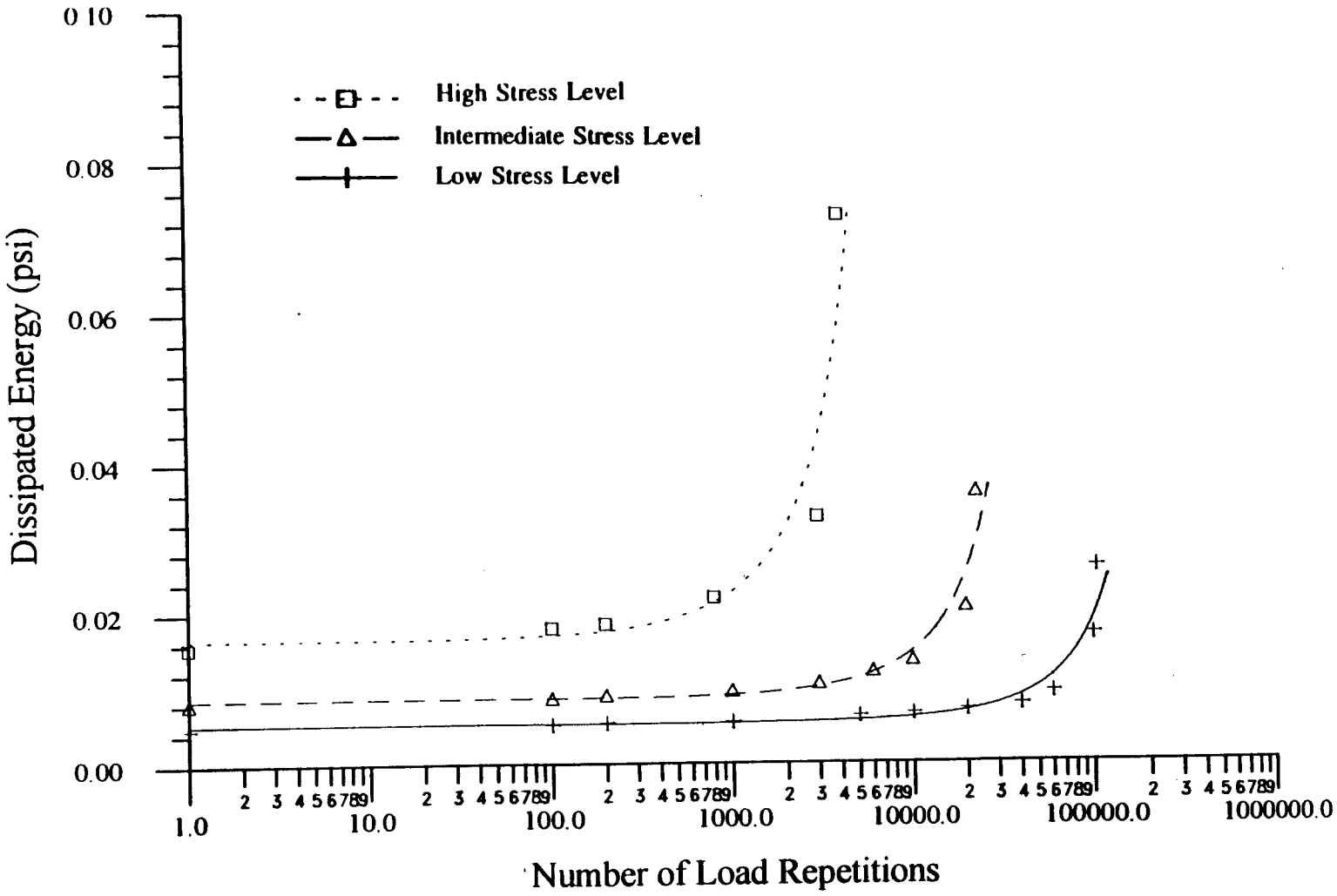

Figure 6.7 Dissipated energy versus number of load repetitions in controlled-stress tests.

During the SHRP A-003A project at NCSU, the controlled-strain diametral fatigue test procedure was developed. The test was conducted by controlling the recoverable horizontal deformation of the diametral specimen in the remote control mode using a computer program. Figure 6.8 shows the change of dissipated energy as a function of the load cycle number from tests conducted using a controlled-strain mode.

The dissipated energy increases with increasing number of load applications in the controlled-stress mode test, whereas in the controlled-strain mode test, the dissipated energy decreases with increasing number of load applications. This result showed a good agreement with the test results reported by Tayebali et al. (1992, 1993) using the flexural beam and trapezoidal fatigue tests.

When an asphalt concrete pavement is subjected to repetitive random wheel loads (varying load levels with different rest periods), two principal mechanisms take place within the asphalt concrete: (1) relaxation of stresses in the material due to the viscoelastic nature of asphalt concrete and (2) damage accumulation. If the applied stress level in the diametral test is as low as that in the resilient modulus test, which is called a nondestructive test, the major portion of the dissipated energy is generated because of the time-dependent viscoelastic property of the asphalt concrete mixture. Also, the amount of the dissipated energy from the hysteresis loop does not change with the increasing number of load applications in a specimen. Therefore, the damage growth within the asphalt concrete specimen is almost negligible if any.

As mentioned before, however, the main source of the dissipated energy in the fatigue test is from the intrinsic viscoelastic material property of an asphalt concrete mixture and the damage growth within the asphalt concrete specimen. The dissipated energy is gradually increased with an increasing number of load applications. The primary reason is due to the development of internal damage growth in the asphalt concrete specimen especially in the fairly high stress level of a fatigue test. As a result, separating the time dependency and the internal damage growth in a specimen may be difficult, quantitatively. However, estimating the internal damage ratio with increasing number of load applications is possible. Therefore, in the following two sections, two general approaches with damage growth and modified shell

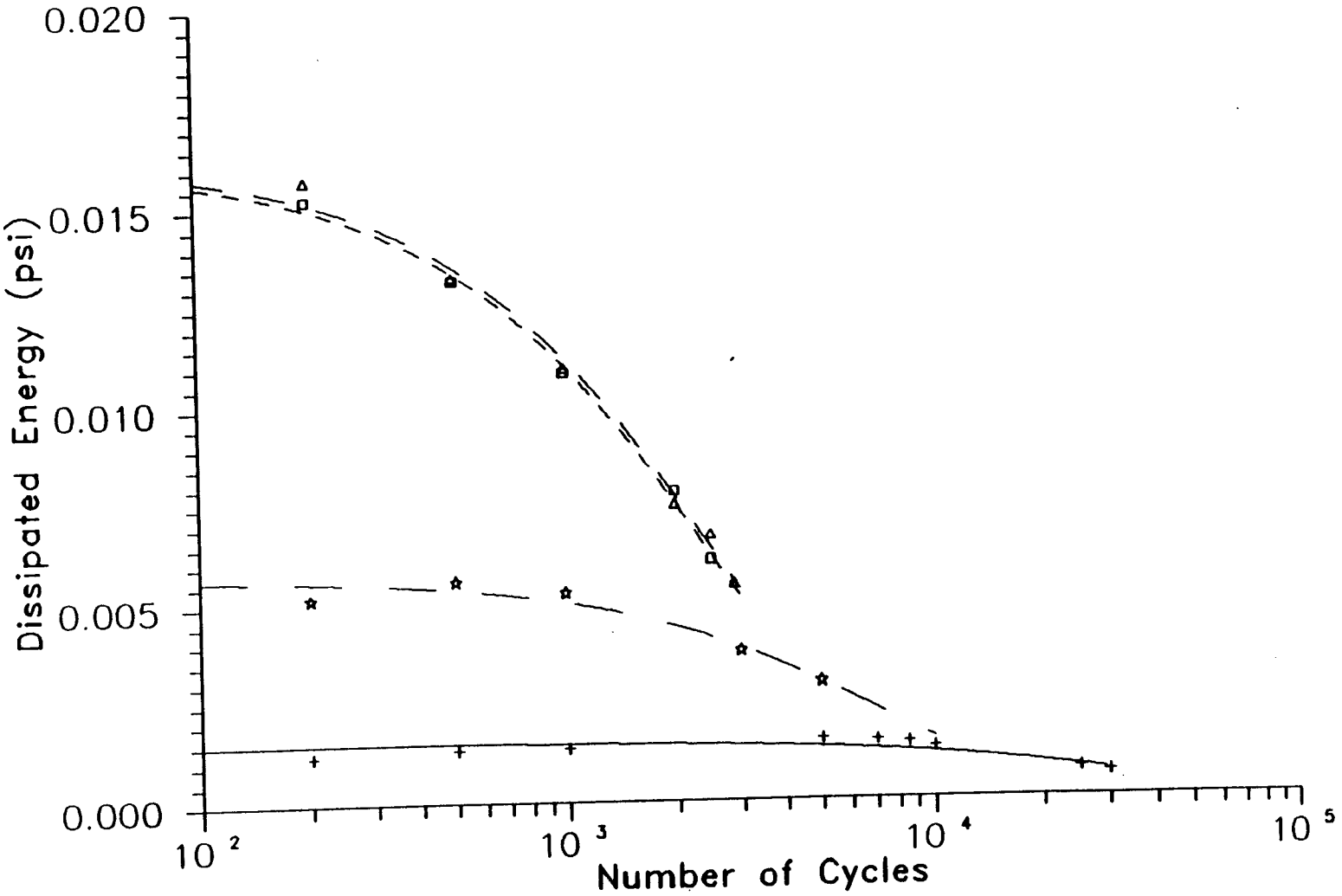

Figure 6.8 Dissipated energy versus number of load repetitions in controlled-strain tests.

method will be presented to develop the performance prediction models on fatigue cracking.

6.4.1 Damage Growth Approach

Based on the concepts discussed above, the internal damage ratio (IDR) at a certain number of load repetitions is defined as the ratio of the dissipated energy change to the initial dissipated energy at the 200th cycle. That is,

$$IDR_n = \frac{w_n - w_i}{w_i} \qquad (6.11)$$

where IDR_n = internal damage ratio at n-th load repetition,

w_n = dissipated energy at n-th load repetition, and

w_i = initial dissipated energy at 200th cycle.

In the initial stage of the fatigue tests, the dissipated energy from the hysteresis loop reaches the steady state in controlled-stress and controlled-strain mode tests. However, the dissipated energy increases with an increase in number of load repetitions due to damage accumulation within the specimen after a certain period of the initial steady state. Therefore, the change in dissipated energy (w_n-w_i) at a certain number of load repetitions after the steady state is attributed to the damage growth within the specimen. In addition, the normalization of the internal damage ratio by dividing the dissipated energy change by the initial dissipated energy makes it possible to describe the internal damage ratio growth as a function of the number of load repetitions. That is, the growth of internal damage ratio defined in Equation (6.11) can be expressed with similar mathematical form regardless of the testing conditions and the mixture variables.

To estimate the internal damage ratio growth of the specimen with the increasing number of load applications during the test, the internal damage ratio was plotted against the number of load repetitions on a semi-log scale. The general trend of the internal damage ratio with increasing number of load applications, is expressed in an appropriate exponential form. Regardless of the testing conditions and the mixture variables in this research, the growth in the internal damage ratio showed an exponential trend. As an example, Figure 6.9 presents

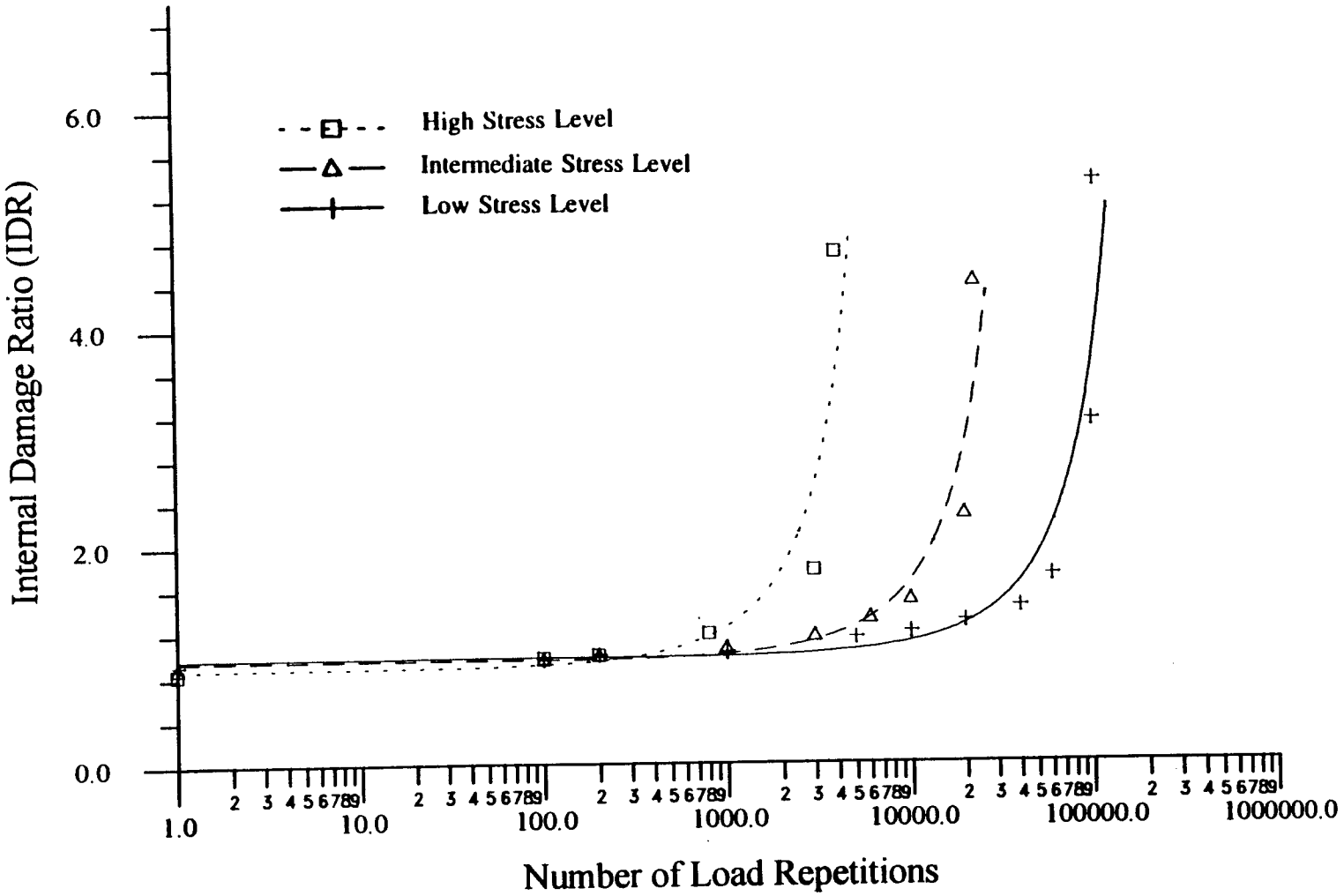

Figure 6.9 Internal damage ratio versus number of load applications with HDS mixture at 32°F (0°C).

the change in internal damage ratio with increasing number of load applications for HDS mixture at 32°F (0°C). Thus, the growth of the internal damage ratio with an increasing number of load repetitions can be described by the following mathematical form:

$$IDR_n = A\exp(BN_n) - 1 \qquad (6.12)$$

where IDR_n = internal damage ratio at n-th load repetitions,

A = regression coefficient (approximatley one),

B = damage growth indicator, and

N_n = n-th number of load applications.

Regardless of testing conditions and mixture variables, the internal damage ratio growth of the specimen with increasing number of load applications showed that the internal damage ratio increased dramatically on approaching failure (see Figure 6.9). Therefore, an arbitrary value of four was selected as the critical internal damage ratio (IDR_c). This failure criterion was decided with the consideration of the previous sample failure criteria described in Section 6.3.4. That is, the failure criteria in Section 6.3.4 were determined based on dramatic increase in total horizontal deformations, whereas the failure criterion in this section was determined based on dramatic increase in internal damage ratio. However, the internal damage ratio at the final number of load repetitions was in the range of three to five. Therefore, it is noted that this specimen failure criterion with internal damage ratio does not violate the previous failure criteria explained in Section 6.3.4.

Since all the internal damage ratio growth curves display an exponential shape, they can be superposed by horizontally shifting these curves. This observation simplifies the modeling of damage growth significantly. One can now develop a damage growth law for a reference condition, and use this reference for other conditions by shifting the reference curve by a predetermined amount (shift factor). In the following sections, the application of this concept to performance prediction modeling is described in more detail.

Growth of Internal Damage Ratio

Preliminary study on the relationship between different test parameters and the

horizontal shift has suggested that the initial tensile strain at 200th cycle can be used in constructing the shift factor.

The horizontal tensile strain shift factor (a_ε) is defined as:

$$a_\varepsilon = \frac{N_{\varepsilon i}}{N_{\varepsilon r}} \qquad (6.13)$$

where a_ε = tensile strain shift factor,

$N_{\varepsilon i}$ = fatigue life at a certain tensile strain level, and

$N_{\varepsilon r}$ = fatigue life at reference tensile strain level.

Rearranging Equation (6.13) we obtain:

$$N_{\varepsilon r} = \frac{N_{\varepsilon i}}{a_\varepsilon} \qquad (6.14)$$

For the reference internal damage ratio curve, Equation (6.12) can be expressed as follows:

$$IDR_r = A_r \exp(B_r N_{\varepsilon r}) - 1 \qquad (6.15)$$

Substituting Equation (6.14) into Equation (6.15) yields:

$$IDR_r = A_r \exp(\frac{B_r N_{\varepsilon i}}{a_\varepsilon}) - 1 \qquad (6.16)$$

Equation (6.16) is an internal damage ratio growth equation for the entire fatigue life in the reference condition. In this research, the failure is defined as the moment when IDR reaches a critical value of IDR_c. Thus, when $IDR = IDR_c$, $N = N_f$.

Applying this failure criterion to Equation (6.16) results in:

$$IDR_{r,c} = A_r \exp\left(\frac{B_r N_{f,\varepsilon i}}{a_\varepsilon}\right) - 1 \qquad (6.17)$$

Rearranging Equation (6.17) produces:

$$N_{f,\varepsilon i} = \frac{a_\varepsilon}{B_r} \ln\left(\frac{IDR_{r,c} + 1}{A_r}\right) \qquad (6.18)$$

where $N_{f,\varepsilon i}$ = fatigue life at a certain initial tensile strain level,

$IDR_{r,c}$ = critical internal damage ratio,

A_r = regression constant (approximately one),

a_ε = tensile strain shift factor, and

B_r = damage growth indicator at reference strain.

The specimen fails when the reference internal damage ratio reaches the critical value of four, which is defined as $IDR_{r,c}$. The only unknowns in Equation (6.18) are a_ε and B_r. B_r can be determined by the regression analysis on the reference internal damage ratio curve. This requires the selection of the reference curve for different testing conditions.

Since the shift factor was a function of the initial tensile strain, one reference strain value was selected for all the conditions tested in this study. With the consideration of a common initial tensile strain range for all the cases, the initial tensile strain of 0.00018 was selected as a reference initial tensile strain regardless of the testing conditions and the mixture types used in this research. Each reference damage growth indicator corresponding to the reference tensile strain was estimated with the relationships shown in Figures 6.10(a) through 6.10(c). That is, a total of nine reference damage growth indicators corresponding to the reference tensile strain, 0.00018, were determined from three different mixtures and three different testing temperatures. In the following sections the behavior of the tensile strain shift factor and the reference damage growth indicator will be studied as a function of test parameters, such as temperature, material properties, etc.

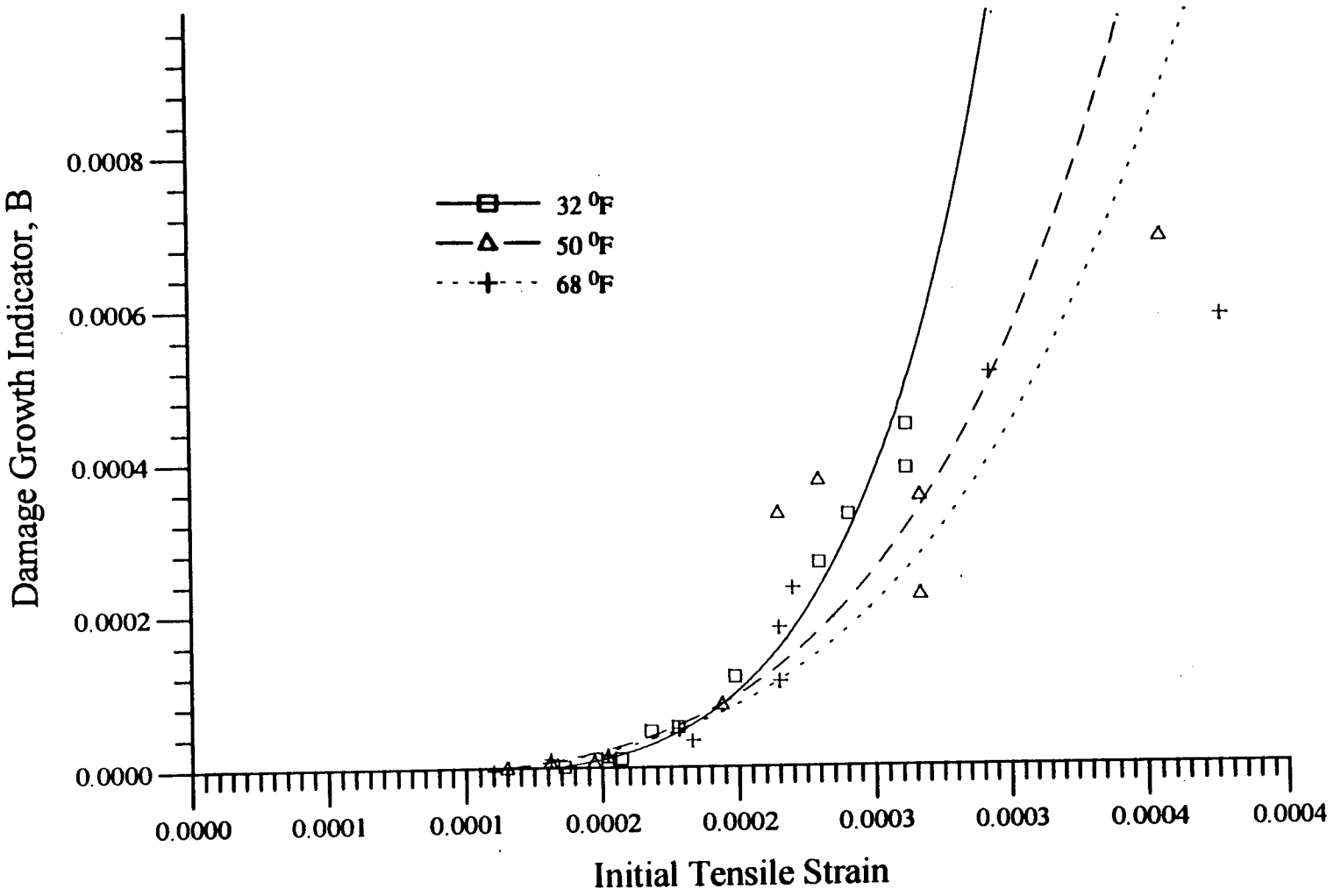

Figure 6.10(a) Damage growth indicator versus initial tensile strain with HDS mixture.

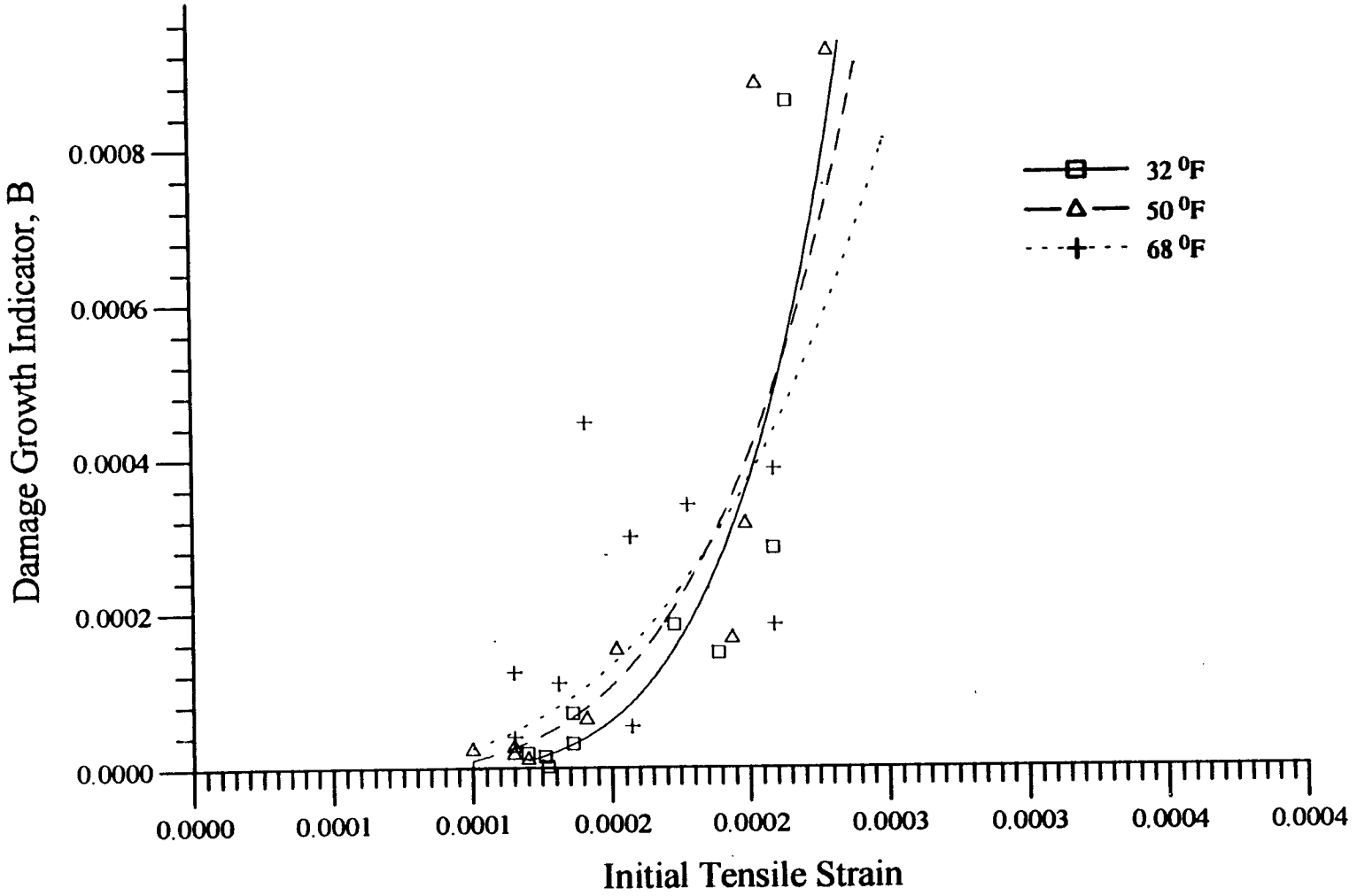

Figure 6.10(b) Damage growth indicator versus initial tensile strain with HDB mixture.

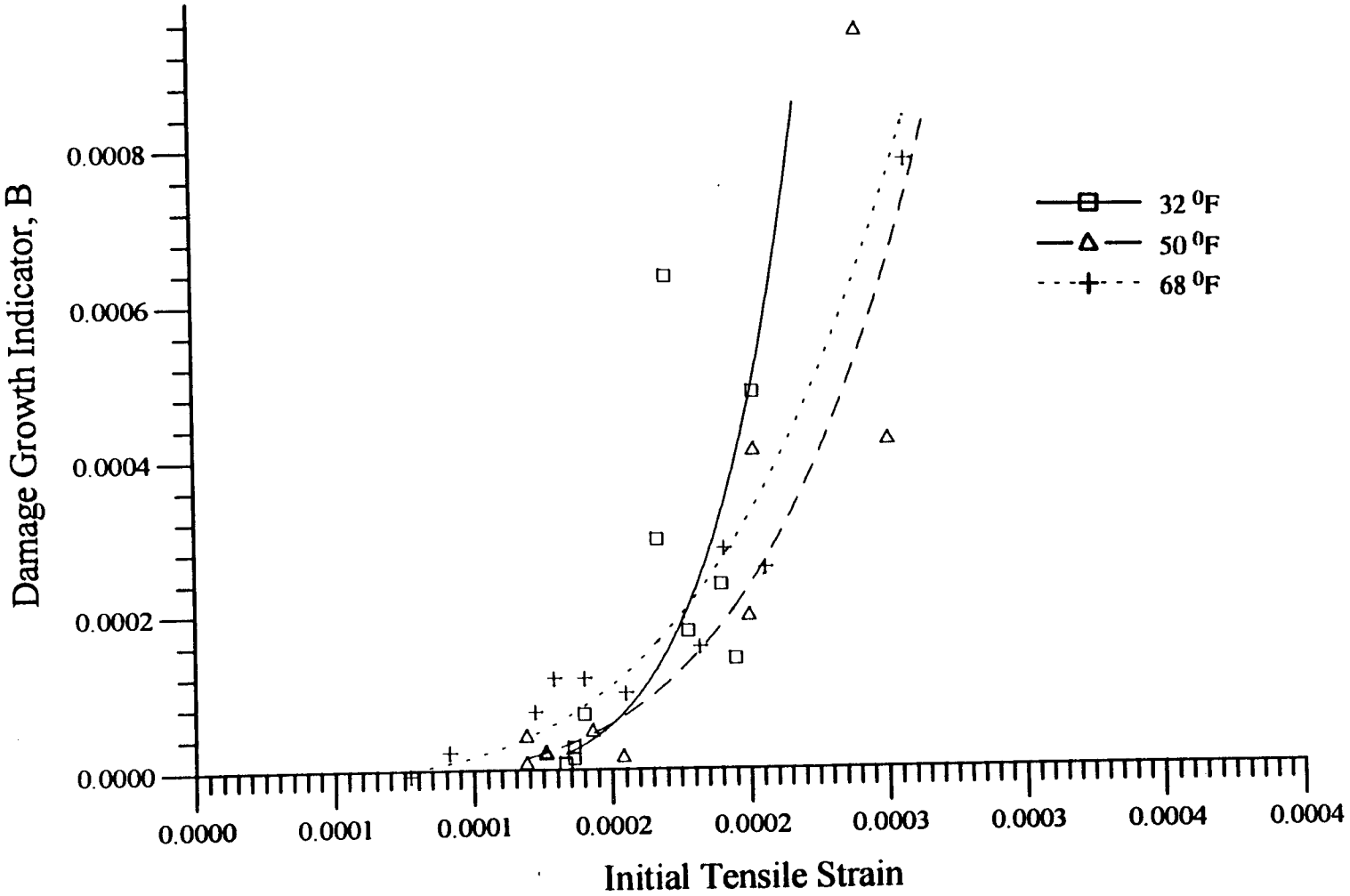

Figure 6.10(c) Damage growth indicator versus initial tensile strain with HB mixture.

Tensile Strain Shift Factor

Horizontal shifts were conducted from the internal damage ratio curves of each specimen with respect to the reference curve. Logarithmic tensile strain shift factors were estimated, and they were plotted against the corresponding initial tensile strain. The results along with the best-fit regression curves through the points are presented in Figures 6.11(a) to 6.11(c). Generally, the effect of the mixture type on the logarithmic tensile strain shift factor was almost negligible at similar temperatures, whereas the effect of temperature on that shift factor was noticeable and consistent for each mixture type. As a result, the effect of the mixture type on the logarithmic tensile strain shift factor for similar temperatures was neglected.

The regression curves developed from the relationship between the logarithmic tensile strain shift factors and the initial tensile strains are based on the theory that the tensile strain shift factor approaches infinity when the corresponding initial tensile strain is close to zero. Therefore, it can be assumed that there will be no specimen failure with the application of that infinitesimal level of initial tensile strain.

However, in reality, this infinitesimal level of the initial tensile strain is temperature dependent, since the elastic property of asphalt mixtures is higher at lower temperatures. Also, it is well known that most paving materials are not elastic but experience some permanent deformation after each load application. However, if the load is small compared to the strength of the material, the deformation under each load repetition is nearly completely recoverable and can be considered as elastic. As a result, the actual level of the initial tensile strain which caused the infinite fatigue life should be a certain higher value than the value close to zero.

The general concept of the threshold tensile strain is illustrated in Figure 6.12. As shown in the figure, the threshold tensile strain level at 32°F (0°C) should be higher than that at 68°F (20°C) since the elastic range of the tensile strain increases as the temperature decreases. Also, it explains that the number of load repetitions to failure can be infinite with the application of a certain threshold tensile strain to the specimen. In this research, a certain initial tensile strain, which results in an infinite fatigue life was defined as the threshold tensile

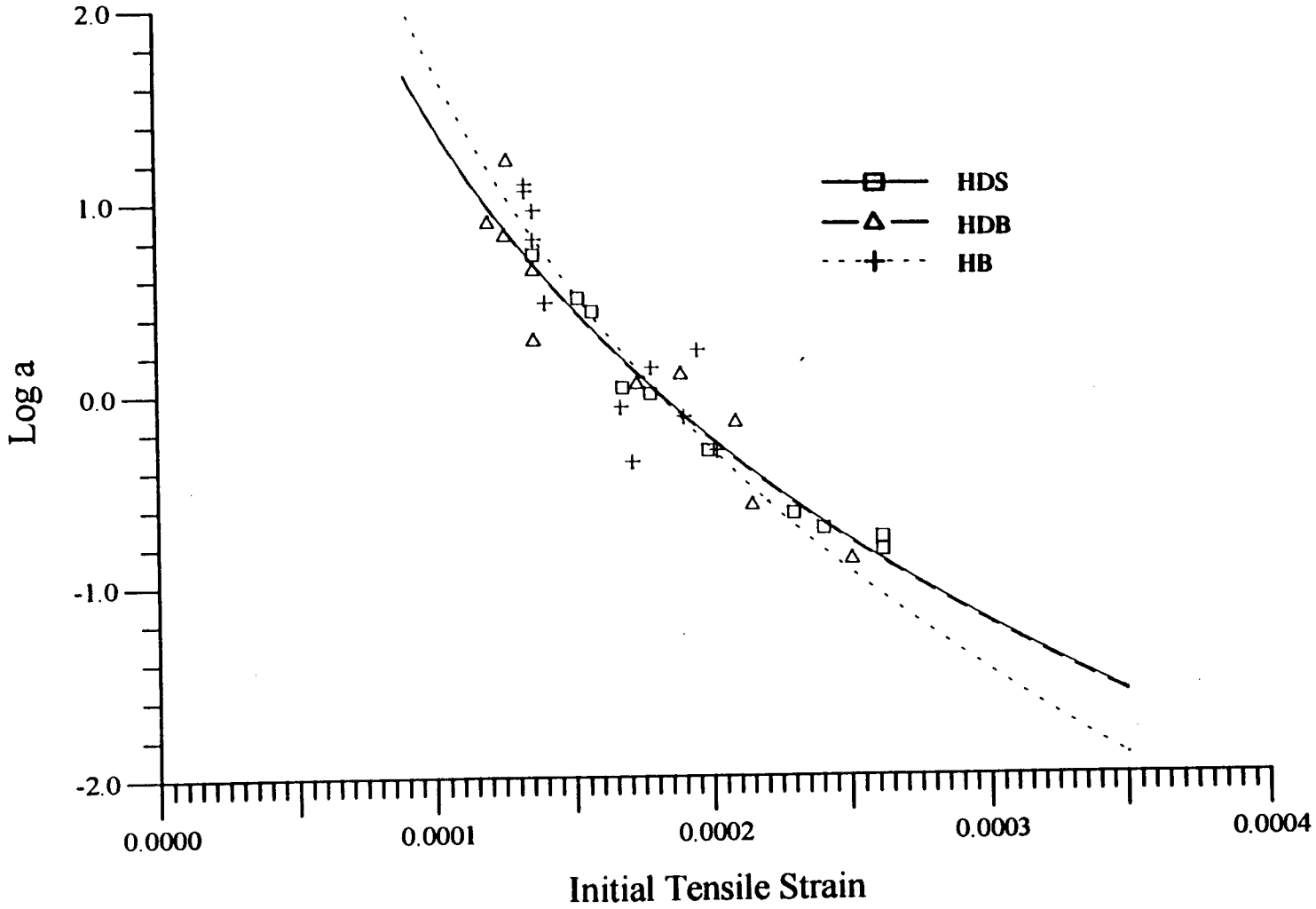

Figure 6.11(a) Log a_ε versus initial tensile strain at 32°F (0°C).

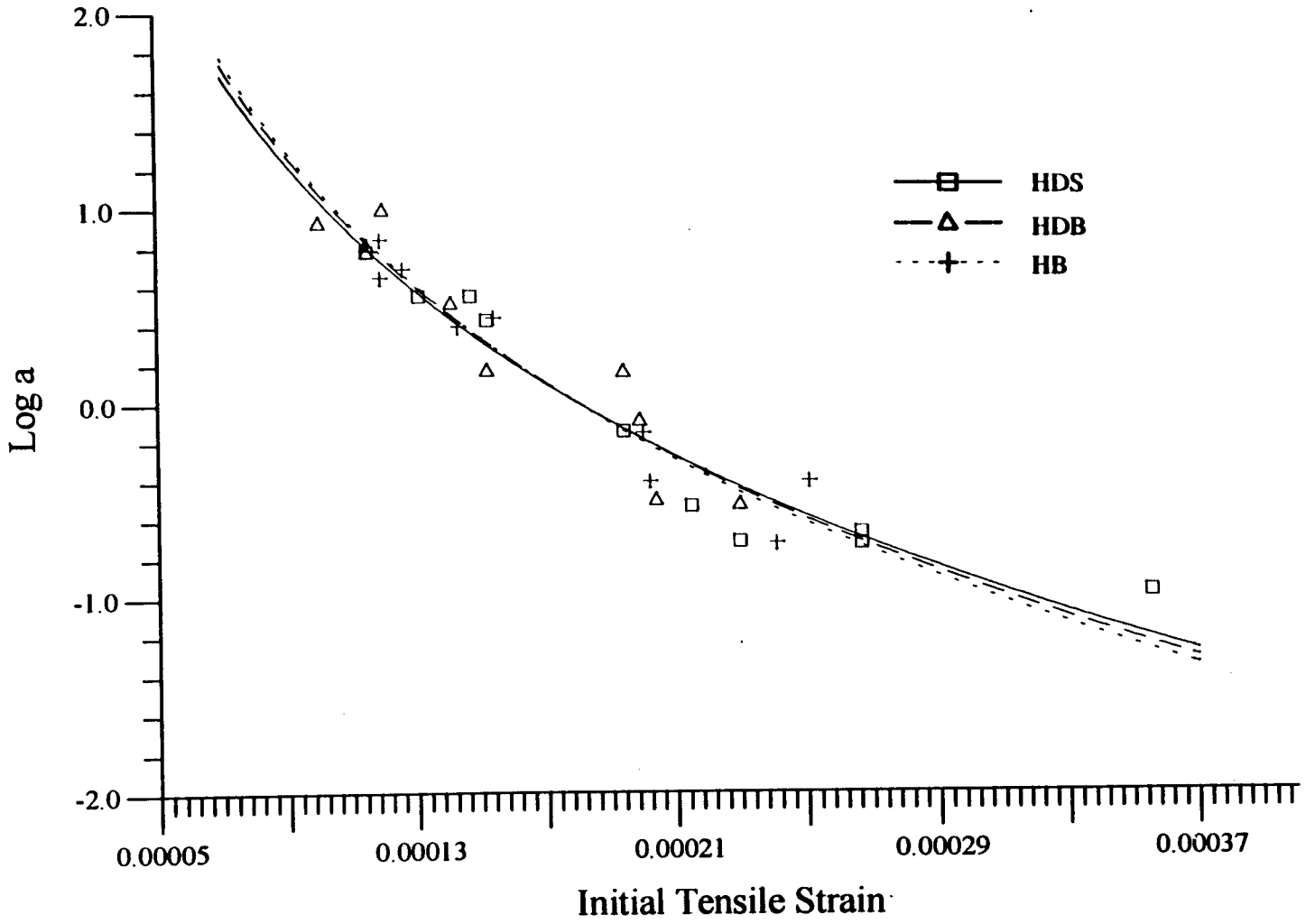

Figure 6.11(b) Log a_ε versus initial tensile strain at 50°F (10°C).

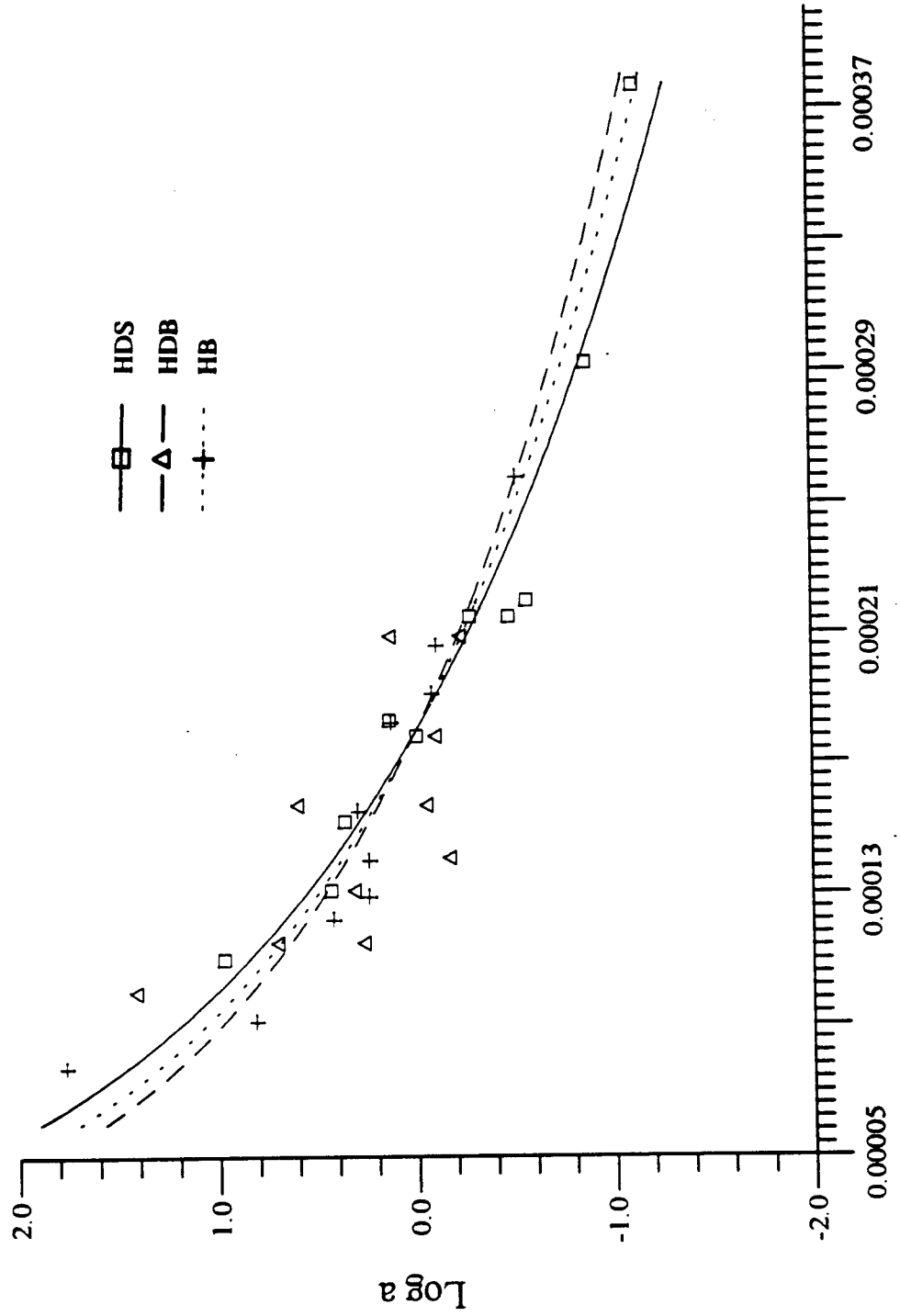

Figure 6.11(c) Log a_ε versus initial tensile strain at 68°F (20°C).

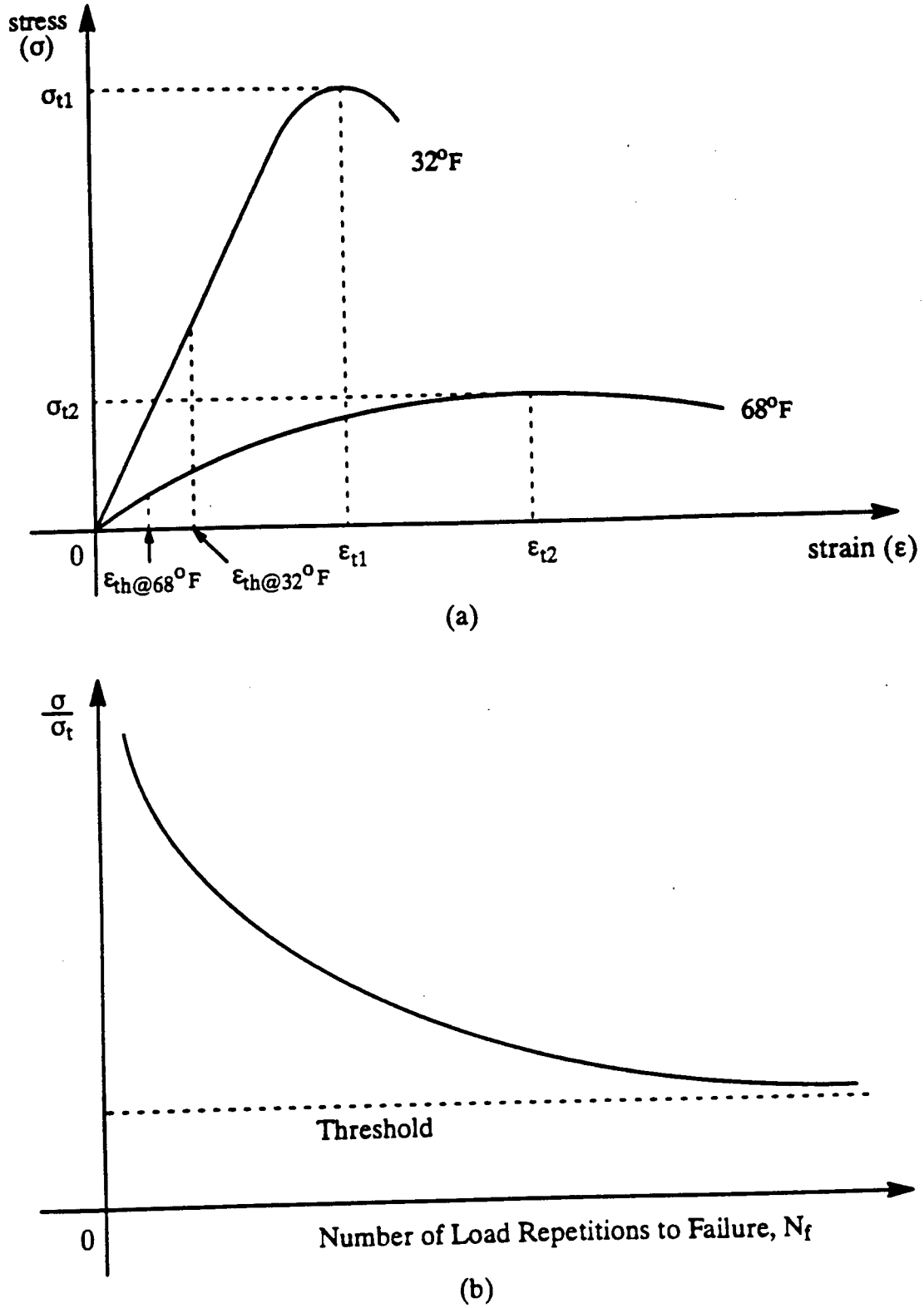

Figure 6.12 General concept of threshold tensile strain.

strain.

With careful observation of the regression curves shown in Figures 6.11(a) to 6.11(c), it can be found that the regression curves can fit better through the points plotted with the introduction of an appropriate threshold tensile strain. In particular, the regression curves can fit better through the points plotted at higher fatigue life.

Therefore, considering the fatigue test results in this research, initial tensile strains of 0.00008, 0.00006, and 0.00004 were selected as the threshold tensile strain at 32, 50, and 68°F (0, 10, and 20°C), respectively. To get more realistic regression curves between the logarithmic tensile strain shift factor and the initial tensile strain, Figures 6.11(a) to 6.11(c) were replotted in Figure 6.13 with the introduction of the selected threshold tensile strains. Regardless of the effect of the mixture type, the figure was plotted and the advantage of the introduction of the threshold tensile strain is shown. Namely, the regression curves can fit better the points plotted at higher fatigue life.

From the regression analysis with the threshold tensile strains defined above, the

$$a_\varepsilon = (2.130\times10^{-5}T^{1.124})^{\log(\frac{\varepsilon_i-\varepsilon_{th}}{\varepsilon_r-\varepsilon_{th}})} \qquad (6.19)$$

general function of the tensile strain shift factor (a_ε) can be expressed as follows:

where a_ε = tensile strain shift factor,

ε_i = initial tensile strain,

ε_{th} = threshold tensile strain,

ε_r = reference tensile strain, and

T = temperature (°F).

To properly relate the nine reference damage growth indicators with the relationships of appropriate engineering parameters, various approaches have been executed. Figure 6.14 suggests that the reference damage growth indicators are not temperature dependent, but mixture type dependent. Thus, the reference damage growth indicators were related to the initial mixture stiffness (S_i) as shown in Figure 6.15. The reference damage growth indicators

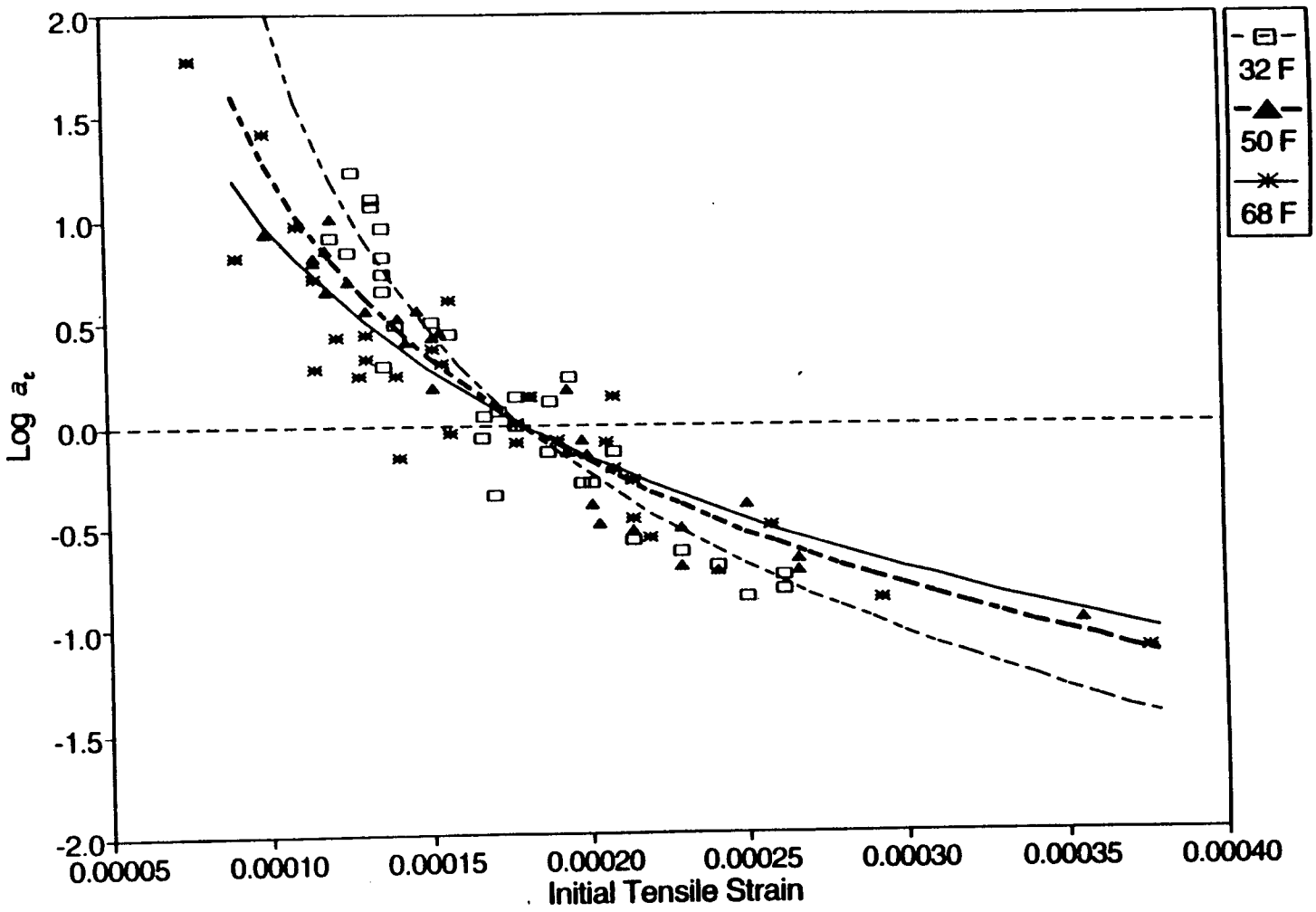

Figure 6.13 Log a_ε versus initial tensile strain with introduction of threshold tensile strain at three temperatures (32, 50, and 68°F (0, 10, and 20°C)).

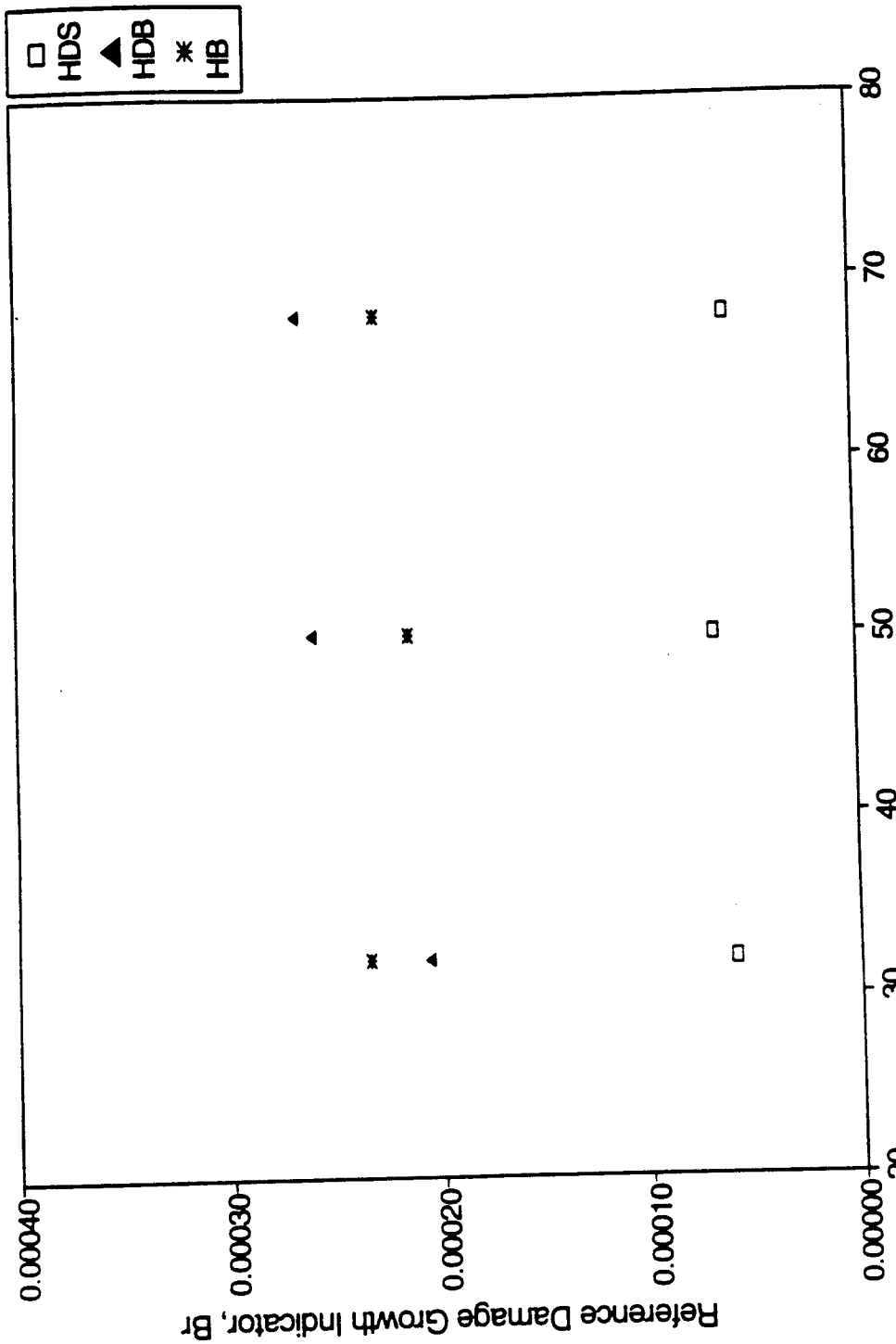

Figure 6.14 Reference damage growth indicator (B_r) versus temperature.

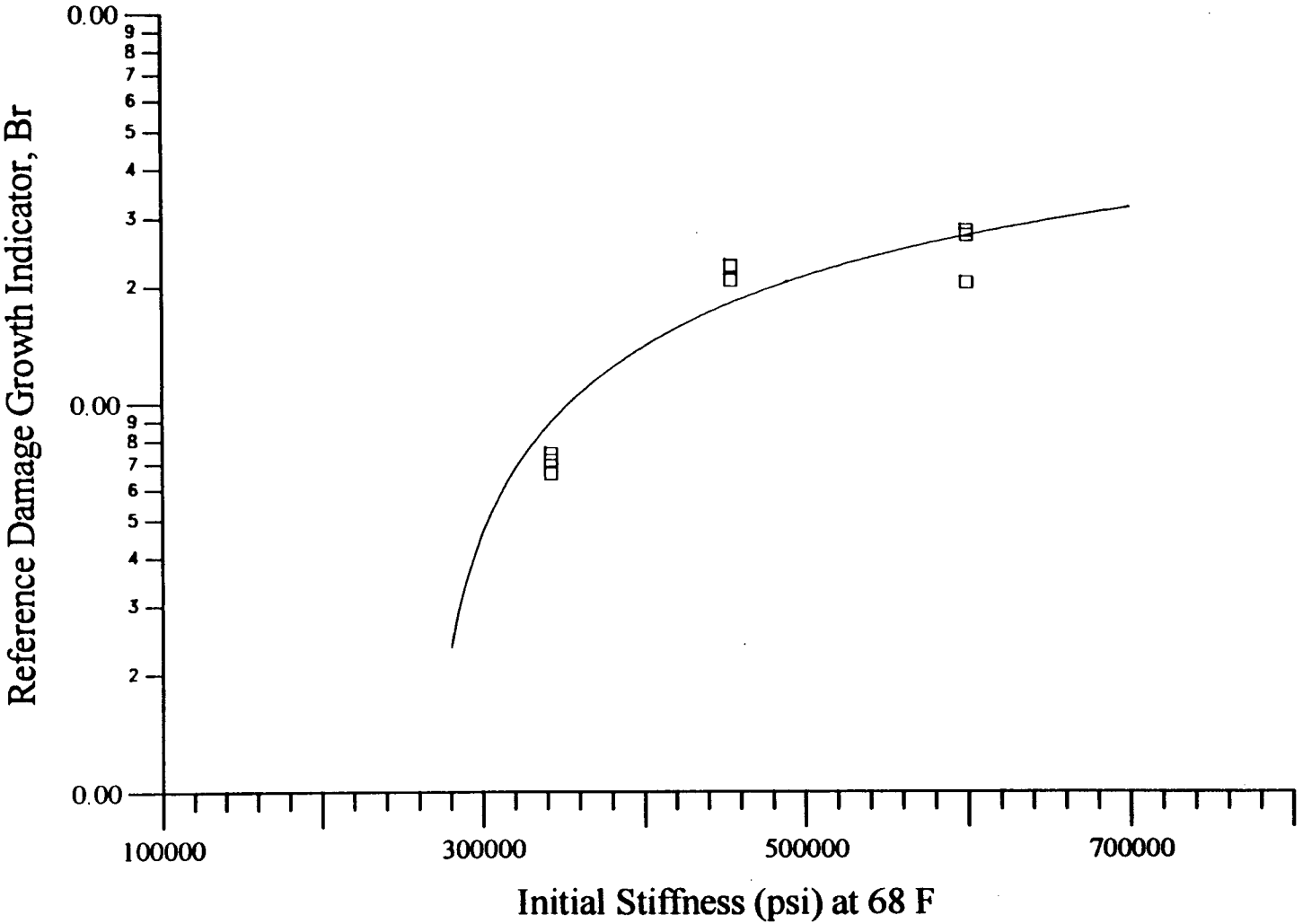

Figure 6.15 Initial mixture stiffness (S_i) versus reference damage growth indicator (B_r).

at the reference tensile strain can be related to the following function:

$$B_r = -4.056\times10^{-3} + 7.470\times10^{-4}\log(S_i) \qquad (6.20)$$

where B_r = reference damage growth indicator and

S_i = initial stiffness (psi) at 68°F (20°C).

Substituting Equations (6.19) and (6.20) into Equation (6.18) generates the general fatigue equation as follows:

$$N_{f,\varepsilon i} = \frac{1.609(2.130\times10^{-5}T^{1.124})^{\log\left(\frac{\varepsilon_i-\varepsilon_{th}}{\varepsilon_r-\varepsilon_{th}}\right)}}{-4.056\times10^{-3}+7.470\times10^{-4}\log(S_i)} \qquad (6.21)$$

where $N_{f,\varepsilon i}$ = fatigue life at an initial tensile strain,

T = temperature (°F),

ε_i = initial tensile strain,

ε_{th} = threshold tensile strain,

ε_r = reference tensile strain, and

S_i = initial stiffness (psi) at 68°F (20°C).

6.4.2 Modified Shell Method

Many investigators (Chomton et al., 1972; Pronk et al., 1990; Tayebali et al., 1992) including Shell researchers (van Dijk, 1975; van Dijk et al., 1977) have suggested various performance prediction models using the dissipated energy approach for fatigue testing. They have used an energy approach for describing fatigue behavior and have shown that the total cumulative dissipated energy to failure is related to the fatigue life. As a result, they have suggested the following representative phenomenological relationship:

$$W_t = A(N_f)^z \qquad (6.22)$$

where W_t = total cumulative dissipated energy,

N_f = number of load repetitions to failure, and

A, z = experimentally determined coefficients.

In Equation (6.22), the fatigue life is related to a terminal test condition, namely, the total cumulative dissipated energy. However, the main focus in this study is to express the fatigue life as a function of the initial engineering parameters instead of the total cumulative dissipated energy. It is noted that this should be conducted without sacrificing the advantages of the total cumulative dissipated energy approach. Therefore, the following general derivations to express the fatigue life as a function of the initial engineering parameters are based on the previous research results conducted by several researchers including Shell investigators.

The dissipated energy per load repetition due to sinusoidal loading conditions can be expressed by:

$$w_n = \frac{\pi}{4}\sigma_n \varepsilon_n \sin(\phi_n) \qquad (6.23.1)$$

or

$$w_n = \frac{\pi}{4}\varepsilon_n^2 S_n \sin(\phi_n) \qquad (6.23.2)$$

where w_n = dissipated energy at load cycle n,

σ_n = stress amplitude at load cycle n,

ε_n = strain amplitude at load cycle n,

S_n = initial mixture stiffness at load cycle n, and

ϕ_n = phase angle between the stress and strain wave signals.

The total cumulative dissipated energy obtained through the summation of the individual dissipated energy during the fatigue test is as follows:

$$W_t = \sum_{n=1}^{N_f} w_n \qquad (6.24)$$

Assuming a controlled-dissipated energy test, the initial dissipated energy per load repetition (w_i) remains constant during testing and the pseudo-total cumulative dissipated energy during the test can be described as follows:

$$W_{pt} = w_i N_f \qquad (6.25.1)$$

or

$$W_{pt} = \frac{\pi N_f \varepsilon_i^2 S_i \sin(\phi_i)}{4} \qquad (6.25.2)$$

where W_{pt} = pseudo-total cumulative dissipated energy to failure,

w_i = initial dissipated energy per load cycle, and

N_f = number of load cycles to failure,

However, the controlled-stress or controlled-strain modes of testing are easily accessible rather than the controlled-energy mode of testing to perform fatigue tests. Despite the advancement in computer controlled testing and data acquisition systems, controlled-dissipated energy testing would be extremely difficult to conduct at this time (Tayebali et al., 1992). The stress or strain, the phase angle change, and the dissipated energy per cycle all change during the test. Therefore, an energy ratio factor that is dependent on the mode of loading is introduced and defined as the ratio between the pseudo-total dissipated energy and

the total cumulative dissipated energy:

$$\psi = \frac{W_{pt}}{W_t} \tag{6.26}$$

Substituting Equations (6.22) and (6.25.2) into Equation (6.26) yields:

$$N_f = \left(\frac{4A\psi}{\pi \varepsilon_i^2 S_i \sin\phi_i}\right)^{\frac{1}{(1-z)}} \tag{6.27}$$

and generalizing for the purpose of regression analysis:

$$N_f = A(\psi)^b(\varepsilon_i)^c(S_i)^d(\sin\phi_i)^e \tag{6.28.1}$$

However, additionally initial air voids content (%) and testing temperature, were added to Equation (6.28.1), since the fatigue performance of the asphalt concrete mixtures could not be completely explained with the engineering parameters described in Equation (6.28.1). With the additional two terms, the following generalized regression equation was obtained:

$$N_f = A(\psi)^b(\varepsilon_i)^c(S_i)^d(\sin\phi_i)^e(V_i)^f(T)^g \tag{6.28.2}$$

The fatigue models estimated herein were based on Equation (6.28.2). Based on Equation (6.28.2), multi-regression analysis was conducted between the fatigue life and the initial laboratory testing parameters. The regression analysis yields the following relationships:

$$N_f = 6.23x10^{-3}(\psi)^{1.363}(\varepsilon_i)^{-4.813}(S_i)^{-1.837}(\sin\phi_i)^{-0.902}\exp(0.101V_i - 0.046T) \tag{6.28.3}$$

or

$$N_f = 1.71x10^{-7}(\psi)^{1.782}(\varepsilon_i)^{-4.601} (S_i)^{-1.082}\exp(0.217V_i - 0.046T) \quad (6.28.4)$$

or

$$N_f = 4.21\times(\psi)^{1.241}(w_i)^{-1.991} \exp(0.162V_i - 0.027T) \quad (6.28.5)$$

The strain-dependent model, Equation (6.28.3), requires the use of a multi-layered elastic system for the mechanistic analysis of pavement structures, while the energy-dependent model shown in Equation (6.28.5), requires energy-based viscoelastic analysis.

The following sections describe the general concepts of energy ratio factor and phase angle in more detail. In particular, the energy ratio factors and the phase angles were estimated from the controlled-stress diametral fatigue tests on three asphalt concrete mixtures.

Energy Ratio Factor

The energy ratio factor (Ψ) is defined as the ratio of the pseudo-total cumulative dissipated energy (Wpt) to the total cumulative dissipated energy (Wt) to failure measured during the test. The total cumulative dissipated energy to failure from the diametral fatigue test is the area under the number of cycles versus the dissipated energy shown in Figure 6.7. The total cumulative dissipated energy (measured to failure) is determined by Equation (6.24) while the pseudo-total cumulative dissipated energy is estimated with Equations (6.25.1) or (6.25.2).

In this research, the energy ratio factor was estimated at different stiffnesses with three mixtures in the controlled-stress diametral fatigue test. Generally, within the limitations of this research, the range of the energy ratio factor was between 0.35 and 0.50. Figure 6.16 shows the relationship between the energy ratio factor and initial mixture stiffness for three

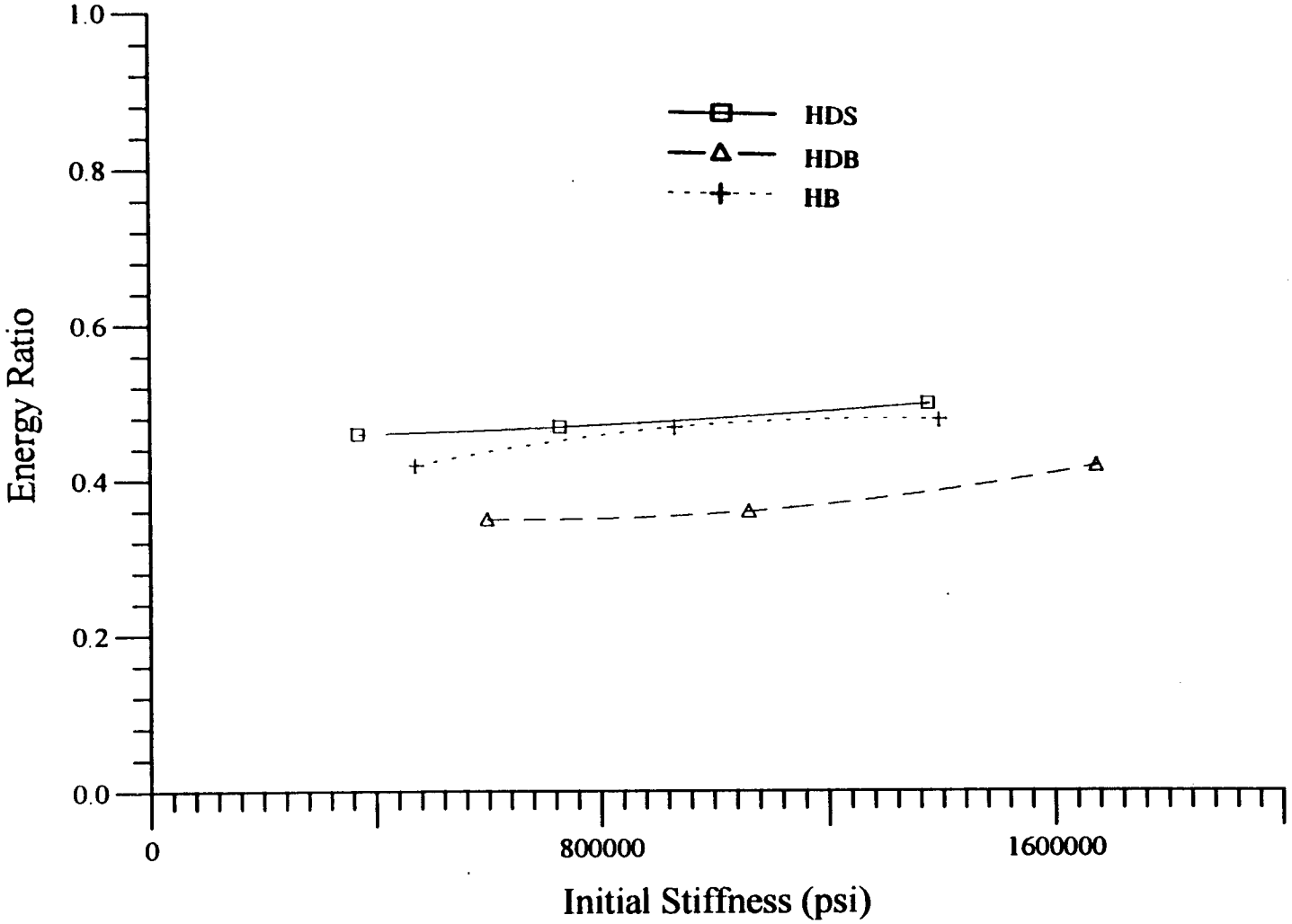

Figure 6.16 Energy ratio factor (Ψ) versus initial mixture stiffness (S_i).

mixtures (HDS, HDB, and HB).

It is noted that the energy ratio increased with increasing the initial stiffness in the controlled-stress diametral test. This finding is in good agreement with the research results reported by van Dijk and Visser (van Dijk et al., 1977) that the energy ratio factor of the controlled-stress beam fatigue test increased with increasing initial stiffnesses.

Phase Angle

The phase angle is defined as the angle between the stress and strain wave signals at a certain load repetition. The phase angle between the stress and strain wave signals stems from the intrinsic time dependent asphalt mixture behavior. The phase angle is zero for a purely elastic material and 90 degrees for a purely viscous body.

However, at a fairly high stress level in the fatigue test, in the nonlinear viscoelastic range, it is considered that the phase angle results from the time dependency and the internal damage development of the asphalt specimen. In this research, the dissipated energy per cycle at a certain load repetition was computed using Equation (6.10). Also, the dissipated energy per load repetition due to the sinusoidal loading condition can be expressed by Equation (6.25.2). Therefore, by equating the two relationships to one another, the following relationship can be obtained:

$$\phi_i = \sin^{-1}\left(\frac{4\int \sigma d\varepsilon}{\pi \varepsilon_i^2 S_i}\right) \qquad (6.29)$$

Based on this equation, the phase angle was computed and the relationship between the initial mixture stiffness and the initial phase angle is presented in Figure 6.17. The figure shows that the phase angle decreased with increasing initial mixture stiffness. The same trend has been reported by van Dijk and Visser (1977), based on controlled-stress beam fatigue tests.

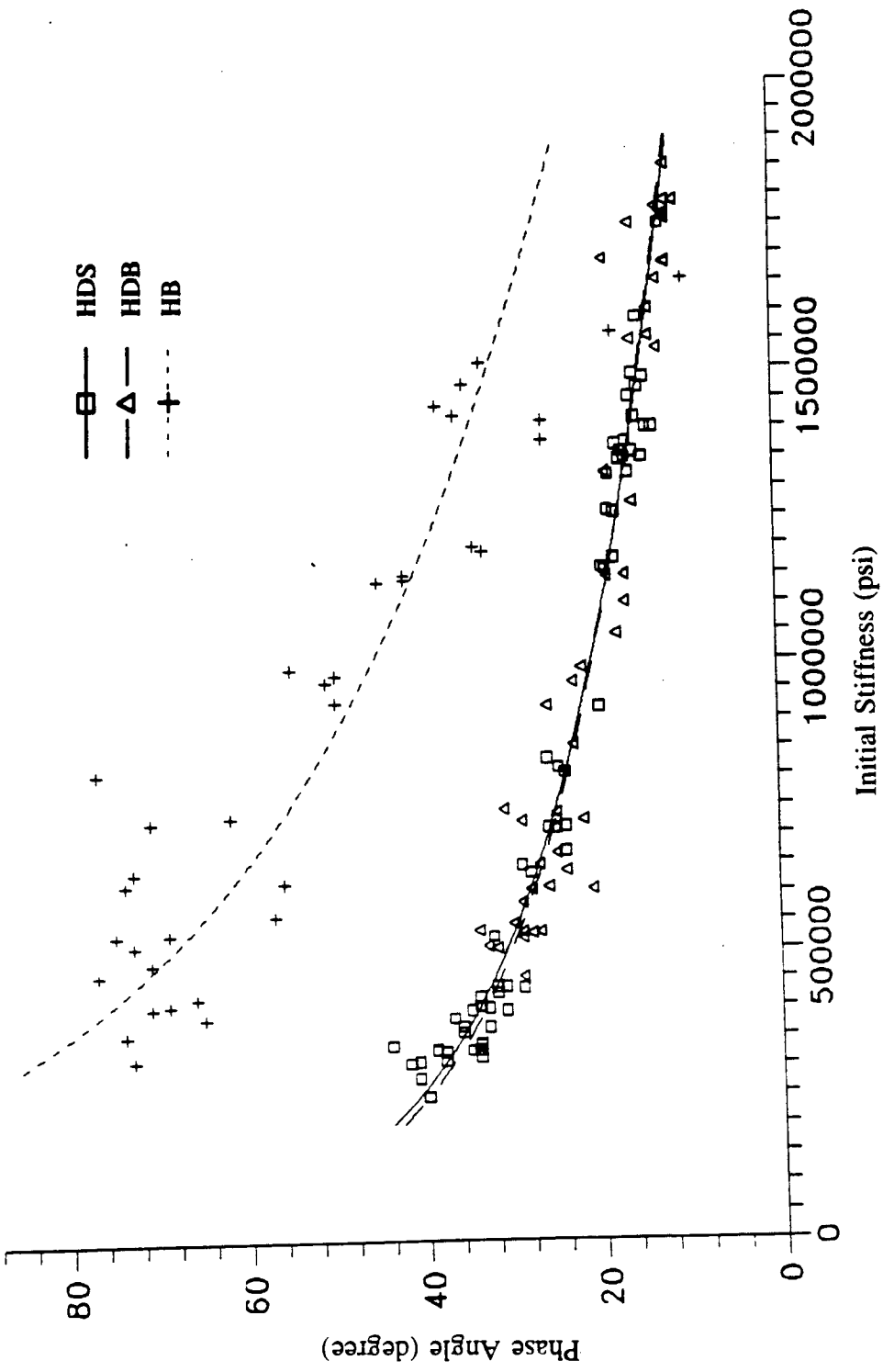

Figure 6.17 Initial phase angle (Φ_i) versus initial mixture stiffness (S_i).

6.5 Validation of Fatigue Prediction Models

6.5.1 Damage Growth Approach

The comparison between the fatigue life predicted from Equation (6.21) and the laboratory-determined fatigue life is presented in Figures 6.18(a) through 6.18(c). These figures demonstrate that the comparison between the predicted and measured fatigue life for the HDS mixture shows excellent results while the comparison for the HDB and HB mixtures demonstrate larger variation than that for the HDS mixture. The primary reason for the larger variation with the HDB and HB mixtures is probably related to less homogeneous asphalt-aggregate structures from these mixtures due to larger nominal maximum aggregate sizes. The comparison between the predicted fatigue life using Equation (6.21) and the laboratory-measured fatigue life (Nf) with all different testing temperatures and with different mixtures is presented in Figure 6.19. The overall R-square value between the predicted and laboratory-measured values was about 0.87.

6.5.2 Modified Shell Method

After the direct measurement or computation of several initial engineering parameters and the energy ratio of individual specimens, the final fatigue life was expressed with the corresponding engineering parameters through the multi-regression analysis technique. Figures 6.20(a) to 6.20(c) present the comparison between the predicted fatigue life using Equation (6.28.3) and the laboratory measured fatigue life. The general comparison showed similar results as to those with the damage-based prediction model. The comparison between the predicted fatigue life using Equation (6.28.3) and the laboratory measured fatigue life with all different testing temperatures and with different mixtures is presented in Figure 6.21. The overall R-square value between the predicted and measured values was about 0.88. It is noted that the overall R-square values between the laboratory-measured and predicted fatigue lives using Equations (6.28.4) and (6.28.5) were 0.87 and 0.79, respectively.

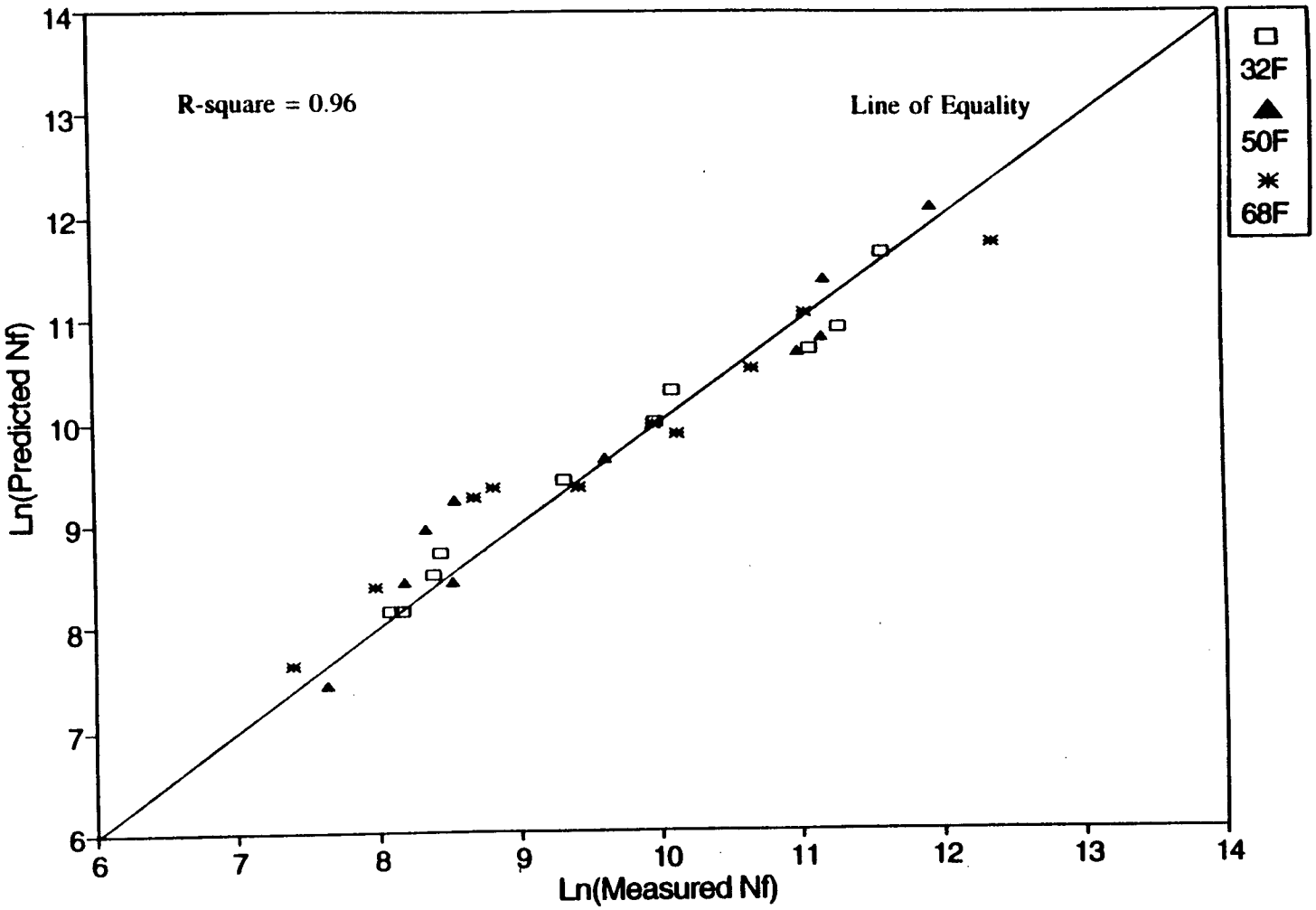

Figure 6.18(a) Laboratory-measured versus predicted fatigue life (N_f) for HDS mixture.

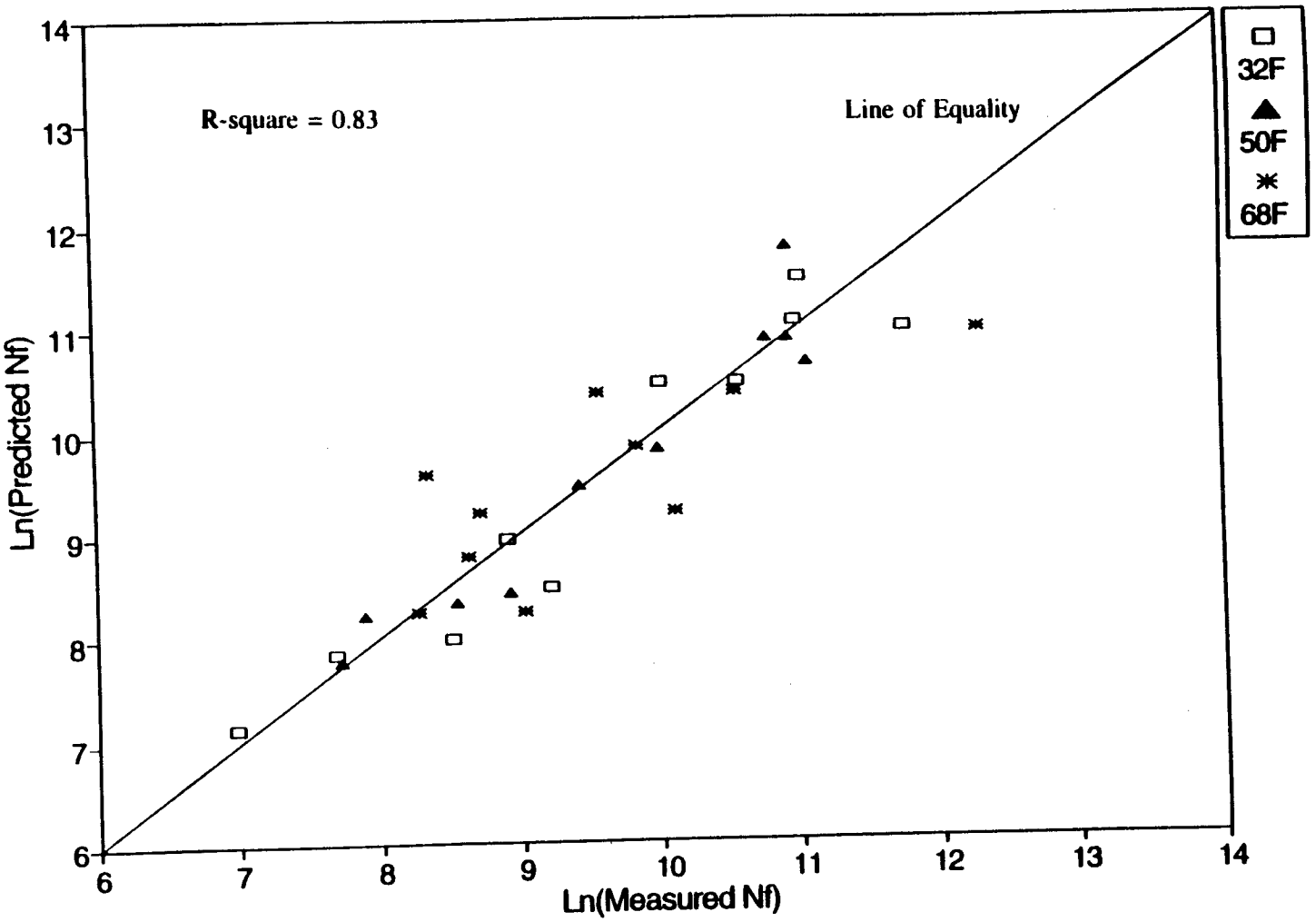

Figure 6.18(b) Laboratory-measured versus predicted fatigue life (N_f) for HDB mixture.

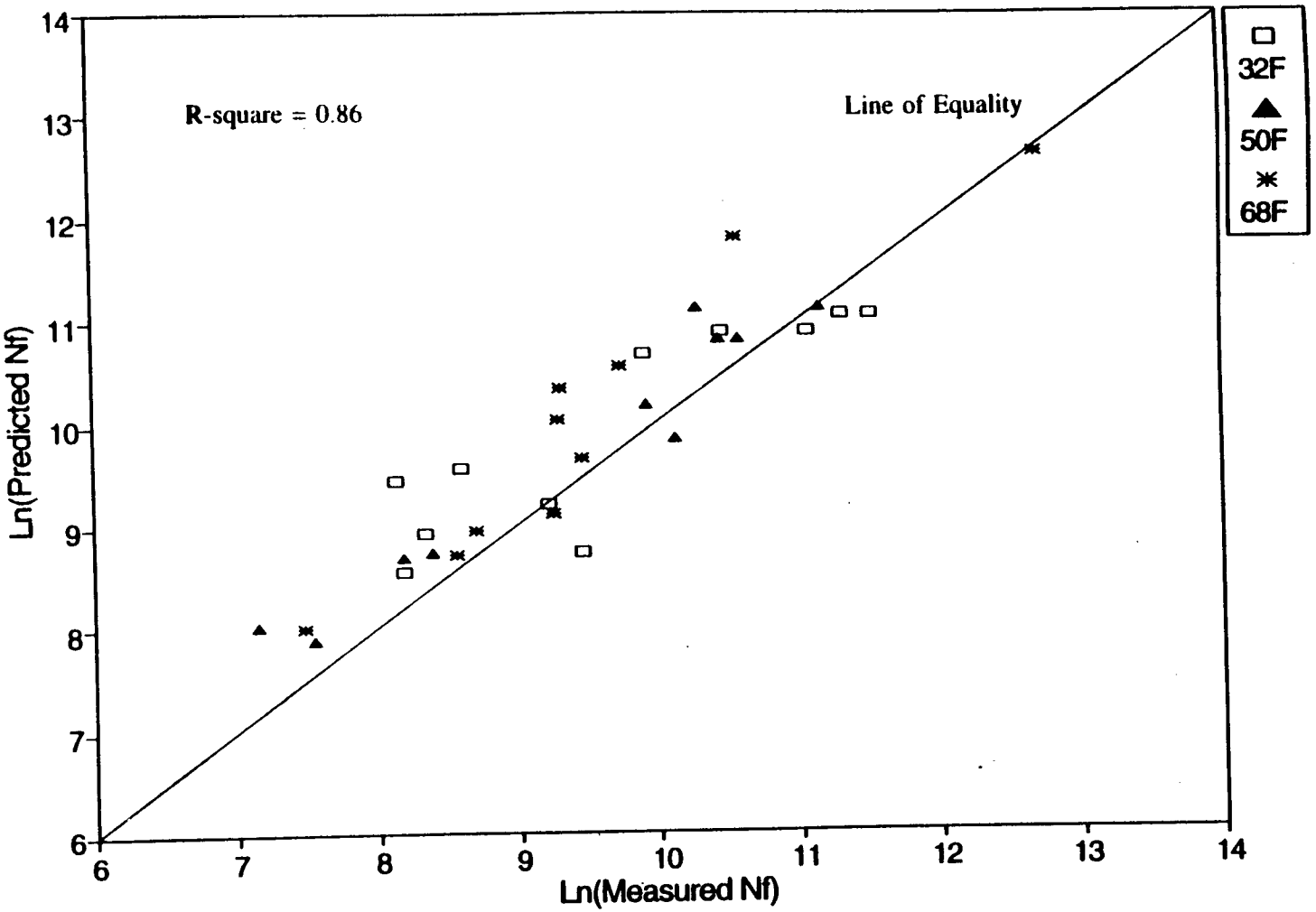

Figure 6.18(c) Laboratory-measured versus predicted fatigue life (N_f) for HB mixture.

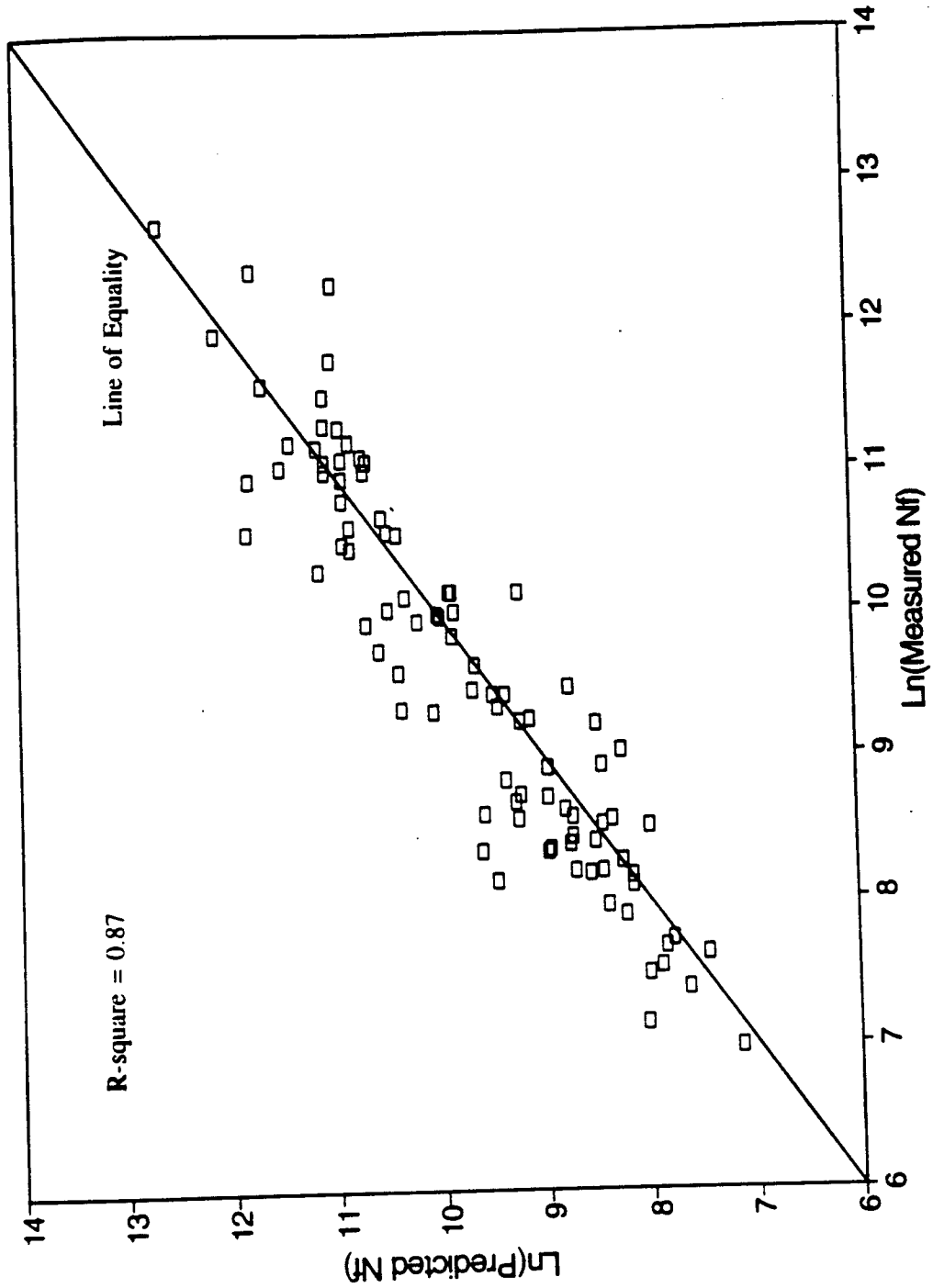

Figure 6.19 Measured versus predicted fatigue life (N_f) for the three mixtures (HDS, HDB, and HB).

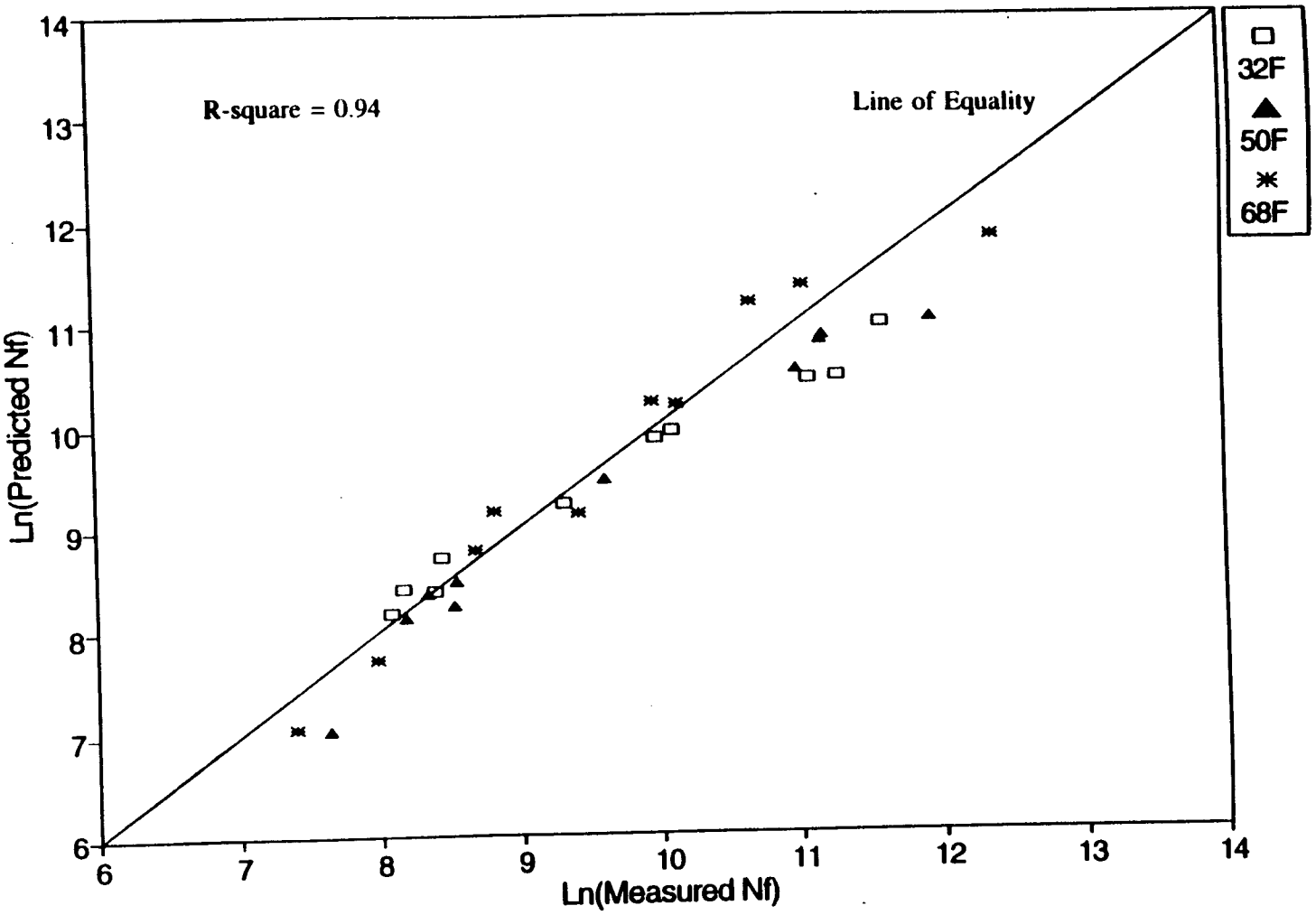

Figure 6.20(a) Measured versus predicted fatigue life (N_f) for HDS mixture.

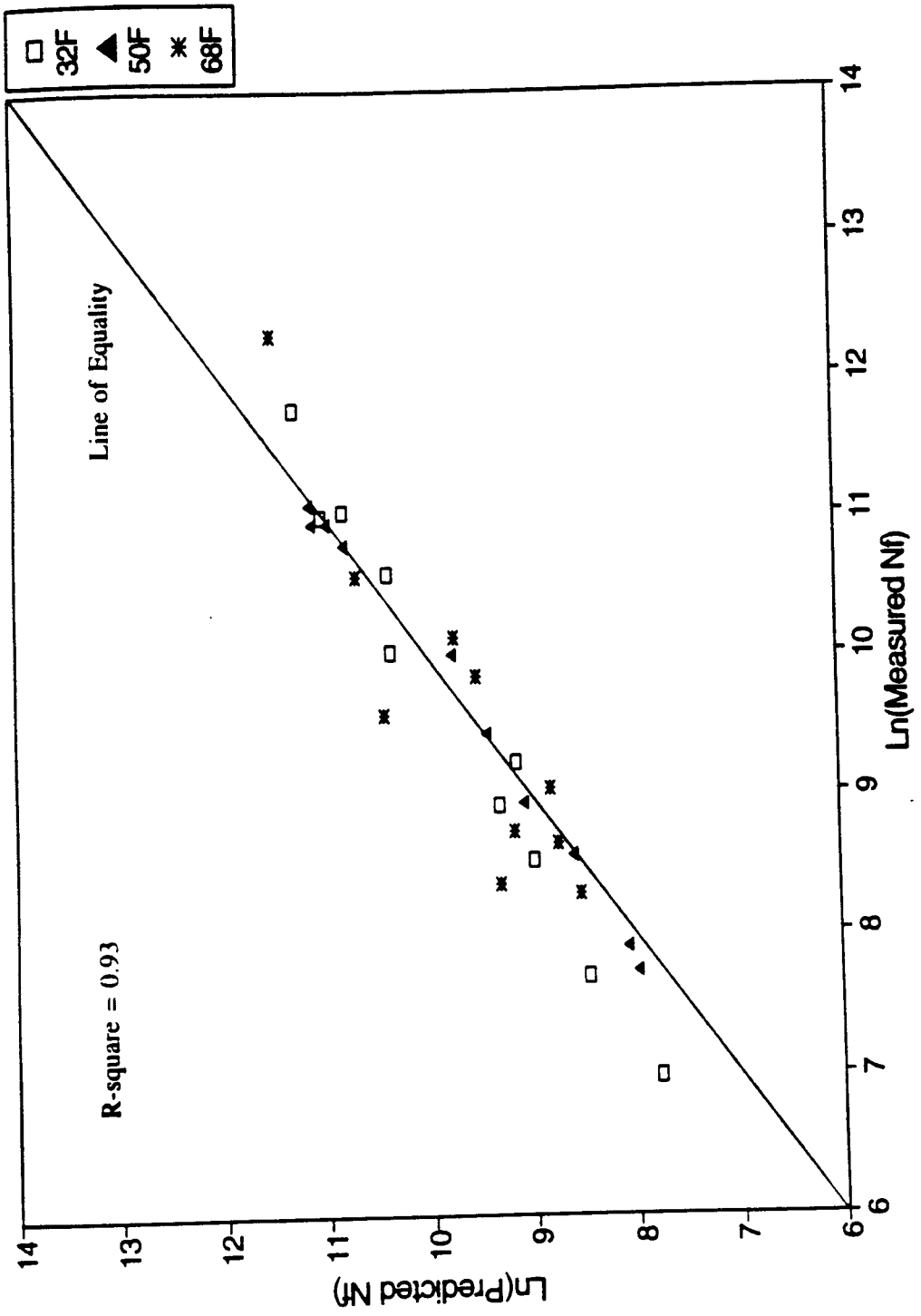

Figure 6.20(b) Measured versus predicted fatigue life (N_f) for HDB mixture.

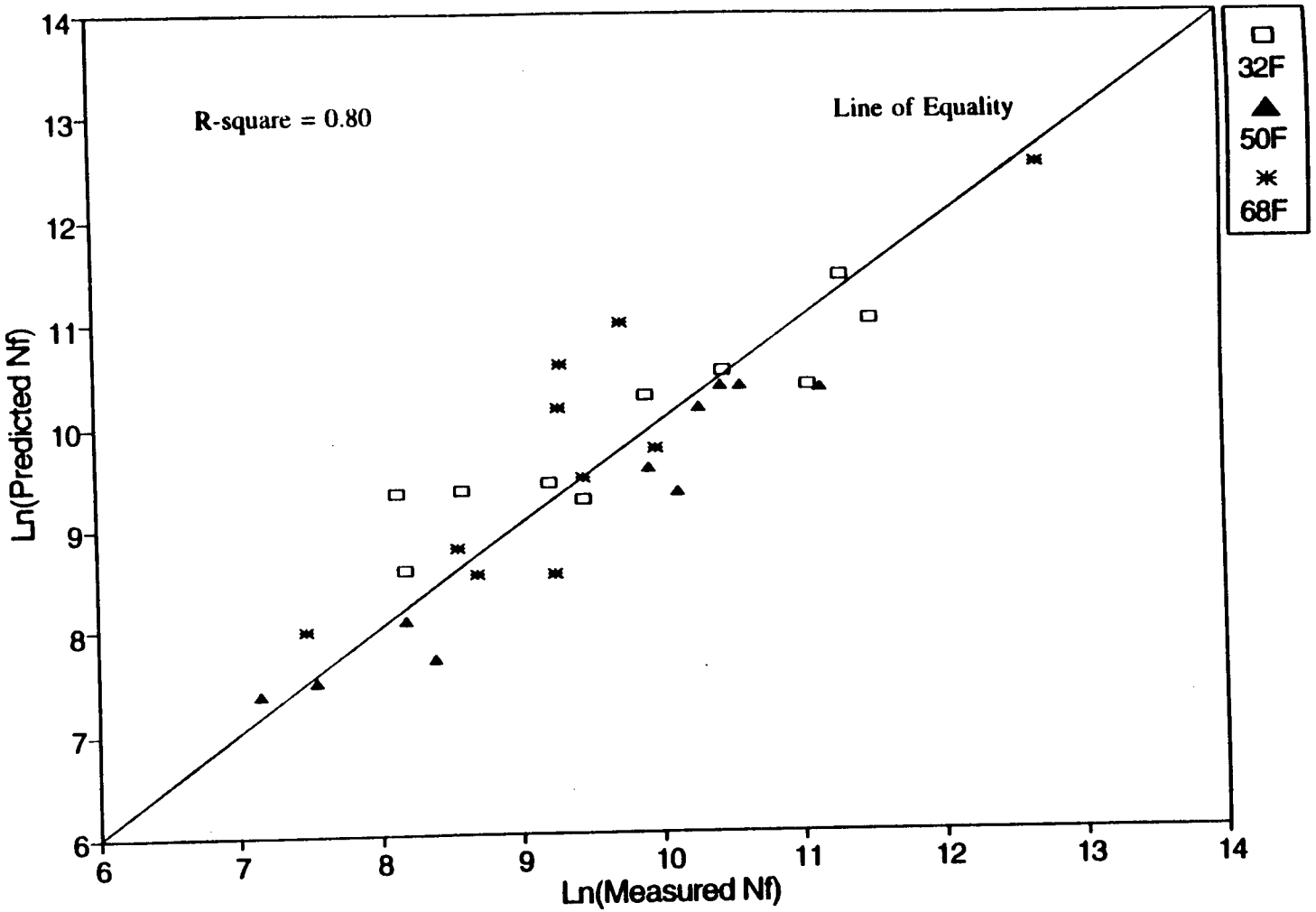

Figure 6.20(c) Measured versus predicted fatigue life (N_f) for HB mixture.

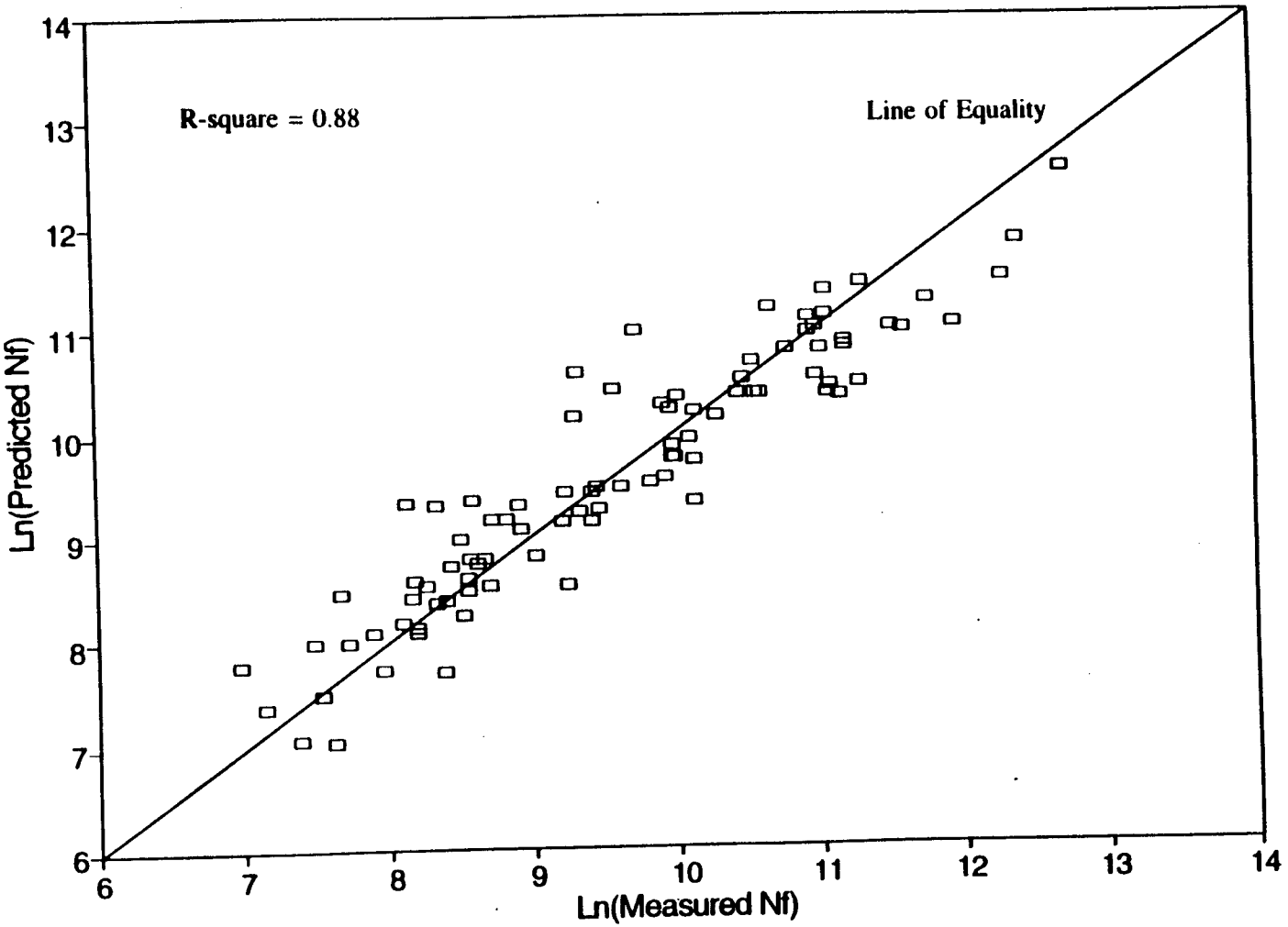

Figure 6.21 Measured versus predicted fatigue life (N_f) for the three mixtures (HDS, HDB, and HB).

CHAPTER 7

PERFORMANCE PREDICTION MODEL FOR PERMANENT DEFORMATION

7.1 Permanent Deformation

Rutting or permanent deformation, refers to the depressions or ruts in the pavement structure under the wheel path. These depressions or ruts are of concern for two reasons;

(1) If the surface is impervious, the ruts will trap water, thereby increasing the potential for hydroplaning, and

(2) increase in rutting could cause steering problems, leading to safety concerns.

7.2 Literature Survey

Little formal work has been done prior to 1960, with regard to rutting potential. At the First International Conference on the Structural Design of Asphalt Pavements in 1962, the Shell Oil Company (Dorman, 1962), presented the first pavement design approach that considered both fatigue and rutting as mechanisms of distress. As a part of this design method, Dorman and Metcalf, developed a relationship between vertical compressive strain in the subgrade and number of load repetitions that could be used to limit rutting.

Barksdale (1972), and Romain (1972), presented a paper in the Third International Conference (1972) outlining a layer strain approach for predicting the amount of rutting due to traffic loads.

In the Fourth International Conference (1977), a wide variety of papers were presented on design methods, which could limit rutting. Finn et.al. (1977), using data from the AASHO Road Test, used stepwise regression techniques to relate rutting to stress, surface deflection and number of load repetitions. Claessen et. al. (1977) modified the shell approach utilizing the creep test approach developed by van der Loo (1974), Barksdale (1977), and Hills (1974).

A large number of rutting prediction models, have been developed over the last

couple of years. Many different testing configurations have also been developed. Table 7.1 shows a summary of the many methods for rut depth predictions. A report prepared by Sousa et.al. (1989) provides a detailed description of various factors involved in rut depth predictions.

7.3 MDD Rutting Evaluation of Asphalt Concrete (AC) Layer

From the selected eight test sections (Sections 1-3, 6-9, and 11) with MDD device, the permanent deformation of the asphalt concrete layers can be separated from overall pavement deformation measured from the surface. The surface pavement deformation is an indication of the cumulative permanent deformation of the sublayers (asphalt, base, subbase, and subgrade). Similarly, the permanent deformation at the bottom of the asphalt layer represents cumulative permanent deformation coming from underlying sublayers (base, subbase, and subgrade).

Therefore, the permanent deformation of an asphalt concrete layer is calculated by subtracting the accumulated permanent deformation at the bottom of the asphalt layer from the surface permanent deformation. The surface permanent deformation of the pavement was measured by walk-through distress survey with a 4.5-foot (1.37 m) straight edge. The permanent deformation at the bottom of the asphalt layer was calculated from corresponding MDD module readings. The cumulative permanent deformation (rutting) under each MDD module was computed using the following calibration formula provided by the Texas Transportation Institute (TTI):

$$PD = \frac{(DV)(LVDT\ Type)\times 0.5}{10} \qquad (7.1)$$

where PD = cumulative permanent deformation and

DV = differential voltage (volt), or original offset - current offset.

Most of the surface pavement deformations of the selected test sections were between 0.20 (0.51 cm) and 0.40 inches (1.02 cm). It has been found from the MDD sections,

Table 7.1 Summarized overview of permanent deformation models developed by several authors (Sousa et al., 1990)

Author	Pavement Analysis	Laboratory Test	Observations
Kirwan Snaith Gynn (1977)	DEFPAV Non-linear Finite Element Layer Strain Method	Uniaxial Compression Dynamic Loading Creep Test	Calculated values of rut depth higher than Nottingham Test Track
Monismith Inkabi Freeme McLean (1977)	ELSYM Layered Elastic Theory Layer Strain Method	Repeated Triaxial Test	Consideration of traffic axle load and lateral distribution
Brown Bell (1979)	Computer Program DEFPAV Non-Linear Finite Element	Axial Creep Tests	Relatively Good Agreement with test track results
Meyer Haas (1977)	Computer Program FEPAVE II Finite Element Layer Strain Method	Repeated Triaxial Test	Measured values rut depth on the Brampton Test Road Section. Good agreement between measured and predicted.
van de Loo (1976)	BISAR Elastic layer Theory	Axial Creep Test	Basis of SHELL Method Generally overestimates rut depth
Thrower (1977)	Viscoelastic Theory Separative Method		
Battiato (1977)	Computer Program MOREL Viscoelastic Theory Two layer viscoelastic incompressible system	Uniaxial Creep Tests	Asphalt mix is represented by a Maxwell Model
Mahboub Little (1988)		Uniaxial Creep Tests	
Tseng Lytton (1986)		Repeated Load Testing	

Table 7.1 Summarized overview of permanent deformation models developed by several authors (Sousa et al., 1990) (continued)

Author	Pavement Analysis	Laboratory Test	Observations
Lai Anderson (1973)		Uniaxial Creep Tests	
Kenis (1977)	VESYS Probabilistic linear viscoelastic solution	Uniaxial Repeated Tests	Basis of the VESYS approach
Francken (1977)		Triaxial Dynamic Tests	Acceptable correlation with rut depth measure in 16 in-service roads
Verstraeten Romain Veverka (1982)	Computer Program ORN093 elastic layer theory Layer Strain Theory	Triaxial Dynamic Tests	Acceptable correlation with rut depth measure in 16 in-service roads
Huschek (1977)	BISAR Elastic layer theory	Uniaxial Creep Tests Cyclic Load Creep Tests	Asphalt mix is represented by a Maxwell element: spring and dashpot in series.
Celard (1977)	ERDT/ESSO Three layer elastic system	Dynamic Creep Tests	Developed Isocreep curves
Khedr (1986)	OSU Model	Multi-step Dynamic Test	

excepting Section 1, that the major portion of the surface pavement deformation was composed of permanent deformation from the asphalt concrete layer. It suggests that the major portion of the permanent deformation in asphalt concrete pavements stems from the asphalt concrete layer rather than from the subgrade layer, provided that the pavements are structurally well designed and properly constructed.

Generally, the MDD readings of Section 1 were unreliable due to its earlier mechanical failure. The comparison between the surface rutting and the AC layer rutting values failed to show the compatibility throughout the data acquisition period. Therefore, the precision of MDD readings on Section 1 is questionable. Table 7.2 presents a summary of permanent deformations from the test sections with MDD devices.

To find out how the permanent deformation changes at different depths within the asphalt layer, detailed analysis was conducted. Sections 7 and 9 had two MDD modules each at the depths of 3.6 inches (9.14 cm) and 10.0 inches (25.40 cm) within the asphaltic layers. Therefore, it was possible to collect the permanent deformations at two locations, both within the asphalt layer. The permanent deformations of asphalt concrete layers from these sections showed that the major part of the total surface permanent deformation occurred within the top 3.6 inches (9.14 cm) of the asphalt concrete layer (see Figure 7.1).

This phenomenon is easily understandable and convincing since the pavement temperature and the stresses under the wheel load are higher at the pavement surface and diminish rapidly as the depth increases. As a result, the pavement material within the top 3.6 inches (9.14 cm) of the asphalt concrete layer (HDS and HDB) is softer than the lower portion of the asphalt concrete layer (HB).

In summary, it has been found that, at least for reasonably stiff supporting materials, most pavement rutting is confined to the asphalt concrete layer. In addition, the primary portion of the total surface permanent deformation in a flexible pavement stems from the upper part (top 3.6 inches (9.14 cm)) of the asphalt concrete layer. The permanent deformations from base, subbase, and subgrade layers were negligible, if any. As a result, the pavement surface rutting measured directly with a 4.5-foot (1.37-m) straight edge was assumed to occur from the asphalt concrete layers throughout this research.

Table 7.2 Summary of comparisons between the surface rutting and the rutting from AC layer in MDD test sections.

Date: Oct'91

Section #	Surface Rutting[1]	AC Layer Rutting[2]
1	0.19"	0.10"
2	0.15"	-
3	0.25"	0.24"
6	0.24"	0.23"
7	0.20"	0.21"
8	0.21"	-
9	0.24"	-
11	0.15"	0.15"

Date: Mar'92

Section #	Surface Rutting[1]	AC Layer Rutting[2]
1	0.19"	0.11"
2	0.16"	-
3	0.25"	0.24"
6	0.24"	0.25"
7	0.20"	0.22"
8	0.23"	-
9	0.24"	-
11	0.19"	0.19"

Date: Jun'92

Section #	Surface Rutting[1]	AC Layer Rutting[2]
1	0.20"	0.11"
2	0.17"	-
3	0.25"	0.25"
6	0.24"	0.24"
7	0.22"	0.23"
8	0.24"	0.22"
9	0.24"	-
11	0.19"	0.19"

Table 7.2 Summary of comparisons between the surface rutting and the rutting from AC layer in MDD test sections (continued).

Date: Oct'92

Section #	Surface Rutting[1]	AC Layer Rutting[2]
1	0.22"	0.29"
2	0.19"	-
3	0.29"	0.29"
6	0.25"	0.24"
7	0.22"	0.24"
8	0.24"	0.21"
9	0.27"	0.26"
11	0.20"	0.20"

Date: Feb'93

Section #	Surface Rutting[1]	AC Layer Rutting[2]
1	0.22"	0.12"
2	0.19"	-
3	0.29"	0.30"
6	0.25"	-
7	0.22"	0.25"
8	0.24"	-
9	0.27"	0.31"
11	0.20"	0.21"

Note: 1. Measured with a 4.5-foot (1.4 m) straight edge.
2. Estimated by (Surface Rutting - Rutting at the bottom of AC layer).

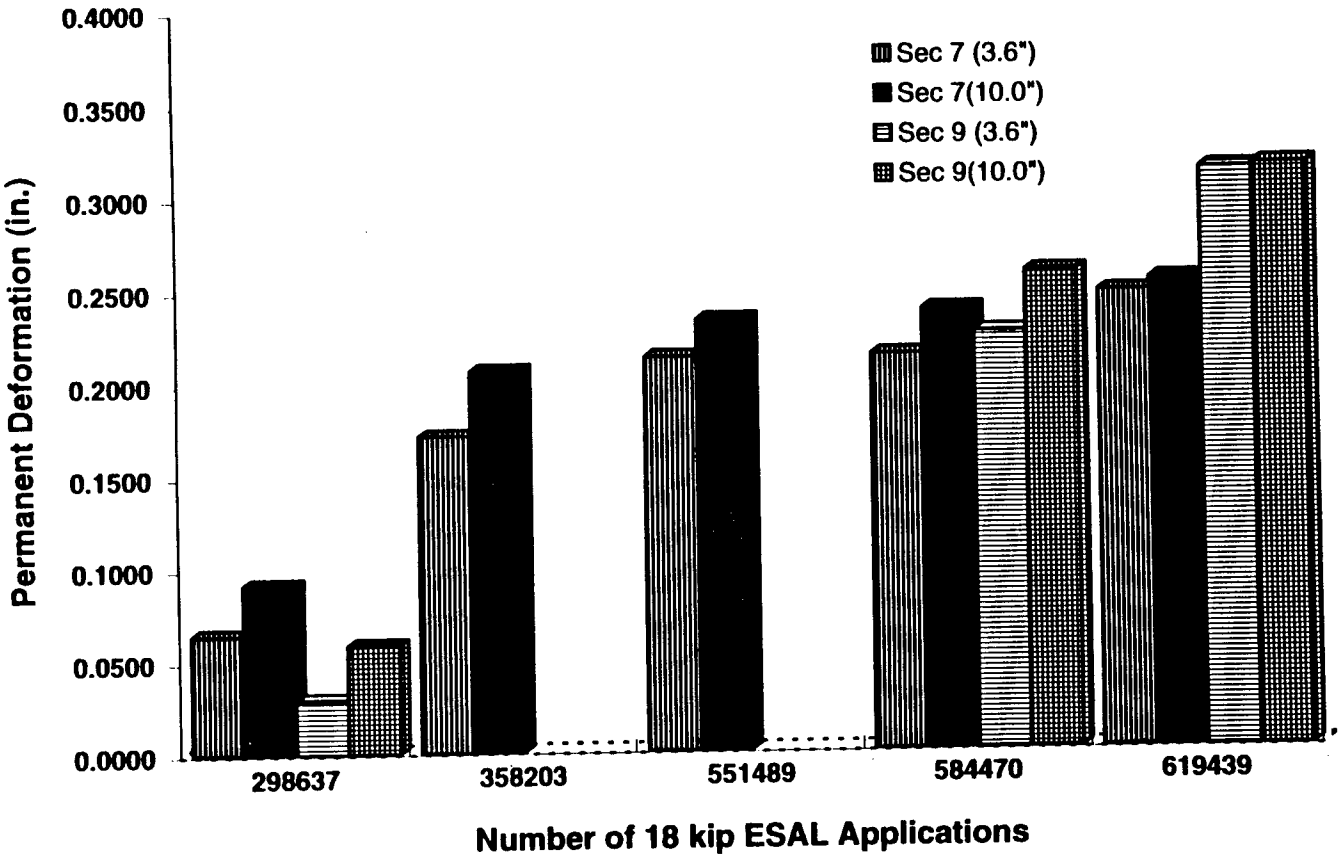

Figure 7.1 Permanent deformation (rutting) at two different locations within asphalt concrete layer.

These findings are in good agreement with the previous research works conducted by several researchers (HRB, 1962; Hofstra et al., 1972; Uge et al., 1974). Hofstra and Klomp (1972) reported that the permanent deformation in the asphalt-concrete layer was greatest near the loaded surface and gradually decreased at lower levels. Because rutting is caused by plastic flow, such a distribution of rutting with depth is reasonable, considering that the vertical stress encountered is smaller and also because of increased resistance to plastic flow at greater depths.

Uge and van de Loo (1974) found that the permanent deformation within an asphalt concrete layer (thickness reduction under the action of pneumatic tires) did not increase with increasing layer thickness beyond a certain threshold (5.12 inches (13 cm) in their studies). Measurement at the AASHO Road Test (1962) indicated that the surface rut depth reached a limiting value for asphalt concrete thickness of about 10 inches (25.40 cm). That is, a thicker asphalt concrete layer did not cause additional rutting.

In most flexible pavement design systems currently adopted by many highway agencies, the subgrade compressive stress criterion is used to limit the permanent deformation within an acceptable range. This design strategy is based on an assumption that the major part of the permanent deformation stems from permanent deformation of the subgrade layer rather than any other upper layers. However, the field test results on permanent deformation in this research along with advances in pavement construction technique suggest a new and realistic design criterion on permanent deformation of flexible pavements.

The necessity of a new and realistic design criterion on permanent deformation of flexible pavements has been proposed by some researchers. In 1982, Freeme et al. used the Heavy Vehicle Simulator (HVS) to evaluate the flexible pavement behavior. They concluded that permanent deformation in the asphalt concrete pavement could not be completely accounted for by the vertical subgrade stress criterion.

7.4 Selection of Test Method

As described earlier in the literature review, the general objective of materials testing is to simulate in-situ field conditions as closely as possible, including loading conditions,

climatic conditions, etc. Also, the test method should be easy, inexpensive, simple, and efficient to conduct, so as to become an acceptable standard laboratory testing method for state highway agencies.

A haversine load with a 0.05-second load duration and 0.25-second rest period was repeated until the number of load applications reached 100,000 cycles. The 0.05 second of loading time was selected based on measurements (measured responses) made at speed limit of 55 miles (88.50 km) per hour at three-inch depths within the asphalt concrete layer. The main reason for using repeated loading instead of creep loading was that the loading history of the cyclic loading was considered to be a better approximation of actual traffic loading than that simulated by constant creep loading. Also, it has been reported (Barksdale et al., 1977; Monistmith et al., 1988) that the repeated loading tests may be more sensitive to mixture variables than the creep tests.

In 1977, Barksdale et al. reported that, on the basis of the Shell creep tests, an increase in the asphalt content of a particular mixture from 4.5 to 5.5 percent would not have a significant effect on the rut depth. Results of repeated load triaxial tests on the same mixture, however, indicated that such an increase in asphalt content could increase the rut depth by 16 percent. From extensive testing, it was concluded that the repeated load triaxial test, rather than a creep test, measures rutting characteristics better.

Monismith and Tayebali (1988) reported similar conclusions. They compared the response of three mixtures under both creep and repeated loading. They could not find any noticeable differences among the mixtures for creep loading while they noticed differences in the repeated load data. These findings suggest that the repeated loading test may be a more appropriate laboratory testing method to characterize the permanent deformation of asphalt mixtures than the simple creep test.

Field condition simulation study

To simulate the field stress conditions better, structural analysis was performed using WES5 on three typical asphalt concrete pavement design types with aggregate base, cement-treated base, and full depth. Figures 7.2(a) through 7.2(c) show the three typical asphalt

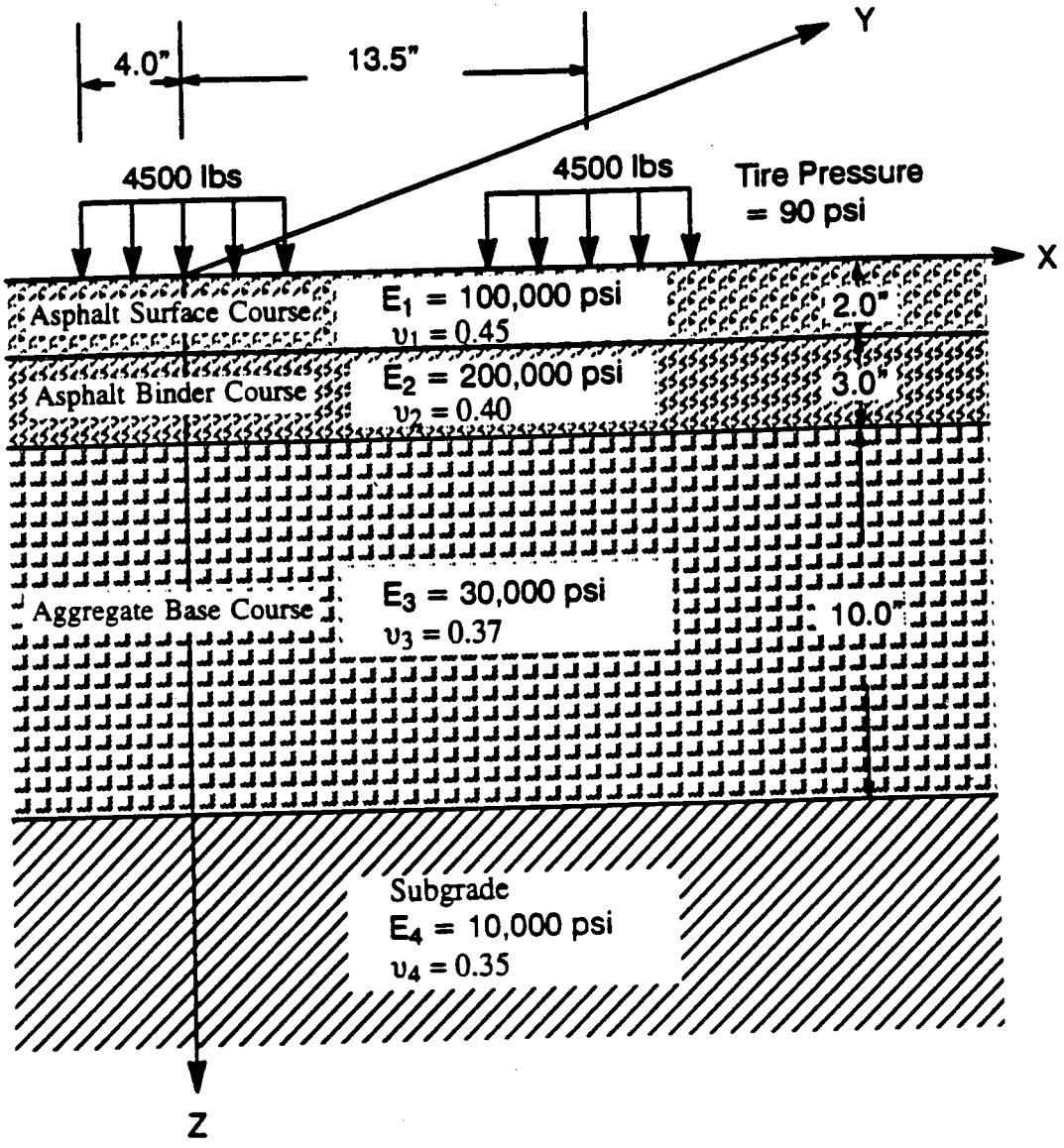

Figure 7.2(a) Typical asphalt concrete pavement design type with aggregate base course.

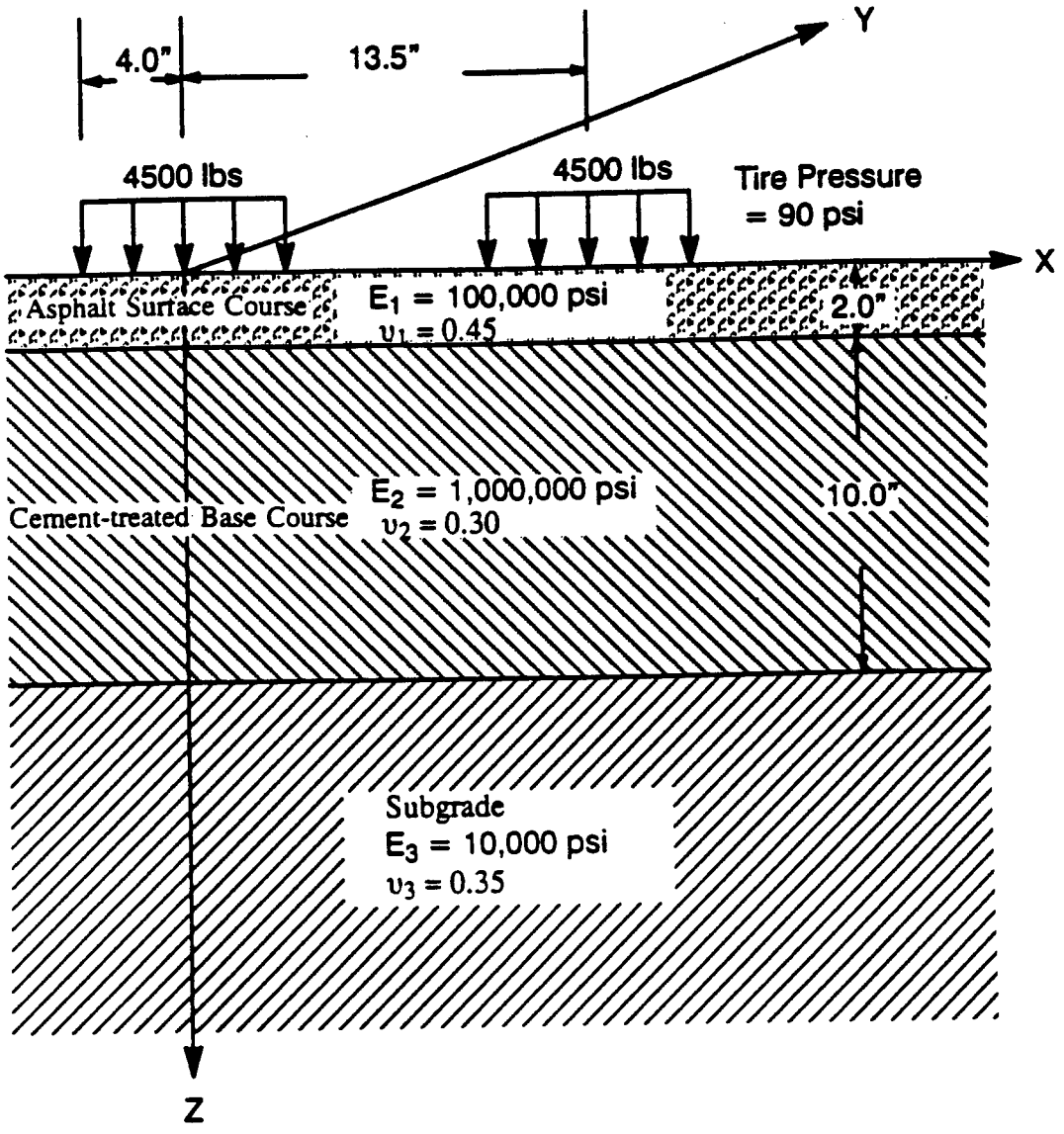

Figure 7.2(b) Typical asphalt concrete pavement design type with cement-treated base course.

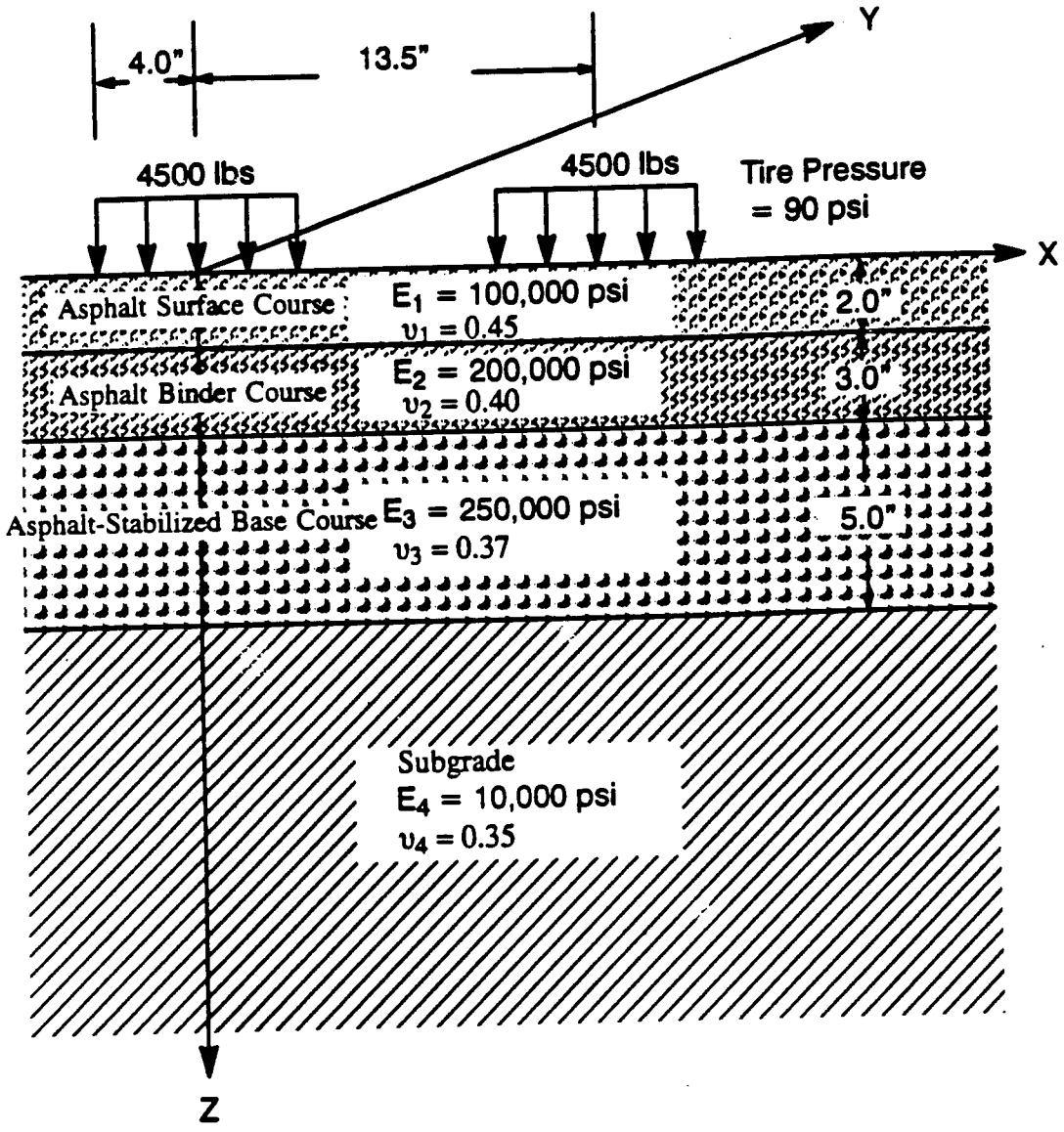

Figure 7.2(c) Typical asphalt concrete pavement design type with full depth AC course.

concrete pavement design types. The field stress (computed using WES5) conditions corresponding to the three typical asphalt concrete pavement design types are presented in Figures 7.3 to 7.5. It is noted that the negative sign was used for compressive stresses. These figures show how the stresses change at different locations within the asphalt concrete layer. For the structural analysis, a tire pressure of 90 psi (620 Kpa) was assumed with an axle loads of 18 kip (80.06 KN). Based on this analysis, vertical stresses of 90, 80, and 50 psi (620.73, 551.76, and 344.85 KPa) were determined to characterize the permanent deformation of AC layer for the top surface layer (less than 2 inches (5.08 cm)), the intermediate layer (between 2 and 5 inches (5.08 and 12.70 cm)), and the deep layer (deeper than 5 inches (12.70 cm)), respectively.

The history behind the use of vertical stress levels can be found from literature review (Little et al., 1993; Von Quintus et al., 1991). In 1991, Von Quintus et al. used linear elastic theory to calculate the distribution of vertical compressive stresses within the asphalt concrete layer. They suggested using 65 psi (448.31 KPa) in the uniaxial static creep test at 140°F (60°C). Little et al. (1993) reported that for most designs a uniaxial stress of between 50 and 60 psi (344.85 and 413.82 KPa) would be appropriate.

The temperatures used were 104°F (40°C) for the surface materials (less than 2 inches (5.08 cm)) and 95°F (35°C) for the other materials (deeper than 2 inches (5.08 cm)). The temperature of 104°F (40°C) for the surface materials was selected based on the range of measured pavement temperatures. Also AAMAS has traditionally used this temperature for creep testing. The selected testing conditions for loadings and testing temperatures are summarized in Table 7.3.

The selection of the test temperatures in this study can be supported by the following previous researches (Bonnot, 1986; Mahboub et al., 1988). Bonnot (1986) selected a test temperature of 140°F (60°C) for wearing-course asphalt concrete and 122°F (50°C) for base courses, based on typical temperatures in France. Mahboub and Little (1993) reported that the permanent deformation was very minimal at temperatures below 50°F (10°C). A testing temperature of 104°F (40°C) was selected by Little et al. (1993) for creep testing .

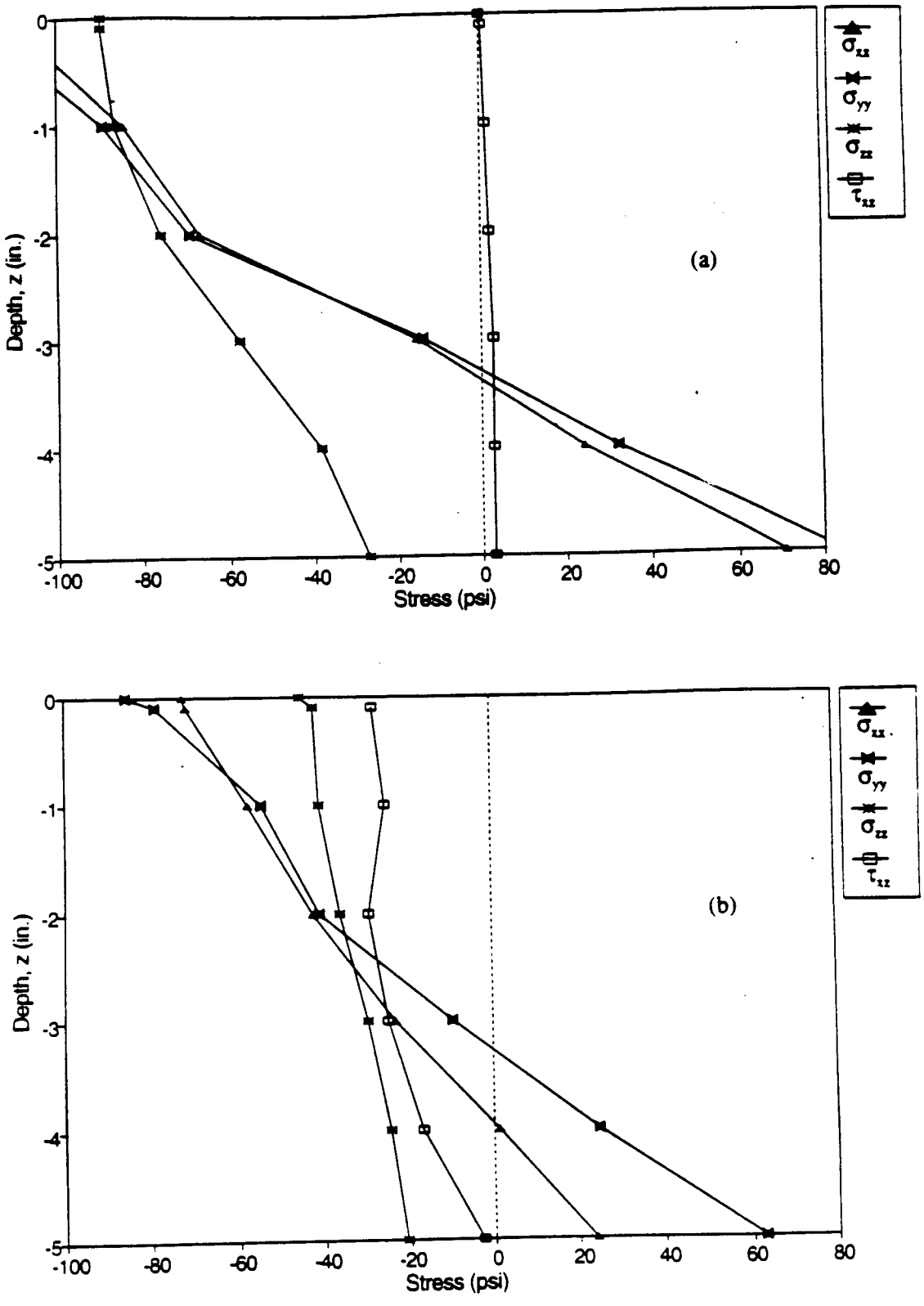

Figure 7.3 Stress distributions in pavement section shown in Figure 7.2(a) (a) at X=0, Y=0 and (b) at X=4 in. (10.20 cm), Y=0.

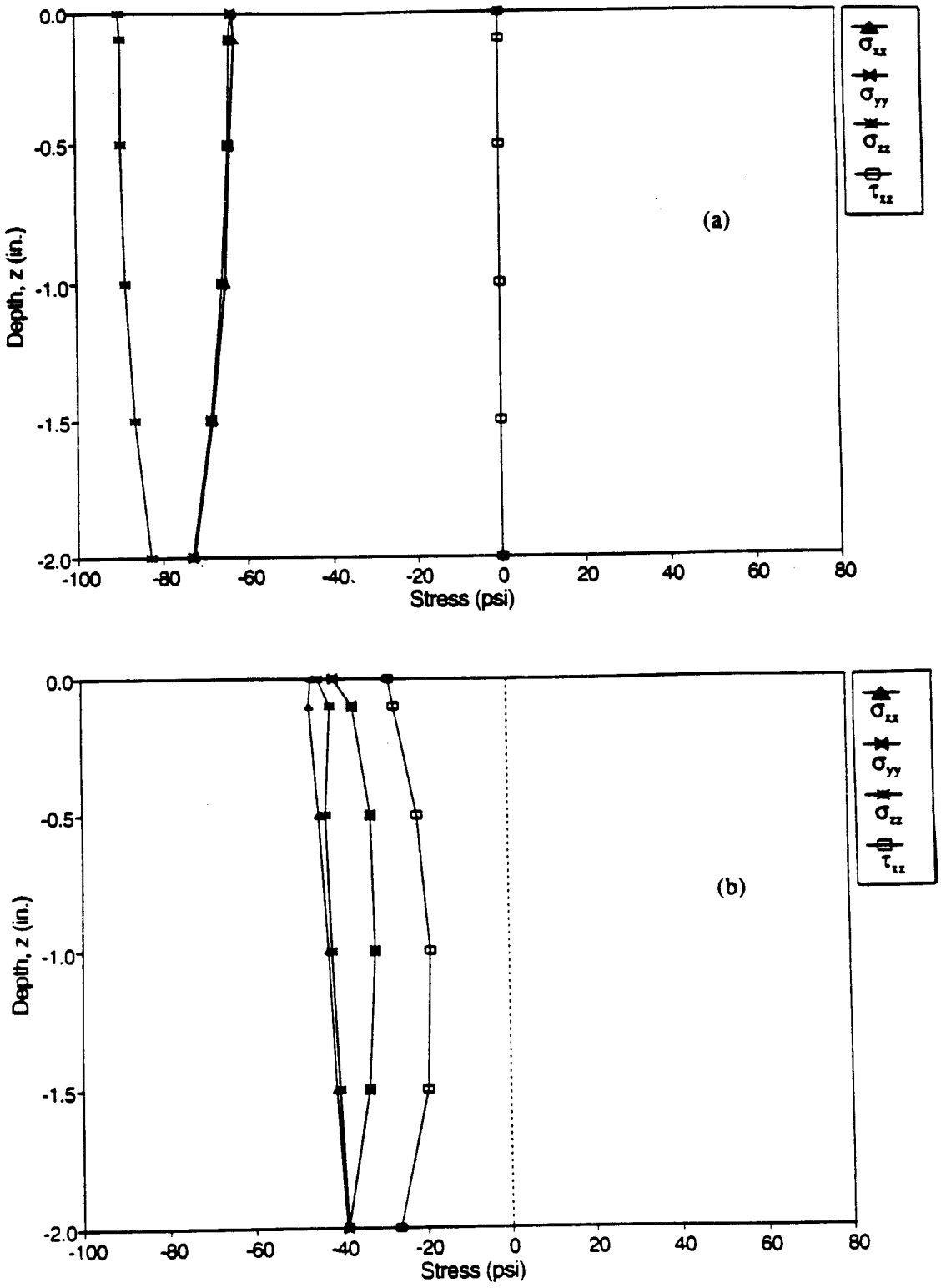

Figure 7.4 Stress distributions in pavement section shown in Figure 7.2(b) (a) at X=0, Y=0 and (b) at X=4 in. (10.26 cm), Y=0.

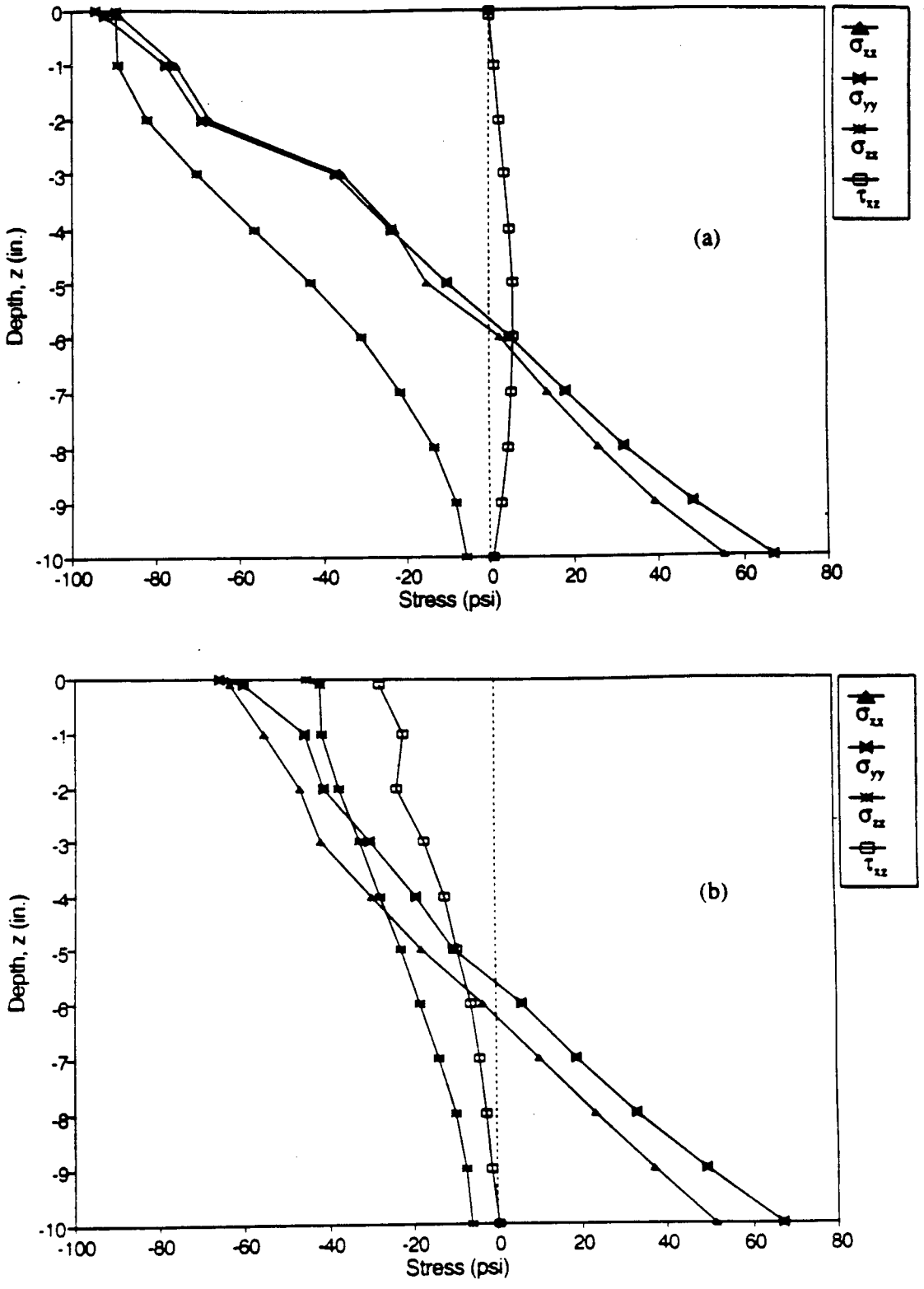

Figure 7.5 Stress distributions in pavement section shown in Figure 7.2(c) (a) at X=0, Y=0 and (b) at X=4 in. (10.26 cm), Y=0.

Table 7.3 Selected rutting test conditions.

Position in AC Layer	Vertical Stress (psi)	Temperature (°F)
Top 2 inches	90	104
Between 2 and 5 inches	80	95
Below 5 inches	50	95

Table 7.4 Experimental design for rutting characterization.

Temperature	Vertical Stress	Mix Type		
(°F)	(psi)	HDS[1]	HDB[2]	HB[2]
104	90	x		
95	80		x	x
95	50		x	x

Note: 1. Three replications in each cell.
2. Two replications in each cell.

Structural Analysis of Testing Configuration

To estimate the stress distribution in the specimen under the new testing configuration (repetitive axial loading test with confinement), the structural analysis was conducted using finite element method (FEM). The loading condition and the specimen geometry of the testing configuration were axisymmetric and the corresponding axisymmetric structural analysis was performed. The structural analysis using FEM was conducted for the three testing conditions according to Table 7.4. The same material properties (elastic modulus and Poisson's ratio) for AC layers were used as presented in Figure 7.2.

To check the validity and compatibility of the stress conditions, the stress conditions from the laboratory testing configuration using FEM were compared with those from the field (using WES 5). The comparison results between the field stress (computed using WES5) conditions and the laboratory stress conditions for the three typical asphalt concrete pavement design types are presented in Figures 7.6 through 7.8. Generally, the vertical stresses from the laboratory testing method showed a good agreement with those from the field throughout the different design types. However, the stresses at the loading edge from the laboratory testing configuration were lower than those from the field throughout the different design types. In particular, the vertical stress and the shear stress at the loading edge may affect the laboratory rutting performance significantly due to the selected laboratory rutting test configuration. Also, it should be noted that the lateral confining pressures from the laboratory testing configuration were lower than those from the field.

7.4.1 Test Fixture and Measurement

Based on these reasons, a new test method employing repetitive axial load with confinement was developed to evaluate the permanent deformation of asphalt concrete. For a more accurate representation of field stress conditions, a lateral confining pressure was applied. This was achieved by applying the axial load through a 4-inch (10.16-cm) diameter loading plate on a 6-inch (15.24-cm) diameter specimen. The material that is not underneath the loading plate creates a lateral confining pressure on the material that is underneath the loading plate.

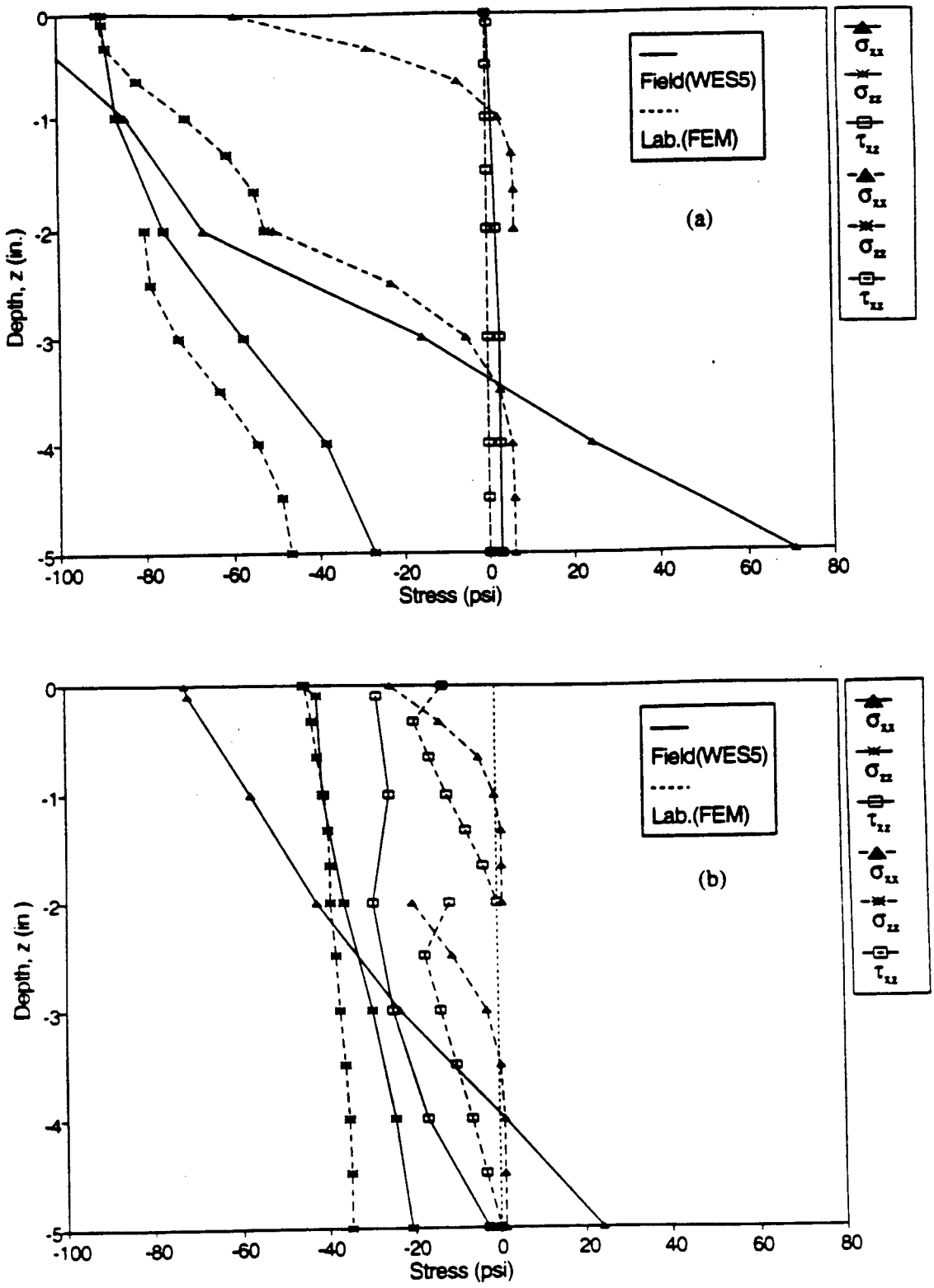

Figure 7.6 Comparison of stress distributions in pavement section shown in Figure 7.2(a) (a) at X=0, Y=0 and (b) at X=4 in. (10.26 cm), Y=0.

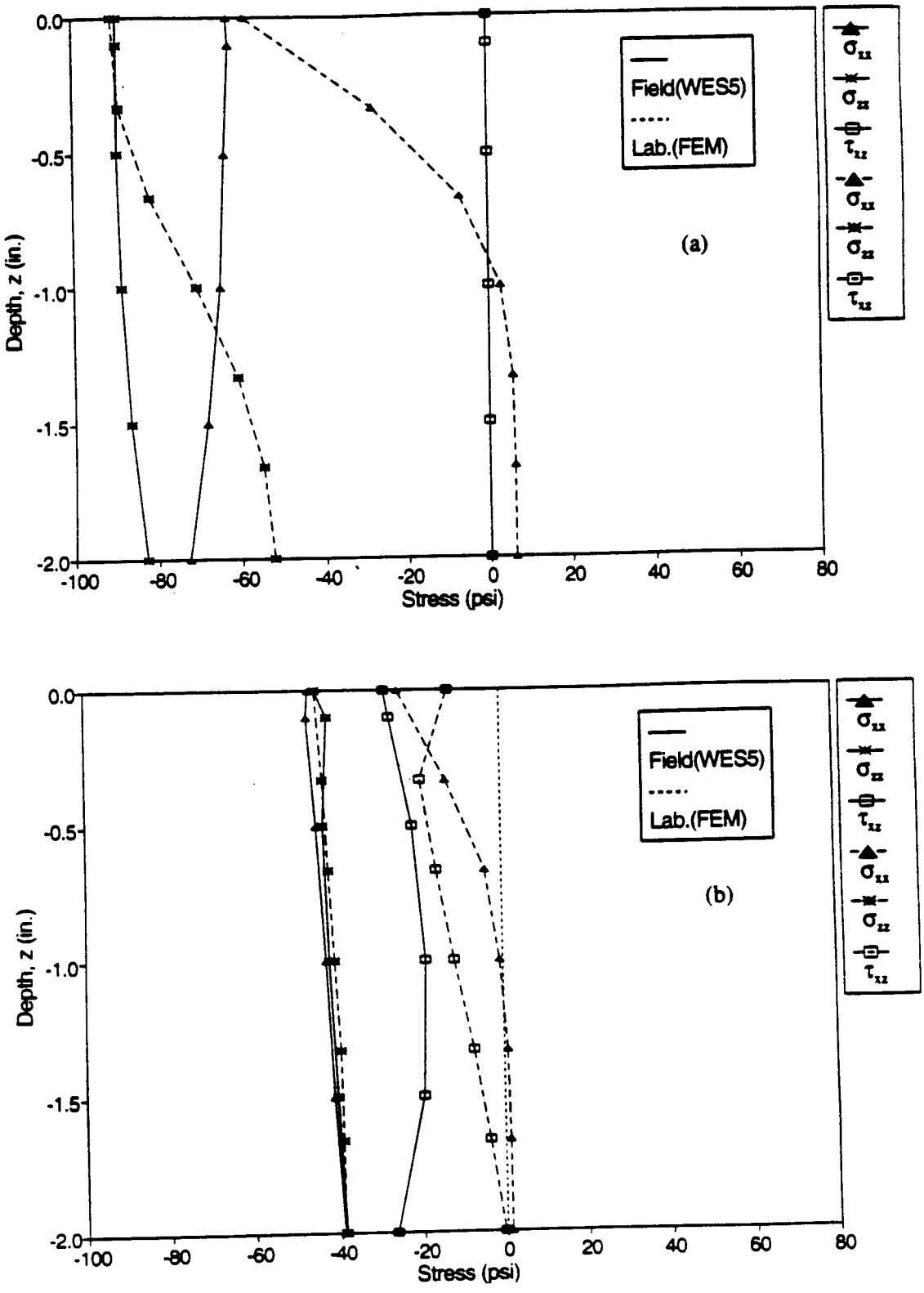

Figure 7.7 Comparison of stress distributions in pavement section shown in Figure 7.2(b) (a) at X=0, Y=0 and (b) at X=4 in. (10.26 cm), Y=0.

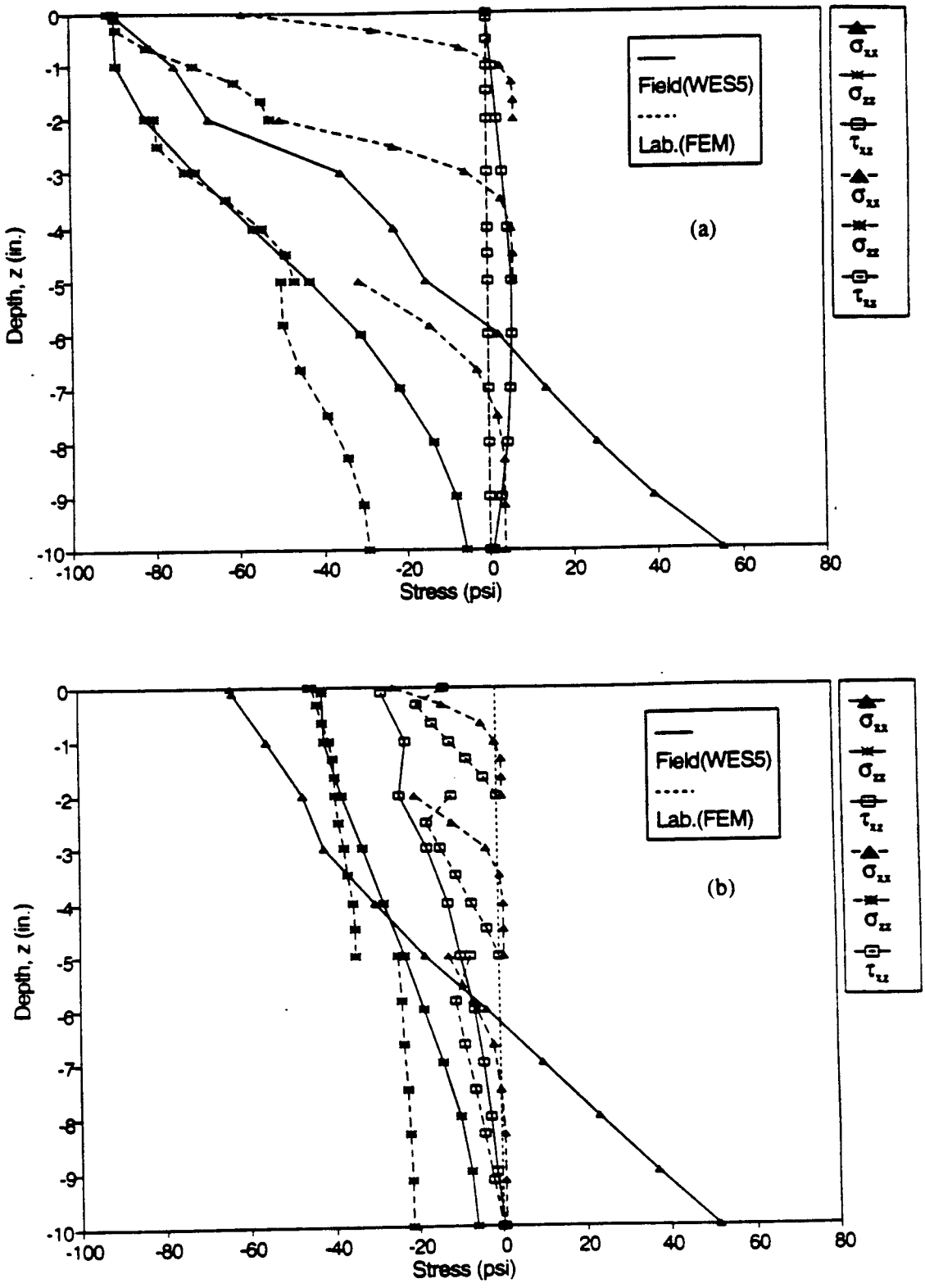

Figure 7.8 Comparison of stress distributions in pavement section shown in Figure 7.2(c) (a) at X=0, Y=0 and (b) at X=4 in. (10.26 cm), Y=0.

In addition, the testing mode can avoid the discontinuity between the loading and unloading parts of the specimen by using the ring-shaped ligament outside the 4-inch (10.16-cm) diameter cylindrical specimen. This is one of the advantages of this test method compared to the conventional triaxial test in which the lateral confining pressure is supplied by pneumatics or hydraulics. The schematic drawing of the repetitive axial loading test with confinement is presented in Figure 7.9. This testing method can be conducted using conventional uniaxial testing equipment and therefore, easily adoptable to many state highway agencies.

7.4.2 Experimental Design for Rutting Characterization

In the design of this experiment, the effects of the asphalt mixture, temperature level, and vertical loading level on the permanent deformation (rutting) of the test specimens were investigated. Table 7.4 shows the experimental design setup.

Independent (Controlled) Variables

The test was performed with three asphalt mixture types (HDS, HDB, and HB) at two temperature levels (95 and 104°F (35 and 40°C)) and three vertical stress levels (50, 80, and 90 psi (344.85, 551.76, and 620.73 KPa)).

Dependent (Response) Variables

The response variables evaluated were the permanent deformation (rutting) parameters. These parameters were used to evaluate the pavement rutting performance.

7.4.3 Test Method

The repetitive axial load was applied on top of a 6-inch (15.24-cm) diameter specimen through a 4-inch (10.16-cm) diameter upper loading plate, causing a confining lateral pressure from the ring-shape ligament outside of the 4-inch (10.16-cm) diameter specimen. The diameter of the bottom plate was kept 6 inches (15.24-cm) so as not to introduce any extraneous deformation due to the weight of the unsupported portion of the specimen. Test data of each channel were collected at the speed of 400 readings per second (0.0025 second

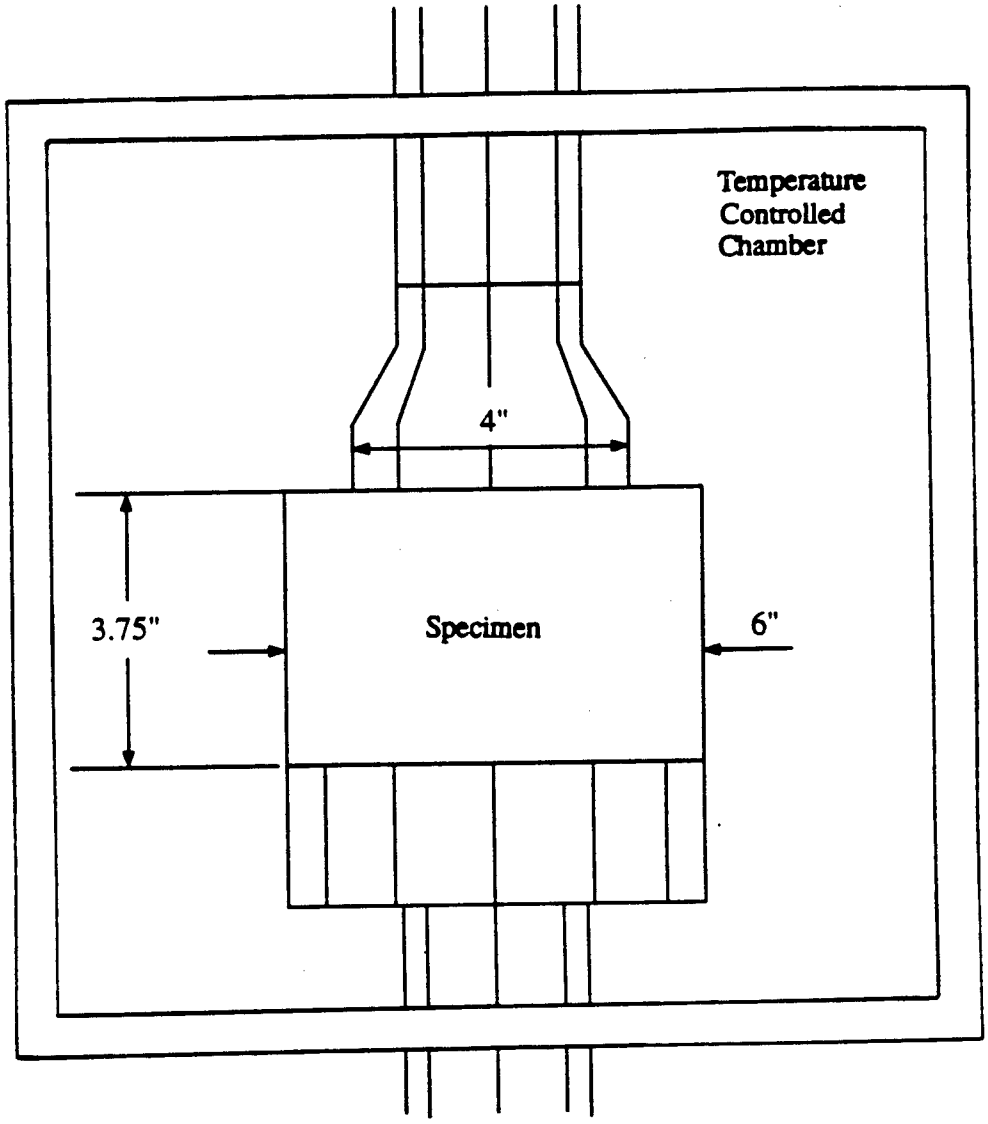

Figure 7.9 Schematic drawing of the repetitive axial loading test with confinement.

per reading). Vertical load and corresponding cumulative permanent vertical deformation were measured. The repetitive axial loading test with confinement was conducted as follows:

(1) Several test specimens and the test fixture were placed in the temperature controlled chamber until they reached a specified test temperature.

(2) The top and bottom plates were lubricated with silicon grease to reduce any eccentric loading.

(3) The specimen was centered on the bottom loading plate. Necessary adjustments to the electronic measuring system were carried out.

(4) Before the actual loading, the specimen was preconditioned with seating loads. Ten repetitions of haversine loading with 0.05-second loading time, 0.25-second rest period, and 10 psi (68.97 KPa) amplitude was applied and followed by a five-minute rest period.

(5) Haversine loading with 0.05 second of loading time and 0.25 second of rest period was repeated until the specimen failed. The failure criteria used in this study are described in the next subsection. The number of vertical loads and the corresponding vertical permanent deformations were measured using a data acquisition system at 10th, 100th, 1,000th, 10,000th, 30,000th, and 100,000th cycles.

(6) Permanent deformation versus the number of load cycles was plotted on a log-log scale.

(7) A straight line representing the best-fit through the points was constructed, and the corresponding regression equation was reported.

7.4.4 Failure Criteria

Test results of the HDS mixture under the testing conditions of 90 psi and 104°F (40°C) display that the vertical deformation increases in three stages: initial, secondary, and tertiary (see Figure 7.10). When the tertiary stage data were plotted with the initial and secondary stage data on a log-log scale, they deviated from the best fit straight line ,increasingly, as the number of repetitions increased. Since some hairline cracks were observed on the side of the specimens at the beginning of the tertiary stage, it was concluded

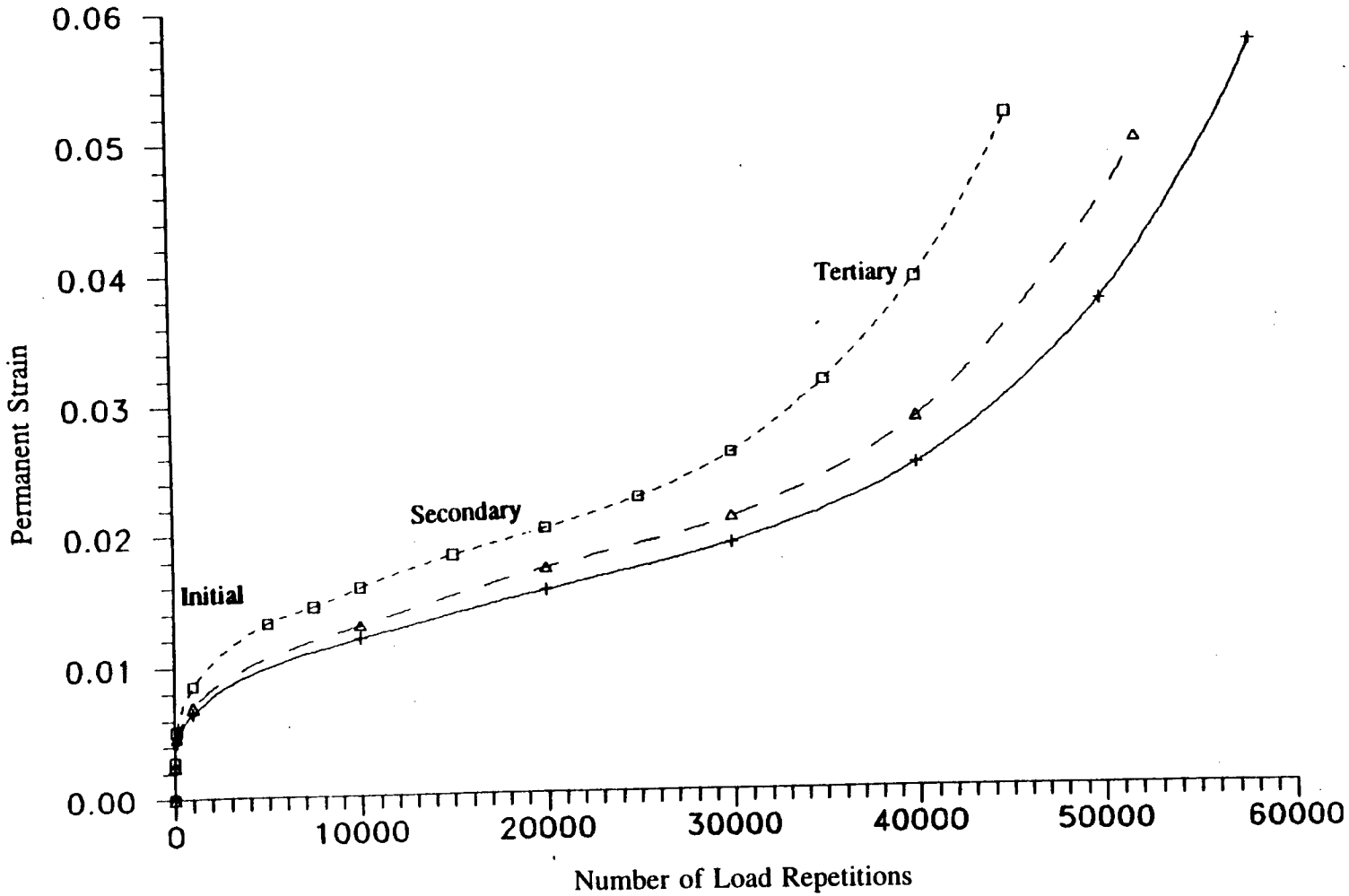

Figure 7.10 Vertical permanent deformation versus number of load repetitions with HDS mixture.

that the main reason for the tertiary stage was due to shear failure around the top loading plate.

A wide range of test results from different mixtures have been studied, and 0.02 inch/inch of vertical strain was selected as the general transition point to denote a change from the secondary to the tertiary stages. Hence the permanent deformation failure was defined in this study as the moment the permanent strain reaches 0.02 inch/inch.

7.4.5 Permanent Deformation Test Results

The permanent strain during the repeated uniaxial loading is plotted against the number of repetitions on a log-log scale. The complete test results with three mixtures (HDS, HDB, and HB) at different testing temperatures are presented in Figures 7.11 based on the experimental design in Table 7.4.

As expected, the permanent deformation from the top two inches of the asphalt layer, subjected to harsher testing conditions (higher temperature and higher vertical stress level), showed more permanent deformation. The permanent deformation of the asphalt concrete layer deeper than 2 inches (5.08 cm) was almost negligible compared to that of the top two inches of the asphalt layer. The regression coefficients of the test results are summarized in Table 7.5.

7.5 Proposed Prediction Model

A mechanistic and analytical rutting performance prediction model was decided based on the laboratory characterization of materials. The approach employed in this study is a laboratory-based approach, which utilizes laboratory characterization of the materials under simulated field conditions such as loading forms, loading levels, loading times, and the testing temperatures. As a mechanistic and analytical approach, a layer-strain theory was used to predict the permanent deformation of the asphalt concrete layer.

Based on the layer-strain theory, the asphalt concrete layer is divided into three sublayers to estimate the amount of permanent deformation that would occur after a given number of wheel load applications. Then, with the vertical stress used for the laboratory

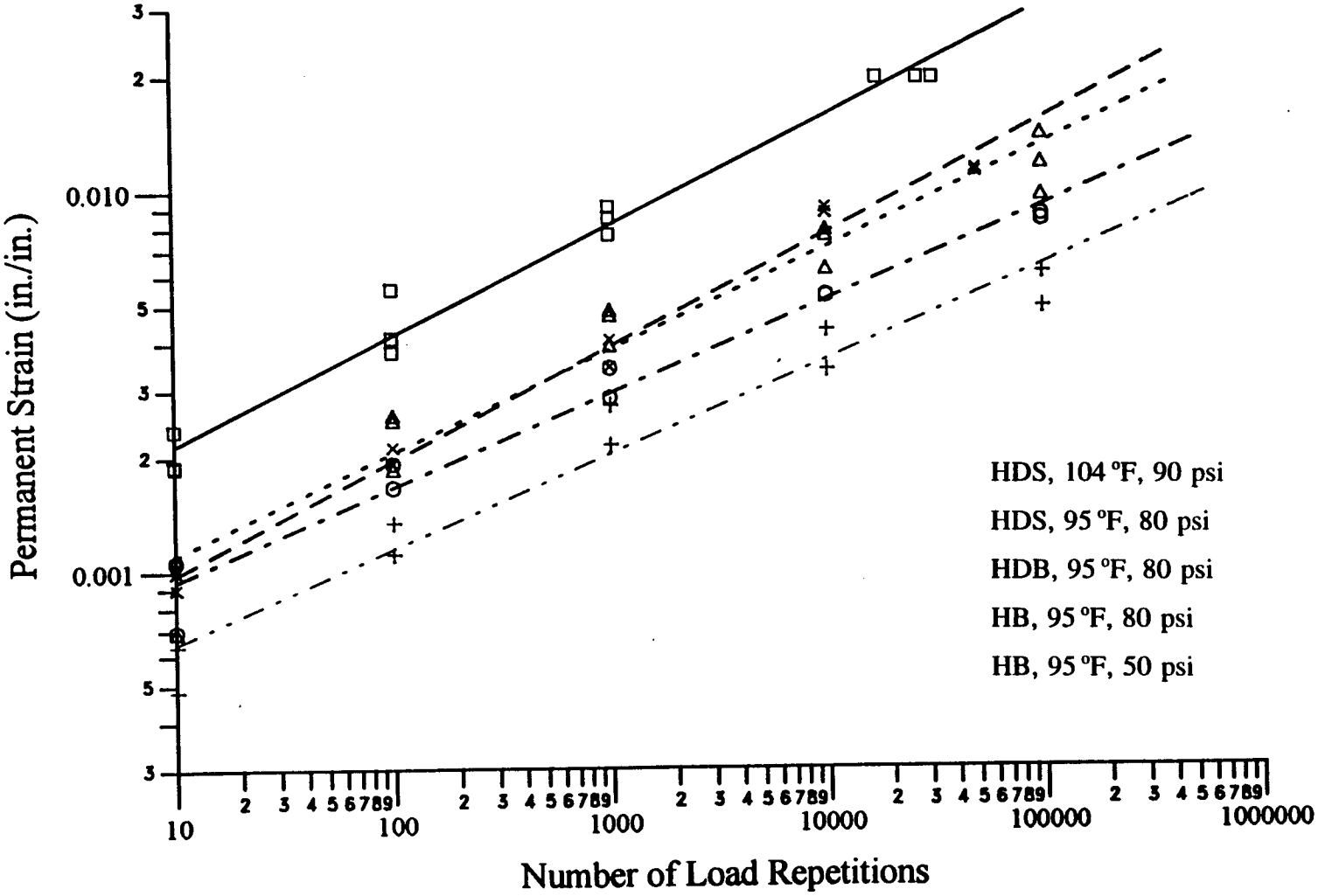

Figure 7.11 Permanent deformation (rutting) test results.

Table 7.5 Regression coefficients from rutting tests.

Mix Type	Testing Temperature (°F)	Vertical Stress (psi)	Regression Constant A	Regression Constant B
HDS	104	90	0.00110	0.2897
HDS	95	80	0.00049	0.2999
HDB	95	80	0.00059	0.2708
HDB	95	50	0.00038	0.2636
HB	95	80	0.00053	0.2471
HB	95	50	0.00036	0.2492

characterization of each sublayer, the corresponding axial plastic strain is evaluated from the results of each laboratory characterization. As a result, the total rut depth for a given number of load repetitions is obtained by summing the products of the average plastic strain occurring from each sublayer and the corresponding sublayer thickness.

The proposed rutting performance prediction model for the asphalt concrete layer is as follows:

$$RD = \sum_{i=1}^{n} (A_i)(a_i N^{b_i})(h_i) \qquad (7.2)$$

where
- RD = total cumulative rut-depth,
- A_i = calibration factor for i-th layer,
- a_i, b_i = experimentally determined regression constants from i-th layer,
- h_i = i-th layer thickness,
- N = number of load repetitions, and
- n = total number of layers.

CHAPTER 8

FLEXIBLE PAVEMENT ANALYSIS AND DESIGN - THEORY AND APPLICATION

8.1 Design Philosophy

The basic consideration for the development of a design method was that the design procedure should be mechanistic. By mechanistic, we mean an analytical-empirical method involving the calculation of pavement response linked to pavement performance. The analysis most often used is based on the application of the theory of elasticity to a system of layers, each with different elastic constants. To this end, researchers have been initiating projects dealing with development of mechanistic design and performance models, which are based on combinations of analysis of a layered system and various distress modes and mechanisms. The mechanistic design system therefore, considers the effect of individual distress in the performance of the pavement. Figure 8.1 shows a typical detailed block diagram for conducting a mechanistic study. The main feature of any mechanistic-based procedure is a multi-layer analysis program that performs an analysis, based on a given pattern of loading on a pavement whose material properties are known, to yield pavement responses. Performance models use these response parameters to predict the evolution of distresses and therefore the time to failure of these pavements. To understand the necessary subgroups in a mechanistic design procedure, a detailed explanation of the primary subgroups or modules integral to any form of mechanistic analysis is presented below:

8.1.1 Material Characterization

Material characterization consists of determining the layer moduli and Poissons ratio of the various constituent layers of the pavement. Details of various aspects of material characterization are provided in Chapter 5.

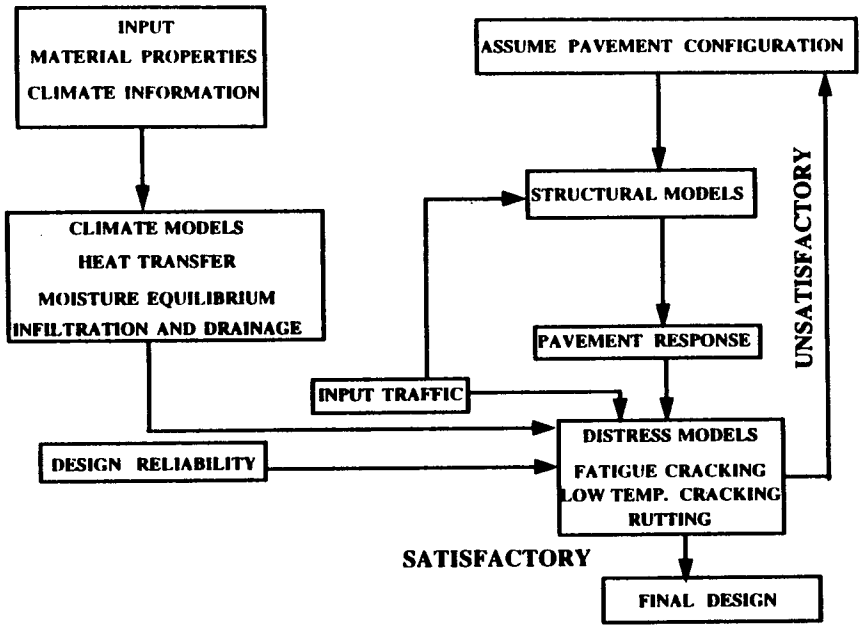

Figure 8.1 Flowchart for a generic mechanistic design procedure for flexible pavements (Huang, 1993).

8.1.2 Structural Analysis

Various structural Analysis modules are currently available for analyzing pavement systems. In 1944, Burmister presented a method for determining stresses and displacements in a 2-layer system. Since then several computer programs have been developed that calculate pavement responses (stresses, strains and deflections) of various layered systems. Although essentially most programs adopt a linear elastic analysis, programs that use visco-elastic analysis are also available. Programs like the VESYS makes use of an approximated or simplified visco-elastic approach. Programs that consider non-linearity in the layer materials are also now available. Finite-element programs that include non-linear materials, inertial effects, discontinuities etc., also exist. Of these linear elastic models is the most popular option. Research by Huang (1993) has clearly demonstrated some problems associated with the use of a finite-element method.

The elastic layer program takes in, as input, the material properties and the nature of loading. The primary purpose in using a multi-layer elastic program is to obtain critical strains and stresses that can be correlated with the onset of failure in the pavement system. It is a common practice to consider the strain at the bottom of the AC layer to be critical in causing fatigue cracking. Permanent deformation or rutting is usually controlled using the stress or strain on the subgrade. Details regarding the use of one such program (WES5 - Multi-layer Elastic Analysis) is included in Chapter 4.

8.1.3 Performance Prediction

Pavement performance models are relationships that yield quantitative descriptors of time-dependent trends in the structural condition of the pavement, usually as a function of the number of 18-Kip (80 KN) equivalent single axle load applications. The relationships are determined by testing material specimens in the laboratory under realistic temperature and loading conditions. The two primary distresses in pavement systems are namely;

1. Fatigue Cracking, and
2. Permanent Deformation

A detailed look at the determination of these two common modes of distresses for

flexible pavements is included.

(a) Fatigue Failure

A model based on dissipated energy concepts has been used for modeling fatigue cracking in asphalt. The details for this model can be found in Chapter 6 .

(b) Permanent Deformation (Rutting)

A detailed review of various rutting models available is provided in Chapter 5 of this report. Details regarding the asphalt concrete rutting model developed at NCSU is also provided in Chapter 7. This model utilizes the layer strain approach to determine rutting in ac layers.

8.1.4 Traffic Analysis

An estimate of the traffic in terms of 18-Kip (80 KN) Equivalent Single Axle Load (ESAL) is needed in the fatigue models. Mixed traffic is converted to 18-Kip (80 KN) ESAL to maintain uniformity over different methods and to allow determination of loading conditions for laboratory specimens.

In this study it was noticed that distress measurements made for the North Bound Lane and South Bound Lane showed significant variation, indicating the existence of other variables than just ESALs in determining pavement performance. In order to be able to use data from both the North Bound and the South Bound lanes, a correction factor was applied to the ESAL count. A detailed study on the field data revealed that the performance of flexible pavements is affected by both the traffic loading and the changing environment(age factor).Thus, a composite indicator was developed in this study which utilizes both the traffic and the age information with appropriate weighting factors. This indicator, so-called corrected number of 18-kip (80 KN) ESAL applications, is calculated from the following:

$$CN = 0.4TM + 0.6N \quad (8.1)$$

where

CN = corrected number of 18-kip (80 KN) ESAL applications,

TM = elapsed time in minutes, and

N = number of 18-kip (80 KN) ESAL applications.

The weighting factors of 0.4 and 0.6 were determined on the basis that the performance curves in SBL and NBL should superpose one another if corrected weighting factors were used. Details regarding this can be found elsewhere (Kim, N., 1994).

8.1.5 Calibration

The process of calibration is performed to relate lab determined pavement lives to those observed in the field. All mechanistic models, utilize some form of analytical-empirical prediction models. These models need to be calibrated. By "calibration," we mean a "shift" factor that needs to be incorporated into the prediction model. This is inevitable, considering the large number of uncertainties that exist in the design process. These uncertainties, develop from three separate problems, namely;

(a) Variation due to traffic or design factors:
Variance occurring from sampling errors in estimating traffic factors.

(b) Variation due to inadequacy of design approach:
This could arise due to certain simplifying assumptions used in the design process, or due to omission of certain design factors.

(c) Variation due to climactic factors:
Inability to accurately model climactic changes and their effects on design variables could cause increased uncertainties.

Despite our improved efforts to model this variability, a certain amount of inherent variation will continue to exist. These make the use of a calibration factor imperative and unavoidable. It should be also noted that calibration factors are dependent upon the prediction model, testing method, and the laboratory loading history. For example, the longer the rest

period, the greater is the fatigue life. This would result in smaller calibration factors for fatigue cracking than those suggested in this study. Therefore, any proposed calibration factors on fatigue cracking and rutting of asphalt concrete layers suggested are limited to the performance prediction models, testing methods, and the laboratory loading histories used in a given study.

Fatigue Model Calibration

The fatigue model needs to be calibrated based on observed fatigue cracking results. The calibration factor is in essence a multiplication factor. Based on Miners hypothesis, the pavement is determined to have failed when the Damage index equals a factor of 1.0. This stage can be defined in terms of various levels of fatigue cracking (such as 10%, 15% etc.) based on the definition of "failure" or "time for overlay", as stipulated by the particular transportation agency. The time to failure thus obtained by the laboratory model needs to be adjusted based on specific failure levels observed by the transportation agency. Equation 8.2 given below clearly indicates the role of the calibration factor.

$$N_{f(meas)} = CF \quad X \quad N_{f(pred)} \qquad (8.2)$$

where

$N_{f\,(meas)}$ = number of cycles to failure as measured in the field

$N_{f\,(pred)}$ = number of cycles to failure as predicted in the lab

CF = calibration factor

Rutting Model Calibration

The calibration process for rutting is fairly simple. Based on rutting observed in the laboratory and those actually observed in the fields, multiplication factors need to be introduced to calibrate the laboratory models to yield realistic rutting estimates.

8.1.6 Pavement Life

Pavement life can be evaluated based on either Fatigue Cracking criteria or the Rutting criteria. Evaluation based on both of these conditions are detailed below.

Fatigue Life Evaluation

The evaluation phase consists of fatigue life estimation, that is, estimation of the cumulative damage induced in the trial pavement, by the loading anticipated during the design life. A structurally efficient pavement is one for which the cumulative damage during the fatigue life is estimated to be exactly one. If d_{ij} is the damage induced by one application of the ith load to the pavement in the jth physical state, and if that load is repetitively applied to the pavement in that state, then d_{ij} can be estimated to be as follows:

$$d_{ij} = \frac{1}{N_{ij}}$$

where N_{ij} represents the number of applications to failure. It is known that the magnitudes of traffic loads and the physical state of the pavement continuously vary for in-service pavements. Therefore, obviously, N_{ij} cannot be directly measured. It is therefore treated as an estimated or derived quantity that is usually related to the level of applied strain.

The traffic forecast yields an estimation of n_{ij}, the predicted number of applications of load I on the pavement in state j during the design life. The total cumulative predicted damage D, during the design life is then estimated as follows:

$$D = \sum_j \sum_i d_{ij} n_{ij} = \sum_j \sum_i \frac{n_{ij}}{N_{ij}}$$

The pavement is considered failed when D equals or exceeds one. The above equation represents the well-known hypothesis of linear summation of cycle ratios, also called Miner's hypothesis. It has been routinely used in the design of aircraft structures. Previous laboratory

investigations have indicated the validity of Miner's Hypothesis under randomly varied loads when the physical state is held constant. Research conducted at the University of Nottingham confirms the validity of these assumptions even when the physical state is varied.

Rutting Failure -Evaluation

Rutting in pavements has been generally attributed to the development of permanent strains in the various layers. This has been linked with measured vertical compressive strains and used to calculate rutting. In this research, having noticed that almost all rutting occurred in the AC course, a different approach was adopted. The testing configuration used for arriving at the model parameters were developed after a critical study of the various confining stresses, and temperatures developed at the various depths in the AC layer. The rutting model utilizes a database approach. Depending on the depth and nature of the AC layer, typical coefficients are chosen and rut depths computed. Coefficients have been provided only for materials tested at NCSU, although similar coefficients can be obtained for newer materials. Details regarding this method are provided in Chapter 5.

8.2 Design Software

Computer programs for the design of flexible pavement systems are not easily accessible to the design community. Many multi-layer models are presently available, that help to calculate pavement response parameters. These are useful to the research community, but for the pavement engineer, whose ultimate aim is to select final thickness, these are of little help. Non-mechanistic methods like the AASHTO design, because of their easy usability, can be programmed using a spreadsheet. However, the method is more empirical than mechanistic. Other packages released by academic and research organizations alike, that profess to help in this respect, are very few and come with their share of problems. Any program that utilizes a mechanistic approach needs to have a comprehensive methodology that goes with it. The models need to be calibrated to conditions that the engineer would encounter. It is therefore, almost an impossible task for any design agency to be able to utilize a computer program directly without conducting detailed studies into the applicability of the

various performance prediction models built into the system. Even systems that avouch to have clearly mechanistic or fundamental models, which could be universally applicable, still require a specific testing protocol. If the design agency does not possess the capability of adopting the required testing protocol, or if it chooses to obtain the parameters from a different testing setup, the whole model would have to be declared void. For example, widely varying moduli values can be obtained, based on whether the testing is performed on diametral or beam specimens. Also, failure criteria may be different for different agencies. Further, most programs do not allow a user friendly interface for the designer to try out various design options. With all this in mind, the Department of Civil Engineering at NC State University, developed a computer program that could be used by the NC Department of Transportation for the design of flexible pavement structures. Figure 8.2 shows the flowchart of the adopted procedure called NCFLEX. The performance models were calibrated for different types of section designs, based on a long term study of test pavements in North Carolina.

The program was written in Fortran (MICROSOFT VER. 5.0). To make it amenable to later changes, the code was written in a modular manner. The actual code is provided in the APPENDIX A. Essentially the program reads in data from a file, and outputs information regarding the time to failure of the pavement. Two different forms of distress were studied in this study, namely fatigue and rutting. The program outputs the fatigue and rutting predictions as a function of time. The program also allows for user specified increases in the thickness of given layer so as to arrive at a final design value that satisfies the necessary design criteria. This process is carried out in an iterative manner. The criteria checked for are minimum design years, minimum design ESALs, and maximum allowable rutting. The program is stopped on reaching any of the above design criteria. The program is available in two versions - a DOS version and a microsoft WINDOWS version. Detailed explanations regarding the actual use of the program can be found in the NCFLEX design manual (Satish, S., 1996). A chart for the various important computational modules present in the program are shown in Figure 8.3. Complete details regarding the program, its features etc., can be obtained from the NCFLEX design manual (Satish, S., 1996). Only the important features of

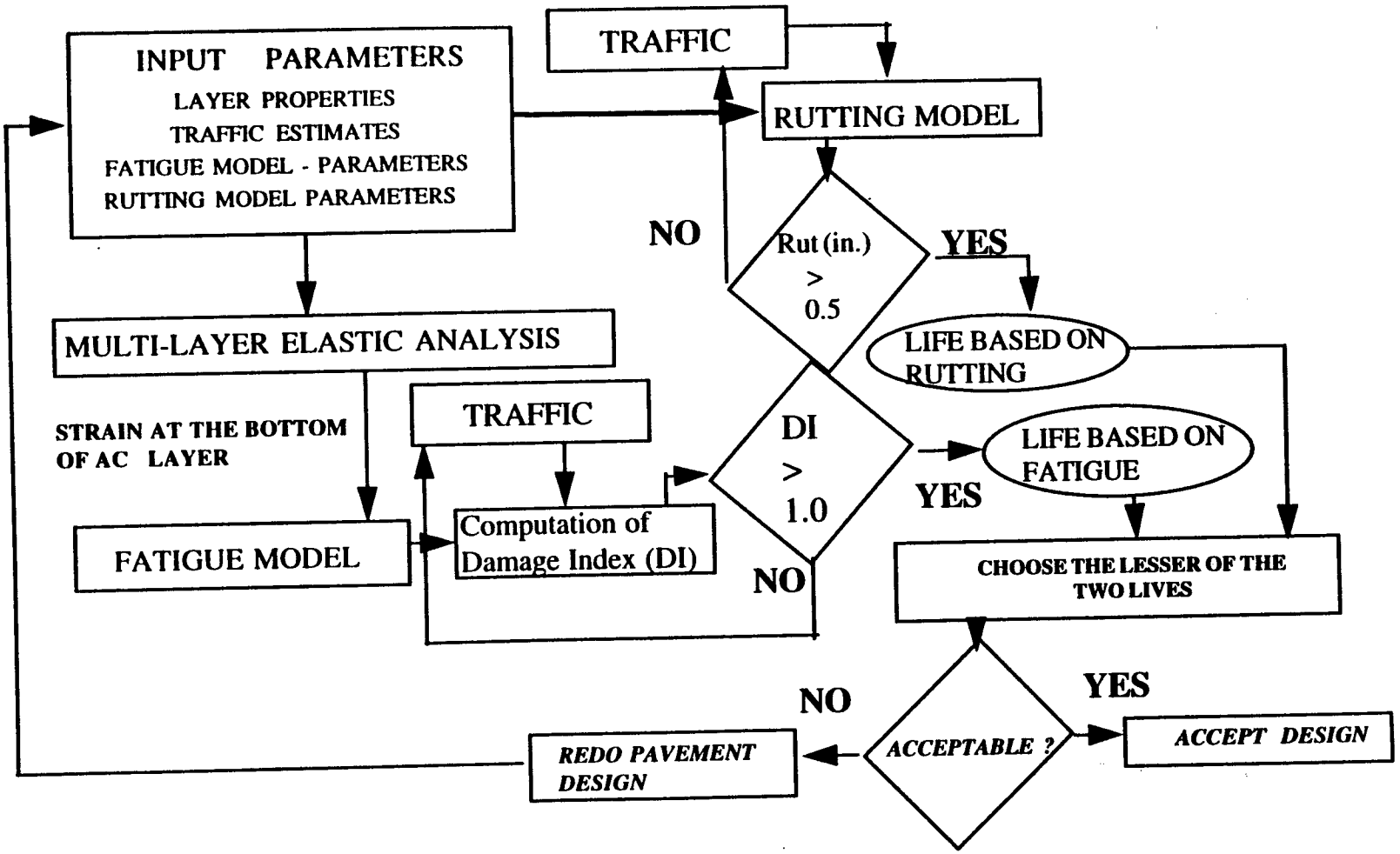

Figure 8.2 Flowchart for the mechanistic design procedure (NCFLEX.) adopted at NCSU.

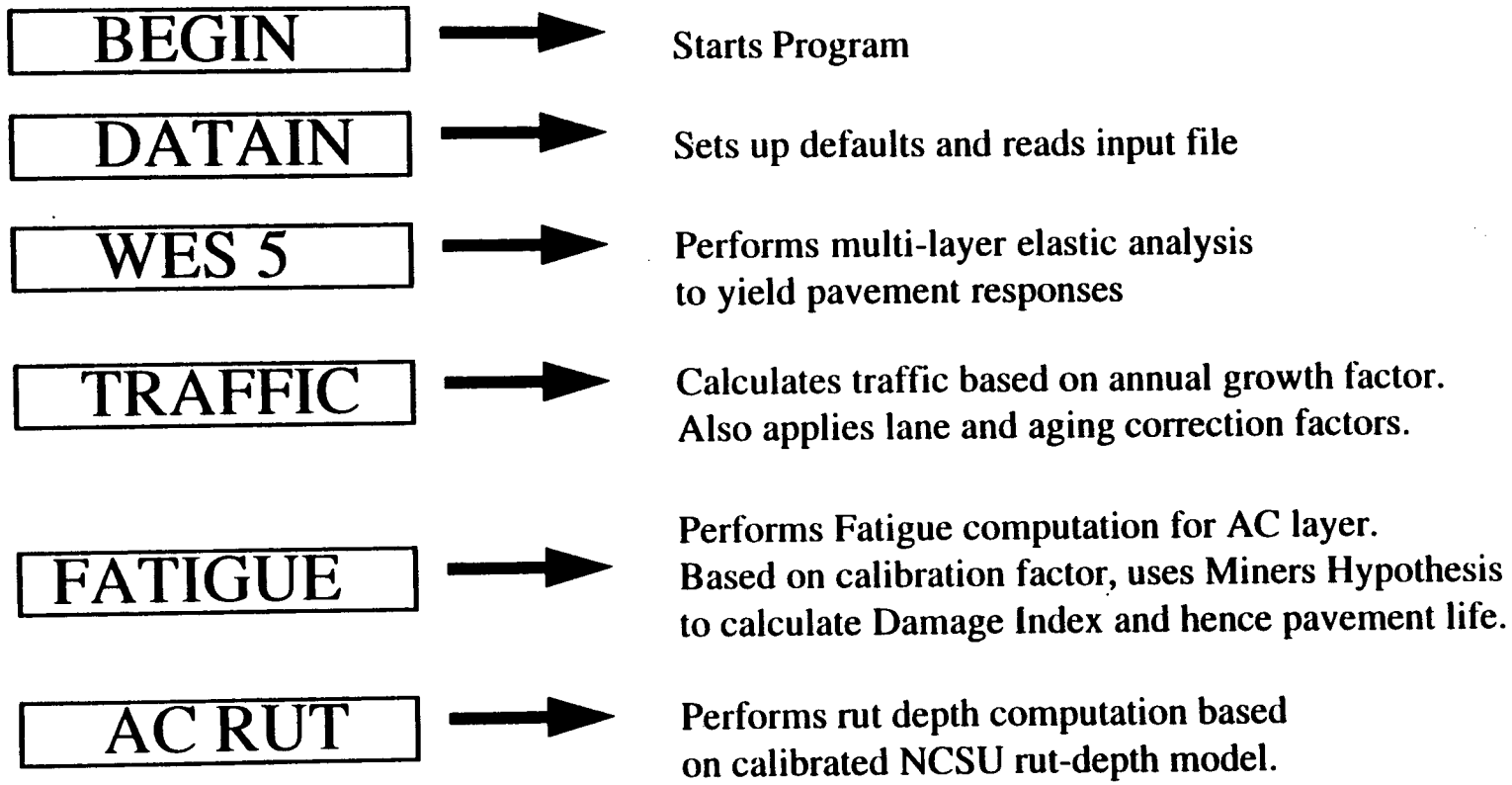

Figure 8.3 Flow diagram for the NCFLEX pavement analysis and design software.

these modules used in the program are discussed below. The names of the modules are descriptive of the nature of task performed.

(1) BEGIN

Allows the user to start the program. The names for input and output files are handled in this routine.

(2) DATAIN

Opens the required data file, and reads in input parameters, like layer moduli, layer Poisson ratios, layer thicknesses, estimated traffic, growth factor for traffic etc. A clear description, of all the variables involved are explained in the Software Users Manual. The layer moduli used in this study are included in Table 8.1.

(3) WES 5

Calculates the pavement response parameters at various locations. Strains calculated at the bottom of the AC layer are used in the fatigue model. This module is adopted from the WES5 analysis package.

(4) TRAFIC

Initial traffic estimates are used along with the growth factor to estimate increased traffic counts for every following year. For fatigue life computation, a corrected ESAL count is used rather than the input traffic estimate. This correction is applied to deal with lane distribution of traffic and pavement aging.

(5) FATIG

Fatigue cracking was considered as one of the important distress mechanisms observed in this project. Two laboratory fatigue models were developed in this research study. These Models are detailed in Chapter 5. These models were used to predict the number

Table 8.1 Layer moduli used in the calibration studies.

Layer Type	Spring	Summer	Fall	Winter
HDS	1.05×10^6	0.67×10^6	0.60×10^6	0.35×10^6
HDB	1.30×10^6	0.85×10^6	0.80×10^6	0.50×10^6
HB	1.20×10^6	0.75×10^6	0.70×10^6	0.40×10^6
ABC	30,400	30,400	30,400	30,400
CTB	995,200	995,200	995,200	995,200
CSSB	207,600	207,600	207,600	207,600
LSSB	61,000	61,000	61,000	61,000
Subgrade	14,200	14,200	14,200	14,200

Note: HDS = Asphalt surface course
HDB = Asphalt binder course
HB = Asphalt-stabilized base ciurse
ABC = Aggregate base course
CTB = Cement-treated base course
CSSB = Cement-stabilized subbase
LSSB = Lime-stabilized subbase

of cycles to reach fatigue failure. Fatigue computation was made over 4 seasonal periods in each year. The details regarding calculation of the damage index, as used by NCFLEX is provided in the following page.

Determination of Damage Index using Miner's Hypothesis.

1. In the procedure developed, the year was divided into 4 seasons. Traffic estimates were made for each season.

2. Knowing the material properties for different seasons and the various structural thicknesses, an estimate of strain (at the bottom of the AC layer) for each of the 4 seasons was made.

3. Using Miner's hypothesis, the damage for each season was obtained.

$$d_{xy} = \frac{n_{xy}}{N_{xy}}$$

where

d_{xy} = damage for season x and year y

x = season Number , 1 to 4

y = year Number , typically 1 to 35

N_{ij} = number of applications to failure (as determined in the lab)

n_{ij} = estimated traffic (Number of 18-kip (80 KN) ESALs)

The Cumulative damage is given by

$$D = d_{11}+d_{12}+d_{13}+d_{14}+d_{21}+d_{22}+...$$

or expressed mathematically;

$$D = \sum_y \sum_x \frac{n_{xy}}{N_{xv}}$$

where D = damage index

and x, y, N_{ij}, n_{ij} continue to be defined as shown above.

Failure Criteria for Fatigue Cracking

As explained earlier, the pavement was considered to have failed when the Damage index equaled or exceeded 1. This is in line with the basic concept of the Miner's Hypothesis.

Calibration for Fatigue Cracking Model

The computer program NCFLEX was subject to multiple-runs using material parameters that mimic field conditions. For each run a different calibration factor was used. For each of these runs, the predicted life of the pavement was compared with the actually observed life. The Calibration factor adopted was one for which the predicted fatigue life equaled the observed life.

The Calibration factors obtained for various test sections using the following fatigue performance model is shown in Table 8.2 As can be seen from the Table 8.2, a clear trend is visible, that distinguishes calibration factors for ABC sections and those obtained for full depth AC sections. As a significant spread is noticed, even within a particular design category, an ANOVA analysis was carried out to determine the relevant factors that affect the Calibration factor. Table 8.3 shows a statistical analysis performed on the calibration factors.. A satisfactory model (R square = 0.94) was obtained for the following predictive equation.

C F = 223.495 - 24.81 Lime1 + 5.344 RTACBS + 104.932 SECTYPE
- 6.467 THICBS - 40.878 THICAC

where

C F = calibration factor

Table 8.2 Calibration factors obtained for the fatigue model using data available from US 421 test sections.

Section No.	Layer 1 Thickness (inches)	Layer 2 Thickness (inches)	Layer 3 Thickness (inches)	Layer 4 Thickness (inches)	Fatigue Calibration Factor
1	2	1.5	12		150
23	2	1.5	12		100
2	2	12	7		200
24	2	12	7		200
3	3.25	3	8		30
16	2	3	8		75
5	2	1.5	8	7	100
17	2	1.5	8	7	200
7	2	1.5	5.5		28
20	2	1.5	5.5		36
9	2	3	4		20
22	2	3	4		27
11	2	5.5	7		4
14	2	5.5	7		5
12	2	1.5	4	7	18
13	2	1.5	4	7	13

Table 8.3 Statistical analysis of individual calibration factors for the NCFLEX fatigue model

DEP VAR: CALIBRATION FACTOR N: 16
MULIPLE R: .923 SQUARED MULTIPLE R: 0.949
ADJUSTED SQUARED MULTIPLE R: .923 STANDARD ERROR OF ESTIMATE: 20.462

VARIABLE	COEFFICIENT	STD ERROR	STD COEF	TOLERENCE	T	P (2 TAIL)
CONSTANT	223.495	45.075	0.000		4.958	0.001
LIME1	-24.481	8.624	-0226	0.8042985	-2.839	0.018
RTACBS	5.344	11.939	0.134	0.0568559	0.448	0.664
SECTYPE	104.932	21.800	1.467	0.0550630	4.813	0.001
THICBS	-6.467	6.343	-0.411	0.0315347	-1.019	0.332
THICKAC	-40.878	11.138		0.1345283	-3.670	0.004

ANALYSIS OF VARIANCE

SOURCE	SUM-OF-SQUARES	DF	MEAN-SQUARE	F-RATIO	P
REGRESSION	77678.841	5	15535.768	37.106	0.000
RESIDUAL	4186.909	10	418.691		

CALIBRATION FACTOR = 223.495 - 24.481 LIME 1 + 5.344 RTACBS + 104.932 SECTYPE -6.467 THICBS -40.878 THICKAC

Lime 1 = 1 for lime treated subbases and 0 for cement treated subbases

RTACBS = ratio of asphalt concrete surface thickness to base course thickness

SECTYPE = 1 for aggregate base course and 0 for Full depth

THICBS = thickness of base course

THICAC = thickness of AC course

Such a regression equation is a useful tool in deciding the calibration factors for pavements different (different in structural thicknesses) from those used in the test study. In the program the user is given the added flexibility of changing the calibration factor for fatigue. Early failure of CTB sections, made it difficult to calibrate the models for CTB sections. It is advisable that the user use an external calibration option in this case. This regression was found to be most accurate for sections structurally similar to those used in the study. Large variations in structural thicknesses from those used in this study could make this equation untenable. In such cases, based on other studies (Shook et al., 1982) fixed values of 100 for aggregate base course and 20 for full depth sections are suggested.

(6) ACRUT

The permanent deformation module used is not completely mechanistic in the traditional sense of the term. It utilizes results obtained from laboratory testing and traffic estimates to provide an estimation of ac rutting.

Calibration for Permanent Deformation Model

As rutting was primarily noticed in the AC layers, an alternative model, was used that applies a calibration factor to measured rutting. A single calibration factor of 1.5 applied to the rutting computed for the top 2 inches (5.08 cm), was decided upon, for all the sections included in this study. For the remaining depths a factor of 1 was used. The rutting equation along with the calibration factor is shown below. Detailed description of the model used, and the computation involved is provided in chapter 5 (Section 5.2.2.1). The proposed rutting performance prediction model for the asphalt concrete layer is given below:

$$RD = \sum_{i=1}^{n} (A_i)(a_i N^{b_i})(h_i)$$

where

RD = total cumulative rut-depth

A_i = calibration factor for i-th layer

($A_1 = 1.5$, $A_{2..} = 1.0$)

a_i, b_i = experimentally determined regression constants from i-th layer

h_i = i-th layer thickness

N = number of load repetitions, and

n = total number of layers

Failure Criteria for Permanent Deformation

The pavement is expected to have failed due to rutting when the rutting reaches a level of 0.5 inches (1.27 cm). In the test pavements used for calibrating the model, such high levels of rutting was not noticed and the pavements had to be overlaid prior to rutting failure, due to high levels of fatigue cracking.

(7) STOP

Allows the user to end the program.

8.3 Design examples

Design examples for the prediction of fatigue life and rutting are provided in the NCFLEX design manual. Sample Input and Output files are provided in Tables 8.4 (a) and 8.4 (b).

Table 8.4(a) Sample input file for NCFLEX program

```
FILENAME
**********
 SEC1
 DATE&TIME
**********
12- 3-1995 @ 13:24
LAYER# ID  NU    THICK.,IN      SLIP
*****************************************
 1      1   .35      2.00          1.
 2      2   .35      1.500         1.
 3      4   .35      12.000        1.
 4      8   .40      20.000        1.
 5      8   .40      SEMI-INFIN
LAYER MODULI IN PSI
 SEASON  TEMP    1          2          4          8         8
*************************************************************
 1   60.00  600000.00  800000.00   30400.00  14200.00  14200.00
 2   42.00 1050000.00 1300000.00   30400.00  14200.00  14200.00
 3   58.00  670000.00  850000.00   30400.00  14200.00  14200.00
 4   74.00  350000.00  500000.00   30400.00  14200.00  14200.00
 TOTAL NUMBER OF ESALS/YEAR
*****************************************
        150000
 TRAFFIC ANNUAL GROWTH FACTOR
*****************************************
          1.0
 STRAIN AT THE BOTTOM OF LAYER #
*****************************************
          2
 FATIGUE EQUATION PARAMETERS
*****************************************
 ID   TEMP   PHI(DEG)   ZHI   VOIDS(%)
 2   60.00     28.00    .40     6.00
 2   42.00     15.00    .40     6.00
 2   58.00     25.00    .40     6.00
 2   74.00     30.00    .40     6.00
 RUTTING COEFFICIENTS
 ************************************
0.0011 0.00049 0.00059 0.00038 0.00053 0.00036
0.2897 0.2999 0.2708  0.2636 0.2471 0.2492
 INCREMENT LAYERS
 ************************************
 1        0.5
 CALIBRATION FACTOR FOR FATIGUE MODEL
*****************************************
          0.0
 MIN DESIGN LIFE   MIN DESIGN ESALS    MAXIMUM ALLOWABLE RUTTING (inches)
 ***************   ****************    **********************************
      20                0.0                          .5
```

Fatigue calculated over 4 seasons

Increment any one layer at a time for arriving at thickness design

For internal calibration of fatigue use 0.0 in input.

3 Design criteria - Minimum Design Life
- Minimum Design ESALs
- Maximum Allowable rutting

Need to choose a minimum of 1 out of the three.To skip any one criteria enter 0.0

Table 8.4(b) Sample output file from NCFLEX program.

```
PROJECT TITLE
*************
SEC 1
DATE&TIME
*************
12- 3-1995 @ 13:24
LAYER#        ID       NU      THICK.,IN       SLIP
************************************************
  1           1        .35      2.000          1.
  2           2         35      1.500          1.
  3           4        .35      12.000         1.
  4           8        .40       .000          1.
  5           8        .40
--------------
LAYER MATERIAL -> ID
HDS-> 1  HDB -> 2 HB -> 3 ABC -> 4 CTB -> 5
LIME_SUBGRADE -> 6 CEMENT_SUBGRADE -> 7 SUBGRADE -> 8
-------------------------------------------------
      MODULI   MODULI   MODULI   MODULI
     SEASON 1 SEASON 2 SEASON 3 SEASON 4
LAYER:1 600000.00 1050000.00 670000.00 350000.00
LAYER:2 800000.00 1300000.00 850000.00 500000.00
LAYER:3  30400.00  30400.00  30400.00  30400.00
LAYER:4  14200.00  14200.00  14200.00  14200.00
LAYER:5  14200.00  14200.00  14200.00  14200.00
-------------------------------------------------
LAYER ID--> 1 2 4 8
 H1   H2   H3   H4  FAT.LIFE(MONTHS)  ESALS TO FAT.
-----------------------------------------------------------------------
2.00 1.50 12.00  .00          24              .60E+06
2.50 1.50 12.00  .00          36              .89E+06
3.00 1.50 12.00  .00          48              .12E+07
3.50 1.50 12.00  .00          72              .18E+07
4.00 1.50 12.00  .00          96              .24E+07
4.50 1.50 12.00  .00         138              .35E+07
5.00 1.50 12.00  .00         192              .49E+07
5.50 1.50 12.00  .00         255              .68E+07
 H1   H2   H3   H4  RUT LIFE  ESALS TO RUT  MAX. RUT
-----------------------------------------------------------------------
2.00 1.50 12.00  .00  20          .61E+07      .43
2.50 1.50 12.00  .00  20          .61E+07      .43
3.00 1.50 12.00  .00  20          .61E+07      .44
3.50 1.50 12.00  .00  20          .61E+07      .45
4.00 1.50 12.00  .00  20          .61E+07      .46
4.50 1.50 12.00  .00  20          .61E+07      .48
5.00 1.50 12.00  .00  20          .61E+07      .50
5.50 1.50 12.00  .00  18          .55E+07      .50
```

Input data

Rutting of ac layers - based on a maximum design life of 20 years or a maximum rut depth of 0.5 inches

CHAPTER 9
VARIABILITY IN FIELD MEASUREMENTS AND COMPUTATION OF RELIABILITY

Variability is an important fact of life when dealing with laboratory and field data. Also, varying assumptions in the predictive models used induce additional uncertainties. All these necessitate the need for calibration studies to correlate the various predictions with actual field observed results. Assumptions used at various junctions of the pavement design process are dealt with in the respective chapters. This chapter will look at the variability existing in field data and methods to account for these in the design process.

Spatial as well as seasonal variability exists in data obtained from field measurements. While spatial variability describes the variation of pavement material properties over distance, seasonal variability describes the variation of properties over time. Due to the sufficiently large data base assimilated during the conduct of this project, data is available to study the variation in the backcalculated stiffness measurements. This chapter is divided into two different sections dealing with - (1) the nature and extent of seasonal variability observed and, (2) a suggested approach (methodology) to handle the pavement design problem from a probabilistic standpoint.

9.1 Variability in Measurement of In-situ Material Properties

9.1.1 Literature Survey of Variability in Design Inputs

In recent years, Long Term Pavement Performance (LTTP) sites have been set up to precisely monitor the performance of various test sites, and to draw statistical conclusions by reducing large amounts of similar information. One such study was conducted in Kentucky to evaluate the long term pavement performance of several pavement sections. The test was conducted by the Kentucky Transportation Center along with the state Department of Transportation (Allen et al.,1994). A total of 20 sites were monitored, throughout the state, seven of which were included in the LTTP program commissioned by the Strategic Highway

Research Program. Although the express concern of this study was to monitor performance, testing on these sites yielded valuable information regarding variability. This study found a high degree of variability in subgrade modulus within each test site with coefficients of variability as high as 75 percent. The study also found a large amount of variability in backcalculated moduli (testing done using a Road Rater) within a 500 foot test section.

Isada (Isada, 1966) conducted a series of deflection tests monitoring two pavement sections over a period of two years, during which he noticed a seasonal variation of about 70% in the maximum deflection under an impulsive loading.

9.2 Observed Variability in Data Obtained from US421 Test Sections

The following sections deal with the seasonal variation observed during the different testing cycles. Observed variation in temperature and stiffness during the different testing periods are provided, along with a statistical analysis of the variation.

9.2.1 Analysis of Temperature Variation During Different Testing Periods

Table 9.1 shows a statistical analysis of temperature data obtained during the different testing periods. Figure 9.1 shows a graphical representation of temperature variation.

9.2.2 Analysis of Seasonal Variability in Backcalculated Moduli

Varying environmental conditions, coupled with the shortcomings in the techniques of backcalculation of moduli, cause considerable variability in the computed values of in-situ stiffness of the different layers in the pavement structure. Different back-calculation programs yield varying modulus values, depending on the nature of the algorithms used. Molenaar (Molenaar, 1994) states that backcalculation of layer moduli can still be regarded as some kind of an art. A single backcalculation procedure could produce different moduli values depending on the seed moduli input by the user. Also, stiffness values are dependent on temperature and moisture conditions. Table 9.2 (a)-(c), shows the variation of backcalculated moduli for aggregate base course, cement treated base corse, and full-depth ac sections measured during different seasons (varying temperature, and moisture conditions). Assuming the integrity of the backcalculated moduli values, a statistical analysis can be performed to

Table 9.1 Surface and air temperature measurements.

SEC #	DEC90 AIR	DEC90 SURFACE	FEB91 AIR	FEB91 SURFACE	MAR91 AIR	MAR91 SURFACE	MAY91 AIR	MAY91 SURFACE	AUG91 AIR	AUG91 SURFACE	OCT91 AIR	OCT91 SURFACE	MARCH92 AIR	MARCH92 SURFACE	OCT92 AIR	OCT92 SURFACE	FEB93 AIR	FEB93 SURFACE	JUNE93 AIR	JUNE93 SURFACE
1	62	62	80	80	76	76	89	104	87	100	63	77	75	88	78	87	61	73	93	116
2	61	61	90	90	76	76	94	114	83	85	63	77	79	91	73	86	61	74	92	109
3	61	61	87	85	96	96	94	118	82	86	56	64	83	94	73	80	58	68	89	102
4	47	47	80	80	96	96	88	100	92	108	65	67	83	95	64	88	53	58	86	96
5	47	47	89	89	89	89			90	100	69	82	84	100	86	101	47	47	97	123
6	41	41	84	82	88	88	88	109	88	97	64	79	82	95	82	96				
7	41		43	43	88	88	84	92	88	97	63	74	80	84	74	76	56	67	95	115
8	45		55	55	75	75	78	83	92	116	60	88			64	65				
9	62		47	47	80	80	83	92	98	121	79	91	80	97	85	95	55	66	91	109
10	45	45	83	83	81	81	85	115	85	102	86	90	72	83	85	98	48	59	89	107
11	59		73	73	71	71	85	97	90	110	75				82	97	46	53	86	95
12	62	62	53	53	64	63			93	115	71	78	74	98	61	82	37	40	82	118
12	62	62	58	58	64	63			91	115	69	74	77	98	73	81	40	46	93	119
13	76	76	52	52	92	92	84	100	87	103	66	73	65	75	77	85	38	48	91	112
13	76	76	58	58	97	97	84	100	89	109	69	75	88	86			40	48	91	112
14	78		52	52	92	92	83	97	82	93	66	73	67	74	79	90	38	51	86	107
15	78		54	54	80	80	83	93	84	90	58	80								
16	78	78	54	54	81	81	98	85	90	116	76	77	67	75	80	92	43	57	90	101
17	67	67	54	54			90	111	95	123	78	80	65	74	72	80	38	54	89	125
18	67		54	54	72	72	92	117	94	122	79	85	62	66	60	65	33	47	89	116
19	89	89	88	88	72	72	88	102	91	122	76	84								
20	89	89	89	89	99	99	87	100	84	95	72	78	59	61	74	88	53	60	83	107
21	83	83	84	84	99	99	88	113	78	85	69	73	57	58	74	91	54	61	82	97
22	83	83	89	89	101	101	84	100	93	108	55	58	64	76	72	85	55	65	79	90
23	89	89	59	59	99	99	82	101	95	110	72	83	65	82	88	74	56	67		
24			54	54	99	99			94	109	72	83	86	80	81	84	55	64	74	84
Average	65.92	67.66667	64.73077	64.57692	83.48	83.4	86.68182	101.9545	88.88462	105.2692	68.88462	75.88	71.54545	83.09091	73.69565	82.78261	48.40909	57.77273	88.42857	107.619
Std Dev	15.25233	15.53848	14.21418	14.10721	12.36162	12.49	4.751903	9.65532	4.684893	11.63403	7.515763	8.363349	8.266731	11.93509	7.821013	11.57192	8.526211	9.219208	5.314593	10.61211
C.V.	0.231376	0.229633	0.219589	0.218456	0.148079	0.14976	0.05482	0.094702	0.052708	0.110517	0.109107	0.110218	0.115545	0.143639	0.106126	0.139787	0.176126	0.159577	0.0601	0.098608

AIR Air Temperature (F)
SURFACE Surface Temperature (F)

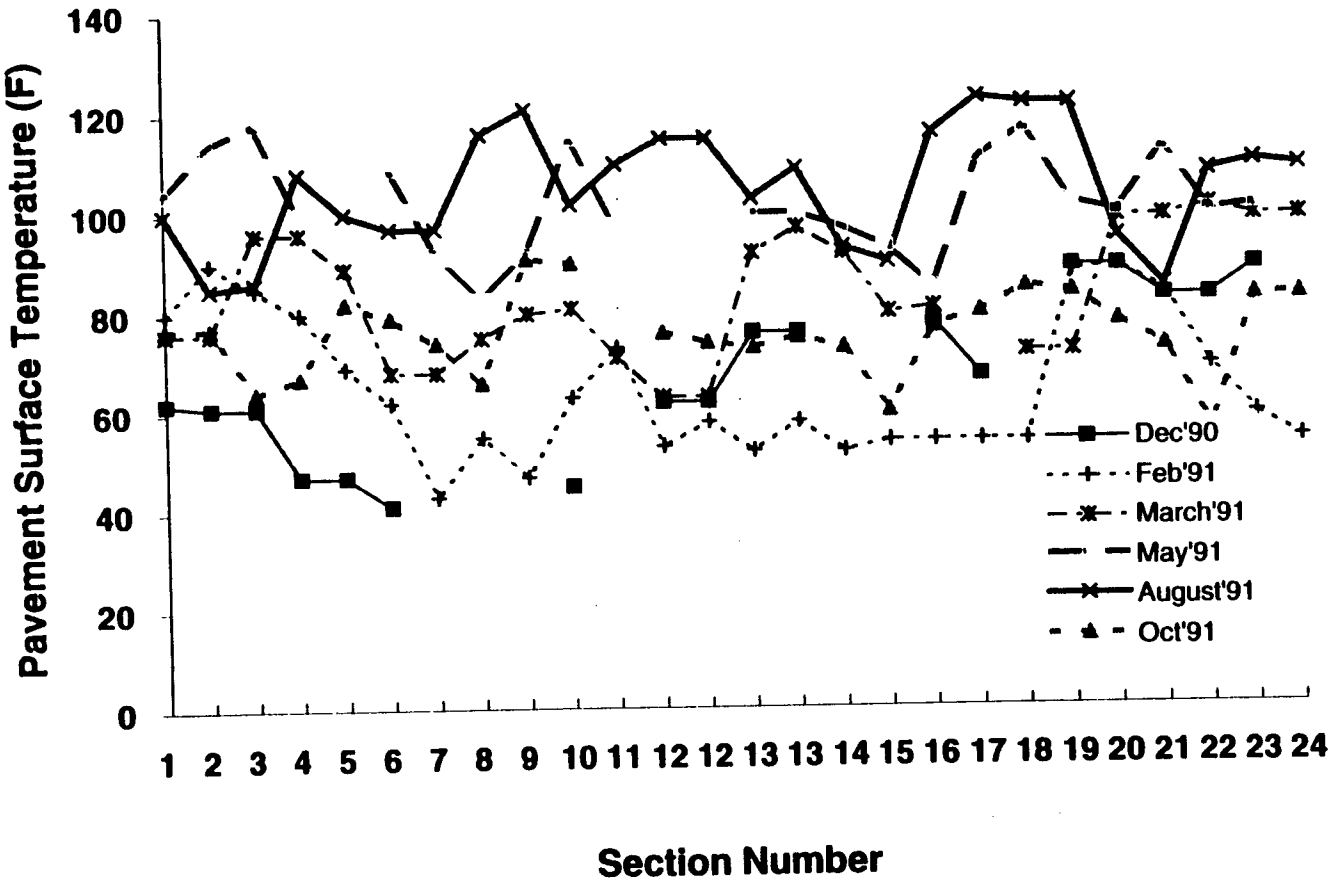

Figure 9.1 Temperature variation during different testing periods for different sections.

Table 9.2(a) Statistical parameters of backcalculated moduli for aggregate base course sections.

		Backcalculated Moduli (ksi)				Temperature (Fahrenheit)	
Section #		AC Layer	Base	Subbase	Subgrade	Air	Surface
1	Average	473.4	15.01		5.21	76.4	86.3
	Std. Dev	239.8	4.16		1.93	10.90	15.44
	C.V.	0.51	0.28		0.37	0.14	0.18
2							
	Average	502.6	47.16	188.27	18.02	77.2	86.3
	Std. Dev	242.9	7.85	65.23	6.91	12.03	15.18
	C.V.	0.48	0.17	0.35	0.38	0.16	0.18
3							
	Average	297.5	14.15		6.67	77.9	85.2
	Std. Dev	161.3	5.33		1.24	14.21	17.27
	C.V.	0.54	0.38		0.19	0.18	0.20
5							
	Average	671.22	27.94	273.11	22.45	75.55	85.11
	Std. Dev	569.82	4.92	97.39	2.19	17.66	24.99
	C.V.	0.85	0.18	0.36	0.097	0.23	0.29
16							
	Average	782.8	48.46		14.16	75.5	79.7
	Std. Dev	478.50	5.9		2.4	15.88	14.63
	C.V.	0.61	0.12		0.17	0.21	0.18
17							
	Average	625.44	33.26	103.62	18.52	72	85.33
	Std. Dev	442.07	9.63	66.01	1.59	17.42	26.11
	C.V.	0.71	0.29	0.64	0.09	0.24	0.31
23							
	Average	507.22	13.48		5.17	75.78	86.22
	Std. Dev	291.85	4.22		1.50	14.85	18.13
	C.V.	0.58	0.31		0.29	0.19	0.21
24							
	Average	635	38.71	56.25	9.65	71.88	79.63
	Std. Dev	368.36	5.34	16.54	2.41	15.76	17.37
	C.V.	0.58	0.14	0.29	0.25	0.22	0.22

Table 9.2(b) Statistical parameters of backcalculated moduli for cement treated base course sections.

		Backcalculated Moduli (ksi)				Temperature (Fahrenheit)	
Section #		AC Layer	Base	Subbase	Subgrade	Air	Surface
8	Average	754.5	281.8	103.73	17.15	66.71	76.67
	Std. Dev	427.55	73.74	38.89	4.9	14.42	19.62
	C.V.	0.57	0.26	0.37	0.28	0.22	0.26
10							
	Average	547.78	2301.6	97.03	17.35	73.9	84.1
	Std. Dev	494.12	388.13	22.21	1.27	15.6	24.43
	C.V.	0.90	0.17	0.23	0.07	0.21	0.25
15							
	Average	706	865.06	62.73	20.82	72.83	75.4
	Std. Dev	411.20	250.47	5.37	1.93	12.12	15.74
	C.V.	0.58	0.29	0.09	0.09	0.17	0.21
18							
	Average	607.89	399.26		17.45	70.2	82.7
	Std. Dev	385.18	106.11		4.37	18.18	27.16
	C.V.	0.63	0.27		0.25	0.26	0.33
19							
	Average	361	1114.2	63.48	14.82	83.67	92.83
	Std. Dev	185.44	256.35	10.33	2.12	7.09	15.73
	C.V.	0.51	0.23	0.16	0.14	0.08	0.17
21							
	Average	779.5	228.52		18.09	76.11	84.55
	Std. Dev	498.35	44.4		2.15	13.64	17.02
	C.V.	0.64	0.19		0.12	0.18	0.20

Table 9.2(c) Statistical parameters of backcalculated moduli for full depth ac sections.

		Backcalculated Moduli (ksi)				Temperature (Fahrenheit)	
Section #		AC Layer	Base	Subbase	Subgrade	Air	Surface
7	Average	528.6			7.61	69	79.56
	Std. Dev	257.21			3.48	17.33	19.45
	C.V.	0.49			0.46	0.25	0.24
9							
	Average	459.9			6.89	75.8	88.67
	Std. Dev	327.67			3.29	15.08	20.84
	C.V.	0.71			0.48	0.19	0.24
11							
	Average	391.56		55.68	12.43	74.11	74.5
	Std. Dev	234.55		42.65	3.33	13.4	33.02
	C.V.	0.6		0.77	0.27	0.18	0.44
12B							
	Average	693.22		25.02	12.4	60.33	79.33
	Std. Dev	421.62		8.26	4.17	22.42	24.23
	C.V.	0.61		0.33	0.34	0.37	0.31
12A							
	Average	897.66		19.37	14.32	67.4	76.33
	Std. Dev	561.56		7.5	3.5	16.8	26.15
	C.V.	0.63		0.39	0.24	0.25	0.34
13B							
	Average	204.88		9.45	8.24	74.67	84.56
	Std. Dev	110.73		3.47	1.70	17.05	20.95
	C.V.	0.54		0.37	0.21	0.23	0.25
13A							
	Average	638.9		14.61	11.99	72.8	81.6
	Std. Dev	373.8		5.94	3.39	16.75	19.99
	C.V.	0.59		0.41	0.28	0.23	0.24
14							
	Average	572.7		30.19	9.24	72.3	81
	Std. Dev	278.17		7.22	2.55	15.87	18.65
	C.V.	0.49		0.24	0.28	0.22	0.23

determine the variation in the different layer moduli with the different seasons. Mean, Standard Deviation and Coefficient of Variation of the moduli values (for the different test sections) are provided in Tables 9.2 (a)-(c). Information useful for selecting stiffness values based on the data (Table 9.2 (a)-(c)) can be garnered from further analysis as detailed in the following page.

Analysis of Seasonal Variation in AC Backcalculated Moduli

Any variation in the stiffness values for similar mixes is essentially based on the temperature at which the measurements were obtained. This arises from the visco-elastic nature of asphaltic materials. Backcalculation in this study was performed using MODULUS 4.0. During this analysis, the asphaltic layers were grouped into one layer, i.e. the surface and binder were treated as one layer of asphaltic concrete, in spite of the different mixes used. This is essential in backcalculation involving pavements with very thin asphalt courses. Detailed explanations for these can be found in Section 4. Hence, the ac moduli arrived at is essentially a composite ac moduli. Due to the nature of the specific backcalculation procedure used in this study, composite ac moduli for layers lesser than 4 inches (10.54 cm) in depth were selected based on a temperature-moduli relationship present in the MODULUS 4.0 program. Any variation in backcalculated moduli obtained in such a case was solely because of temperature differences. This also ruled out computation of variability in backcalculated ac moduli within a test section as the variability obtained in FWD deflection measurements were not reflected in the ac moduli backcalculated. For sections with ac courses deeper than 4 inches (10.54 cm), although ac moduli were backcalculated using more rigorous backcalculation principles the backcalculated values for ac course obtained using MODULUS 4.0 were essentially the same.

Figure 9.2 shows spatial variation in FWD measured peak deflection for aggregate base course section measured during March 1992. The coefficient of variation are shown in parentheses. Section 24 and Section 7 are similar in design and appear to show comparatively lower levels of variation (C.V. lesser than 10%). Coefficient of Variation along Section 16 was as high as 68%. Peak deflections corrected to temperature (68 F) is shown in Figure 9.3.

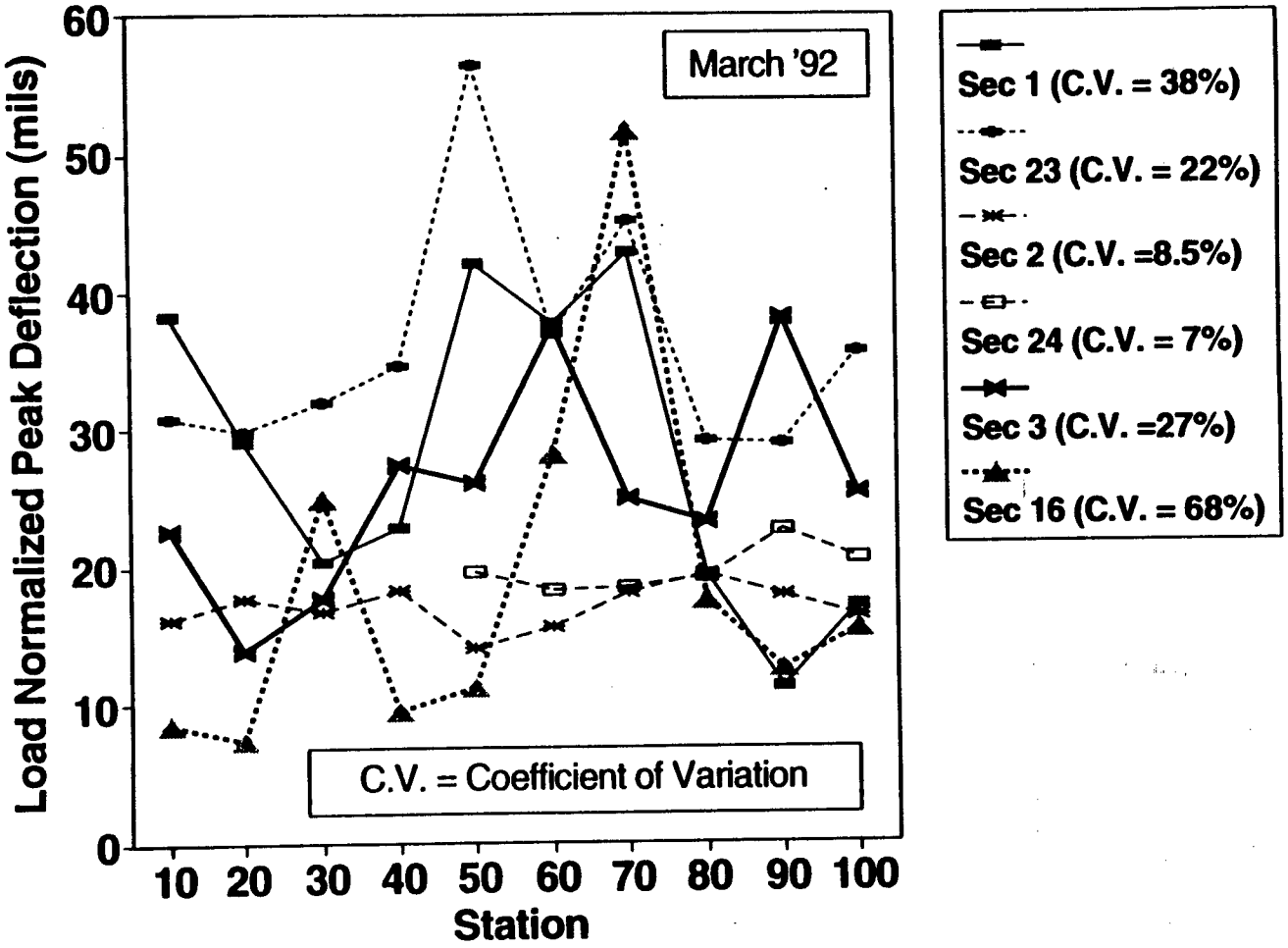

Figure 9.2 Spatial variation in peak FWD deflections measured for ABC sections (March 1992).

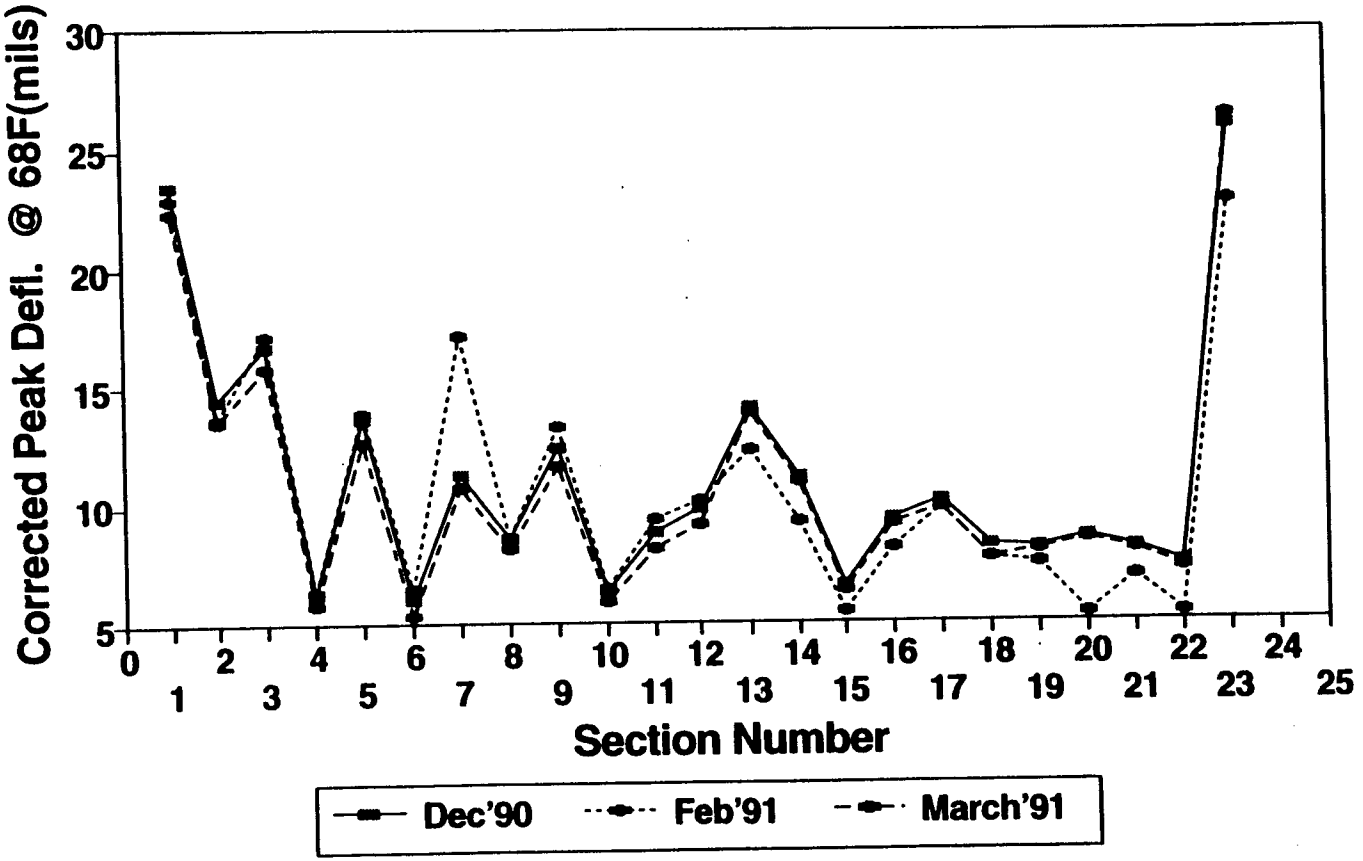

Figure 9.3 Seasonal variation in temperature corrected Peak FWD measurements for different test sections.

The peak deflection measurements were corrected based on established AASHTO procedures. It would be expected that with effective temperature correction, the deflections would be a function of only pavement condition. In spite of the temperature correction, it appears that the August readings for the different Sections appears to be the maximum. This indicates that the correction for temperature has not been totally successful. Figure 9.4 shows backcalculated moduli for aggregate base course sections corrected to 68 degree F. The correction procedure adopted was based on a moduli-temperature correction procedure developed at North Carolina State University. The relation developed was specific to this project and is provided below:

$$MR_{68}=10^{(0.0153 \; x \; (T_{md}-68) \; x \; MR_{md})}$$

where

MR_{68} = Resilient modulus of AC layer at 68 °F

T_{md} = Temperature at the mid-depth of AC layer

MR_{md} = Resilient modulus of AC layer at T_{md}.

As noted in Figure 9.4 a general trend in decreasing stiffness (stiffness corrected for temperature) with time, indicates the weakening of the pavement.

The corrections adopted in this section were performed only to illustrate the need for temperature correction and for illustrating the effectiveness of temperature corrected deflection/moduli in predicting pavement performance. These correction procedures were not adopted in the presentation of the various results in this report, as season sensitive moduli (moduli measured during different seasons) were required for the purpose of analysis. The correction procedure for the resilient modulus has been verified for the results of this study only. Other correction procedures are available for correcting the modulus of AC layers for temperature effects.

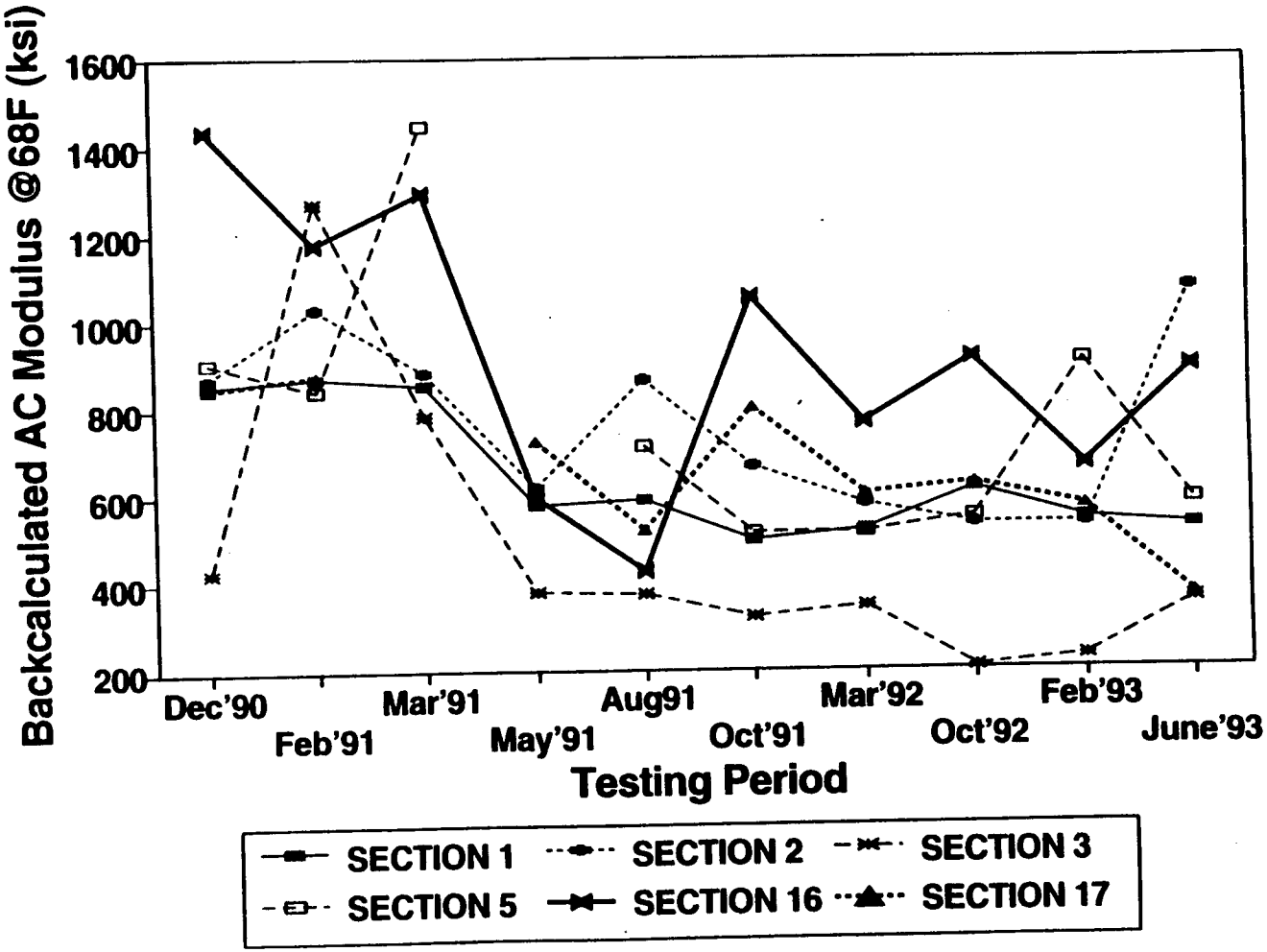

Figure 9.4 Seasonal variation in temperature corrected backcalculated moduli for different test sections.

Analysis of Seasonal Variation in Aggregate Base Course and Subgrade Backcalculated Moduli

Deflection data obtained from FWD testing was used to backcalculate the moduli. A summary of the backcalculated moduli is included in Chapter 4. Subgrade moduli varied within each test section and between test sections. As FWD backcalculation was conducted primarily in the vicinity of the sensors in each test section, data from these specific regions of each test section was used to study the variability of these subgrade moduli for different seasons. A method is suggested below to pick up representative subgrade and aggregate moduli for four different seasons. The method suggested, utilizes a statistical approach. The method can also be used to obtain a stiffness estimate within user specified levels of reliability. Although, the data presented here may be typical for the sections tested, the methodology is useful for selecting unique values of subgrade or aggregate base moduli based on seasonal considerations. This would be useful for a designer attempting to select "a given seasonal value" for the modulus of any given pavement layer to be utilized in the design.

Subgrade moduli values for different test sections were normalized by season to the maximum backcalculated subgrade modulus for that season. Table 9.3 shows partial results from normalization performed on subgrade moduli, for the season extending from December to February. The normalization was performed for all 24 test sections. It is common practice to use this normalization practice over an entire project length of raoadway. This was done for a total of 68 data points. The percentage of data points in each 10 percent increment of the maximum backcalculated subgrade modulus was determined as shown in Table 9.4. Subtracting the numbers in column 3 (cumulative distribution) of Table 9.4 from 100 percent yields the percent reliability of design. The results of the calculation for subgrade moduli are shown in Figure 9.5(a). For example, if the designer wished to obtain a subgrade modulus value for the period of Dec-Feb at a reliability level of 80 percent, a subgrade modulus value that is approximately 30 percent of the maximum subgrade modulus would be used (30% of 23 = 6.9 KSI). Similar computation was performed to obtain the moduli of aggregate base for different seasons and at different reliability levels. The results for these calculations are shown in Figure 9.5 (b).

Table 9.3 Partial results for computation of Normalized Subgrade Modulus during December - January

Backcalculated Subgrade Moduli (ksi)	Normalized Data
8.5	0.37
13.8	0.60
8.8	0.38
22.0	0.96
20.10	0.87
22.90	1.00 (*)
12.80	0.56
15.60	0.68
12.20	0.53
19.10	0.83
18.70	0.81
18.90	0.82
14.30	0.62
10.80	0.47
17.60	0.77
12.50	0.54
23.00	1.00
15.90	0.69
18.30	0.80
...	...
...	...
...	...

(*) Normalization performed based on a mximum backcalculated value of 22.90 ksi

Table 9.4 Computed values used to determine subgrade moduli - reliability curves

	December - January			March - May		
Data Range % of Max Modulus	% of Data Points in Range	Cumulative Distribution	Reliability	% of Data Points in Range	Cumulative Distribution	Reliability
0-10	0	0	100	0	0	100
10-20	2.9	2.9	97.1	6	6	94
20-30	5.8	8.7	91.3	14.93	20.93	79.07
30-40	11.6	20.3	79.7	13.43	34.36	65.64
40-50	7.25	27.55	72.45	8.95	43.31	56.69
50-60	14.5	42.05	57.95	13.43	56.74	43.26
60-70	11.6	53.65	46.35	14.93	71.67	28.33
70-80	17.4	71.05	28.95	7.46	79.13	20.87
80-90	13.04	84.09	15.91	13.43	92.56	7.44
90-100	14.5	98.59	1.41	5.97	98.53	1.47
100	1.41	100	0	1.47	100	0

	June-July			September - November		
Data Range % of Max Modulus	% of Data Points in Range	Cumulative Distribution	Reliability	% of Data Points in Range	Cumulative Distribution	Reliability
0-10	6.38	6.38	93.62	0	0	100
10-20	21.27	27.65	72.35	6.12	6.12	93.88
20-30	23.4	51.05	48.95	14.29	20.41	79.59
30-40	12.77	63.82	36.18	8.16	28.57	71.43
40-50	12.77	76.59	23.41	18.37	46.94	53.06
50-60	8.51	85.1	14.9	14.29	61.23	38.77
60-70	6.38	91.48	8.52	16.33	77.56	22.44
70-80	6.38	97.86	2.14	12.24	89.8	10.2
80-90	0	97.86	2.14	6.12	95.92	4.08
90-100	0	97.86	2.14	2.04	97.96	2.04
100	2.14	100	0	2.04	100	0

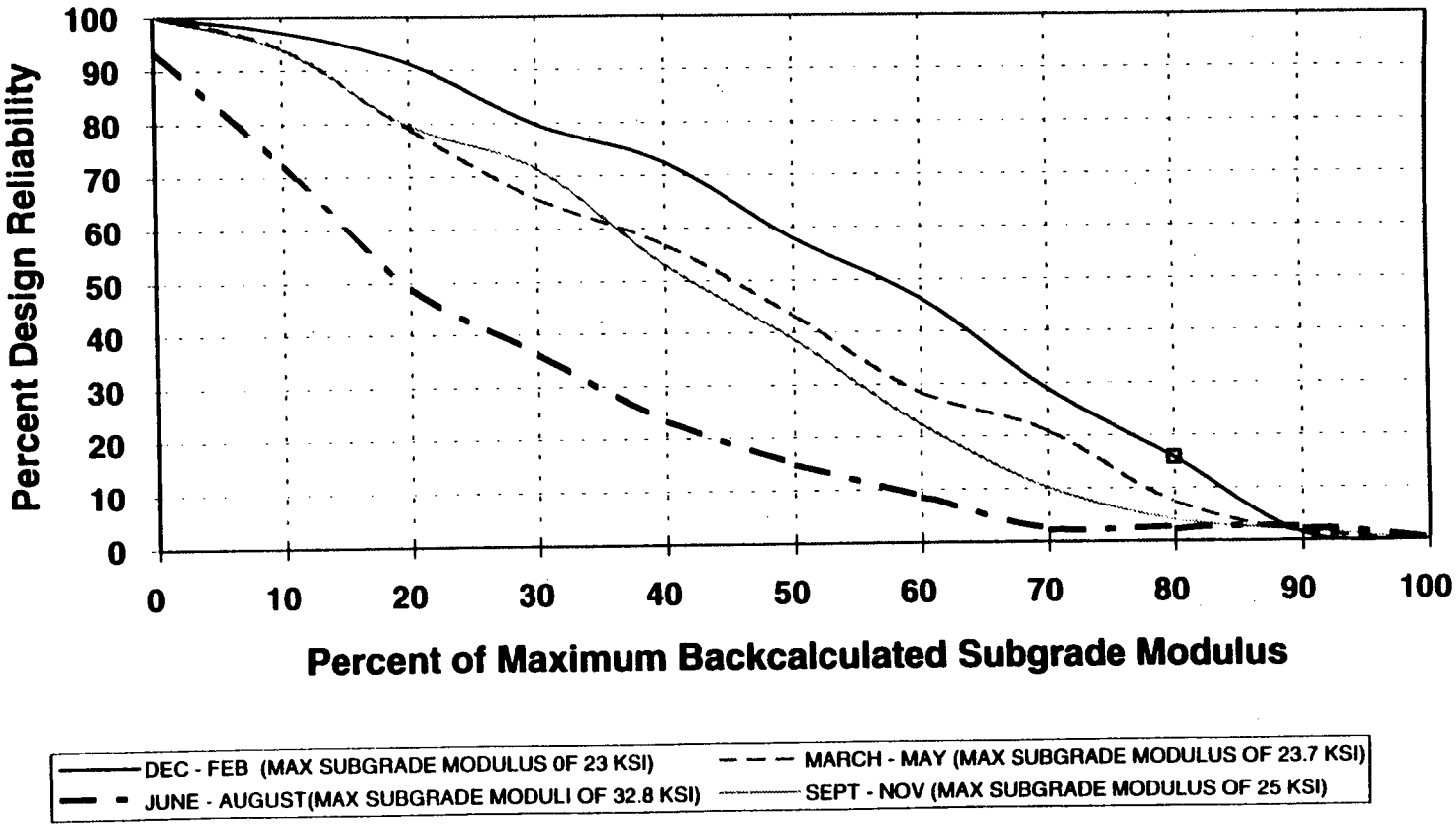

Figure 9.5(a) Design reliability curve for subgrade modulus for different seasons.

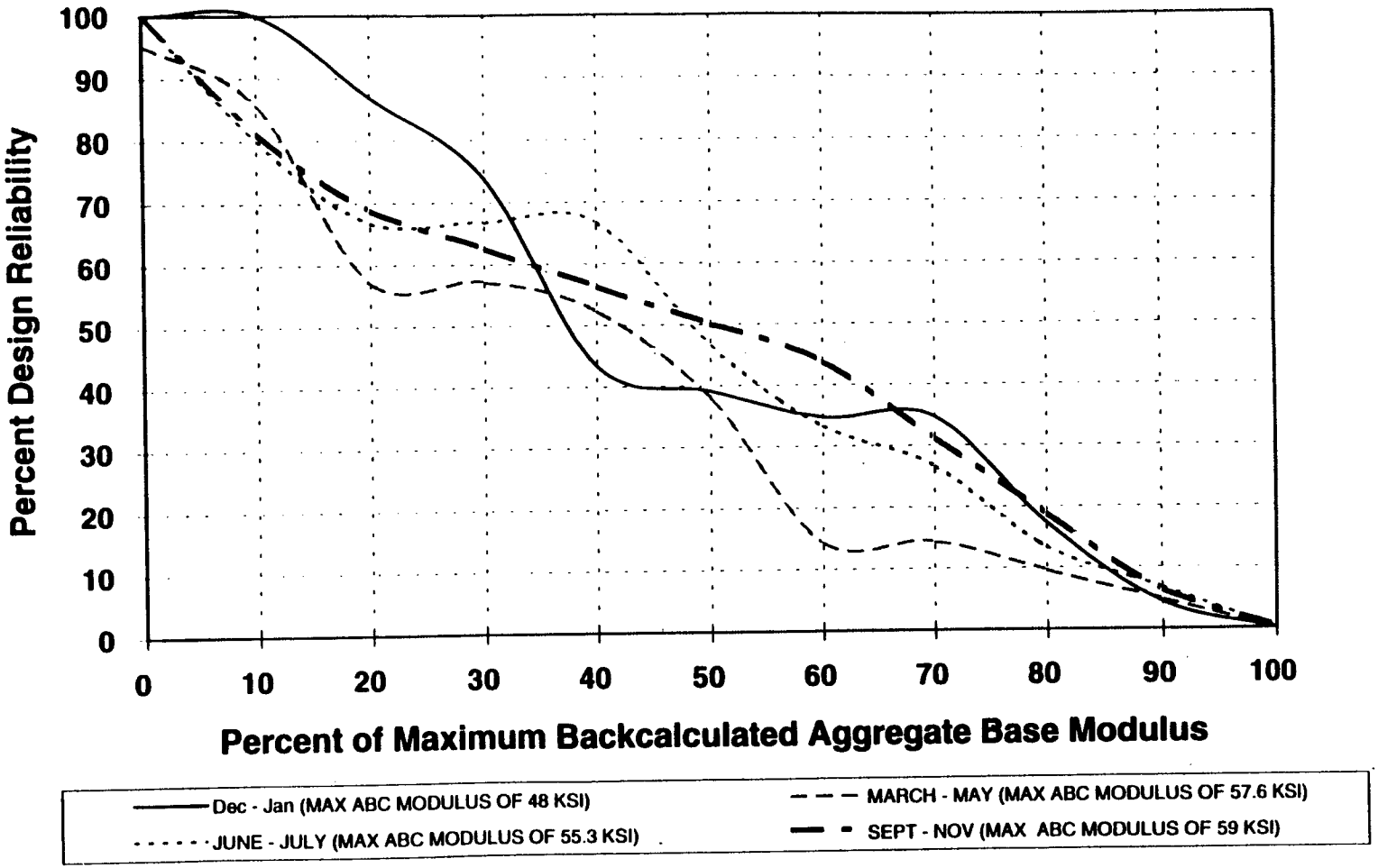

Figure 9.5(b) Design reliability curve for aggregate base course modulus for different seasons.

The combined probability of a successful design (design reliability) is the product of the individual design reliabilities of the various design factors (ac stiffness , base stiffness, subgrade stiffness,...) involved. For example an overall design reliability of 60 percent for the project can be obtained in the following manner.

A percent ac modulus reliability x B percent base modulus reliability x C percent Subgrade modulus reliability = > 60 percent overall design reliability

i.e. AxBxC = 60 for various combinations of A, B and C.

This method of computation of reliability based on individual reliabilities is useful when design is performed based on simple design charts, but for mechanistic methods, a more involved method may be necessary. Nevertheless, figures 9.5(a) and (b) can be used to arrive at estimates of stiffness (at desired levels of reliability) to be used as input parameters for more involved methods of pavement design. A detailed look at the various concepts involved with reliability and its application from a mechanistic pavement design standpoint is discussed in Section 9.5.

9.3 Seasonal Variability in Strain and Stress Measurements for US421 Test Sections

Figures 9.6(a) show the mean (computed over different seasons) and coefficient of variation observed for strain at the bottom of the ac layer for aggregate base course and full depth sections. It can be seen that the coefficient of variation (C.V)for the ABC sections are around 40 percent or less, whereas the C.V for full depth sections are considerably higher than 50 percent. It is therefore possible to assume ranges of strain values for ABC sections with a higher degree of reliability as opposed to assuming them for full depth sections. The strain values measured are a function of the materials used in the pavement and the depth of the asphalt cover.

Figure 9.6(b) shows the mean (computed over different seasons) subgrade stress in

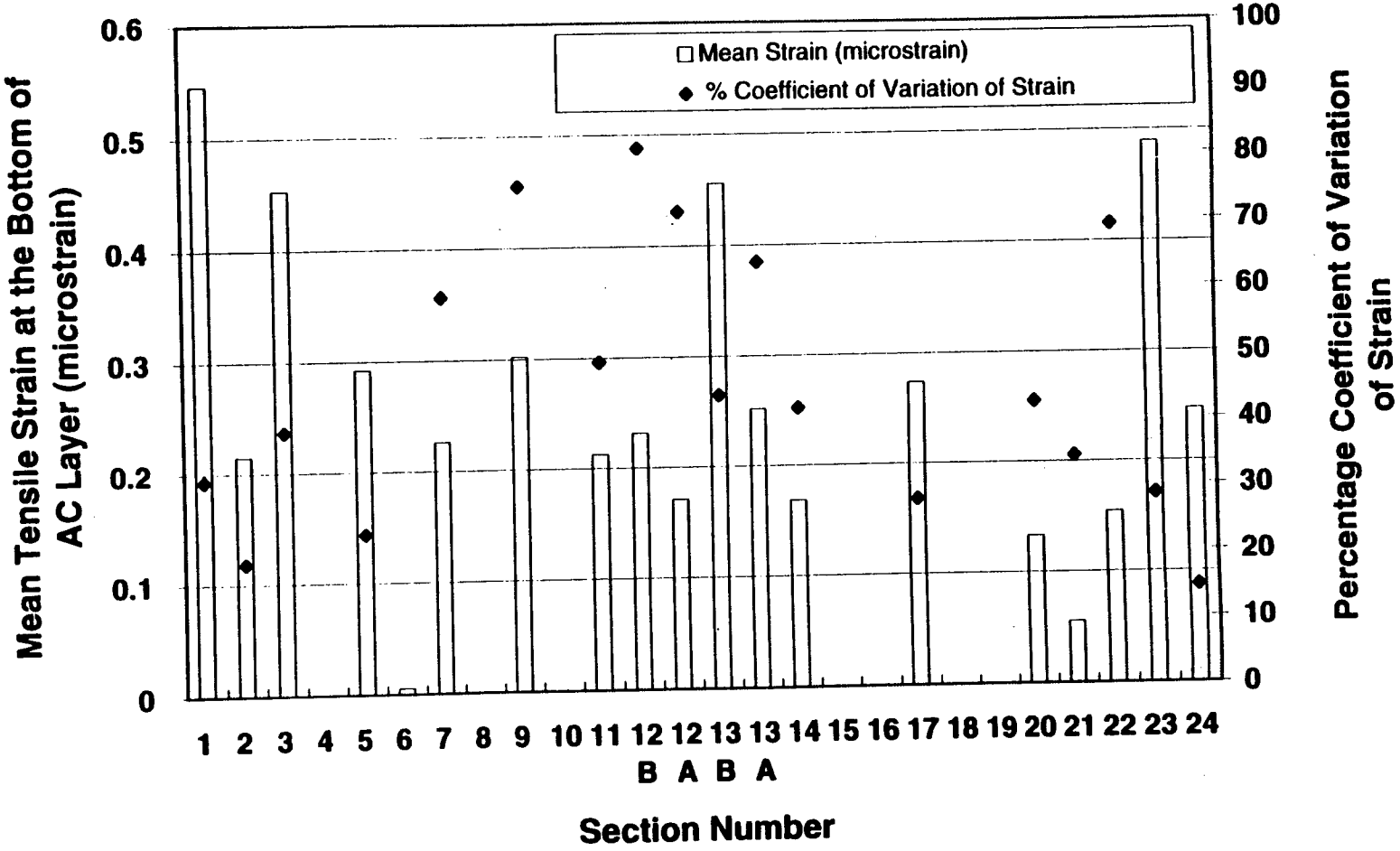

Figure 9.6(a) Mean and coefficient of variation of strain at the bottom of ac layer.

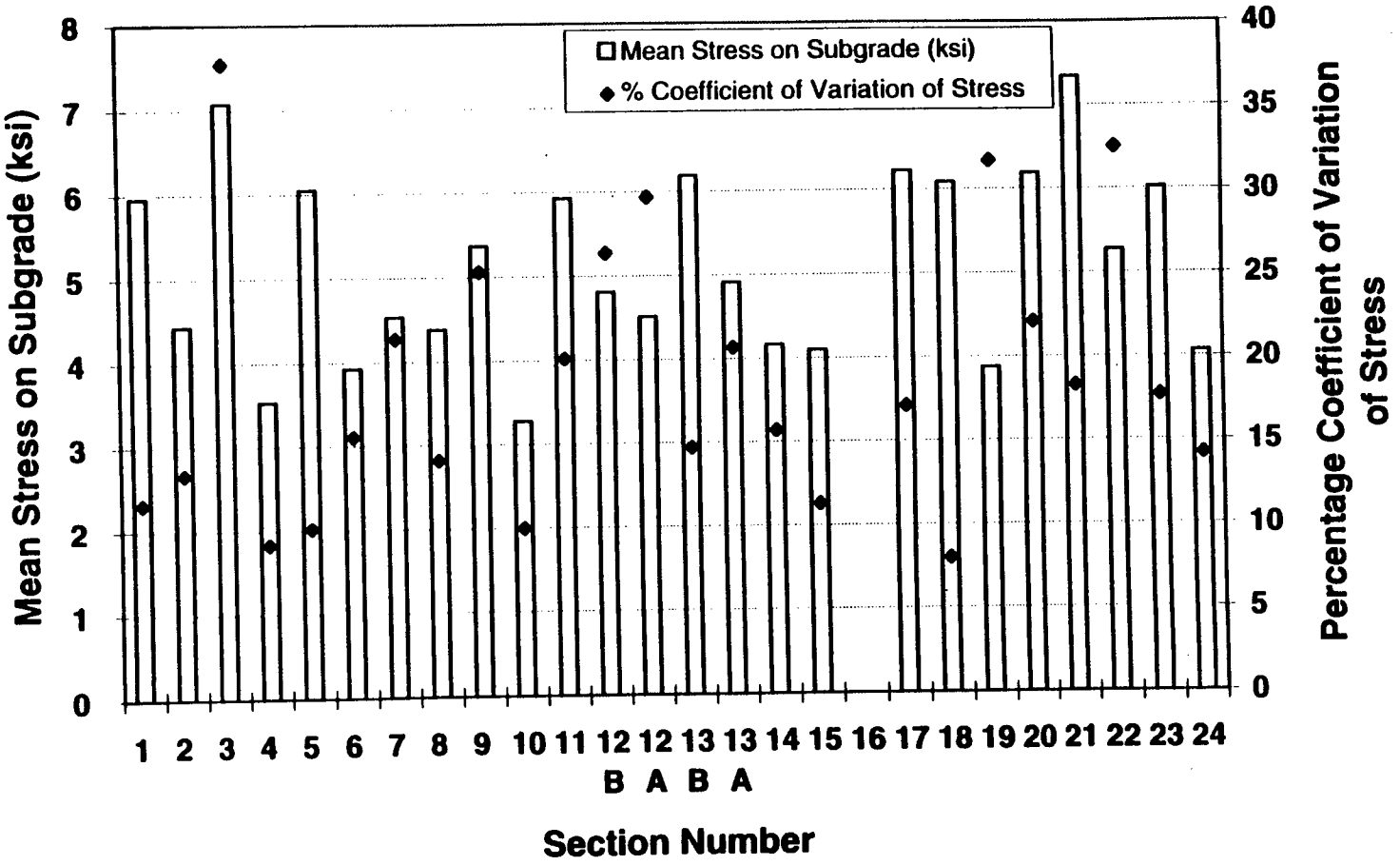

Figure 9.6(b) Mean and coefficient of variation of stress at the bottom of ac layer.

ksi. Unlike for the strains, the C.V. for stresses is not dependent on the type of pavement. The C.V. is limited to a maximum of 40 percent for all 24 test sections.

9.4 Sensitivity of Modified Shell Fatigue Model to Variation in Asphalt Modulus and Thickness

Field backcalculated moduli for the asphalt concrete were chosen from trips made during the months of October to March. The data was grouped into two groups based on measurements made during October to December (temperature of 65F) and measurements made during January-March (temperature of 78F). Mean and standard deviations of the moduli during these periods were determined. Strain at the bottom of the AC layer were computed for section 1 for both these groups independently, by varying the surface moduli by one standard deviation on either side of the mean. During this process the AC thickness was also varied from a value of 3.25 inches to a maximum of 3.75 inches. Therefore for each period (say, OCT-DEC) a total of nine data points were obtained. Fatigue estimates were made using the fatigue law illustrated in equation 6.28.3 in Chapter 6. This fatigue relationship is shown below:

$$N_f = 6.23x10^{-3}(\psi)^{1.363}(\varepsilon_i)^{-4.813} (S_i)^{-1.837}(\sin\phi_i)^{-0.902}\exp(0.101\,V_i - 0.046\,T)$$

where

N_f = number of cycles to failure

Ψ = energy Ratio

ϵ_i = initial Strain (Strain @ 200th cycle)

S_i = initial Stiffness

ϕ_i = phase Angle

V_i = voids

T = AC temperature

Computation for fatigue was performed treating only the stiffness and strains as varying, while the remaining factors were assumed constant. Computations were performed using a specially written program capable of repeated calculation of the strain and fatigue lives using various combinations of AC moduli and AC thicknesses. The results are shown in Figure 9.7. the lines shown represent computation made with similar surface moduli, but varying thickness measurements. It can be seen that in the OCT-DEC data set, fatigue life decreases with increasing stiffness, whereas for the FEB-March data set, fatigue life decreases with decreasing stiffness. This happens due to the interplay between the variables of stiffness and strain in the fatigue equation. The apparent decrease in fatigue life for increasing stiffness estimates during the OCT-DEC trip is minuscule and may be treated as almost constant. This shows that the model is more sensitive for stiffness changes greater than 30 ksi. As the data used to generate the plot was based on statistical variations observed in field measurements, it indicates the variation in fatigue lives that can be observed using the model developed at NCSU.

9.5 Reliability Analysis - An Introduction

The ways in which civil engineering systems fail, the occurrence and frequency of failure, demonstrate considerable difference between idealized and actual systems. The failure of a system is assessed by its inability to perform its intended function adequately on demand for a period of time under specified conditions. The measure of success is called "reliability". It is thus evident, that any meaningful scale of success or failure must be addressed in probabilistic terms due to the inherent variability and lack of determinacy of civil engineering systems. Probabilities of failure are the most significant indices of reliability. Being objective, and quantifiable they lend themselves as effective tools for comparisons of the risk of failure of different systems.

Any attempt at reliability analysis requires the computation of the mean and the standard deviation of requisite variable (distribution of the variable) being studied, based on available information on the distribution characteristics of related variables. The next section

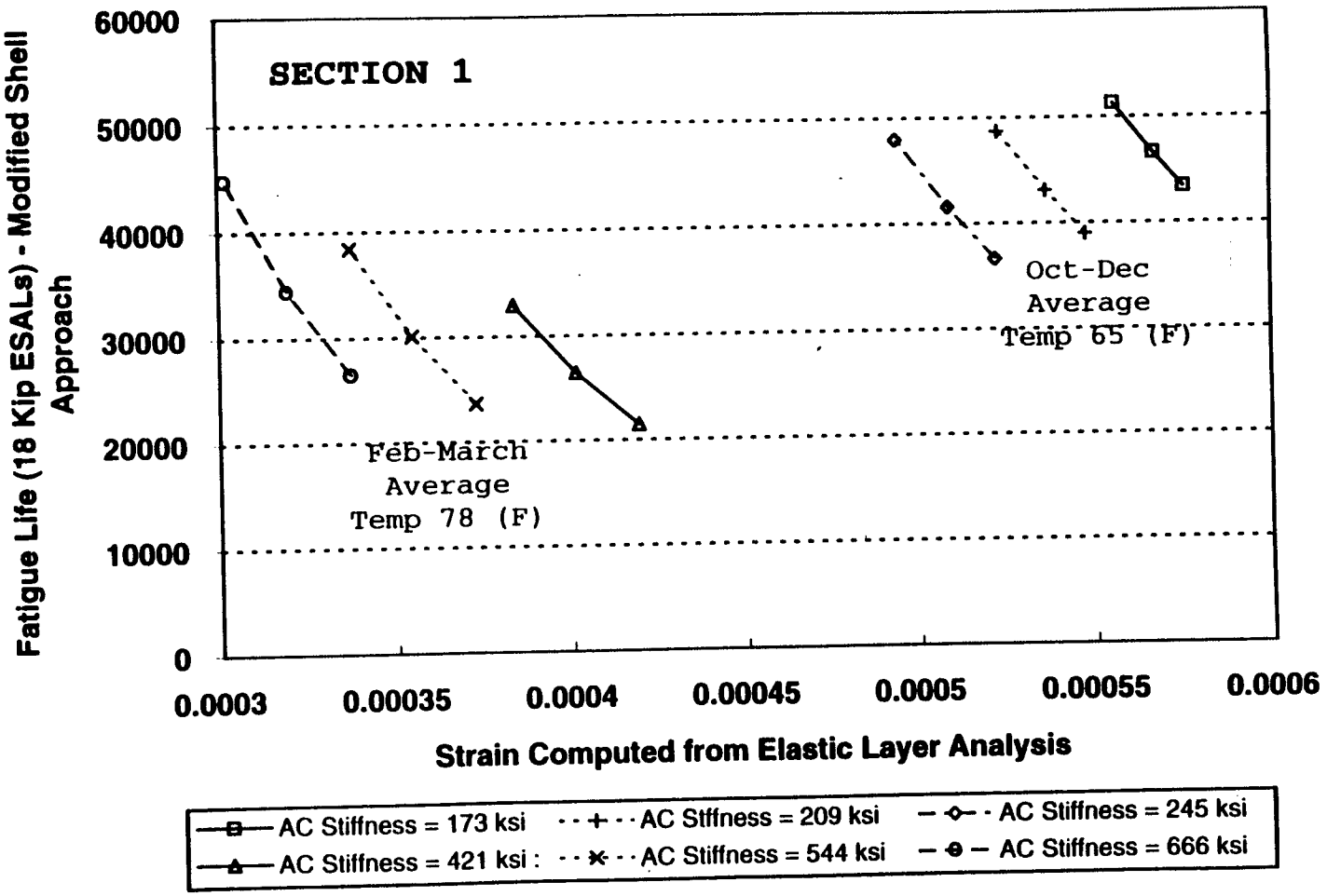

Figure 9.7 Effect of variation in ac thickness and field observed variation in ac moduli on computed strain and fatigue life predictions. (NCSU model).

details available methods to determine the distribution of any random variable.

9.5.1 Methods to Determine Distributions of Random Variables

Several methods have been developed which provide the distribution of random variables. These can be categorized as follows:

(1) Exact Methods

(2) First Order, Second-Moment (FOSM) Method

(3) Point Estimate Method (Harr,1987)

(1) Exact Methods

The exact methods are usually computer-oriented and require several numerical integrations. In these methods, the probability distribution function must be known for the component variables associated with a random variable. Numerical integration and Monte Carlo methods are included in this category.

The Monte Carlo method requires the probability distribution functions of all component variables to be completely known. The method uses a hit-or-miss procedure, where the density function of the desired random variable is obtained by using large sets of random numbers, that model the distributions of the input random variables, in a series of simulations. Harr (Harr,1987) has shown how the randomly generated inputs can be associated with the assumed distribution of the independent variables. He has also shown examples of the number of simulations to achieve a particular level of reliability. It is important to realize that the number of simulations or trials increase in proportion to the power of the number of independent variables.

(2) First-Order Second Moment (FOSM) Methods

The FOSM methods result from the truncation of the multivariate expansion of Taylor's series about the expected value of the variables. Only first-order (linear) terms are retained. The method is computationally intensive as it requires the evaluation of partial derivatives. This becomes quite impossible, when most relationships are given in the form of

charts or graphs.

(3) Point Estimate Method (PEM)

The difficulties using the FOSM method were ameliorated by the use of Rosenblueth's point estimate method (PEM). The method is simple and based on the finite difference procedure. Unlike the Taylor series expansion that required the knowledge of each term in the function and the existence and continuity of the first and second derivatives, Rosenblueth's PEM can be used directly to determine the mean and variance of any function without knowing its formulation. To reiterate, the Rosenblueth's method does not make use of the Taylor series, but instead uses calculated values of the function of x and y at different points, with each calculated value weighted to produce estimates of the expected value and variance of the function. The Rosenblueth method can be used to determine the probabilistic solutions from the deterministic solutions. Any deterministic design method can be easily converted to a probabilistic method solely, based on a number of deterministic solutions. Consider a function f(x) on which conditions of existence or continuity of first and second derivatives have not been imposed. Then, Point estimates of the function (for one variable) can be used in an expression for the expected value:

$$E(g(x)) = \tfrac{1}{2}\,(g(x)_{+} + g(x)_{-})$$

This expression expanded to multiple variables (m):

$$E(g(x)) = 1/2^{m}\,(g(x)_{+++++} + \ldots\ldots + g(x)_{-----}) \text{ for M variables}$$

M M

The total number of variables involved in the above equation is 2^{M}. The values of the function f (x) at the + and - levels correspond to the mean value of the first variable x plus or minus the associated standard deviation of the x variable.

9.5.2 Pavement Design - A Probabilistic Perspective

The area of pavement design provides a classical case study for the complexities involved in incorporating a rigorous probabilistic approach in the design of pavement systems.

It also clearly indicates the importance of such an approach in the design considerations. For long, pavement design has primarily been conducted at an empirical level. The factors that go into the design of a pavement system are very many, and the variables involved have large variances. The discussions in this chapter will pertain to the probabilistic considerations in the design of flexible pavement systems. Several definitions for design reliability have been provided by various agencies. An example from the AASHTO guide , defines reliability in the following manner: "Reliability is the probability that the pavement will perform its intended function over its design life and under the conditions encountered during operation."

The important factors that go into the design of a road system are:

(a) **Material properties:**

Elastic Moduli, Thickness, Poissons ratio,

(b) **Environmental conditions:**

Temperature, Moisture, Amount of rainfall

(c) **Loading Conditions:**

Nature of the load, Axle configurations, Tire pressures

The AASHTO method of pavement design evolved from field tests run in Illinois in the early 60's, and to date provides the most widely recognized pavement design procedure. Over the years, wide ranging improvements in computational power and material testing equipment have taken place. Specific failure mechanisms for various pavement types have been identified and explained. All these have necessitated the move towards a mechanistic design framework. By mechanistic, the pavement engineer obviously refers to a mechanistic empirical procedure.

In analyzing a pavement structure in probabilistic and reliability terms, the expected value and variance of a function (such as the computed stresses, strains, or load repetition) should first be determined, and the reliability of the design (fatigue life) can then be evaluated. The next section provides a framework for designing pavements under a probabilistic framework.

9.6 Proposed Framework for Designing a Pavement under Probabilistic Considerations

To understand this, one needs to understand the mechanistic design procedure. The easiest way to understand this complex procedure is to study the flow chart shown in Figure 8.1 (chapter 8). The design involves a structural analysis model at its core which calculates the pavement response to a certain loading condition for a given set of layer properties. As is evident, there is variability involved in each of the modules. The pavement engineer is interested primarily in variation caused in the most significant design parameter due to changes in material parameters (stiffness, thickness, loading,...).

The two most significant design parameters for flexible pavement design are:

(a) **Strain at the base of the asphalt layer:** This strain has to be minimized to decrease the level of fatigue cracking. This occurs due to the constant application of load which tends to fatigue the asphaltic course.

(b) **Stress at the top of the subgrade:** This is to minimize rutting or permanent deformation. With increasing stress on the subgrade, depressions are caused along the wheel path which could lead to loss of steering control and Hydroplaning.

Test sections are designed based on available material and the stress and strain levels are computed using a multi-layer elastic or visco-elastic theory. The strain levels are used to compute the predicted service life (number of cycles to failure). A novel approach would be to carry out this entire computation under a probabilistic framework. Due to the complexities involved in a rigorous probabilistic formulation, one simplified approach, would be to use Rosenblueth's Point Estimate Method (sec 9.31(3)) . The actual procedure to determine a proabilistic estimate of strain is explained in the following pages. The whole process can be programmed so as to minimize the time and effort taken to consider the large number of computations.

From the elastic layer theory, we understand that the strain at any given location in the pavement structure due to the passage of a load can be expressed as a function of the parameters like load, stiffness, Poissons ratios and thicknesses. Mathematically strain can thus be expressed as:

Strain at the bottom of ac layer = $f(P,e1,e2,h1,\nu_1,\nu_2)$ for a 2 layer pavement with an ac layer over a subgrade.

where

P = Load on the Pavement

e1 = Layer 1 Moduli

e2 = Layer 2 Moduli

h1 = Layer 1 Thickness

ν_1 = Poissons ratio for Layer 1

ν_2 = Poissons ratio for Layer 2

Based on the discussion on point estimate method, the following equations are useful to the solution of our problem (calculating the probabilistic estimates of mean and variance for the strain value at a specified depth).

$$E(\epsilon^N) = \tfrac{1}{2}\,(\epsilon^N_{+} + \epsilon^N_{-}) \textit{ for one variable}$$

$$E(\epsilon^N) = 1/2^2\,(\epsilon^N_{++} + \epsilon^N_{+-} + \epsilon^N_{-+} + \epsilon^N_{--}) \text{ for two variables}$$

$$E(\epsilon^N) = 1/2^M\,(\epsilon^N_{+++\cdots+} + \cdots + \epsilon^N_{---\cdots-}) \text{ form M variables}$$

(M) (M)

These expressions are the same as those used to explain the Point Estimate Method. The total number of terms to calculate the expected value of a function ϵ (strain computed using a multi-layer elastic program) which has M variables is 2^M, and if ϵ represents the function f (x) then N is the power of the function and takes on values of either 1 or 2. For N=1 in the above equation, we obtain the first expectation of the strain.

An example of computation for a 2 layer system is given below. The input information from Table 9.5(a) can be input into a linear elastic layer program (WES 5 , ELSYM, BISAR etc..) to find the strain at the bottom of the asphalt surface course. Instead of using the mean values of the input parameters, the added flexibility of changing the input

Table 9.5(a) Sample input used for 2 layer system used in PEM computation.

2 Layer System		
	Mean Modulus (psi)	Coefficient of Variation
Layer 1 (Asphalt)	1000000	0.1
Layer 2 (Subgrade)	9000	0.1
	Mean Thickness (inches)	Coefficient of Variation
Layer 1 (Asphalt)	20	0.1
Layer 2 (Subgrade)	infinite	
	Mean Load (pounds)	Coefficient of Variation
Load	30000	0.1

parameters in a manner dictated by its variance is made use of.

To reduce the number of computations, variations of Poissons ratio of pavement materials are neglected. The independent parameters that are considered but uncertain are Wheel Load (P), elastic modulus and thickness of the asphalt layer (e1 and h1), respectively, and the elastic modulus of the subgrade (e2). Thus it is now a four parameter problem. The total number of terms needed to compute the expected value of a function (strain) is 2^M ($2^4 = 16$). N would take values of either 1 or 2 (2 if we need both mean and mean square values).

If P represents the mean load value of 30,000 lb., then

$P_+ = 33000$ and $P_-=27,000$

Based on the notation shown earlier

$$\epsilon_{+--} = f(P_+, e1_+, e2_-, h1_-)$$
$$= f(33000, 1100000, 8100, 18)$$

Thus 16 (2^4) different strain values can be found based on various combinations (Table 9.5(b)).

The variance is found using the formula:

$$V(X) = E[X^2] - E^2[x].$$

The standard deviation is obtained by taking the square root of the variance. Thus, we now have the mean and standard deviation of the strain. The choice of probability distribution may be a function of mathematical convenience, such as normal or log-normal distributions. The distribution (for strain) in this case is assumed to be normal.

9.6.1 Computation of Mean and Standard Deviation of Strain for US421 Test Sections

Table 9.6 shows the mean and standard deviation for moduli values encountered in

Table 9.5(b) Sample Output obtained from PEM computation of 2 Layer System

# of Runs	Strain Term	P (pounds)	E1 (psi)	E2 (psi)	H1 (inches)
1	e + + + +	30000+3000 =33000	1000000+100000 = 1100000	9000+900 = 9900	20 + 2 = 22
2	e ++ - -	30000+3000 =33000	1000000+100000 = 1100000	9000 - 900 = 8100	20 - 2 = 18
3	e + - + -	30000+3000 =33000	1000000-100000 = 900000	9000+900 = 9900	20 -2 = 18
...	...	...	...	...	...
...	...	...	...	...	...
...	...	...	...	...	...
...	...	...	...	...	...
...	...	...	...	...	...
16	e - - - -	30000 - 3000 =33000	1000000-100000 = 900000	9000 - 900 = 8100	20 - 2 = 18

P = Load (Mean = 30,000 , Std. Dev. = 3000)

E1 = Layer 1 Moduli (Mean = 1000000, Std. Dev. = 100000)

E2 = Layer 2 Moduli (Mean = 9000, Std. Dev. = 900)

H1 = Thickness of Layer 1 (Mean =20, Std. Dev. 2)

Table 9.6 Mean and standard deviation of moduli (3 seasons) for 4 sections .

	Season	Section	Moduli (ksi)			
			AC Layer	Base	Subbase	Subgrade
	Oct-Dec	1				
Mean			209.33	13.73		3.43
Std. Dev.			36.17	2.68		1.33
		23				
Mean			484.67	14.63		5.97
Std. Dev.			115.28	5.86		1.67
		12B				
Mean			778.33		25.43	14.90
Std. Dev.			118.71		7.71	2.83
		13B				
Mean			215.67		11.50	8.97
Std. Dev.			84.51		4.10	1.35
Mean	Feb-March	1	544.00	13.43		5.00
Std. Dev.			122.38	2.41		1.20
Mean		23	520.33	11.80		3.80
Std. Dev.			239.04	2.55		0.73
Mean		12B	810.33		28.40	12.10
Std. Dev.			413.25		10.60	2.62
Mean		13B	196.00		8.47	8.47
Std. Dev.			24.99		0.21	0.21

Table 9.6 Mean and standard deviation of moduli (3 seasons) for 4 sections (contd).

	Season	Section	Moduli (ksi)			
			AC Layer	Base	Subbase	Subgrade
	May-Aug.	1				
Mean			204.50	13.10		3.15
Std. Dev.			43.50	3.10		1.55
		23				
Mean			213.50	16.00		5.25
Std. Dev.			27.50	0.60		0.05
		12B				
Mean			112.50		21.20	6.60
Std. Dev.			7.50		3.20	0.60
		13B				
Mean			83.00		5.85	5.70
Std. Dev.			5.00		0.45	0.60

sections 1, 23 , 12B and 13B, during three different seasons. Sections 1 and 23 are similar in design and so are Sections 12B and 13B. Based on these and assumed values of variation in thicknesses, the mean and standard deviation, for the strains for each of these sections during the different seasons is calculated. A partial list of these computations for Section 1 is shown in Table 9.7.

9.6.2 Computation of Probabilistic Estimates of Fatigue Life for US421 Test Sections

For a given the strain value, a plethora of empirical as well as mechanical relationships exist to arrive at the fatigue life of the pavement structure. It is now possible to predict a reliability level for every value of strain used to predict the fatigue life. Strain repetitions are calculated for the specific failure mode from strain values corresponding to different reliability levels.

Considerable research on fatigue cracking has been performed in recent years to yield mechanistic relationships linking fatigue life to strain. Based on the concepts of dissipated energy, a fatigue model of the following form was developed at North Carolina State University.

$$N_f = f(\Psi, V, t, \epsilon, S^*, \sin\phi)$$

where

ϵ = Strain at the bottom of the asphalt layer.

S^* = Stiffness Modulus.

ϕ = phase angle.

Ψ = Energy ratio

t = temperature

V =voids

N_f = number of cycles to fatigue.

Details regarding this model can be seen in Chapter 6. If variation in phase angle, energy ratio, and void ratios were to be neglected, then fatigue life can simultaneously be

Table 9.7 Partial results obtained using PEM for section 1 (variation of strain due to variation in input parameters).

E1	H1	E2	H2	E3	H3	E4	H4	E5	STRAIN
173160	3.25	16410	11.75	10500	0	10500	0	4760	0.000503
245500	3.75	16410	11.75	10500	0	10500	0	4760	0.00044
245500	3.75	11050	11.75	10500	0	10500	0	4760	0.000545
173160	3.25	11050	11.75	10500	0	10500	0	4760	0.000662
173160	3.25	11050	11.75	10500	0	10500	0	4760	0.000662
245500	3.75	11050	11.75	10500	0	10500	0	4760	0.000545
245500	3.75	16410	11.75	10500	0	10500	0	4760	0.00044
173160	3.25	16410	11.75	10500	0	10500	0	4760	0.000503
173160	3.25	16410	12.25	10500	0	10500	0	4760	0.0005
245500	3.75	16410	12.25	10500	0	10500	0	4760	0.000437
245500	3.75	11050	12.25	10500	0	10500	0	4760	0.000542
173160	3.25	11050	12.25	10500	0	10500	0	4760	0.000659
173160	3.25	11050	12.25	9500	0	10500	0	4760	0.000659
245500	3.75	11050	12.25	9500	0	10500	0	4760	0.000542
245500	3.75	16410	12.25	9500	0	10500	0	4760	0.000437
173160	3.25	16410	12.25	9500	0	10500	0	4760	0.0005
173160	3.25	16410	11.75	9500	0	10500	0	4760	0.000503
245500	3.75	16410	11.75	9500	0	10500	0	4760	0.00044
245500	3.75	11050	11.75	9500	0	10500	0	4760	0.000545
.....	.....	.....	.....	.....	.....	.....	.....	.....	.....
.....	.....	.....	.....	.....	.....	.....	.....	.....	.....
173160	3.75	16410	11.75	9500	0	9500	0	4760	0.000491
173160	3.75	11050	11.75	9500	0	9500	0	4760	0.000628
245500	3.75	11050	11.75	9500	0	9500	0	4760	0.000545
245500	3.25	11050	11.75	9500	0	9500	0	4760	0.000586
173160	3.25	11050	11.75	9500	0	9500	0	4760	0.000662
								Strain (Mean) =	0.000544
								Strain (Std. Dev)=	7.96E-05

(Oct-Dec) Data

	Mean	Std-Dev		Mean	C.V.
E1(psi)	209330	36170	H1(in.)	3.5	0.071
E2(psi)	13730	2680	H2(in.)	12	0.021
E3(psi)	3430	1330	H3(in.)	0	0
E4(psi)	3430	1330	H4(in.)	0	0
E5(psi)	3430	1330			

obtained along with strain estimates.

9.6.3 General Formulation of Reliability for Different Probability Density Functions

The reliability factor, Z_R, may be computed for any probability density function by using the following steps:

(1) Find the mean, μ.

(2) Find the variance σ^2.

(3) Find the area beneath the probability density function, from its lower limit, to the maximum acceptable upper limit, X_{max}. This area is the reliability level, R.

(4) Calculate the reliability factor, Z_R, from

$$Z_R = \frac{X_{max} - \mu}{\sigma}$$

The computation of Z_R is illustrated in Figure 9.8. The reliability factor can be computed for any probability density function, p(x). The risk of failure is 1.0 minus the reliability.

9.6.3.1 Computation of Reliability based Strain and Fatigue Lives for Section 1 (US421 Test Section)

Figure 9.9 shows a reliability strain curves for Section 1. Three curves for three typical seasons are shown. These curves were plotted based on data provided in Table 9.6 (a)and (b). The Point Estimate Method was utilized to derive the reliability strain relationships. Based on Figure 9.9, for variations in seasonal temperatures, different values for strain at the bottom of the ac layer can be chosen based on user specified levels of reliability. Fatigue Lives obtained using these estimates along with the strain values are shown in Figure 9.10.

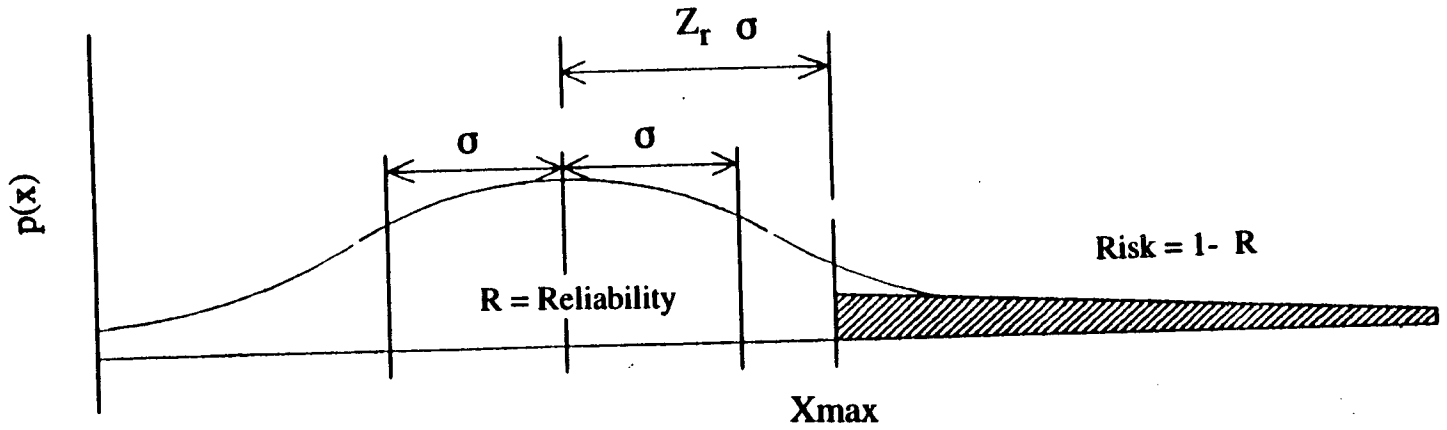

Figure 9.8 Normal probability distribution curve.

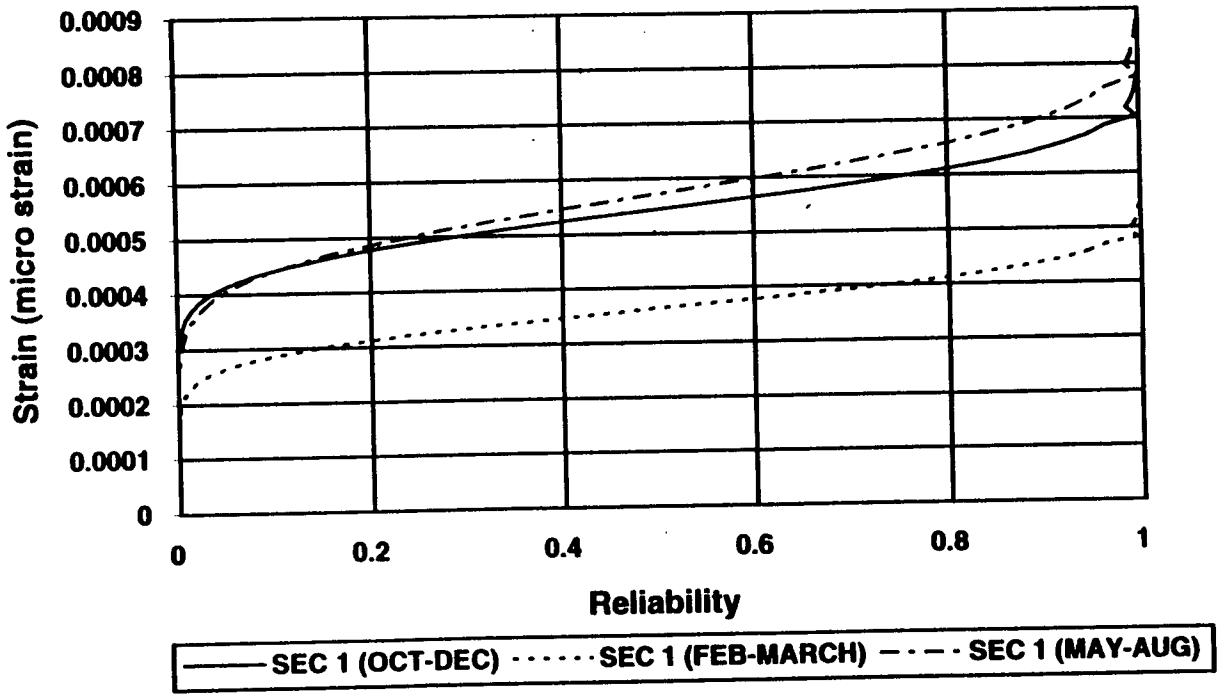

Figure 9.9 Strain reliability curves for section 1 for three different seasons.

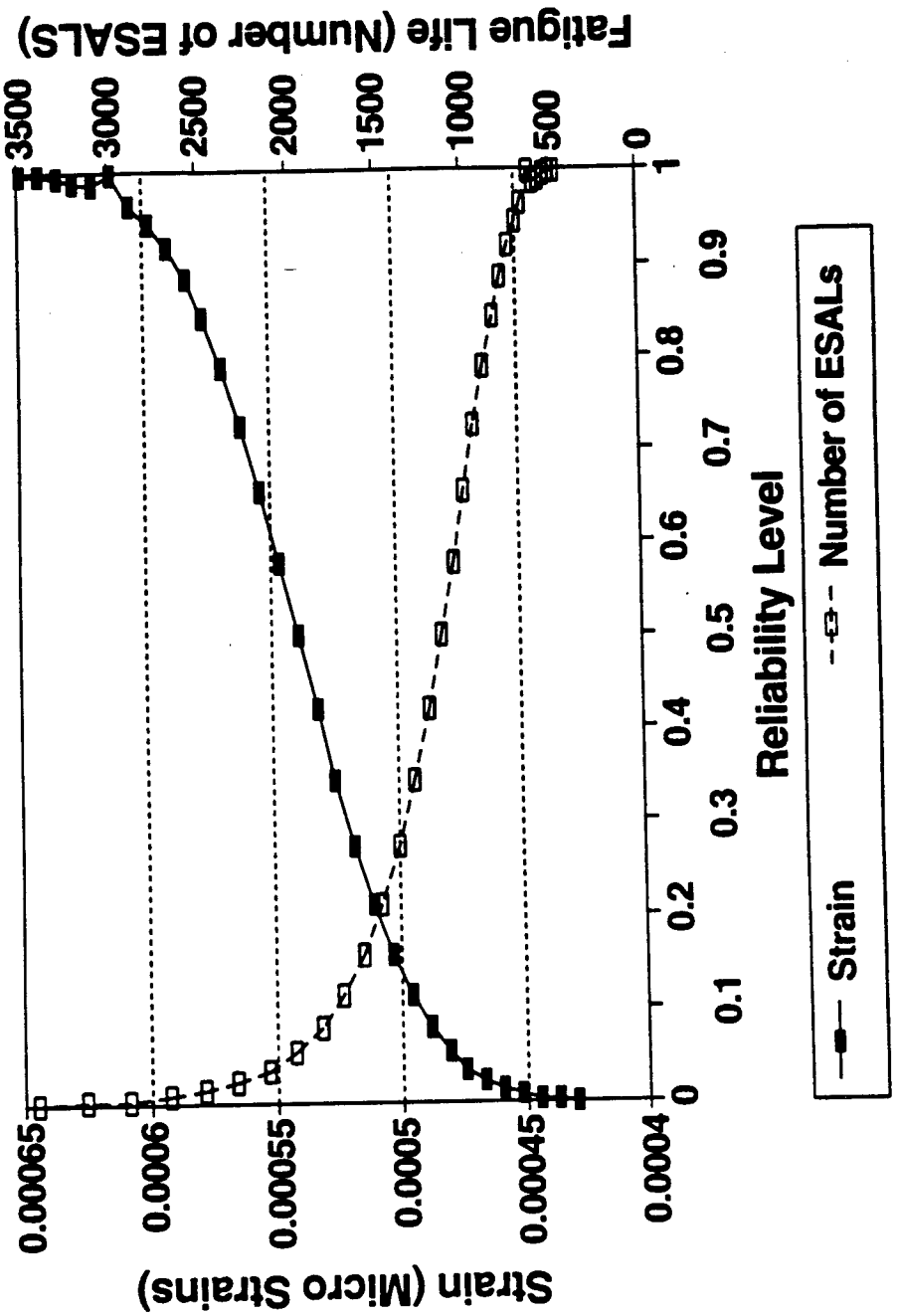

Figure 9.10 Strain and fatigue lives for varying reliability estimates.

9.7 RELPAV - A Program for Computation of Fatigue Life in a Probabilistic Framework.

A Program called RELPAV was developed to carry out the computations for the Point Estimate Method and to develop the reliability-strain and the reliability-fatigue life curves. This program was developed as an analysis tool, and has not been incorporated into the design procedure. The code for the Point Estimate computation utilized the Hamilton Walk algorithm to generate the various permutations and combinations required (section 9.6). Due to the large number of combination runs required, the program requires considerable time to run even with a 486 processor. Structural analysis was carried out using WES 5 (see Section 4.3). Figure 9.11 shows a flow diagram for the computation of the distribution parameters of strain and fatigue lives using the Point Estimate Method. The FORTRAN code for the program is provided in the appendix.

This methodology for RELPAV although simple to use in individual cases. is difficult to incorporate into a regular design method. It has therefore not been incorporated into the NCFLEX system. Other probability based programs, carry out probabilistic-based computation only at the levels involving computation of fatigue, rutting, PSI etc. These methods do not carry out probabilistic based computation during the determination of pavement responses like strain or stress, as these parameters are not evaluated based on simple equations, but require a more involved analysis. The RELPAV program was developed as an analysis tool in this project, and can be used to evaluate the variation that can be obtained in the response parameter (strain at the bottom of the ac layer) due to variation in input layer properties. It performs fatigue computation based on stiffness (estimate for the entire year) and thickness estimates for the various layers. The NCFLEX program although deterministic in nature utilizes 4 seasonal estimates of the stiffness of the different layers thereby accounting, in its own way, for seasonal variability.

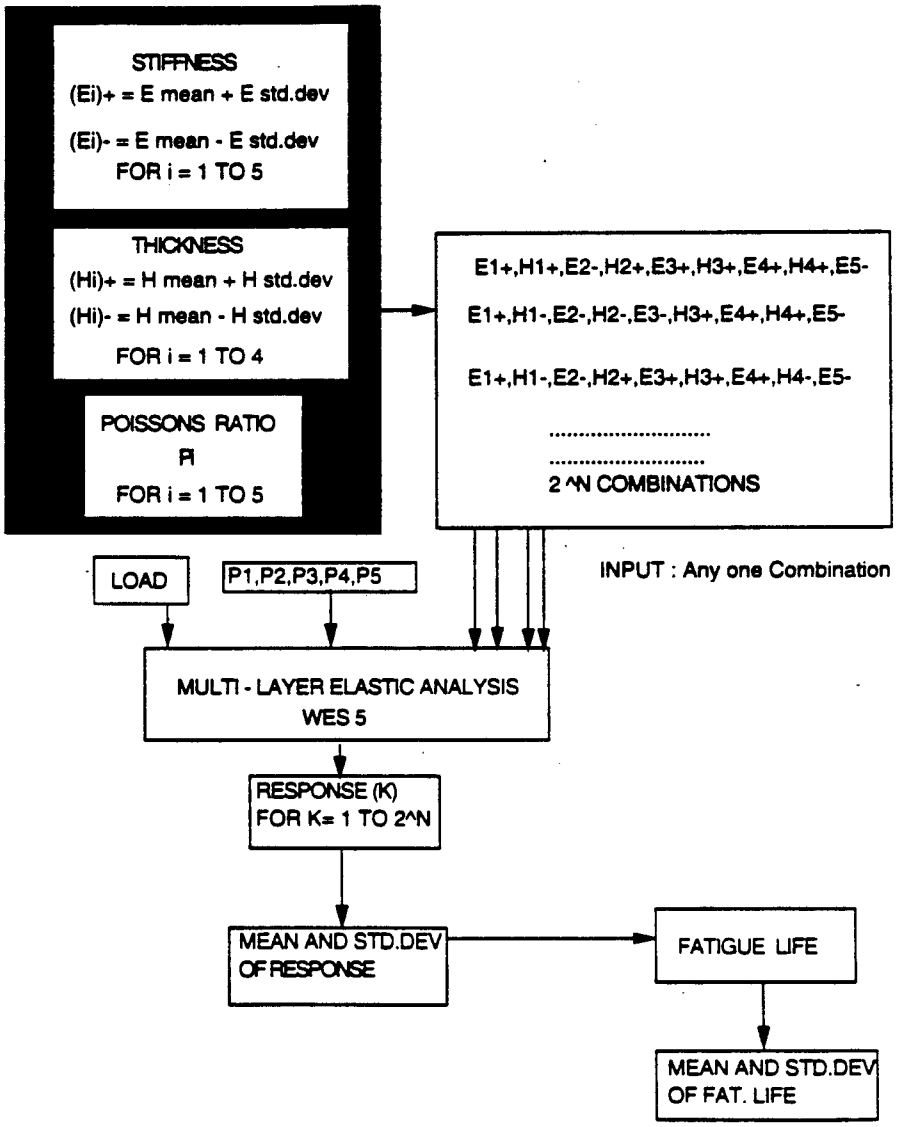

Figure 9.11 Flow diagram illustrating the sequence of computational steps involved in the Point Estimate Method.

CHAPTER 10

COMPARISON OF DIFFERENT DESIGN METHODS

This chapter deals with performance prediction of US421 test sections using existing design methodologies. The AASHTO, VESYS, and the Asphalt Institute method are used in this study. Due to non availability of comprehensive data specific to the application of these design methodologies, assumptions had to be made regarding certain parameters. These assumptions have been mentioned in the respective sections. The various methods used are dealt below.

10.1 AASHTO Design Method

The design procedure recommended by the American Association of State Highway and Transportation Officials (AASHTO) is based upon the results obtained from extensive testing of AASHO Road test sites in Ottawa, Illinois in the late 1950's and early 1960's. It was the first time a functional concept to failure was introduced above the traditional concepts of structural failure. The functional concept stated that the function of any road was to safely and smoothly carry traffic from one point to another. Non compliance with the above stated objective, meant that the pavement system had failed functionally. To quantify such a functional concept, several additional concepts were introduced. The concept of serviceability was introduced. Serviceability was quantified using a term called PSR, or the present serviceability index. The PSR was a rating given to the pavement on a scale from one to five, based on the observations of a select panel of qualified individuals. A later correlation was made relating the PSR to various physical measurements of the pavement. This was called as PSI, or the present serviceability index.

$$PSIi = 5.03 - 1.91\log(1+SV) - 1.38\overline{RD^2} - 0.01(c+p)^{1/2} \qquad (10.1)$$

where

SV = slope variance, a measure of longitudinal roughness

RD = average rut depth

c & p = area of cracking and patching per 1000 square feet

Performance was introduced as a time related function of serviceability. It indicated the ability of a pavement to satisfactorily serve traffic over a period of time. Using the above concepts, the following expression for the design of flexible pavements was developed:

$$\log W_{t18} = 9.36\log(SN+1) - 0.20 + \frac{\log(P_o - P_t)/(P_o - 1.5)}{0.4 + 1094/(SN+1)^{5.19}} + \log(1/R) + 0.372(S_i - 3.0) \qquad (10.2)$$

where

W_{t18} = total load applications at time t of an 18 kip single axle load

SN = structural number of the pavement

P_o = initial serviceability (t=0)

P_t = serviceability at end of time t

S_i = soil support value

The total equivalent 18-kip single axle load applications (W_{t18}) is defined as the total traffic volume expected to pass a point or over a roadway section during a given traffic analysis period (t) adjusted for lane and directional distribution and converted to equivalent 18 kip single axle load applications.

The Structural Number (SN) is an index number derived from analysis of traffic, roadbed soil conditions, and regional factors that may be converted to thickness of variable pavement layers through the use of suitable layer coefficients related to the type of material being used in each layer. The SN is the variable in the AASHTO equation reflecting the actual structural design of the pavement.

The P_t value or the terminal serviceability index is the lowest serviceability level that will be tolerated before reconstruction becomes necessary. The regional factor (R) is used to adjust the structural number of the flexible pavement structure for climatic conditions. The

soil support value (S_i) is an index number that expresses the relative ability of the subgrade to support a given traffic level on a particular flexible pavement structure.

Luhr (NCHRP) developed a simplified performance equation to predict the number of allowable 18 Kip single-axle load applications for each pavement condition using computed subgrade strains obtained from the AASHO road test data.

$$\log_{10}N_x = 2.15122 - 597.622(\epsilon_{sg}) - 1.32967\log_{10}(\epsilon_{sg}) + \log_{10}(PSI_i - TSI)/2.7]^{1/2} \qquad (10.3)$$

where

Nx = number of weighted applications of axle load X before the pavement reaches a specified terminal serviceability index (TSI)

ϵ_{sg} = subgrade compressive strain due to axle load X

PSI_i = initial Present Serviceability Index

TSI = terminal Serviceability Index

This equation, presented by Luhr, makes use of a subgrade compressive strain parameter (ϵ_{sg}) which is obtained from a mechanistic analysis of any pavement system.

10.1.1 AASHTO Analysis of US421 Test Sections

The following section describes the AASHTO method of determining failure times. The analysis is performed on data obtained from the US421 test sections. The traffic estimates from the weigh-in-motion instrumentation were used to determine the number of ESALs that caused failure. Failure due to fatigue cracking was defined as a cracking level of 15 percent of total area, based on the criteria suggested by the North Carolina Department of Transportation. To compare this failure time with those predicted by the AASHTO (1986) method, computations for the number of ESALS to failure of the different sections were

performed. The various steps used in this computation are described below:

(1) Layer coefficients for the various layers were determined based on a survey of literature available on this topic (AASHTO, 1961). Table 10.1 shows some values for layer coefficients that can be used.

(2) Structural number computations were performed as detailed in the 1986 AASHTO guide.

$$SN = a1*m1*h1 + a2*m2*h2 + a3*m3*h3 + a4...$$

where

a = layer coefficients

h = thickness of the layers, and

m = drainage Coefficient

In this analysis, no use was made of the drainage coefficient. The structural numbers so obtained are shown in Table 10.2.

(3) The method requires the use of an effective roadbed soil resilient modulus rather than a single estimate of resilient modulus as obtained from the lab. Table 10.3 shows a sample worksheet (AASHTO,1986) for estimating the effective roadbed resilient modulus. A year is divided into a number of periods during which different roadbed soil resilient moduli are specified. The shortest time period is half a month. These seasonal moduli can be determined from correlations with soil moisture and temperature conditions or from non destructive deflection testing. The relative damage can be obtained from the vertical scale or computed from the equation provided. The average relative damage is then computed, from which the effective roadbed soil resilient modulus can be obtained.

For applying this procedure in the analysis of the test sections in the report, a modified approach had to be taken. Backcalculated subgrade modulus was available for various months, but not necessarily for all the 12 months of the year. Damage factors were calculated for each of these modulus values, averaged and an effective resilient modulus was computed. The conversion from average resilient modulus (M_R) to damage factor, back to an effective roadbed resilient modulus value was performed using the AASHTO recommended equation

Table 10.1 Layer Coefficients for the evaluation of Structural Number (AASHTO, 1961).

PAVEMENT COMPONENT	COEFFICIENT
Surface Course	
Roadmix (low stability)	0.20
Plantmix (high Stability)	0.44
Sand asphalt	0.40
Base Course	
Sandy gravel	0.07
Crushed stone	0.14
Cement-treated (no soil cement)	0.14
Compressive strength at 7 days	
650 psi or more	0.23
400 - 650 psi	0.20
400 psi or less	0.15
Bituminous - treated	
Coarse graded	0.34
Sand asphalt	0.30
Lime-treated	0.15 - 0.30
Subbase Course	
Sandy gravel	0.11
Sand or sandy clay	0.05 - 0.10

Table 10.2 AASHTO structural number (SN) computations for US421 test sections.

SECt#	A.C.	A.C.	BASE	BASE	BASE	SUBBASE	SUBBASE	S.N.
	SURFACE	BINDER	ABC	CTB	FULL-DEPTH	C-STAB	L-STAB	
Layer Coeff	0.44	0.44	0.14	0.2	0.34	0.15	0.1	
1	2	1.5	12					3.22
2	2		12			7		3.61
3	2	3	8					3.32
4	2	1.5		7.5				3.04
5	2	1.5	8			7		3.71
6	2	3		5.5				3.3
7	2	1.5			5.5			3.41
8	2			7.5			7	3.08
9	2	3			4			3.56
10	2	1.5		5.5				2.64
11	2				5.5		7	3.45
12	2	1.5			4		7	3.6
13	2	1.5			4		7	3.6
14	2				5.5		7	3.45
15	2	1.5		5.5				2.64
16	2	3	8					3.32
17	2	1.5	8				7	3.36
18	2	1.5		7.5				3.04
19	2			7.5			7	3.08
20	2	1.5			5.5			3.41
21	2	3		5.5				3.3
22	2	3			4			3.56
23	2	1.5	12					3.22
24	2		12				7	3.26

CTB = CEMENT STABILIZED BASE
C-STAB = CEMENT STABILIZED
L-STAB= LIME STABILIZED

given in Table 10.3. Table 10.4 gives the effective roadbed resilient modulus values for the various test sections. Notice that the value so obtained is not just an arithmetic mean of the various moduli values obtained from various seasons.

(4) With the requisite parameters available, the number of ESALs to failure is obtained from the following equation.

$$\log W_{t18} = Z_R * S_0 + 9.36\log(SN+1) - 0.20 + \frac{\log(P_o - P_t)/(P_o - 1.5}{0.4 + 1094/(SN+1)^{5.1}} + 2.32\log(M_R) - 8.07 \qquad (10.4)$$

where

W_{t18} = total load applications at time t of an 18 kip single axle load

SN = structural number of the pavement

P_o = initial serviceability (t=0)

P_t = serviceability at end of time t

Z_R = normal deviate for a given reliability

M_R = effective roadbed soil resilient modulus

S_o = standard deviation

In this analysis a P_o value of 4.2, P_t value of 2.3, Z_R value of -1.645 and a S_o value of 0.35 were used.

(5) Th entire process is fairly straight-forward and could be easily done with a spreadsheet. The entire design process can be readily programmed using a spreadsheet. This is a convenient way to carry out repetitive computation to check the feasibility of various designs.

10.1.2 Comparison of AASHTO Predicted Failure Times with Observed Distress

From Figure 10.1 the following points can be noted:

(1) The AASHTO method predicts an unreasonably high life to failure for section 5. This

Table 10.3 Worksheet template for estimating effective roadbed soil resilient modulus (AASHTO, 1986).

Month	Roadbed Soil Modulus. M_R (psi)	Relative Damage. u_f
Jan	20.000	0.01
Feb.	20.000	0.01
Mar.	2.500	1.51
Apr	4.000	0.51
May	4.000	0.51
June	7.000	0.13
July	7.000	0.13
Aug.	7.000	0.13
Sept.	7.000	0.13
Oct.	7.000	0.13
Nov	4.000	0.51
Dec	20.000	0.01
Summation: Σu_f =		3.72

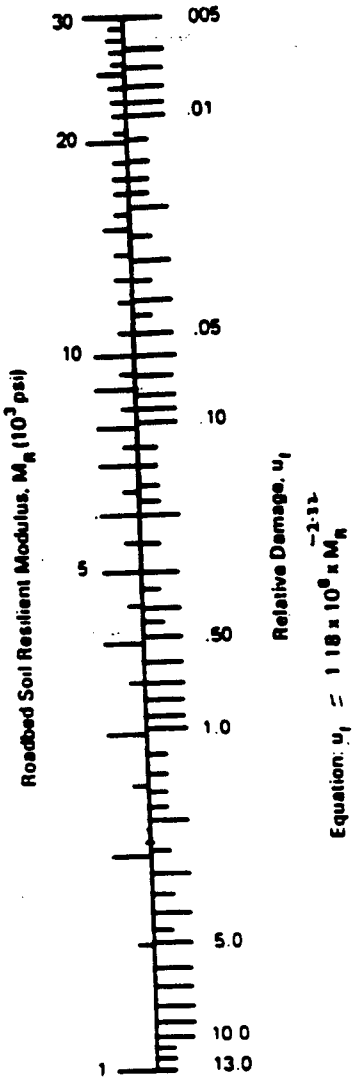

Average: $\bar{u}_f = \frac{\Sigma u_f}{n} = \frac{3.72}{12} = 0.31$

Effective Roadbed Soil Resilient Modulus, M_R (psi) = 5.000 (corresponds to $\bar{u}_f$)

Table 10.4 Effective subgrade modulus values computed for US 421 test sections using AASHTO method

Section Number	Effective Modulus (psi) AASHTO METHOD
1	3463.832
23	8742.243
2	14790.69
24	7832.446
3	6300.026
16	13394.8
5	22117.61
17	18306.82
4	20457.53
18	15349.43
6	10188.24
21	17668.7
8	12370.63
19	14339.16
10	17207.25
15	20510.13
7	5592.552
20	13270.52
9	4713.268
22	10501.74
11	11079.61
14	8170.922
13	9644.438

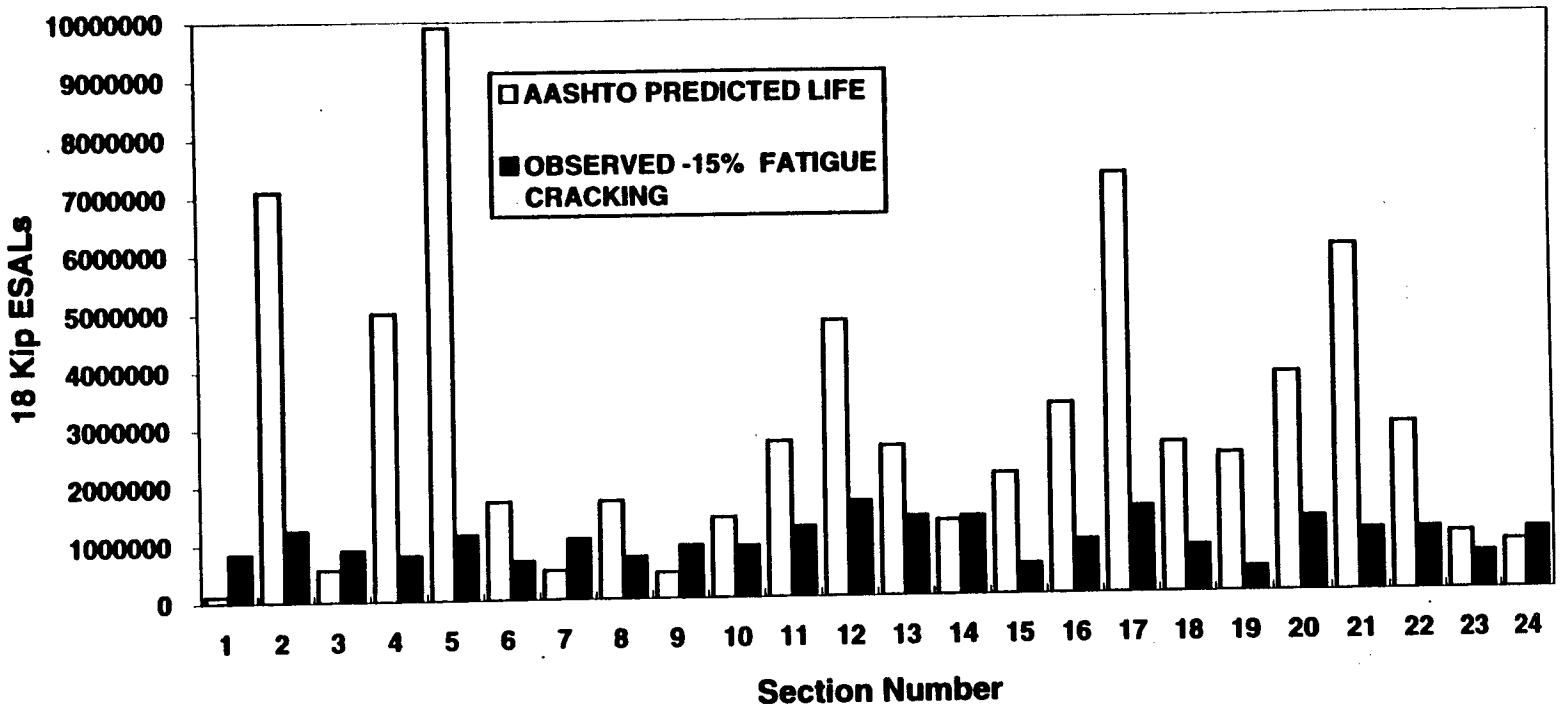

Figure 10.1 Comparison of AASHTO predicted life and observed life (15% fatigue cracking) for US421 test sections.

can primarily be correlated to the combination of a high value obtained for the structural number (3.71) as well a high effective resilient modulus value of 22117 psi.

(2) It is noticed that for most sections, the life to failure as predicted by AASHTO method is much higher than the 15% fatigue life as modeled at NCSU. This is acceptable considering that the AASHTO defined failure is a PSI based approach that takes into consideration factors that include fatigue, rutting, roughness, slope variance etc. Failure of the pavement was defined in this project as a cracking level of 15% over the entire area of the test section.

(3) For sections 1,3,7 and 9, the AASHTO predicted number of ESALs to failure is lower than the 15% fatigue life limit modeled by NCSU. Sections 1 and 3 are aggregate base course sections. Sections 7 and 9 are full depth AC sections. All four sections do not have a stabilized subbase layer.

(4) The AASHTO design of these test sections made use of subgrade modulus values as measured by the FWD, and have been averaged as per AASHTO procedures to yield the effective subgrade resilient modulus. Due to this, different effective subgrade resilient moduli were obtained for sections with similar designs, and even similar subgrades. It is widely believed that the backcalculated subgrade moduli may sometimes over-estimate the moduli by as much as a factor of 3. Lack of information regarding the moisture conditions during the various months of the year made it impossible to accurately predict subgrade moduli values in the laboratory for the various seasons. It was felt that in such a case, the method used in this analysis might serve as a better means to arrive at seasonal subgrade moduli.

The reasons for the differences between the predictions made using the AASHTO method and the observations are therefore many. The AASHTO guide due to its empirical nature, does not seem to be adequately capable of handling various climatic and structural differences. In the decisions made to overlay the pavement, no separate functionality concepts (PSI, roughness, etc.) were considered. In the local practice, fatigue cracking seems to be the most important criteria in deciding when a particular pavement would be resurfaced.

Although, the comparison between these two methods are difficult to make considering the widely different methodology they adopt, the analysis reiterates the importance of the various factors used in the design methodologies. The designer should

therefore exercise whatever method he chooses with caution, and understand the numerous pitfalls.

10.2 VESYS

The VESYS program was developed under the sponsorship of the U.S. Federal Highway administration (FHWA) by a number of prestigious academic institutions, consulting firms and Highway agencies. The program utilizes a two step mechanical-empirical modeling approach. Figure 10.2 illustrates the major components of the VESYS program. The program is composed of 4 major interactive models; primary response, general response, damage and performance. Several versions of the program, have been released to date. VESYS-IIM (1976) considered only a three layer system, but beginning with VESYS-G(1977) up to eight layers may be accommodated. Using VESYS-5(1987), the effects of tandem and tridem axles on the pavement may also be examined. The structural analysis component is essentially a visco-elastic adaptation of a layered elastic analysis. Prediction of damage considers individually the three primary distresses entering the AASHO PSI equation (rutting, cracking, and roughness), and employs calculated responses due to a static or a pulse load. This is done in a probabilistic fashion rather than a deterministic fashion, in order to account for inherent variability in material input parameters, traffic distributions, climatic factors, etc. The VESYS output consists of means and variances of the three primary distresses, and of the combined PSI values.

10.2.1 VESYS Analysis of US421 Test Sections

Four sections were chosen for conducting a detailed VESYS analysis. Section 1 and 3, both aggregate base course sections and section 7 and 9 both Full depth AC sections were chosen, for further analysis. Test results (material properties) for materials and gradation similar to those used in the test sections were used in the analysis. The data regarding the material properties was adapted from a study conducted earlier by Malpass (Malpass,G., 1994). The following conclusions can be drawn from the analysis of the results. The material properties that served as input for the VESYS program are shown in Table 10.5(a)-10.5(d)

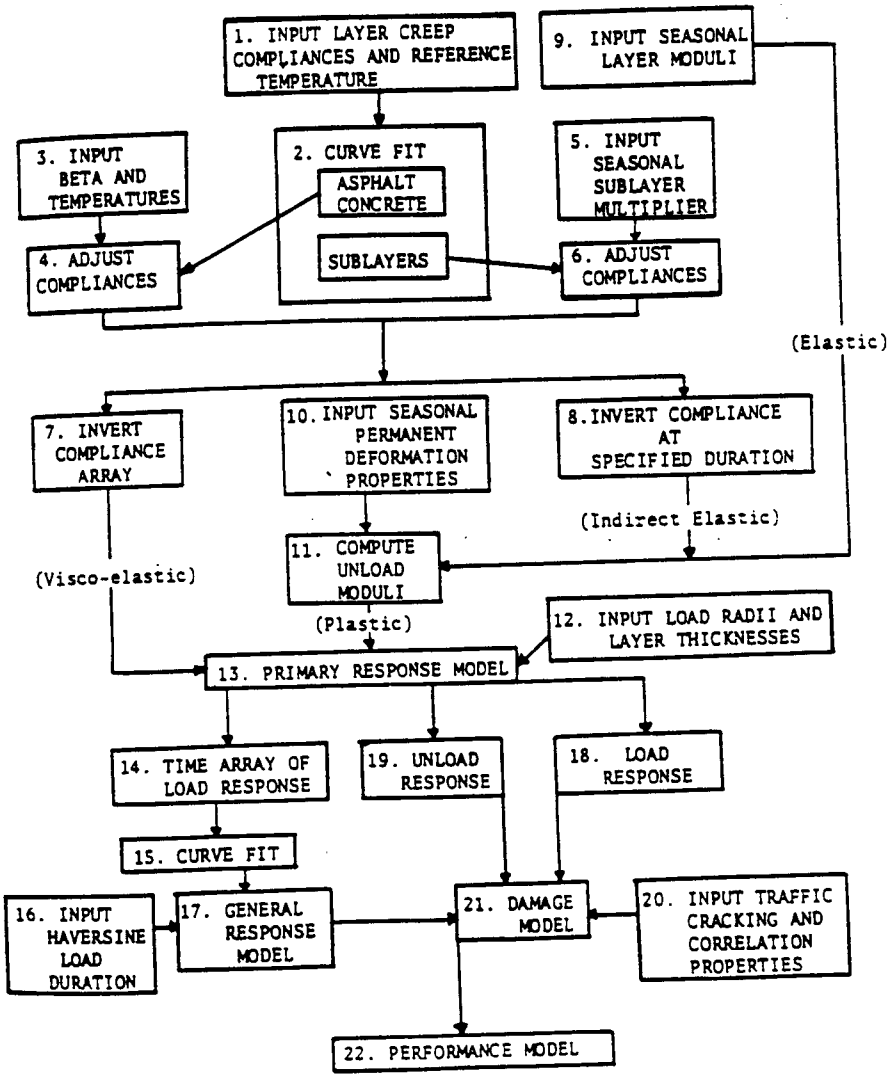

Figure 10.2 Flow chart for VESYS method.

Table 10.5(a) Average seasonal pavement temperature (used as input in the VESYS analysis)

Season	Average Temperature (F)
Winter	40
Spring	70
Summer	100
Fall	70

Table 10.5(b) Resilient moduli values (used as input in the VESYS Analysis)

		Average Pavement Temperature		
		40 (F)	20 (F)	100(F)
Surface Mixture	Mr (psi)	1,494,000	271,000	49,900
Base Mixture	Mr(psi)	3,770,400	700,400	72,500
Binder Course	Mr(psi)	1,880,000	323,000	59,100
Aggregate Base	Mr(psi)	27,000	26,000	29,000
Subgrade Soil	Mr(psi)	4,000	3,000	9,000

Table 10.5(c) Mechanistic properties -K1 and K2 (used as input in the VESYS analysis).

	K1	K2
Surface Course Mixture	2.15 x 10 -3	1.84
Base Course Mixture	1.87 x 10-15	6.91
Binder Course	1.95 x 10 -7	3.75

Table 10.5(d) Mechanistic properties Alpha and Gnu (used as input in the VESYS analysis).

	Average Pavement Temperature		
	40 (F)	20 (F)	100(F)
Surface Course Mixture Alpha	0.183	0.565	0.623
Gnu ($x10^{-3}$)	7.095	35.79	33.50
Base Course Mixture Alpha	0.232	0.415	0.624
Gnu ($x10^{-3}$)	3.490	15.30	21.40
Binder Course Mixture Alpha	0.410	0.620	0.690
Gnu ($x10^{-3}$)	9.0	50.0	38.0
Aggregate Base Course Alpha	0.810	0.840	0.870
Gnu ($x10^{-3}$)	10.0	10.0	5.0
Subgrade Alpha	0.850	0.850	0.720
Gnu ($x10^{-3}$)	160.0	160.0	40.0

10.2.2 Comparison of VESYS predicted Distress with Observed Distress

A comparison of the VESYS analysis of the test sections and actually observed condition of the pavement is presented below.

(1) Comparison of rutting

The rutting prediction for three sections (1,3 and 7) is shown in Figure 10.3. It can be seen that maximum rut depths were noticed for section 3, followed by section 7 and then by section 1. It can be observed from the figure that VESYS over-predicts rutting for all the three sections. It must be noted, that the NCSU model takes into account rutting from the AC layers only in accordance with field observed rutting. It seems quite obvious that the VESYS model is taking into account factors such as aggregate base course and subgrade rutting in its rut depth computation.

(2) Comparison of fatigue life

The fatigue models for both the NCSU and for the VESYS model are based on Miners Hypothesis. A cumulative damage ratio is computed for each year or season based on observed and predicted number of ESALs. In the NCSU model it is hypothesized that the pavement layer is considered to have failed in fatigue cracking when the Damage Index ratio equals 1. The VESYS program works on the hypothesis that a Damage Index of 1 refers to crack initiation at the bottom of the AC layer, and that one must consider factors such as crack propagation etc. Therefore the VESYS calculated DI values may be greater than 1. Damage Index (DI) computation for some typical sections by both the NCSU method and the VESYS method are shown in Figures 10.4 and 10.5 respectively. The VESYS program also computes the area cracked per 1000 square feet by assuming the damage ratio to be normally distributed.

$$A = 1000[1\text{-probability}(C <= 1)]$$

The pavement cracks when C >1, so that the expression within the brackets is the percentage of area that cracks. Figure 10.6 shows the area cracker per 1000 square feet as calculated by VESYS

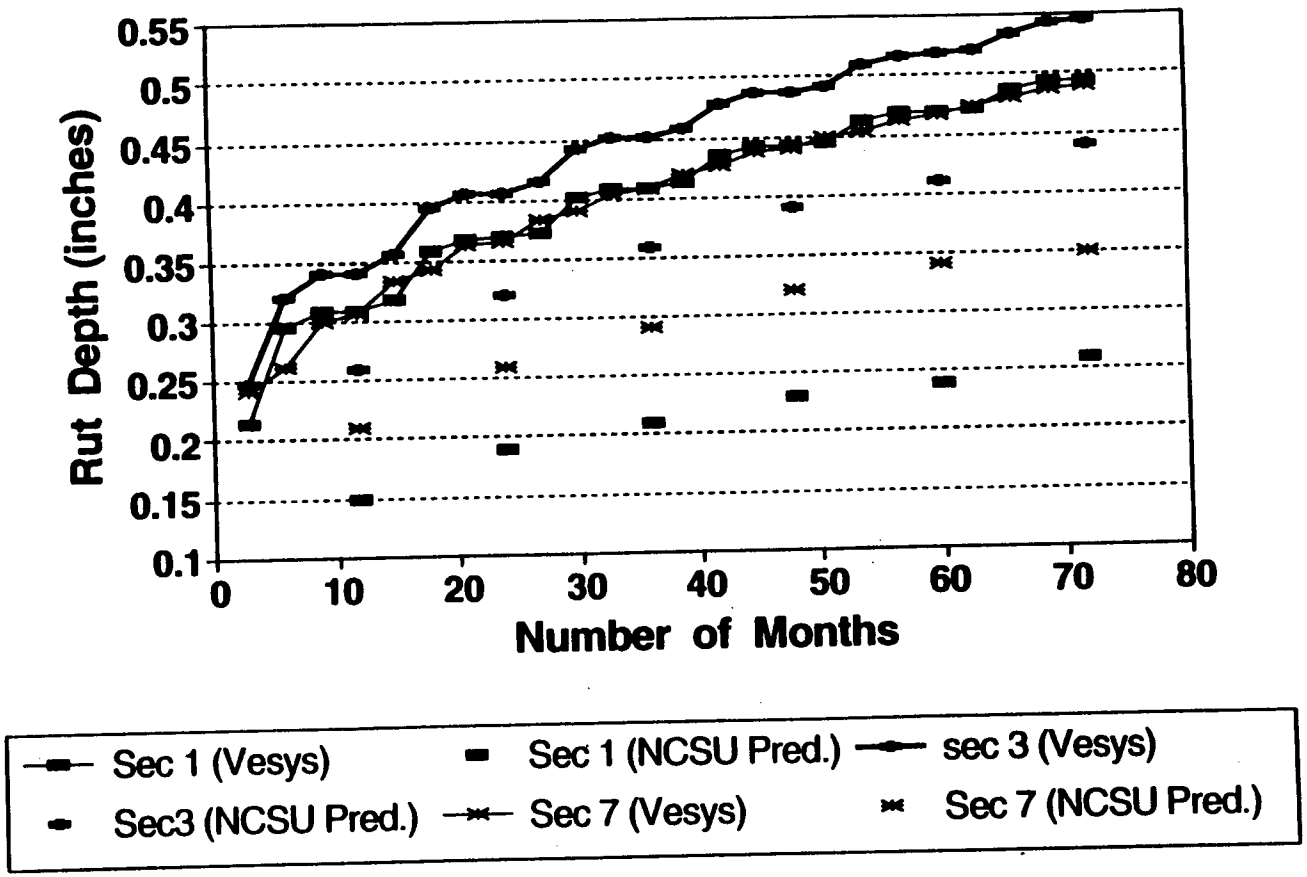

Figure 10.3 Comparison of VESYS prediction of rut depths versus NCSU observed rut depths for US421 test sections.

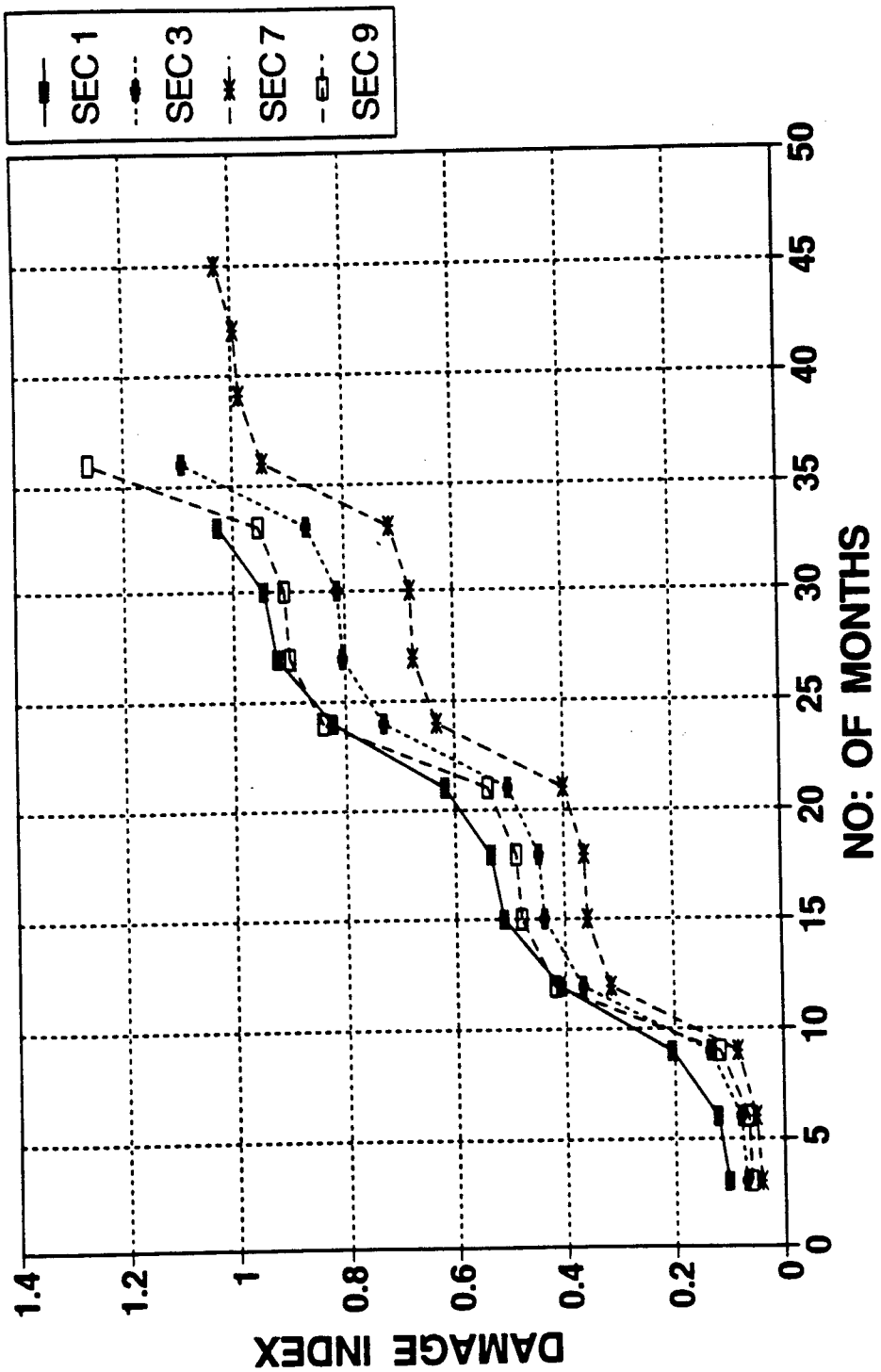

Figure 10.4 Damage Index computation using fatigue model developed at NCSU for US421 test sections.

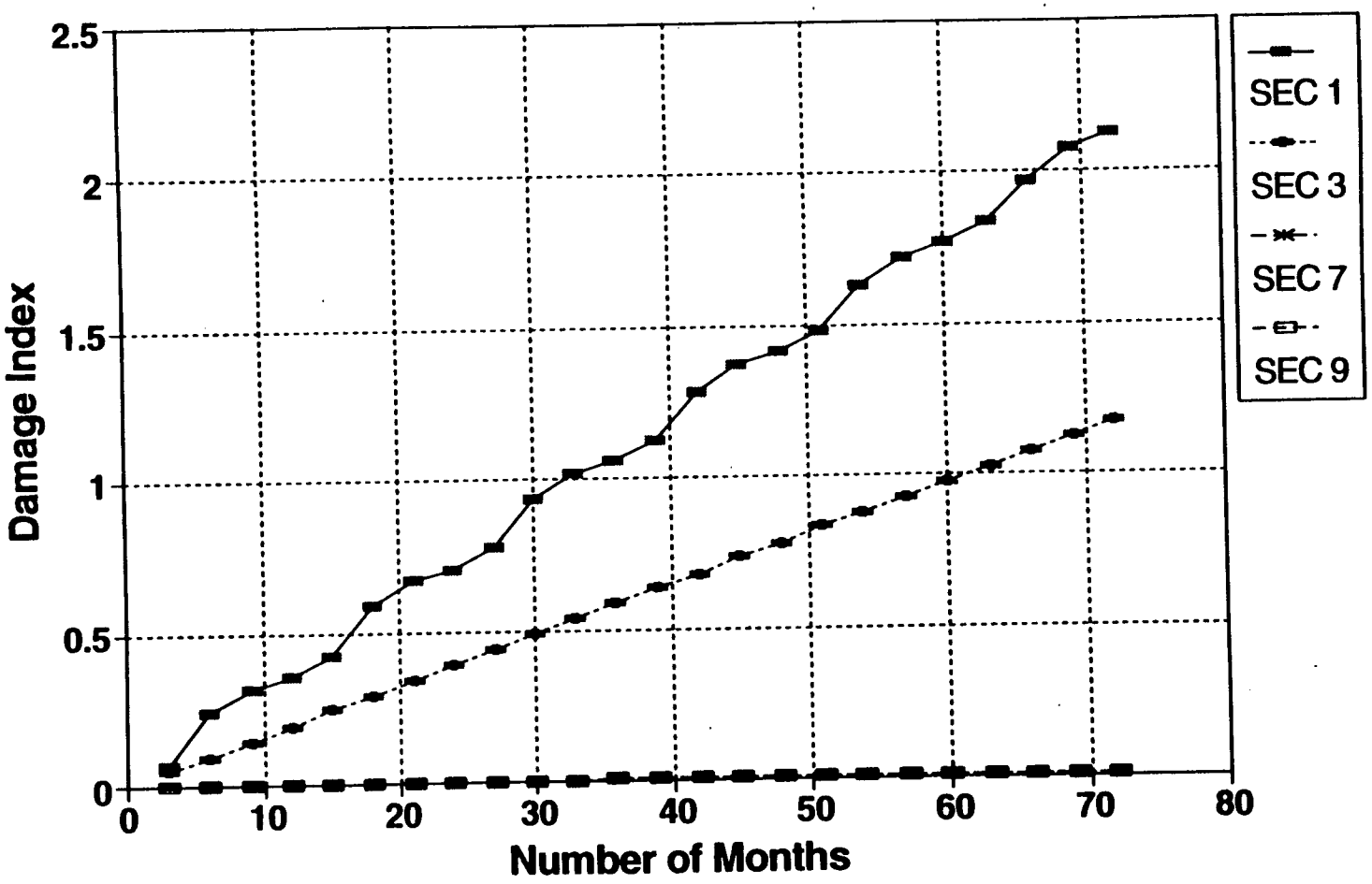

Figure 10.5 Damage Index computation using VESYS for US421 test sections.

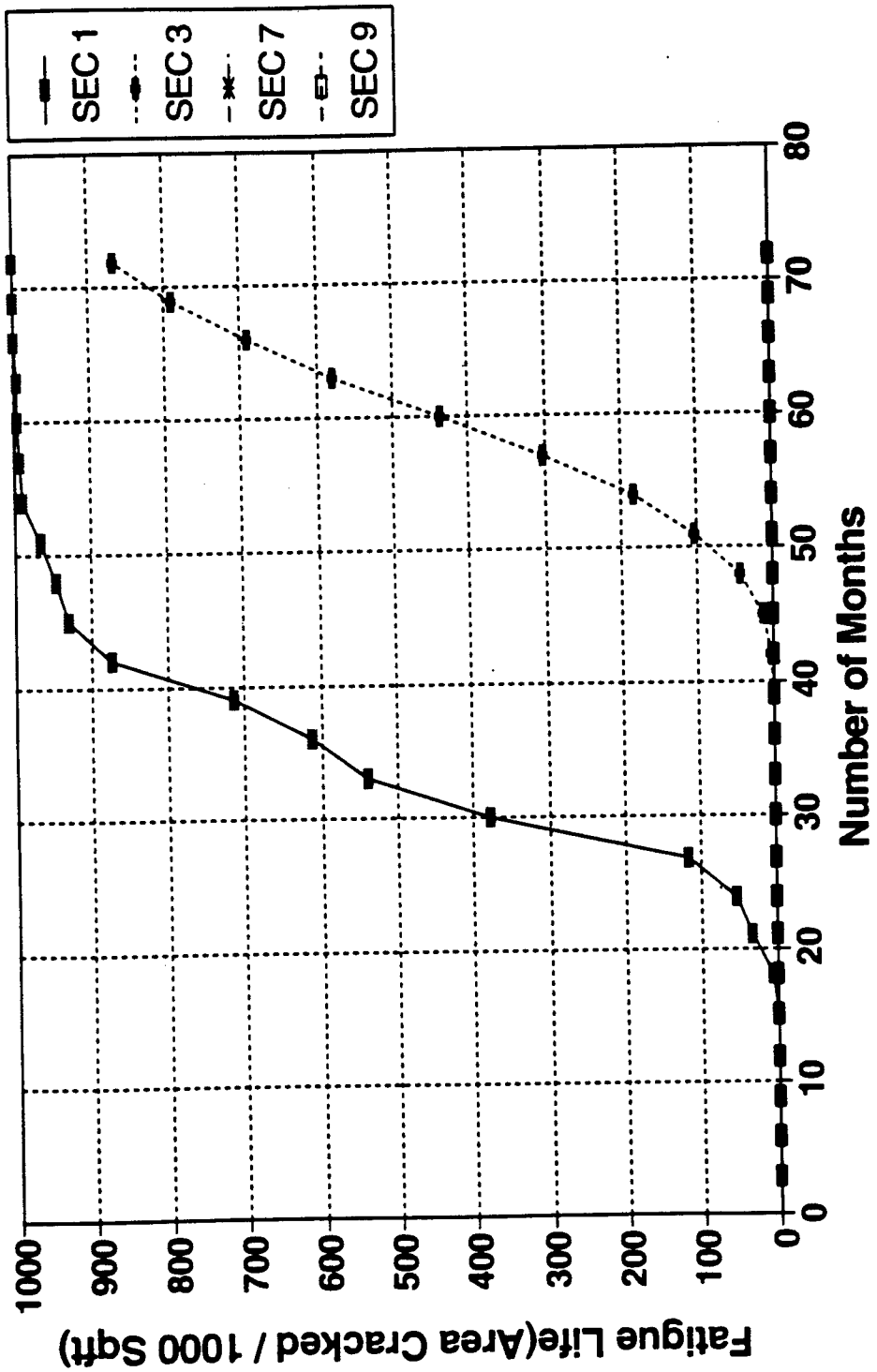

Figure 10.6 VESYS predictions for fatigue cracking predictions (Area cracked/1000 sqft) for US421 test sections.

(3) Computation of PSI using VESYS

The computation for Present Serviceability Index (PSI) used in the VESYS program is based on the following formula.

$$PSI = PSI_0 - 1.91 \log(1+SV) - 1.38\ RD^2 - 0.01\ (A)^{.5}$$

where

PSI_0 = initial serviceability index,

SV = slope variance in 10^{-6} radians

RD = rut depth in inches

A = area cracked in sq.ft/1000 ft^2

Figure 10.7 shows the decrease in PSI with time. Default values were used for SV and PSI_0 in the computation of PSI. As roughness and slope variance measurements were not made during the NCSU study, it was not possible to determine actual PSI measurements for the US421 test sections and hence comparisons between predicted and observed PSI was not possible.

10.3 Asphalt Institute Method

Since 1955, the Asphalt Institute (AI) has published nine editions of its Thickness Design Manual (MS-1). The ninth edition (shook et. al., 1981) successfully incorporated both mechanistic (analytical) and empirical state of the art information into a useful and reliable design methodology. Similar to most mechanistic design methodologies the AI method utilized fatigue and rutting design criteria to evaluate the life of the pavement. The fatigue life is evaluated using stiffness estimates of the asphalt concrete and the strain in the layer. The next section provides a comparison of the fatigue life estimates obtained using the AI method and those obtained using the dissipated energy method developed at North Carolina State University.

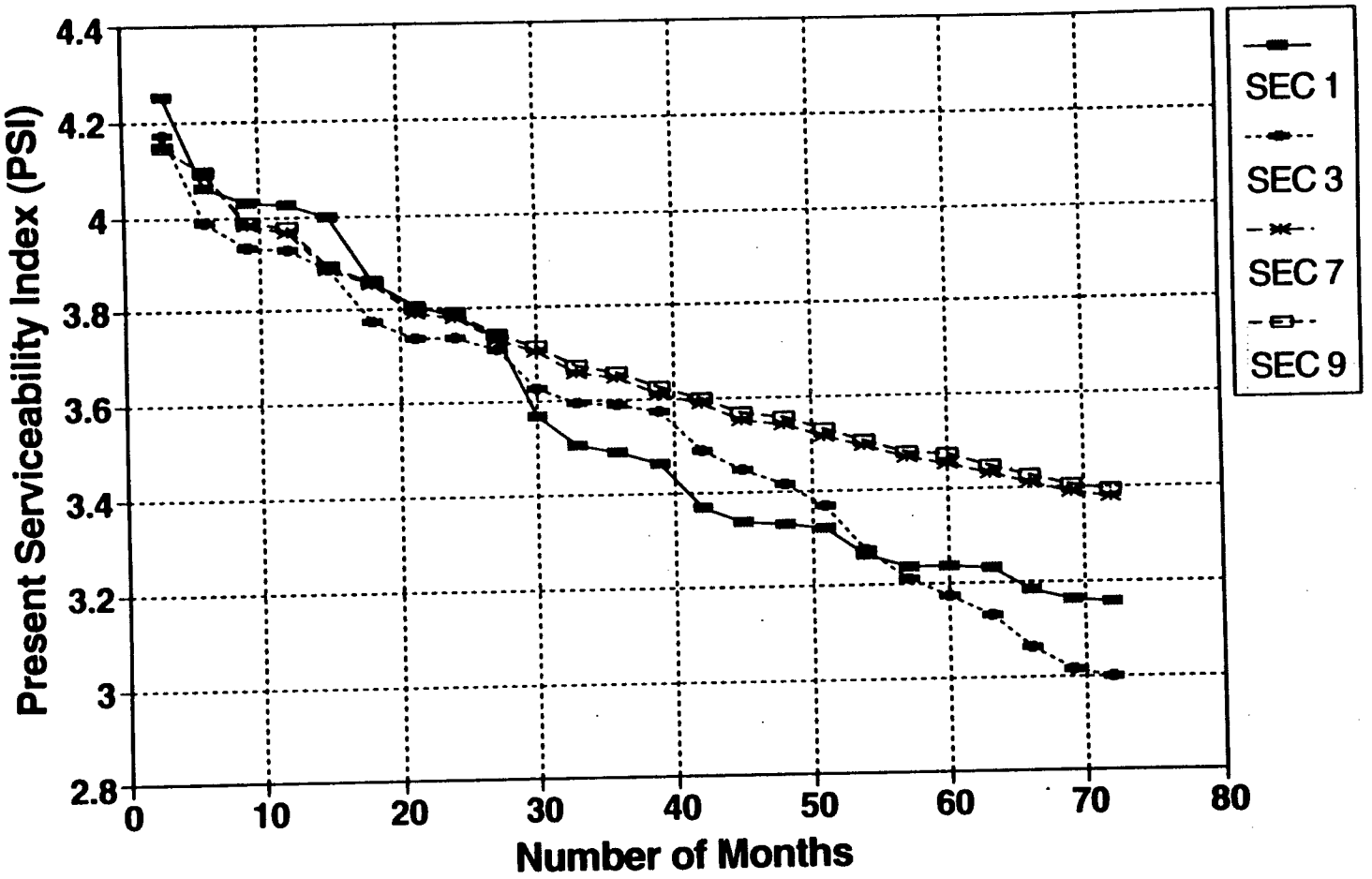

Figure 10.7 Present Serviceability Index (PSI) computation measurements for US421 test sections using the VESYS model.

10.3.1 Comparison of Fatigue Life Predictions using Asphalt Institute Method and Predictions Made using the Modified Shell Approach Developed at North Carolina State University

Like most analytically based design procedures, the AI method uses the tensile strain at the underside of the asphalt bound materials for determination of fatigue. The AI method utilizes a fatigue criteria developed by Finn et. al. (1977) with minor modifications to reflect changes in both the asphalt content and air void content.

$$N=18.4(c) \quad X \quad [4.325x10^{-3}(\epsilon_t)^{-3.291}(E^*)^{-0.854}] \qquad (10.5)$$

where

N = number of 80 KN (18-kip) equivalent single axle loads

ϵ_t = tensile strain asphalt layer (in./in. or mm/mm)

E* = asphalt mixture stiffness modulus, psi

c = function of air voids, Vv, and asphalt volume, V_b

where the correction factor is determined from:

$$c = 10^{M}$$

where

$$M=4.84[\frac{V_b}{V_v+V_b}-0.69]$$

V_b = volume of asphalt

V_v = volume of air voids

The value of c is equal to 1 when V_b = 11.1 and V_v = 5%. In the computations used

for the comparison a c value of 1 has been assumed. Figure 10.8 shows a comparison between fatigue lives predicted using the above model and the equation 6.28.3 (chapter 6). It can be observed that a reasonable match is obtained for sections 1 , 16 and 17 (differences of 16, 28 and 28%), whereas for sections 9, 7 and 12 the fatigue life predictions by both methods differ by 50-100%. Sections 1, 16 and 17 are aggregate base course sections, whereas sections 7, 9 and 12 are full depth asphalt concrete sections. It can be seen that the calibrations used for the Shook equation remains constant irrespective of the design type (depends only on binder volume and volume of voids), whereas the calibration used in the US421 study and in this comparison are specific to the given sections. Also the c factor in Shooks equation was obtained from laboratory fatigue data adjusted to provide an indication of approximately 20 percent or greater fatigue cracking. It can be seen that the Asphalt Institute model consistently over-predicts the fatigue life.

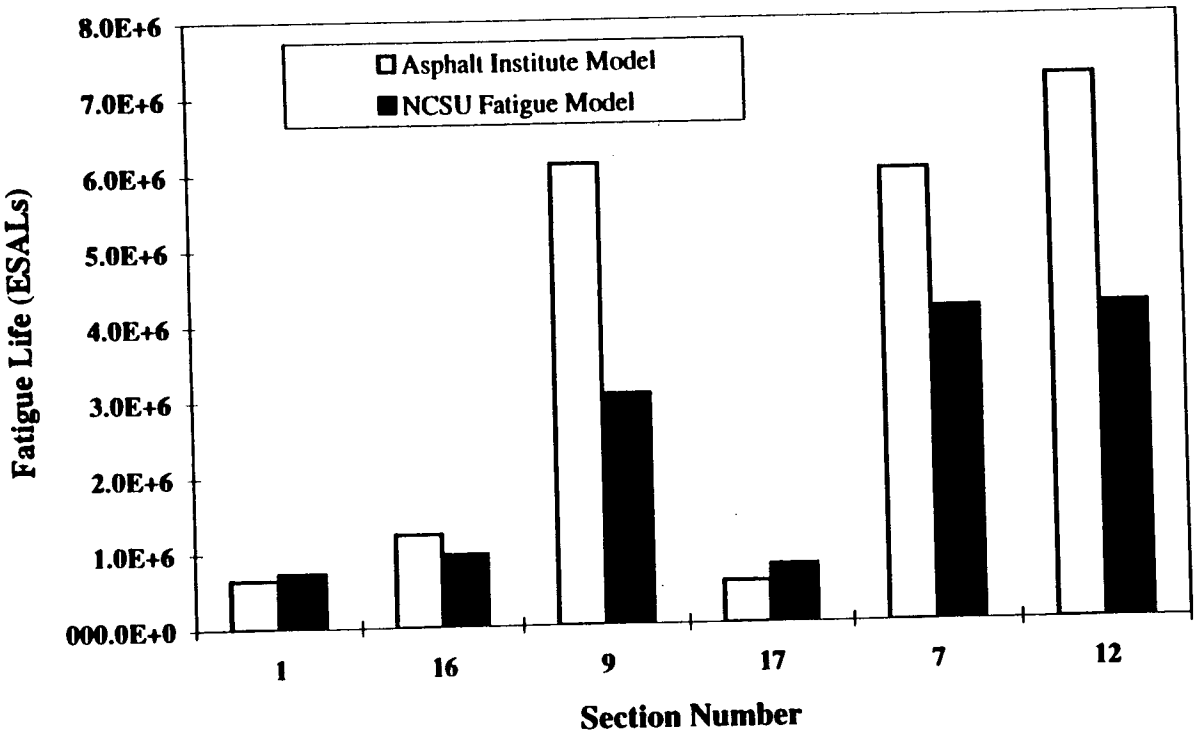

Figure 10.8 Comparison between fatigue predictions made using the Asphalt Institute method and the Modified Shell Method (developed at NCSU).

CHAPTER 11

CONCLUSIONS AND RECOMMENDATIONS

11.1 Conclusions

This research dealt with a field study to compare different designs for flexible pavements. Also, based on extensive field and laboratory testing, a comprehensive design procedure for mechanistic design of flexible pavements was developed. A computer program NCFLEX was developed that would assist the pavement engineer in designing flexible pavements based on fatigue and permanent deformation criteria.

Conclusions relating to various topics, culled from comprehensive observations and analysis performed over a period of 10 years are presented in the following subsections. The conclusions drawn will be dealt under the following broad subheadings:

(a) Field instrumentation, testing, and comparison of the different designs.

(b) Laboratory testing and modeling.

(d) Field variability and reliability computations.

(c) Mechanistic design methodology-Theory and Applications.

(e) Comparison of AASHTO, VESYS and Asphalt Institute design methods with the observed data from the US 421 test sections.

11.1.1 Field Instrumentation, Testing, and Comparison of the Different Designs

Instrumentation

(1) The stress and strain gages, and the multi-depth deflectometers for the most part performed satisfactorily. The moisture gages could not be calibrated, and hence only an approximate idea of the moisture content in the base and subgrade could be obtained from field data.

(2) Traffic data obtained from Weigh-in-Motion was considerably erratic, with periods of missing data. Nevertheless, such data can be more valuable than those obtained

with the conventional means.

(3) Non destructive test measurements made using the FWD were utilized in several ways. Primarily they were used to backcalculate the pavement layer stiffness. The process of backcalculation, its usefulness and limitations are explained in detail in Chapter 4 of this report. Also methods to utilize the surface deflection measurements from the FWD to explain the condition of the pavement were also detailed. Methods to compute Surface Curvature Index, Base Curvature Index, and Base Damage Index were detailed along with the relevance of these parameters. It was noticed that although the Base Damage Index was low for CTB sections in comparison to Aggregate Base Course sections, it did not explain the early deterioration of the CTB sections. These measurements were more useful in determining the condition of a pavement, when used among pavements with similar structural layers.

(4) Response predictions made using WES5 - a multi-layer elastic analysis program was compared with the pavement responses measured from the field instrumentation. For ABC sections, this comparison showed that the multi-layer elastic program over-predicted the tensile strain at the bottom of the asphalt concrete layers. The predicted stresses were less accurate than the predicted strains and deflections for ABC sections.

A major problem in predicting the responses from the multi-layered elastic theory for the CTB sections was the significant underestimation of the tensile strain at the bottom of the asphalt concrete layer. Deflections at different depths and stresses at the top of the subgrade were however over-predicted. The discrepancy in the measured and predicted strains was mainly due to the inability of the analysis models to account for the effects of severely deteriorated cement-treated-base courses.

The prediction of the responses for the full-depth asphalt concrete pavements is a function of how accurately the influence of temperature has been taken into account. Both stresses and strains were over-predicted by the multi-layer elastic theory. The predicted stresses do not adequately indicate the influence of subgrade

stabilization on the stresses at the top of the subgrade. Measured values of stresses however indicate a lowering of stresses on top of the subgrade due to stabilization; although, this decrease is difficult to isolate from any decrease due to the presence of a stiffer layer (black base) above the subgrade.Inspite of some shortcomings in the elastic layer analysis it is felt that such an analysis affords the most convenience, when compared with visco-elastic and finite-element approaches.

(5) The MDD rutting evaluation from the test pavements showed that the most pavement rutting was confined to the asphalt concrete layer. Furthermore, the major portion of the pavement rutting stemmed from the upper part (top 3.6 inches (9.14 cm)) of the asphalt layer.

(6) A method for validation of back-calculated moduli using multi-depth deflectometers is provided. This method, valid for sections instrumented with MDD's, makes use of the discrepancies between the measured deflections and the predicted deflections. Regardless of the ection type, surface deflections were predicted very accurately.

(7) The relationship between the air temperature and pavement temperature was developed from the temperature data measured during the field tests.

(8) Measured responses (strains, stresses, and deflections) for the FWD and 18-kip (80 KN) truck at 55 mph correlated well, irrespective of the design type. This would suggest that the FWD loading with 9-kip (40 KN) weight could be used to approximate the pavement response under a standard 18-kip (80 KN) axle load with dual wheels.

Pavement Distress Measurements and Comparison of Different Design Types Based on Performance

(9) The effects of base type and the stabilized subgrade layer on the fatigue performance were noticeable. Generally, full-depth asphalt pavements showed the best fatigue resistance, and the fatigue performance of the pavements with cement-treated base was the worst. The fatigue performance of aggregate base course sections was significantly improved when the subgrade was treated with cement or lime.

(10) Subgrade stabilization clearly showed a stiffening effect as they reduced the average

vertical strains in the subgrade. In comparing sections with and without subgrade stabilization, it was shown that subgrade stabilization decreased the average vertical strains in the asphalt layer. This could minimize the amount of rutting. Subgrade stabilization may not influence rutting to a large extent in sections with thick asphalt concrete layers where rutting maybe primarily confined to the ac layers.

Base stabilization decreased average vertical strains in the base although this is not very apparent with the cement treated base course sections which exhibited considerable block cracking. Base stabilization decreased the average vertical strains in the subgrade. The most effective form of base stabilization for this purpose was cement stabilization. Stabilization of the base layer using asphalt decreased the average vertical strains in the subgrade to a lesser extent compared to cement stabilization.

The effect of replacing a 12-inch (30.48 cm) thick aggregate base course with a 5.5-inch (13.97 cm) thick asphalt concrete base course indicated that the structural capacities in both cases were nearly the same, as a comparison of average vertical strains in the subgrade yielded similar values. On a similar note, comparisons of Sections 3 and 9 indicated that a 4 inch (10.16 cm) thick asphalt concrete base was equivalent to 8 inches (20.32 cm) of aggregate base course.

For sections without any stabilization, a 1.5-inch (3.81 cm) increase in the AC layer thickness with 4-inch (10.16 cm) reduction of the base layer thickness increased the average vertical strains in the base layer and in the subgrade. This is to say that a pavement section with a 3.5 inch (8.9 cm) AC layer and a 12 inch (30.48 cm) aggregate base layer (Section 1) is not equivalent to a pavement section with a 5 inch (12.70 cm) AC layer with a 8 inch (20.32 cm) aggregate base course (Section 3).

(11) The most commonly encountered distress types were longitudinal cracking, fatigue cracking, patching, and rutting. Sections with cement treated base course, regardless of subgrade stabilization, performed the worst. This could be attributed to the cracking of the CTB layers that manifested themselves as reflective cracks on the surface. Although CTB sections did exhibit extensive cracking, calculation of Base

Damage Index (BDI) for the various sections proved that the structure by itself was considerably sound. Nevertheless, such extensive cracking necessitated early overlays. For ABC sections, subgrade stabilization considerably enhanced their performance. Sections with cement-stabilized subgrade performed relatively better than lime-stabilized sections. Comparison of moduli values clearly indicate that the cement-stabilized subgrades were much stiffer in comparison to the lime-stabilized subgrades.

11.1.2 Laboratory Testing and Modeling

New performance prediction models for fatigue cracking and permanent deformation (rutting) of asphalt concrete layers were developed through extensive field tests and various laboratory material characterization. Within the limits of this study, the following principal conclusions regarding fatigue tests on AC specimens can be drawn:

(1) Diametral fatigue test is a practical tool for evaluating the fatigue performance of asphalt concrete.

(2) The maximum total horizontal deformation values of 0.01, 0.02, and 0.10 inch (0.25, 0.51, 2.54 mm) were found to be appropriate failure criteria at 32, 50, and 68°F (0, 10, and 20°C), respectively, for all the mixtures studied in this research.

(3) The dissipated energy concept has been applied to modeling of fatigue cracking using two different approaches: (I) Internal Damage Ratio growth method which accounts for the damage growth throughout the entire fatigue life and (ii) modified Shell method which relates the dissipated energy at early cycles to the fatigue life

The study on permanent deformation (rutting) of asphalt concrete layers resulted in the following conclusions:

(4) The repetitive axial loading test with confinement was developed as a means of characterizing the rutting performance of asphalt concrete.

(5) A new laboratory test protocol was developed based on the study of the field data. This protocol divides asphalt layer(s) into three categories depending upon the depth. Different temperatures and vertical stress levels were used in these areas.

(6) The layer-strain theory was applied to predict the rutting of the entire asphalt concrete

layers.

11.1.3 Field Variability and Reliability Computations

(1) Seasonal variation in the backcalculated values for the various layers in different test sections was observed. The variability in the ac modulus was primarily due to temperature variation and loss of support. The underlying layers experience varying seasonal moduli values due to different moisture conditions during different seasons. The performance prediction models used in this study were affected more by the variation in the ac layer moduli than the variation in the base and subgrade moduli.

(2) To account for the changing moisture conditions affecting the moduli values of the aggregate base course and subgrade during different seasons, a reliability based chart was created to select stiffness values for the aggregate base course and subgrade values at specified levels of reliability for different seasons. These charts may be used when conditions similar to those observed in the study are experienced. In other cases, based on the methodology provided in this study, similar charts can be created for use in the design process.

(3) A methodology using the Point Estimate Method has been provided, wherein one can predict the variability in fatigue life using available data on variability in layer properties. The application of the following method has been demonstrated in Chapter 9. This methodology could be used to develop design charts for selecting layer thicknesses based on varied levels of reliability.

11.1.4 Mechanistic Design Methodology-Theory and Applications

(1) In order to aid the pavement design process, a mechanistic based computer program (NCFLEX) was designed based on the experience garnered from the field testing carried out during the course of this project. NCFLEX is an analysis and design program for flexible pavement systems that allows the user to design systems that are similar to those employed in this study. The program is generic, and with additional calibration data from further studies, it can be used to design pavements composed

of materials different from those used in this study. The program iteratively alters thickness of any given layer to arrive at a design that satisfies criteria based on fatigue and rutting. The program is a microsoft windows based program and hence is user-friendly.

(2) Based on the comparison between the field and the predicted performances, calibration (shift) factors were proposed for the fatigue prediction model and for the rutting model. Different fatigue calibrations factors are suggested based on the structural design of the pavement. A value of 1.5 is used as the calibration factor for the rutting model for all flexible pavement designs used in this study.

11.1.5 Comparison of AASHTO, VESYS and Asphalt Institute Design Methods with the Observed Data from the US 421 Test Sections

Comparison with AASHTO Analysis

(1) It is noticed that for most sections, the life to failure as predicted by the AASHTO method is much higher than the predicted fatigue life based on a failure criteria of 15% fatigue cracking. This disparity can be explained based on the fact that the AASHTO defines failure based on the serviceability concept that takes into consideration factors that include fatigue, rutting, roughness, slope variance etc., whereas failure as defined in this study was based only on fatigue and rutting.

(2) For sections 1 and 3 (ABC sections), and sections 7 and 9 (full depth ac sections), the AASHTO predicted number of ESALs to failure was lower than the 15% fatigue cracking limit adopted by the North Carolina Department of Transportation to indicate failure.

(3) Although the AASHTO method is a comprehensive method for pavement design, because of its non-mechanistic nature, the method does not provide adequate quantifiable information on rutting and fatigue. Nevertheless, it incorporates concepts such as serviceability that are not available with the NCFLEX method. From

the standpoint of the practice followed by the North Carolina Department of Transportation, overlay decisions are based primarily on fatigue and rutting levels reached, and hence a mechanistic design program like NCFLEX could prove to be very useful.

Comparison with VESYS Analysis

(1) Computation of rutting for sections 1, 3 and 7 were performed using VESYS. It can be seen that maximum rut depths were observed for section 3, followed by section 7, and then by section 1. A comparison of rutting for sections 1, 3 and 7, with field measured rut depths, indicated that VESYS over-predicted the rutting. The VESYS method computes total rutting based on rutting experienced by all layers including the aggregate base course and the subgrade. However, the field testing (with the help of the multi-depth deflectometers) suggested that almost all the rutting occurred in the ac layers only. This could account for the discrepancy in the prediction of rutting by VESYS.

(2) Fatigue computation and calculation of PSI (Present Serviceability Index) values for various US 421 sections were performed utilizing the VESYS method. Although, the NCFLEX program can provide estimates of fatigue and rutting, the method cannot be used to determine serviceability parameters like PSI.

Comparison with the Asphalt Institute Method

Predictions made using the Asphalt Institute fatigue model were compared with the calibrated model developed using the US421 data. A comparison of fatigue lives computed by both the methods indicate a reasonable match for aggregate base course sections (differences in fatigue life predictions of 16-28%), whereas, for full-depth sections the fatigue life predictions by both methods differ by 50-100%. For full depth sections the AI method over-predicted fatigue lives as compared to the calibrated fatigue model used in this study

11.2 Recommendations

Further research is recommended in the following areas to improve the performance prediction procedure of flexible pavements. A few recommendations are listed below:

(1) It is recommended that when using strain and stress gages in the field, a large number of them should be employed to take into account any possible failure, and to increase the confidence in the readings obtained.

(2) This study was limited to only three conventional asphalt concrete mixtures (HDS, HDB, and HB). Additional asphalt concrete mixtures made up of modified asphalts, large stone mixes, etc. should be included in further studies. A broad representation of the roads in different geographical locations with varying materials and environmental conditions will aid in developing a good data bank for establishing calibration factors (for performance prediction models) for future pavement design.

(5) Cement treated pavements showed very early signs of distress . This was attributed to the thin ac cover provided. Further work is needed to accurately model CTB pavements, considering the damage mechanisms are very much different than for full depth and aggregate base course sections.

(6) Nondestructive testing techniques should be used for evaluating the pavements. Also, improvements in the correlations developed between actual laboratory test values and field measurements (measured using nondestructive testing techniques) will aid in the development of a more practical, economical, and realistic design procedure for new pavements.

(7) An extensive database of calibration factors need to be developed so as to make the fatigue model universally acceptable. Use of factors such as healing when incorporated into the fatigue model, could help in decreasing the calibration factor by accounting for a portion of the uncertainty in shifting from laboratory observation to actual field conditions.

(8) The rutting model utilized in this study accounts for rutting in the ac layer only. This was in agreement with observed rutting in the field and as validated by the MDDs. For sections experiencing rutting in all the layers it would be necessary to consider other rutting models that can explain rutting in the non ac layers.

LIST OF REFERENCES

1. AASHTO. (1986). AASHTO pavement design guide. American Association of State Highway and Transportation Officials, Washington D.C.

2. Allen, D.L., and R.C. Graves, Variability in measurement of in-situ material properties.The Fourth International Conference on the Bearing Capacity of Roads and Airfields,1994, Vol 2, pp.989-1006.

3. Barksdale, R.D., "Laboratory Evaluation of Rutting in Base Course Materials," Proceedings, Third International Conference on the Structural Design of Asphalt Pavements, Vol.I, London, 1972.

4. Barksdale, R.D., "Compressive Stress Pulse Times in Flexible Pavements for Use in Dynamic Testing," Proceedings, Highway Research Board, Vol.345, 1971.

5. Barksdale, R.D. and J.H. Miller II, "Development of Equipment and Techniques for Evaluating Fatigue and Rutting Characteristics of Asphalt Concrete Mixes," School of Civil Engineering, Georgia Institute of Technology, 1977.

6. Bazin, P. and J.B.Saunier, "Deformability, Fatigue and Healing Properties of Asphalt Mixes," Proceedings, Second International Conference on the Structural Design of Asphalt Pavements, University of Michigan, 1967.

7. Berry, H.K., and R.C. Panuska, (1987)."Manufacture of an accelerated loading facility (ALF)- Executive summary." FHWA/RD-87/07. Federal Highway Administration. Washington, D.C.

8. Bohn, A.O., R.N. Stubstad, Anders Sorensen, and Per Simonsen, "Rheological Properties of Road Materials and their Effect on the Behavior of a Pavement Section Tested in a Climate Controlled, Linear Track Road Testing Machine," Proceedings, Association of Asphalt Paving Technologists, Vol.46, 1977.

9. Bonnaure, F.P., G. Gest, A. Gravois, and P. Uge, "A New Method of Predicting the Stiffness of Asphalt Paving Mixtures," Proceedings, Association of Asphalt Paving Technologists, Vol.46, 1977.

10. Bonnot, J., "Asphalt Aggregate Mixtures," Transportation Research Record 1096, Transportation Research Board, 1986.

11. Brown, S.F. and C.A. Bell, "The Prediction of Permanent Deformation in Asphalt Pavement," Proceedings, Association of Asphalt Paving Technologists, 1979.

12. Brown, S.F. and C.A. Bell, "The Validity of Design Procedures for the Permanent Deformation of Asphalt Pavements," Proceedings, Fourth International Conference on the Structural Design of Asphalt Pavements, Vol.I, Ann Arbor, 1977.

13. M. Burmister," The General Theory of Stresses and Displacements in Layered Soil Systems", Journal of Applied Physics, August 1944.

14. Byrd, L.G., and R.L. Hutchinson,(1985)."Pavement Testing conference."FHWA/RD-86/078, Federal Highway Administration, Washington, D.C.

15. Chomton, G. and P. J. Valayer, "Applied Rheology of Asphalt Mixes, Practical Applications," Proceedings, Third International Conference on the Structural Design of Asphalt Pavements, London, Vol.I, 1972.

16. Chou, Y.J., J. Uzan, and R.L. Lytton, "Backcalculation of Layer Moduli from Nondestructive Pavement Deflection Data Using the Expert System Approach. In Nondestructive Testing of Pavements and Backcalculation of Moduli," Special Technical Publication 1026, American Society for Testing and Materials, 1989, pp. 341-354.

17. Chua, K.N. , "Evaluation of Moduli Backcalculation Programs for Low-Volume Roads. In Nondestructive Testing of Pavements and Backcalculation of Moduli.," Special Technical Publication 1026, American Society for Testing and Materials, 1989, pp. 398-414.

18. Chou,Y.T., "Probabilistic and Reliability Design Procedures for Flexible Airfield Pavements - Elastic layered mathod", Final report for Department of the Army, US Army Corps of engineers, Washington, D.C. 20314-1000,September 1987.

19. Christison, J.T., D.W. Murray, and K.O. Anderson.,1972, " Stress prediction and low temperature fracture susceptibility of asphalt concrete pavements," Proceedings, Association of Asphalt Paving Technologists, Vol 41, pp.494-523.

20. Claussen,A.I.M., J.M. Edward, P. Sommer, and P.Uge, 1977, "Asphalt Pavement Design - The SHELL Method,"Proceedings, 4th International Conference on the Structural Design of Asphalt Pavements, Vol 1, pp.39-74.

21. Dukatz, E.L.Jr., "Aggregate Properties Related to Pavement Performance," Proceedings, Association of Asphalt Paving Technologists, Vol.58, 1989.

22.. Fairhurst, C.E., Y.R. Kim, and N.P. Khosla, "Resilient Modulus Testing of Asphalt Specimens with ASTM D 4123-82," Proceedings, RILEM Fourth International Symposium, Budapest, Hungary, 1990.

23. Finn, R.N. and C.L. Monismith. Asphalt Overlay Design Procedures, NCHRP Synthesis of Highway Practice #116, Transportation Research Board, Washington, DC, 1984.

24. Finn, F.N., C. Saraf, R. Kulkarni, K.Nair, W.Smith and A.Abdullah, " The use of Distress Prediction Subsystems for the Design of Pavement Structures," Proceedings, Vol I, Fourth International Conference on the Structural Design of Asphalt Pavements, pp. 3-38, 1977.

25. Freeme, C.R., J.H. Maree, and A.W. Viljeon, "Mechanistic Design of Asphalt Pavements and Verification Using the Heavy Vehicle Simulator," Proceedings, Fifth International Conference of the Structural Design of Asphalt Pavements, Vol.I, Delft, The Netherlands, 1982.

26. Frocht, M.M., "Photoelasticity," Vol.2, John Wiley and Sons, New York, 1957.

27. Hadley, W.O. and H. Vahida, "Fundamental Comparison of the Flexural and Indirect Tensile Tests," Transportation Research Record No.911, Transportation Research Board, Washington, D.C., 1983.

28. Harr, M.E. Reliability-Based Design in Civil Engineering, McGraw Hill, N.Y. 1987.

29. Harvey, J.,"Asphalt Concrete Specimen Preparation Protocol SHRP Project A-OO3A," Technical Memorandum 90-4 Prepared for SHRP, Institute of Transportation Studies, University of California, Berkeley, 1990.

30. HRB,1952. Final Report on Road Test one MD,Special Report 4, Highway Research Board.

31. HRB,1955. The WASHO Road Test,Part 2;Test Data, Analysis and Findings, Special Report 22, Highway Research Board.

32. HRB 1962. The AASHO Road Test, Report 5;Pavement Research;Report 6;Special Studies; and Report 7;Summary Report,Special reports 61E,61F,and 61G,Highway Research Board.

33. Highway Research Board, "The AASHO Road Test," Special Report 73," Publication No.1012, Washington, D.C., 1962.

34. Hillel, D. Soil and Water: physical principles and processes. Academic Press, Inc., New York, N.Y. 1971.

35. Hofstra, A. and A.J.G. Klomp, "Permanent Deformation of Flexible Pavement under Simulated Road Traffic Conditions," Proceedings, Third International Conference on the Structural Design of Asphalt Pavement, Vol.1, 1972.

36. Huang, Y.H., "Pavement Analysis and Design," Prentice Hall, New Jersey, 1993.

Huhtala, M., Risto Alkio, Jari Pihlajamäki, Marku Pienimäki, and Pekka Halonen, "Behavior of Bituminous Materials under Moving Wheel Loads," AAPT, February 1990, Albuquerque, New Mexico.

37. Ioannides, A.M, "Mechanistic Performance Modeling: A Contradiction in terms," Proceedings of the 7th International Conference on Asphalt Pavements, Vol 5, 19992.

38. Isada, N.M., "Detecting Variations in Load Carrying Capacities of Flexible Pavements," NCHRP Report No. 21, Highway Research Board, Washington D.C., 1966.

39. Kennedy, T.W. and W.R. Hudson, "Application of the Indirect Tensile Test to Stabilized Materials," Highway Research Board Annual Meeting, 1968.

40. Kennedy, T.W., "Characterization of Asphalt Pavement Materials Using the Indirect Tensile Test," Proceedings, Association of Asphalt Paving Technologists, Vol.46, 1977.

41. Kenis, W.J., "Predictive Design Procedures- A Design Method for Flexible Pavements Using the VESYS Structural Subsystem." Proceedings, Fourth International Conference on the Structural Design of Asphalt Pavements, Vol.I, Ann Arbor, 1977.

42. Khosla, N.P., "Investigation of Premature Distress in Flexible Pavements," Research Report 17845, Center for Transportation Engineering Studies, North Carolina State University, Raleigh, NC, June 1984.

43. Khosla, N.P. and M.S. Omer, "Characterization of Asphalt Mixture for Prediction of Pavement Performance," Transportation Research Record No.1034, Transportation Research Board, Washington, D.C., 1985.

44. Khosla, N.P., Y.R. Kim, S. Satish, and N. Kim, "A Comparative Study of Performance of Different Designs for Flexible Pavements," Interim Report, Research Project No.23241-87-1, Department of Civil Engineering, North Carolina State University, June 1992.

45. Khosla, N.P. and S.J. Zahran," The Role of Modified Asphalt Binders in the Performance of Pavements," Center for Transportation Engineering Studies, Research Report 23241-87-2, 1989.

46. Kim, N., "Effect of Temperature and Mixture Variables on Fatigue and Permanent Deformation of Asphalt Concrete," Master Thesis, North Carolina State University, 1991.

47. Kim, N., "Development of Performance Prediction Models for Asphalt Concrete Layers," Doctoral Dissertation, Department of Civil Engineering, North Carolina State University,1994.

48. Kim, Y.R., N.P. Khosla, and N. Kim, "Effect of Temperature and Mixture Variables on Fatigue Life Predicted by Diametral Fatigue Testing," Published in 1991 Annual Meeting of the Transportation Research Board, 1991.

49. Kim, Y.R., N.P. Khosla, S. Satish, and T. Scullion. Validation of Moduli Backcalculation Procedure Using Multidepth Deflectometers Installed in Various Flexible Pavement Structures. Published in the Symposium Proceeding on Nondestructive Deflection Testing and Backcalculation for Pavements, Transportation Research Board, 1992.

50. Kim, Y.R., N. Kim, and N.P. Khosla, " Effect of Aggregate Type and gradation on Fatigue and Permanent Deformation of Asphalt Concrete," Published in 1992 ASTM STP 1147, 1992.

51. Kim, Y.R. and Y.C. Lee, "Characterization of Damage Growth in Asphalt Concrete," Final Report Submitted to Texas A&M Research Foundation, Department of Civil Engineering, North Carolina State University, December 1992.

52. Langsner, G., T.S. Huff, and W.J. Liddle, "Use of Road Test Findings by AASHO Design Committee," Highway Research Board Special Report 73, Washington, D.C., 1962, pp.399-414.

53. Lenngren, C.A. Relating deflection data to pavement strain. Transportation Research Record 1293

54. Little, D.N., J.W. Button, and H. Youssef, "Development of Criteria to Evaluate Uniaxial Creep Data and Asphalt Concrete Permanent Deformation Potential," Published in 1993 Annual Meeting of the Transportation Research Board, 1993.

55. Lytton, R.L. Backcalculation of Pavement Layer Properties. In Nondestructive Testing of Pavements and Backcalculation of Moduli. Special Technical Publication

1026, American Society for Testing and Materials, 1989, pp. 7-38.

56. Lytton, R.L. and D. Zollinger, "Modelling Reliability in Pavement", presented in the 72nd Annual Meeting, Transportation Research Board, Washington D.c., January 1993.

57. Malpass, G. Use of Ground Tire Rubber in Asphalt Concrete Pavements. PhD Thesis, North Carolina State University, 1994.

58. Mahboub, K. and D.N. Little, "Improved Asphalt Concrete Design Procedure," Research Report 474-1F, Texas Transportation Institute, 1988.

59. Mathew, J., "Variation of Resilient Modulus with water content and applied stress for different soils at constant compactive effort", Report, Department of Civil engineering, North Carolina State University, Dec. 1994.

60.. McLean, D.B., "Permanent Deformation Characteristics of Asphalt Concrete," Ph.D. Dissertation, University of California, Berkeley, 1974.

61. McRae, J.L., "Gyratory Testing Machine," Technical Manual, Engineering Developments Company Inc., Vicksburg, Mississippi.

62.. Moavenzadeh, F. and J.F. Elliat, "A Stochastic Approach to Analysis and Design of Highway Pavements," Proceedings, Third International Conference on the Structural Design of Asphalt Pavements, Vol.I, London, 1972.

63. Molenaar, A.A.A. State of the Art of Pavement Evaluation. Keynote address presented at the Fourth International Conference on the Bearing Capacity of Roads and Airfields,1994, Vol 2,pp.1781-1801.

64. Monismith, C.L., J.A. Epps, and F.N. Finn, "Improved Asphalt Mix Design," Proceedings, Association of Asphalt Paving Technologists, Vol.54, 1985.

65. Monismith, C.L., K. Inkabi, C.R. Freeme, and D.B. Mclean, "A Subsystem to Predict Rutting in Asphalt Concrete Pavement Structures," Proceedings, Fourth International Conference on Structural Design of Asphalt Pavements, Vol.I, Ann Arbor, 1977.

66. Monismith, C.L. and A.A. Tayebali, "Permanent Deformation (Rutting) Considerations in Asphalt Concrete Pavement Sections," Proceedings, Association of Asphalt Paving Technologists, Vol.57, 1988.

67. MTS Reference Manual, "810 Material Test System," Job #948.04, Vol.1, 2, 3 of 3,

1989.

68. Nair, K., W.S. Smith, and G.Y. Chang, "Characterization of Asphalt Concrete and Cement-Treated Granular Base Courses," Materials Research and Development, Technical Report, Oakland, California, 1972.

69. Nunn, M.E., "Prediction of Permanent Deformation in Bituminous Pavement Layers," Research Report 26, Transport and Road Research Laboratory, 1986.

70. OECD, Strain Measurements in Bituminous Layers, Road transport research, Swiss federal office of Highways, Berne 1985.

71. OECD Full-Scale Pavement Test. Report prepared by an OECD Scientific Expert Group, Organisation for Economic Co-operation and Development, 1991.

72. Ong, C.L., D.E. Newcomb, and R. Siddharthan. Comparison of Dynamic and Static Backcalculation Modulus for Three Layer Pavements. Preprint from 1992 Transportation Research Board Annual Meeting, Washington, D.C., 1992.

73. Paterson, W.D.O. and A.D. Chesher, "On Predicting Pavement Surface Distress with Empirical Models of Failure Times", Transportation research Record 1095.

74. Pavement accelerated loading facility (ALF), design, construction and development - Mechanical and structural aspect. (1985). Department of Main Roads, New South wales, Australia.

75. "Predictive Design Procedures, VESYS Users Manual An Interim Design Method for Flexible Pavements Using the VESYS Structural Subsystem," U.S. Federal Highway Administration, Washington, D.C., January 1978.

76. Pronk, A.C. and P.C. Hopman, "Energy Dissipation: the Leading Factor of Fatigue," Conference Proceedings, The United States Strategic Highway Research Program-Sharing the Benefits, London, 1990.

77. Quintus, H.L.V., J.B. Rauhut, and T.W. Kennedy, "Comparisons of Asphalt Concrete Stiffness as Measured by Various Testing Techniques," Proceedings, Association of Asphalt Paving Technologists, Vol.51, 1982.

78. Rada, G.R, C.W. Schwartz, M.W. Witczack, and S. Jafroudi, Analysis of climate effects on performance of unpaved roads. ASCE.

79. Raithby, K.D. and A.B. Sterling, "The Effect of Rest Periods on the Fatigue Performance of a Hot-Rolled Asphalt under Reversed Axial Loading," Proceedings,

Association of Asphalt Paving Technologists, 1970.

80. Rao Tangella, S.C.S., J. Craus, J.A. Deacon, and C.L. Monismith, "Summary report on fatigue response of asphalt mixtures", Report TM-UCB-A-003A-89-3, Institute of Transportation Studies, Berkeley, California, 1990.

81. Road Note 29, A guide to the structural design of pavements for new roads, Third Edition, Road Research laboratory, Department of Environment,London 1978.

82. Road Note 31, A guide to the design of Bitumen Surfaced Roads in Tropical and Sub-Tropical Countries,Third Edition, Road Research laboratory, Department of Environment, Department of Transport,London 1977.

83.. Roberts, F.L., P.S. Kandhal, and E.R. Brown, "Hot Mix Asphalt Materials, Mixture Design, and Construction," NAPA Education Foundation, Maryland, 1991.

84. Romain, J.E., "Rut Depth Prediction in Asphalt Pavements," Proceedings, Third International Conference on the Structural Design of Asphalt Pavements, Vol.II, Ann Arbor, 1972.

85. Rosenblueth, E."Two point estimates in Probabilities", Applied Math Modelling, 1981.

86. Rosenbueth, E., "Point Estimates for Probability Moments", Proceedings, National Academy of Sciences, Mathematics, Vol. 72, No. 10, pp. 3812-3814, 1975.

87. Ruth, B.E. and G.K. Olson, "Creep Effects on Fatigue Testing of Asphalt Concrete," Proceedings, Association of Asphalt Paving Technologists, Vol.46, 1977.

88. Saal, R.N.J., and P.S. Pell, kolloid Zeitschrift MI, Heft 1, pp. 66-71, 1960.

89. Satish, S. "NCFLEX version 1.0 - a Windows Based Computer Program for the Design and Analysis of Flexible Pavement Systems". North Carolina State University, 1996.

90. Sousa, J.B. and J. Craus, "Summary Report on Permanent Deformation in Asphalt Concrete," Institute of Transportation Studies, University of California, Berkeley, 1990.

91. Sousa, J.B., R. Taylor, and A.J. Tanco, "Analysis of Some Laboratory Testing Systems for Asphalt-Aggregate Mixtures," Transportation Research Board Paper No.91-0743, 1991.

92. Sousa, J.B., "Dynamic Properties of Materials for Pavement Design," Ph.D.Thesis, University of California at Berkeley, 1986.

93. Sebaaly, Peter E., Anderson, David A., and Tabatabaee, Nader (1989). "Performance of Full Scale Pavement Under Accelerated Loading.", ASCE, VOL 115, NO. 4 (1989).

94. Schmidt, R.J., "A practical Method for Measuring the Resilient Modulus of Asphalt-Treated Mixes," Highway Research Board Annual Meeting, 1972.

95. Scholz, T., "Evaluation of Cold In-Place Recycling of Asphalt Pavement in Oregon," Master Thesis, Oregon State University, 1989.

96. Scullion, T., R.C. Briggs, and R.L. Lytton. Using the Multidepth Deflectometer to Verify Modulus Backcalculation Procedures. In Nondestructive Testing of Pavements and Backcalculation of Moduli. Special Technical Publication 1026, American Society for Testing and Materials, 1989, pp. 90-101.

97. Scullion.T., J. Uzan, and M. Parades. A microcomputer-based backcalculation system. Transportation Research Record, No. 1260, Transportation Research Board, 1990, pp. 180-192.

98. Scullion, T., J. Uzan, J.I. Yazdani, and P. Chan. Field Evaluation of the Multi-Depth Deflectometers. Research Report 1123-2. Texas Transportation Institute, September 1988.

99. Shook, J.F., F.N. Finn, M.W. Witczak, and C.L. Monismith. Proceedings, Fifth International Conference on the Structural Design of Asphalt Pavements held at The Delft University of Technology, The Netherlands, August 23-26, 1982, Vol. I, pp. 17-44

100. Shook, J.F., F.N. Finn, M.W. Witczak, C.L. Monismith."Development of The Asphalt Institute Thickness Design Manual (MS-1), Ninth Edition", Research Report Number 81-2 (RR-81-2).The Asphalt Institute, College Park, Maryland.

101. Southgate, H.F. and R.C. Deen, "Temperature Distribution within Asphalt Pavements and its Relationship with Pavement Deflections", Highway Research Record 261, Transportation Research Board, Washington, D.C., 1969.

102. Strategic Highway Research Program (SHRP), "Distress Identification Manual for the Long-Term Pavement Performance Studies," SHRP LTPP/FR-90-001, National Research Council, 1990.

103. Stubstad, R.N., N.P. Khosla, and W.W. Wynn. Construction of Fully Instrumented Test Pavements in North Carolina. CRREL Symposium. Proceedings on State of the Art of Pavement Response Monitoring Systems for Roads and Airfields, West Lebanon, N.H., 1989.

104. Tayebali, A.A., G.M. Rowe, and J.B. Sousa, "Fatigue Response of Asphalt-Aggregate Mixtures," Proceedings, Association of Asphalt Paving Technologists, 1992.

105. Tayebali, A.A., J.A. Deacon, and C.L. Monismith, "Modeling Fatigue Response of Asphalt-Aggregate Mixtures," Proceedings, Association of Asphalt Paving Technologists, 1993.

106. Terrel, R.L. and I.S. Awad, "Laboratory Considerations," Proceedings, Association of Asphalt Paving Technologists, 1972.

107. Thompson, M.R. "Environmental factors and pavement systems," Construction Engineering Research Laboratory Technical Report, March, 1970.

108. Thompson., M.R. and R.P. Elliot, 1985." ILLIPAVE - Based Response Algorithms for Design of Flexible Pavements," Transportation Research Record 1043, TRB, pp. 50-57.

109. Thrower, E.N., "Methods of Predicting Deformation in Road Pavements," Proceedings, Fourth International Conference on the Structural Design of Asphalt Pavements, Vol.I, Ann Arbor, 1977.

110. Thrower, E.N., S. Mortazavi, and J.W. Dorgill, "Methods for Predicting Permanent Deformation in Flexible Pavements," Contractor Report 38, Transport and Road Research Laboratory, 1986.

111. Timoshenko, S. and J.N. Goodier, "Theory of Elasticity," 2nd Edition, McGrawHill, New York, 1951.

112. Turnbull, W.J., and R.G. Ahlvin, "Mathematical Expression of the CBR Relations", Proceedings, 4th Internationsl Conference on Soil Mechanics and Foundation Engineering, Vol. 2, pp. 178-180, 1957.

113. Uge, P. and van de Loo, P.J., "Permanent Deformation of Asphalt Mixes," Koninklijke/Shell-Laboratorium, Amsterdam, 1974.

114. Ullidtz, P., Pavement Analysis, Elsevier Science, New York, 1987.

115. Ullidtz, P. and R.N. Stubstad, "Analytical-Empirical Pavement Evaluation Using the Falling Weight Deflectometer," Transportation Research Board, TRR #1022, Washington, DC, 1985.

116. van de Loo, P.F., "Creep Testing, A Simple Tool to Judge Asphalt Mix Stability," Proceedings, Association of Asphalt Paving Technologists, Vol.43, 1974.

117. Van Cauwelaert, F.J., D.R. Alexander, T.D. White, and W.R. Barker. Multilayer Elastic Program for Backcalculating Layer Moduli in Pavement Evaluation. In Nondestructive Testing of Pavements and Backcalculation of Moduli. Special Technical Publication 1026, American Society for Testing and Materials, 1989, pp. 171-188.

118. van Dijk, W., "Practical Fatigue Characterization of Bituminous Mixes," Proceeding, Association of Asphalt Paving Technologists, Vol.44, 1975.

119. van Dijk, W. and W. Visser, "The Energy Approach to Fatigue for Pavement Design," Proceeding, Association of Asphalt Paving Technologists, 1977.

120. Von Quintus, H.L., Scherocman, J.A., Hughes, C.S., and Kennedy, T.W., "Asphalt Aggregate Mixture Analysis System (AAMAS)," NCHRP Report 338, 1991.

121. Yapp, M., R.G. Hicks, and B. Connor. Development of an Improved Overlay Design Procedure for the State of Alaska, Department of Transportation and Public Facilities, Fairbanks, Alaska, 1987.

122. Yoder, E.J. and M.W. Witczak, "Principles of Pavement Design," 2nd Edition, John Wiley and Sons, New York, 1975.

123. Zahran, S.J., "A Mechanistic Evaluation of Modified Asphalt Paving Mixtures," Ph.D. Dissertation, North Carolina State University, Raleigh, NC, 1988.

APPENDIX A

TEST SECTION PROFILES AND GAGE INSTALLATION

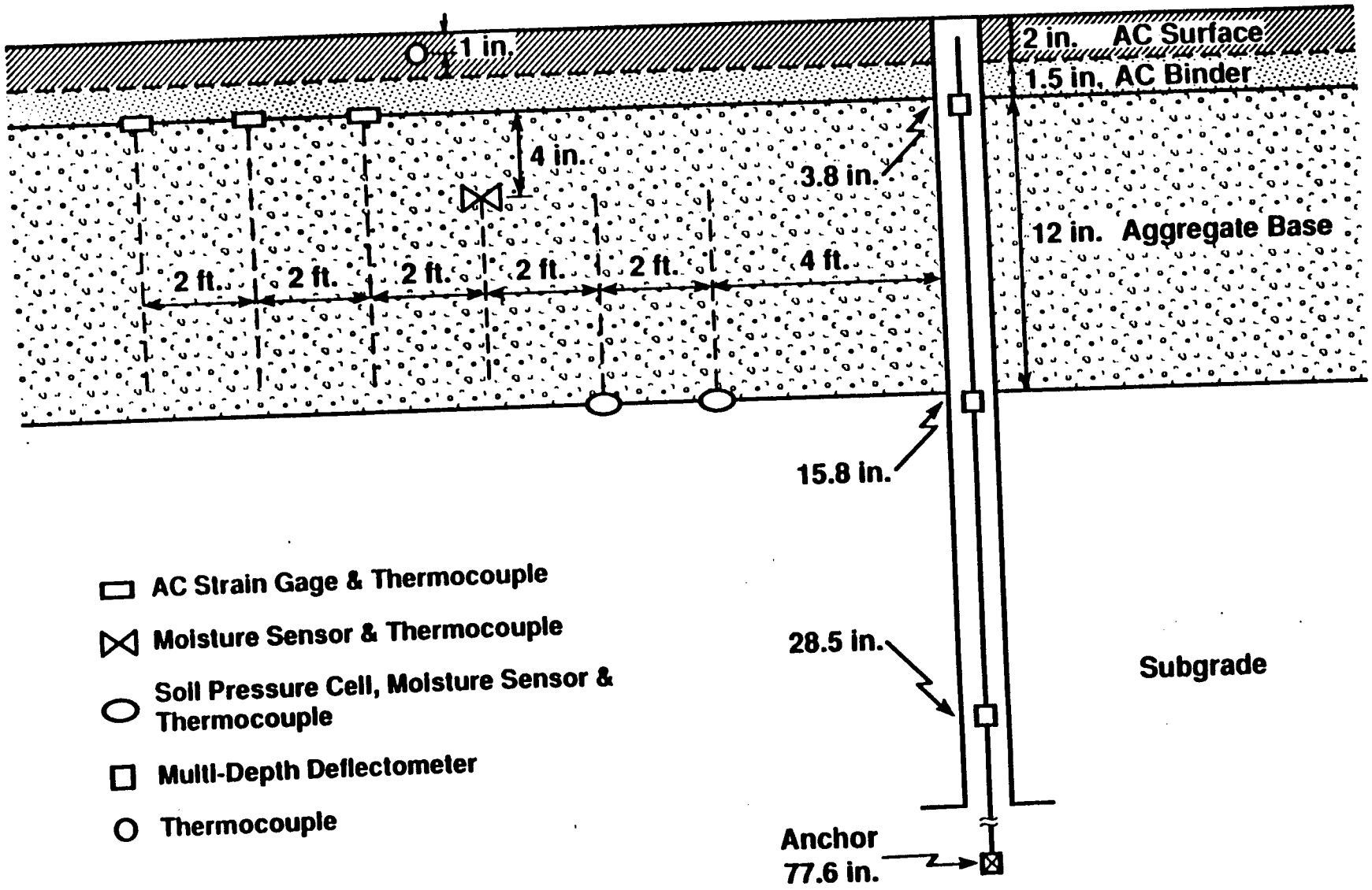

Figure A.1 Section 1* and 23 (* MDD present)

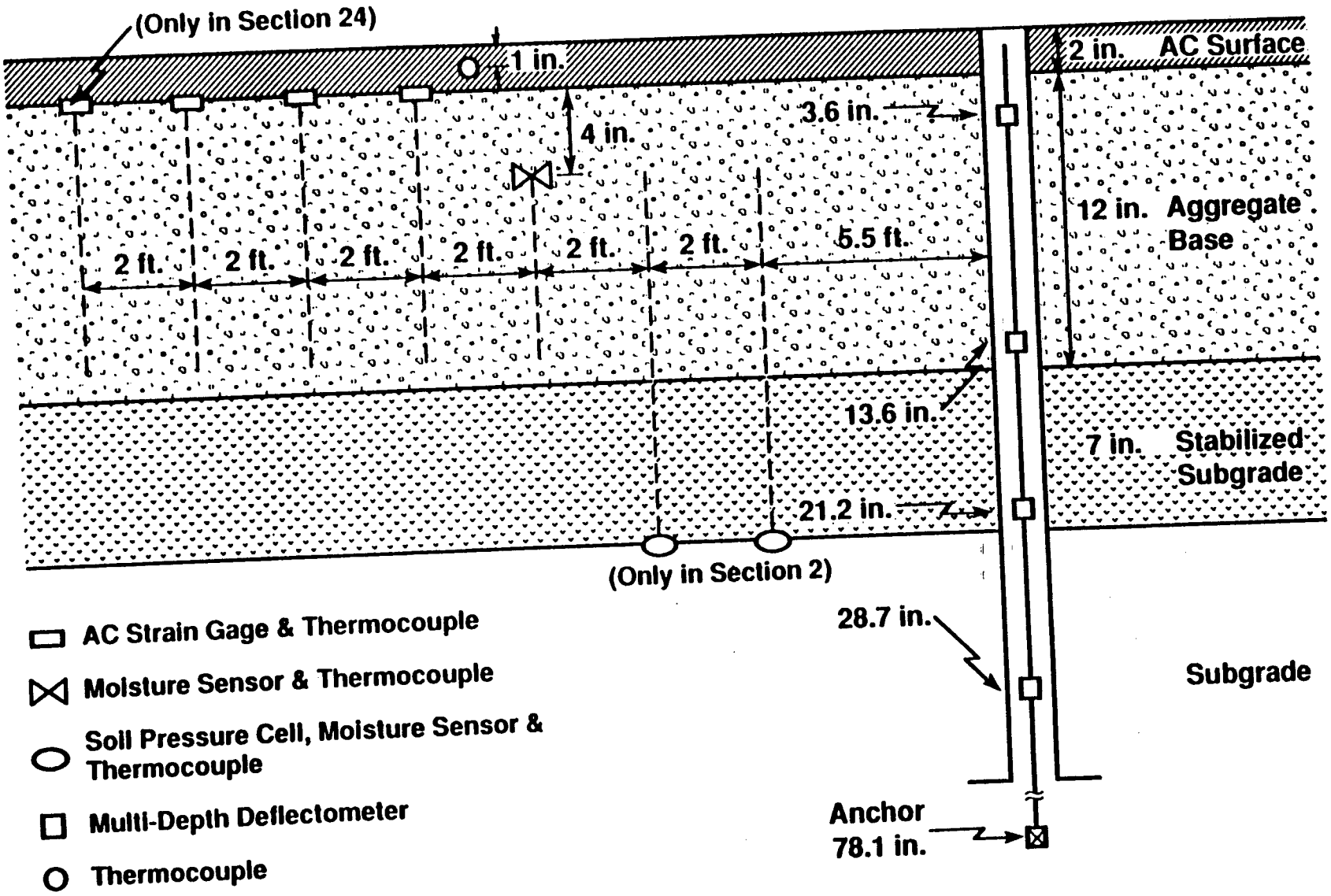

Figure A.2 Section 2* and 24 (* MDD present)

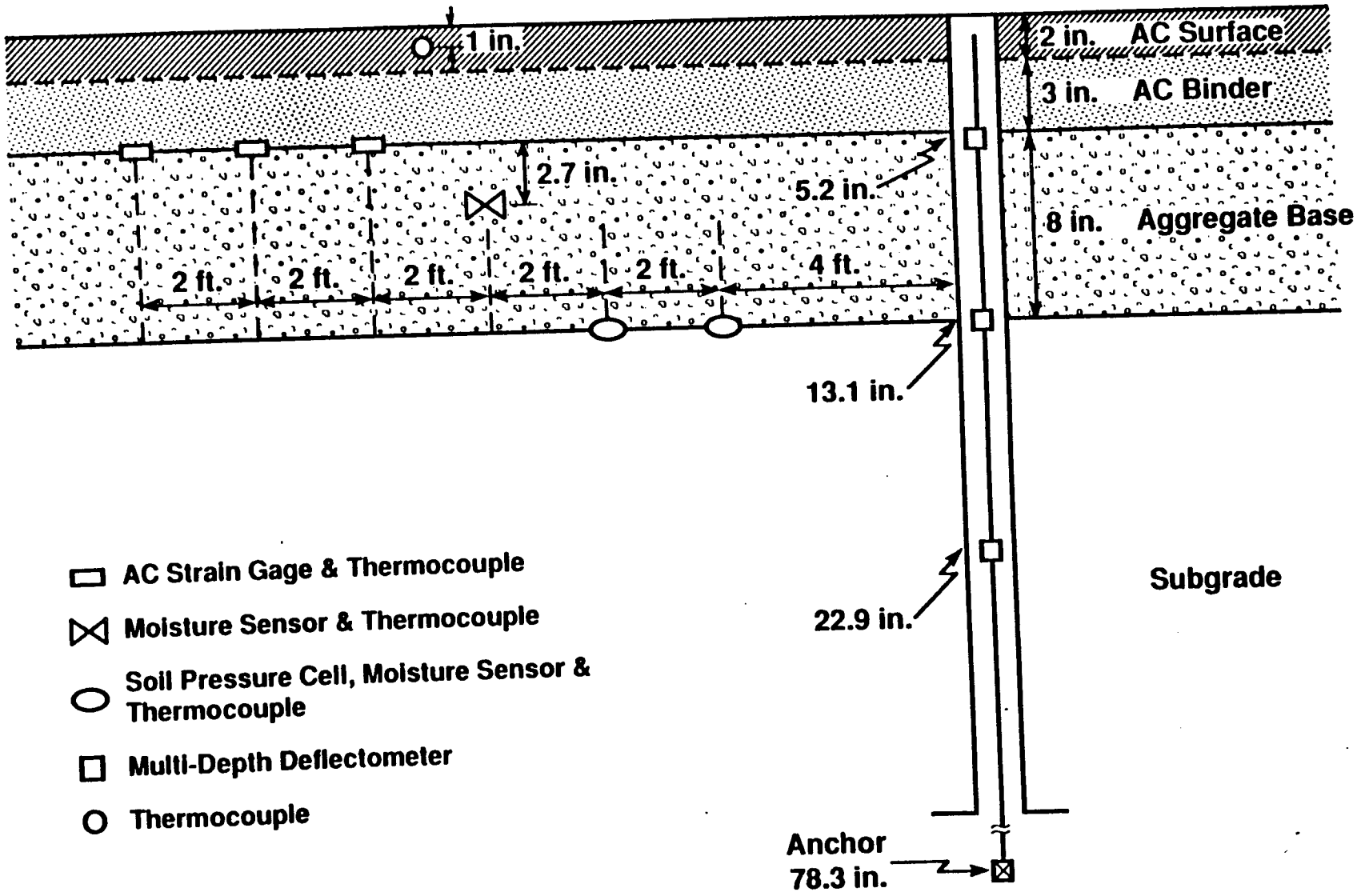

Figure A.3 Section 3* and 16 (* MDD present)

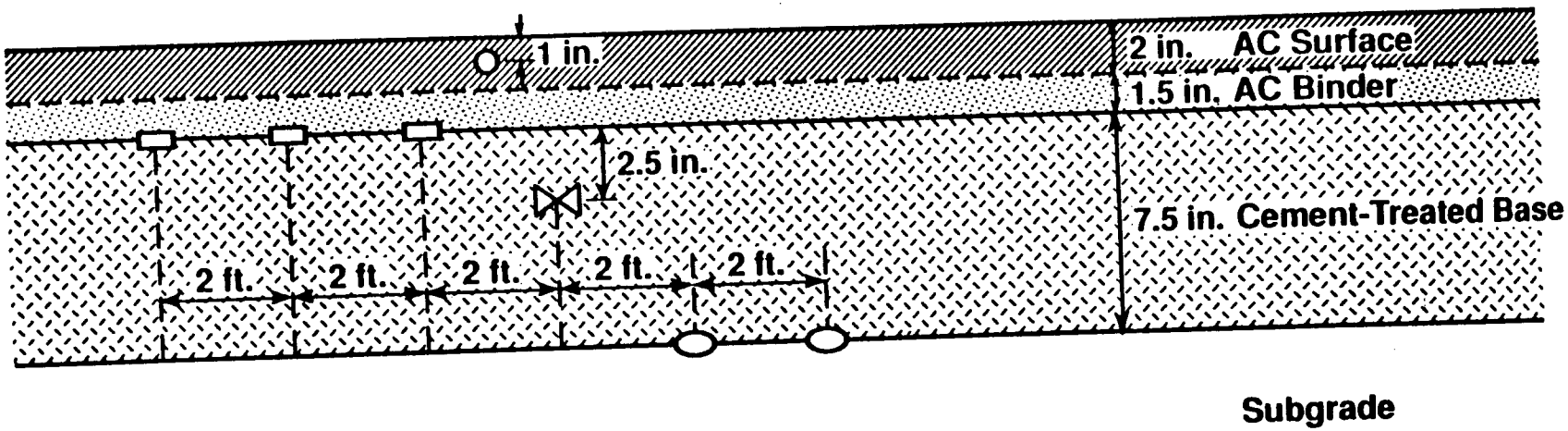

AC Strain Gage & Thermocouple

Moisture Sensor & Thermocouple

Soil Pressure Cell, Moisture Sensor & Thermocouple

Thermocouple

Figure A.4 Section 4 and 18

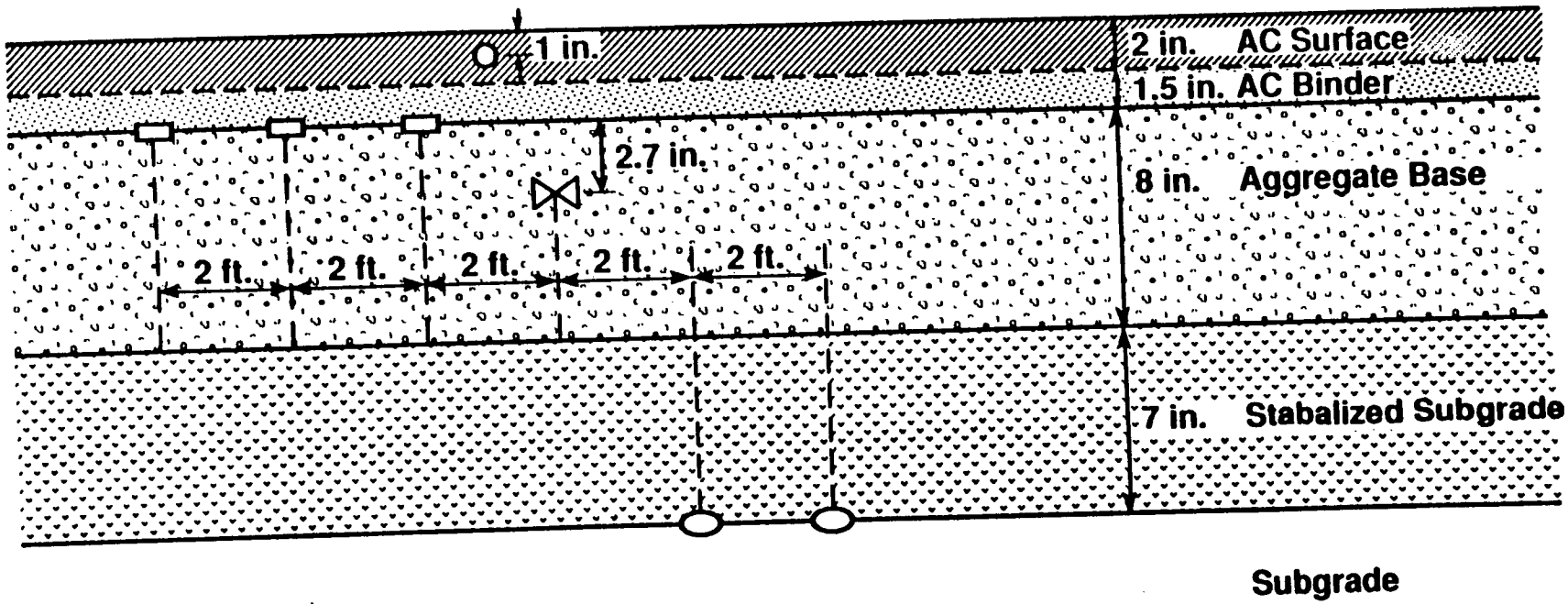

AC Strain Gage & Thermocouple

Moisture Sensor & Thermocouple

Soil Pressure Cell, Moisture Sensor & Thermocouple

Thermocouple

Figure A.5 Section 5 and 17

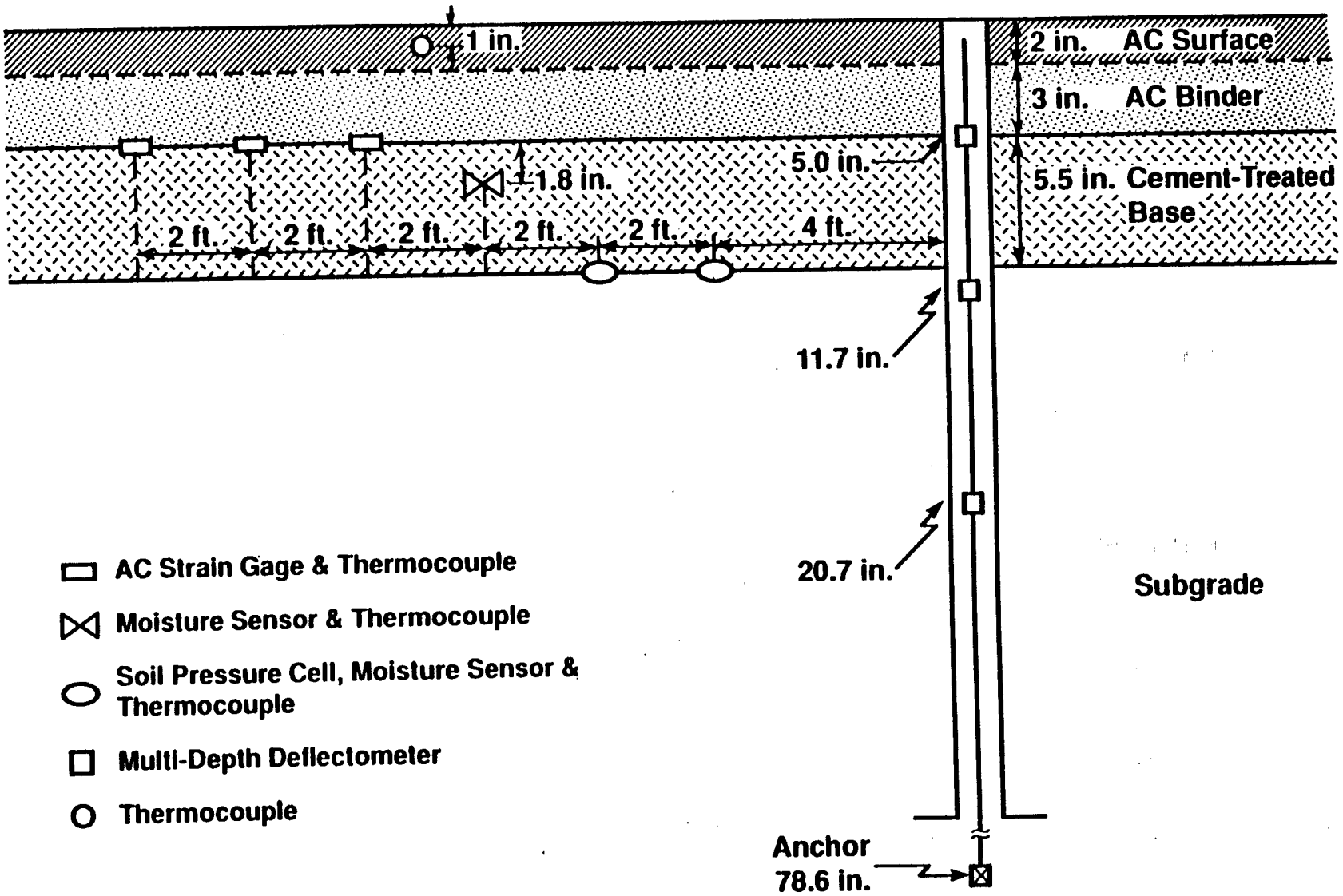

Figure A.6 Section 6* and 21 (* MDD present)

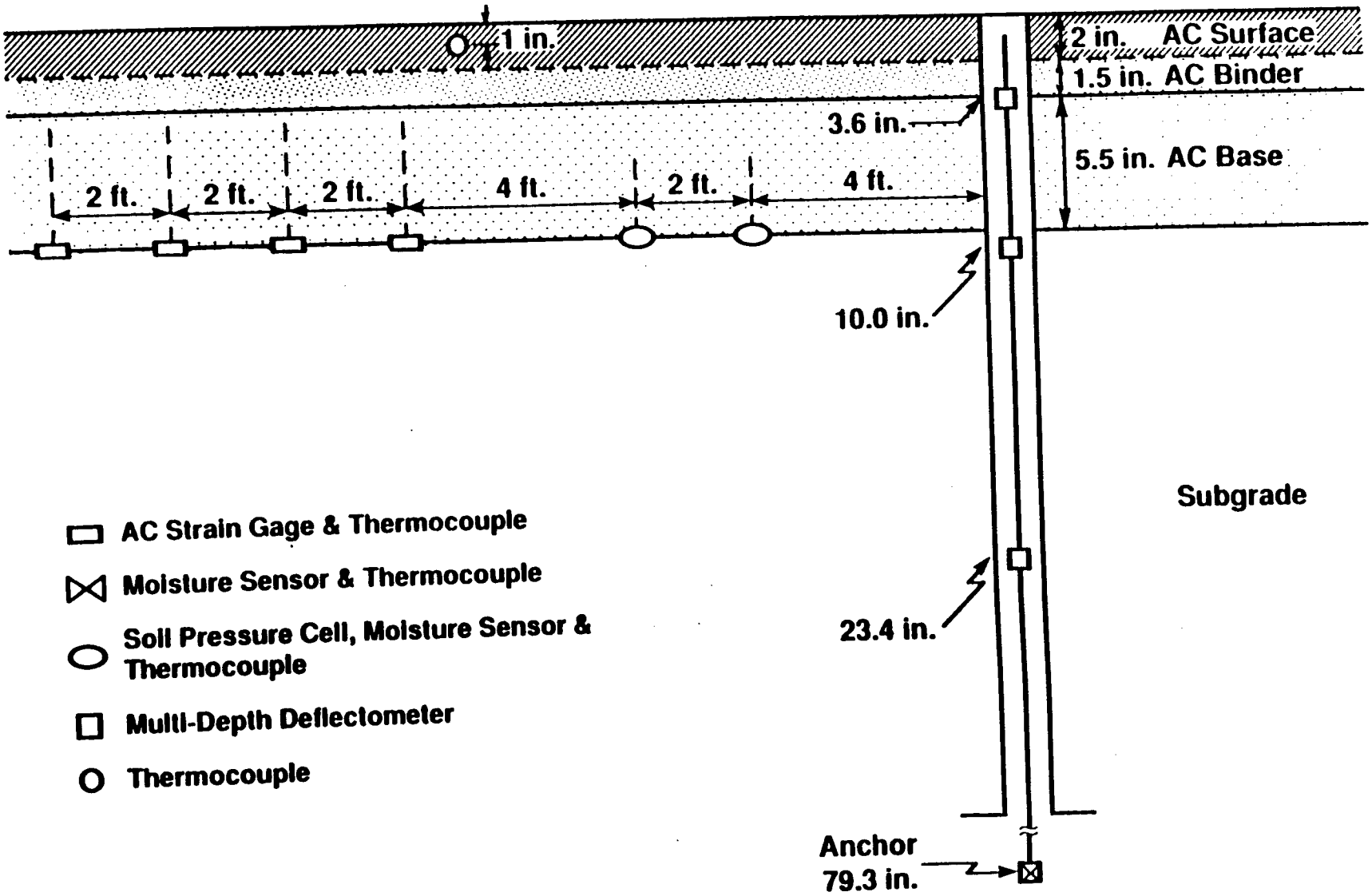

Figure A.7 Section 7* and 20 (* MDD present)

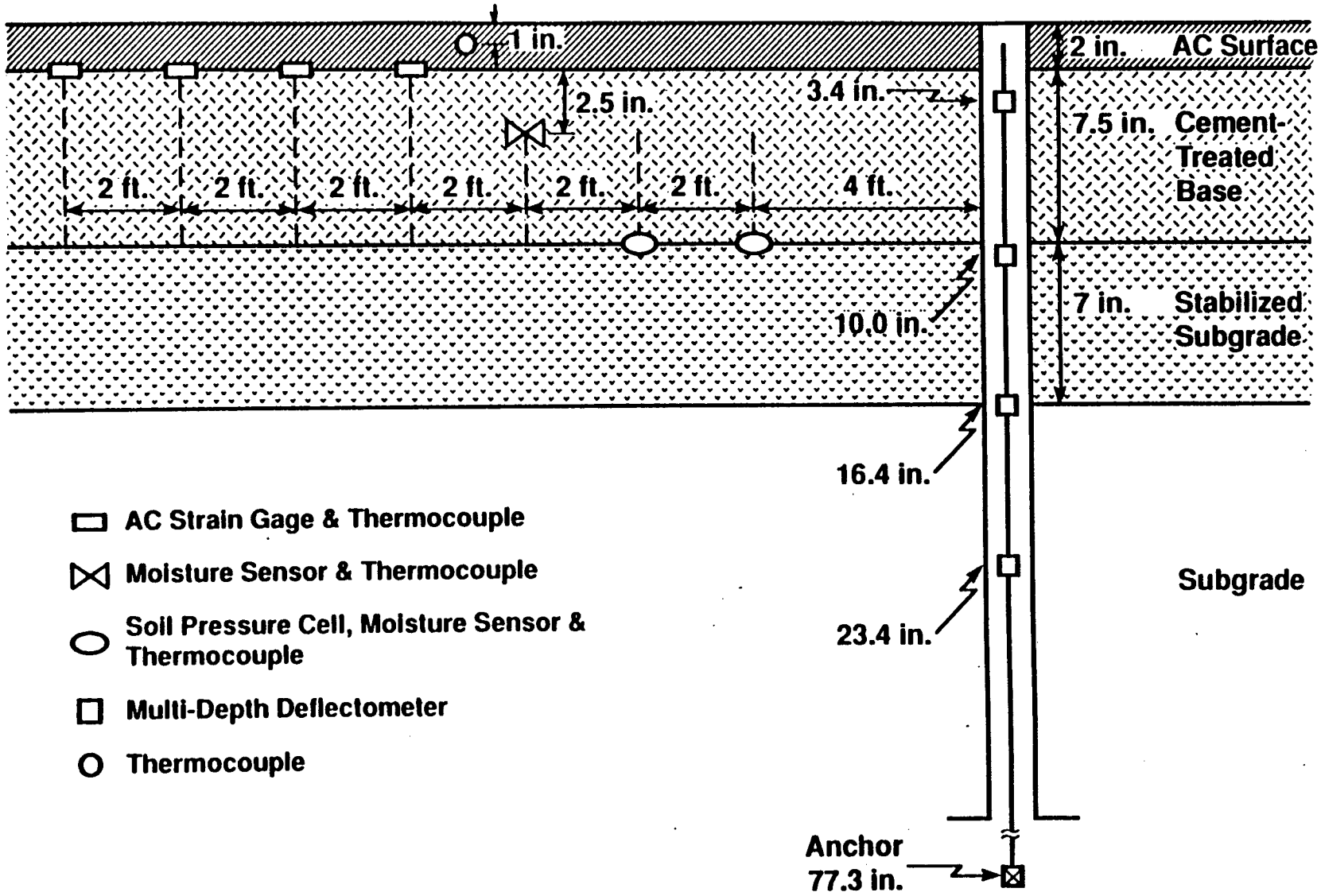

Figure A.8 Section 8* and 19 (* MDD present)

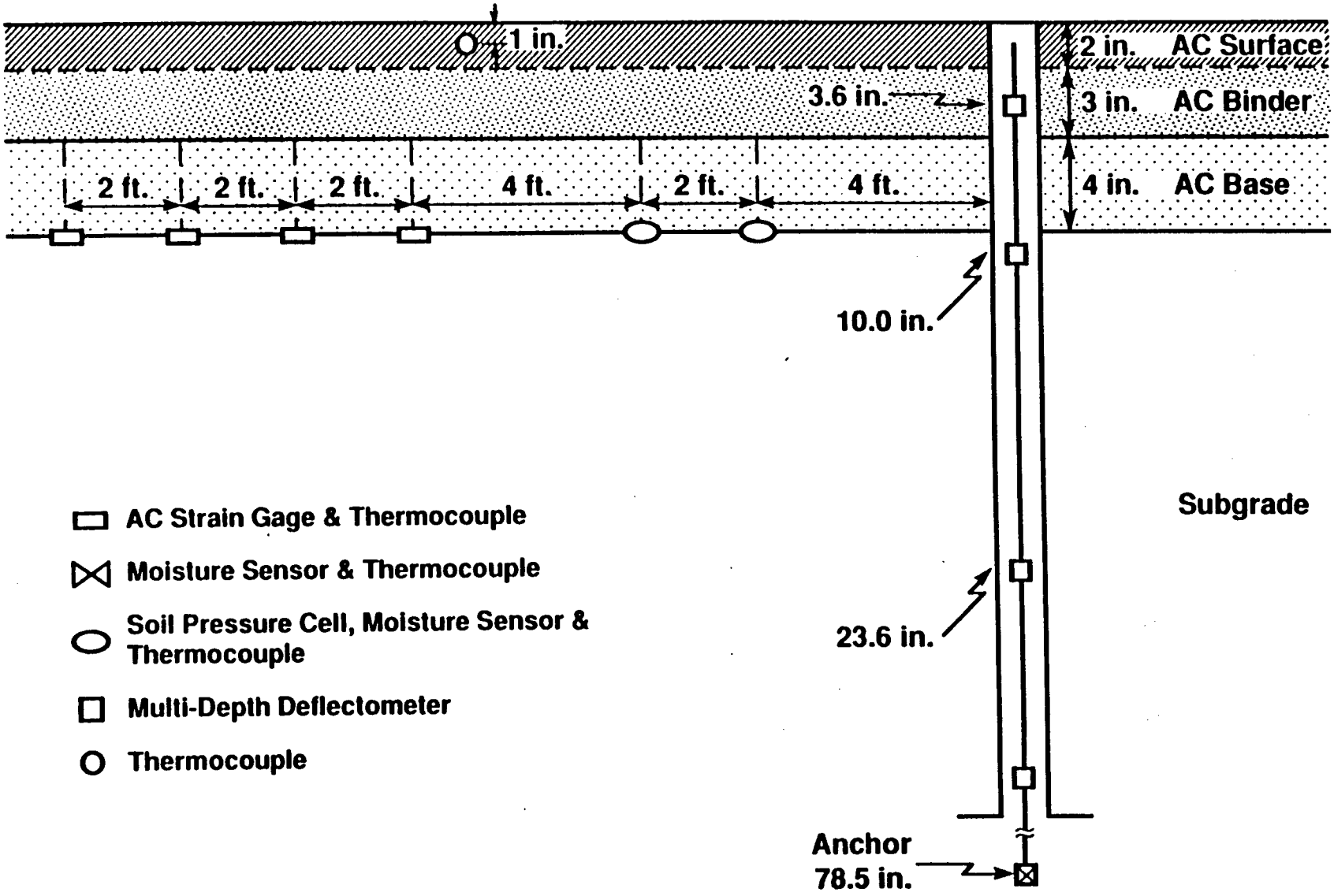

Figure A.9 Section 9* and 22 (* MDD present)

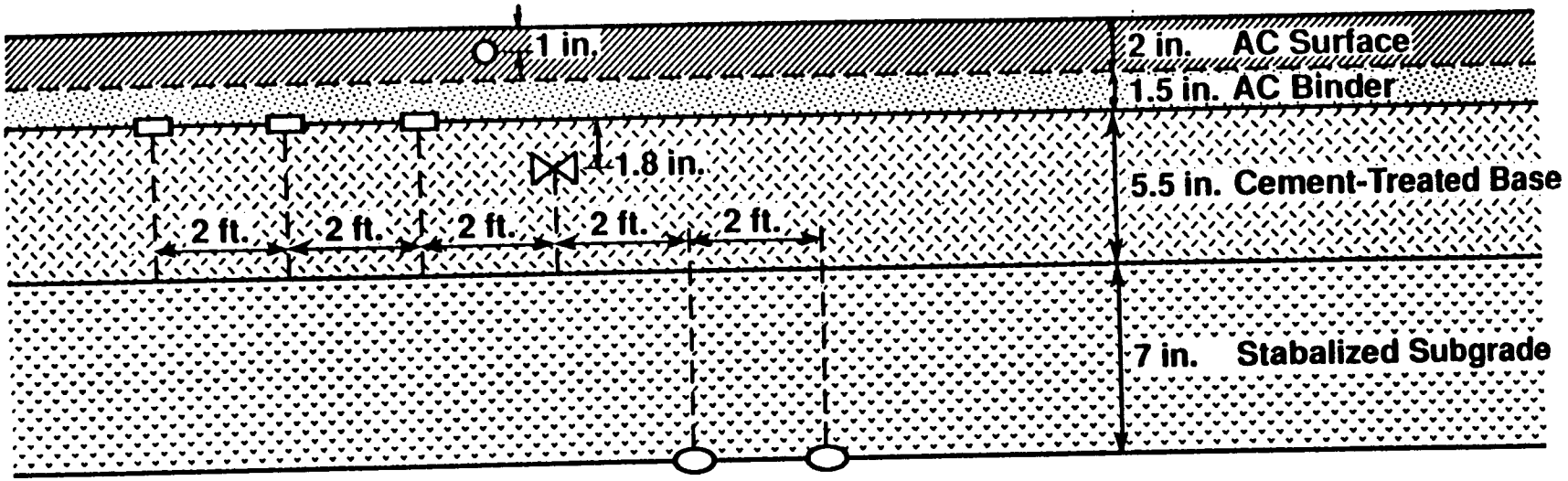

AC Strain Gage & Thermocouple

Moisture Sensor & Thermocouple

Soil Pressure Cell, Moisture Sensor & Thermocouple

Thermocouple

Figure A.10 Section 10 and 15

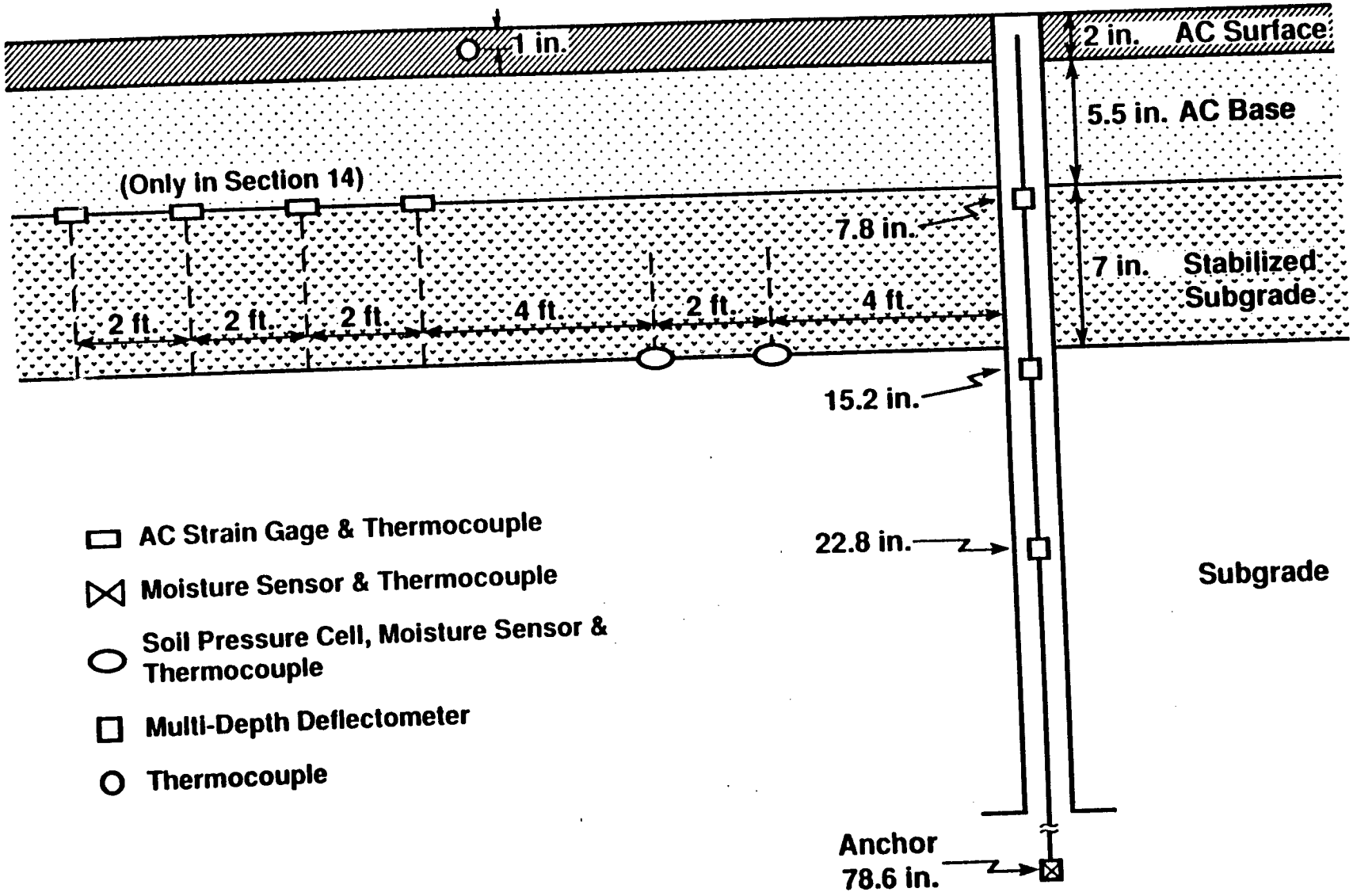

Figure A.11 Section 11* and 14 (* MDD present)

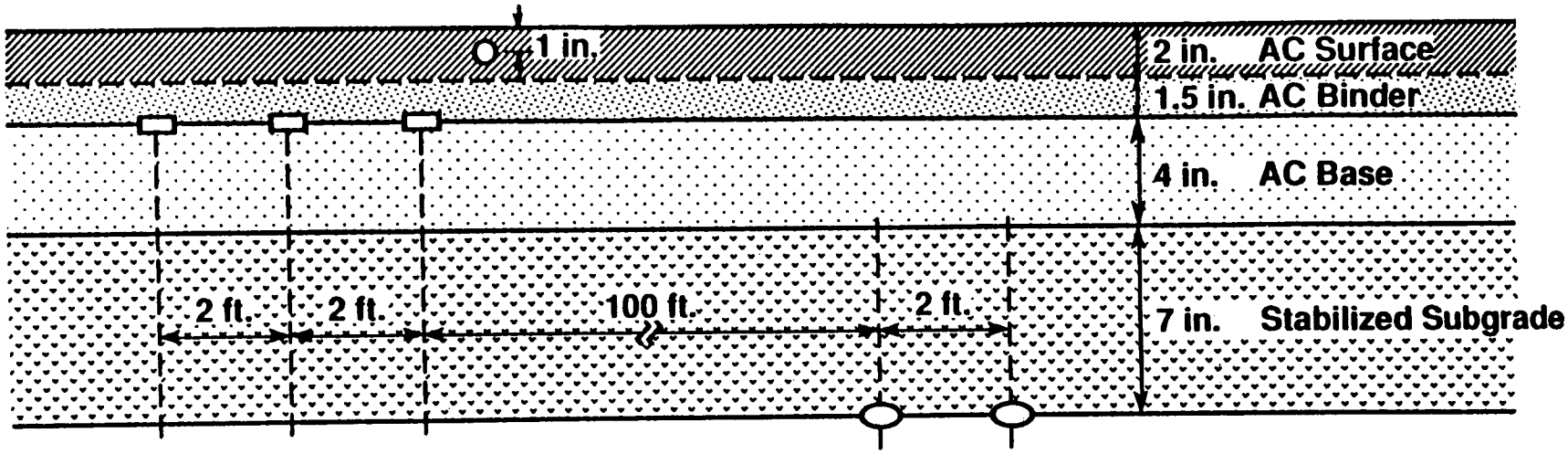

Figure A.12 Section 12 and 13

APPENDIX B

COMPUTER PROGRAMS (FORTRAN CODE)

B.1 NCFLEX.FOR

B2. RELPAV.FOR

```
    THIS PROGRAM - NCFLEX.FOR -IS WRITTEN IN MICROSOFT FORTRAN.
    THE PROGRAM NEEDS TO BE COMPILED ALONG WITH WES.FOR
    INPUT INFORMATION IS PROVIDED FROM AN EXTERNAL INPUT FILE
    PROGRAM DEVELOPED BY SATISH SANKARAN**************

    THIS PROGRAM IS EXPLAINED IN CHAPTER 6
    THIS PROGRAM IS AN ANALYSIS AND DESIGN PROGRAM FOR
    DESIGNING FGLEXIBLE PAVEMENT STRUCTURES

C**********INITIALISATION OF VARIABLES**************

      LOGICAL NEWOLD
      COMMON /WESP/STRAINY,STRESSZ,STRAINZ
      COMMON /FAT/ VOID,PHI,ZHI,LAY
      COMMON /traf/ESAL_Y,TAGF,ESALF,ESALR,CSESAL,CYESAL
      COMMON /STRUCT/P_TYPE,TEMP,N_SEAS
      COMMON /LABL/FILE,TEXT,HLINE,CMDCHAR
      COMMON /DIST/SDAMG,RD
      COMMON /PD1/ID_LAY1,ID_LAY2,ID_LAY3,ID_LAY4,ID_LAY5
      common /out/depth,fat_period,fat_traf,rut_period,rut_traf,np,
     +RUT_MEAS


      integer fat_period(50),rut_period(50),np
      real*8  fat_traf(50),rut_traf(50),depth(4,50),RUT_MEAS(50)

      INTEGER ITER_INP(10),LAY,lay_inc,FAT_LIFE/1/,RUT_LIFE/1/
      REAL*8 R_LIME1,RTACBS,THICBS,THICAC,SECTYPE,calib_fact
      REAL*8 STIFF(5,5),TAGF,CSESAL(35,4),CYESAL(35),FAT_ESAL/0./
      REAL*8 H(4),U(5),LA(4),calibration,inc,RUT_ESAL/0./
      INTEGER ESAL_Y,ESALF(35,4),ESALR(35),DES_LIFE
      REAL*8 STRAINY(15,15),STRESSZ(15,15),STRAINZ(15,15)
      REAL*8 SDAMG(35,4),RD(35),RUT_LIM,DES_ESALS,RUT_AMT/0./
      CHARACTER*1 CMDCHAR
      CHARACTER*72 FILE
      CHARACTER*80 TEXT,HLINE
      INTEGER P_TYPE,N_SEAS
      REAL*8 PHI(4,4),ZHI(4,4),VOID(4,4),TEMP(4),T(4),A_RT(6),B_RT(6)
C*****************************
C FOR WES.FOR ANALYSIS
      INTEGER L,L1,LS(50),IRQST
      COMMON PROV(50,1,9),RES(50,1,9)
      REAL*8 J1(20),RESULTS(50,1,19)
      REAL*8 A(20),P(20),LOAD(20),XC(20),YC(20)
      REAL*8 XS(50),YS(50),ZS(50)
      REAL*8 dev_stress,MR_iter,bulk_subbase,bulk_base

      DATA A(1) /4.00/,LOAD(1) /4500./,P(1) /90./
      DATA A(2) /4.00/,LOAD(2) /4500./,P(2) /90./
      DATA XC(1) /0.0/,YC(1) /0.0/
      DATA XC(2) /13.5/,YC(2) /0.0/
      DATA L /2/,L1 /11/,LS(1) /1/,LS(2) /2/,LS(3) /3/
      DATA LS(4) /4/,IRQST /1/,ZS(0) /0.0/
      DATA LS(5) /1/, LS(6) /1/
      DATA LS(7) /1/,LS(8) /2/,LS(9) /3/,LS(10) /4/,LS(11) /5/
      DATA YS(5) /0.0/,YS(6) /0.0/
      DATA XS(5) /0.0/,XS(6) /2.0/
      data np/1/
C*********************************************
      CALL BEGIN

      CALL DATAIN(STIFF,H,U,LA,CALIBRATION,DES_LIFE,DES_ESALS,
     +RUT_LIM,lay_inc,inc,A_RT,B_RT)
```

```
C*****************************************************************
 216  WRITE(*,*)'          MODULI     MODULI     MODULI     MODULI'
      WRITE(*,*)'         SEASON 1   SEASON 2   SEASON 3   SEASON 4'
      WRITE(8,*)'          MODULI     MODULI     MODULI     MODULI'
      WRITE(8,*)'         SEASON 1   SEASON 2   SEASON 3   SEASON 4'
C     WRITE(*,*)'-------------------------------------------------'
C     WRITE(8,*)'-------------------------------------------------'
      DO 219 IK=1,5
      write(*,218)IK,STIFF(IK,1),STIFF(IK,2),STIFF(IK,3),STIFF(IK,4)
      write(8,218)IK,STIFF(IK,1),STIFF(IK,2),STIFF(IK,3),STIFF(IK,4)
 218  format(1x,'LAYER:',I1,f10.2,1x,f10.2,1x,f10.2,1x,f10.2)
 219  CONTINUE
      WRITE(*,*)'-------------------------------------------------'
      WRITE(8,*)'-------------------------------------------------'
C*****************************************************************

      CALL TRAFIC(DES_LIFE)
 232  call calfactor(H,CALIBRATION,calib_fact,lay_inc,inc)
      DO 100 I=1,4
      ZS(I) = ZS(I-1)+H(I)
      XS(I)=6.75
      YS(I)=0.0
 100  CONTINUE
      ZS(5)=H(1)
      ZS(6)=H(1)
      DO 105 i = 7,11
      zs(i) = h(i-6)/2 + zs(i-7)
      XS(I)=6.75
      YS(I)=0.0
 105  continue
      DO 107 I=1,L1
 107  CONTINUE

 113  format(f6.2,f6.2,f6.2)

      DO 175 I =1,4
      CALL WES(STIFF(1,I),STIFF(2,I),STIFF(3,I),STIFF(4,I),STIFF(5,I),
     +H(1),H(2),H(3),H(4),U(1),U(2),U(3),U(4),U(5),LA(1),LA(2),
     +LA(3),L,P,A,XC,YC,L1,LS,XS,YS,ZS,RESULTS,IRQST)

      DO 180 K=1,L1
      WRITE(*,'(24(/))')
      write(*,*)'computation of strain in progress- PLEASE WAIT'

      STRAINY(K,I)=RESULTS(K,1,17)
      STRESSZ(K,I)=RESULTS(K,1,3)
      STRAINZ(K,I)=RESULTS(K,1,18)

 178  FORMAT(1X,'ZPOSN',2X,F5.2,2X,'STRAIN',2X,E10.4,2X,'STRESS',
     +2X,F6.2)
 180  CONTINUE
 175  CONTINUE

      CALL FATIG(STIFF,calib_fact,DES_LIFE,FAT_LIFE,FAT_ESAL)
      CALL ACRUT(H,CYESAL,RUT_LIM,DES_LIFE,DES_ESALS,RUT_LIFE,
     +RUT_ESAL,RUT_AMT,A_RT,B_RT)

      depth(1,np)=h(1)
      depth(2,np)=h(2)
      depth(3,np)=h(3)
      depth(4,np)=h(4)
      fat_period(np)=fat_life
      fat_traf(np)=fat_esal
      rut_period(np)=rut_life
      rut_traf(np)=rut_esal
```

```
      RUT_MEAS(NP)=RUT_AMT


C     WRITE(8,210)ID_LAY1,ID_LAY2,ID_LAY3,ID_LAY4,ID_LAY5
      WRITE(*,210)ID_LAY1,ID_LAY2,ID_LAY3,ID_LAY4,ID_LAY5
C     write(8,212)h(1),h(2),H(3),H(4)
      write(*,212)h(1),h(2),H(3),H(4)

 210  FORMAT(2X,'LAYER id     ->'4X,I1,7X,I1,7X,I1,7X,I1,11X,I1)
 212  FORMAT(2X,'LAYER THICK ->'2X,F6.3,2X,F6.3,2X,F6.3,2X,F6.3,2X,'
     +SEMI-INFIN')


      WRITE(*,215)FAT_LIFE,FAT_ESAL
C     WRITE(8,215)FAT_LIFE,FAT_ESAL
      WRITE(*,220)RUT_LIFE,RUT_ESAL,RUT_AMT
C     WRITE(8,220)RUT_LIFE,RUT_ESAL,RUT_AMT

  215 FORMAT(2X,'FATIGUE LIFE ->',I4,'MONTHS',2X,
     +'FATIGUE ESALS ->',F11.2)
  220 FORMAT(2X,'RUTTING LIFE ->',I2,'YEARS',2X,
     +'RUTTING ESALS ->',F11.2,2X,'RUTTING(inch)->',F5.2)
C     WRITE(8,*)'*****************************************************'
      IF(FAT_LIFE .GT. (DES_LIFE*12))THEN
       GOTO 275
       ELSE IF(FAT_ESAL .GT. DES_ESALS .AND. DES_ESALS .GT. 0.0)THEN
       GOTO 275
       ELSE IF( RUT_LIFE .LT. DES_LIFE) THEN
       GOTO 275
      ENDIF
C      READ(*,*)IJK
C     write(8,*)'next pass'
C      read(*,*)ijk

      np=np+1
      goto 232
275   call out_life
      OPEN(9,FILE='junk')
      close(9)



      STOP
      END

C*********************************************
      SUBROUTINE BEGIN
      CHARACTER*72 INFILE,OUTFILE

c947  WRITE(6,'(1X,A,\)')'ENTER INPUT DATA FILENAME = '
c     READ(5,1)INFILE
c   1  FORMAT(A)
      OPEN(7,FILE='flexinp.dat')
c 949  WRITE(6,'(1X,A,\)')'ENTER OUTPUT DATA FILENAME = '
c      READ(5,1)OUTFILE
      OPEN(8,FILE='flexout.dat')
c     GO TO 980
c948  WRITE(6,'(1X,A,\)')'INPUT FILE DOES NOT EXIST!!!  TRY AGAIN!'
c      GO TO 947
c 950  WRITE(6,'(1X,A,\)')'OUTPUT FILE ALREADY EXISTS!!!  TRY AGAIN!'
c      GO TO 949
c 980  RETURN
      END
C*********************************************************************
      SUBROUTINE DATAIN(STIFF,H,U,LA,CALIBRATION,DES_LIFE,DES_ESALS,
```

```
     +RUT_LIM,lay_inc,inc,A_RT,B_RT)
      COMMON /FAT/ VOID,PHI,ZHI,LAY
      COMMON /traf/ESAL_Y,TAGF,ESALF,ESALR,CSESAL,CYESAL(35)
      COMMON /STRUCT/P_TYPE,TEMP,N_SEAS
      COMMON /LABL/FILE,TEXT,HLINE,CMDCHAR
      COMMON /PD1/ID_LAY1,ID_LAY2,ID_LAY3,ID_LAY4,ID_LAY5

      REAL*8 STIFF(5,5),TAGF,CSESAL(35,4),CYESAL,A_RT(6),B_RT(6)
      REAL*8 H(4),U(5),LA(4),calibration,inc,RUT_LIM,DES_ESALS
      INTEGER ESAL_Y,ESALF(35,4),ESALR(35),LAY,lay_inc,DES_LIFE

      CHARACTER*1 CMDCHAR
      CHARACTER*72 FILE
      CHARACTER*80 TEXT,HLINE
      INTEGER P_TYPE,N_SEAS
      REAL*8 PHI(4,4),ZHI(4,4),VOID(4,4),TEMP(4),T(4)
      REAL*8 R_LIME1,RTACBS,THICBS,THICAC,SECTYPE
C*******
      DO 115 I = 1,8
      READ(7,95)TEXT
      write(8,95)TEXT
 95   FORMAT(A)
 115  CONTINUE
      READ(7,*)I1,ID_LAY1,U(1),H(1),LA(1)
      WRITE(8,117)I1,ID_lAY1,U(1),H(1),LA(1)
      READ(7,*)I1,ID_LAY2,U(2),H(2),LA(2)
      WRITE(8,117)I1,ID_lAY2,U(2),H(2),LA(2)
      READ(7,*)I1,ID_LAY3,U(3),H(3),LA(3)
      WRITE(8,117)I1,ID_lAY3,U(3),H(3),LA(3)
      READ(7,*)I1,ID_LAY4,U(4),H(4),LA(4)
      WRITE(8,117)I1,ID_lAY4,U(4),H(4),LA(4)
      READ(7,*)I1,ID_LAY5,U(5)
      WRITE(8,118)I1,ID_lAY5,U(5)
      WRITE(8,*)'---------------'
      WRITE(8,*)'LAYER MATERIAL -> ID '
C     WRITE(8,*)'------------------------------'
      WRITE(8,*)'HDS-> 1  HDB -> 2 HB -> 3 ABC -> 4 CTB -> 5'
      WRITE(8,*)'LIME_SUBGRADE -> 6 CEMENT_SUBGRADE -> 7 SUBGRADE -> 8'
      WRITE(8,*)'-------------------------------------------------'
  117 FORMAT(3X,I1,7X,I1,4X,F3.2,2X,F6.3,9X,F2.0)
  118 FORMAT(3X,I1,7X,I1,4X,F3.2)

      READ(7,95)TEXT
      READ(7,95)TEXT
      READ(7,95)TEXT
      DO 155 I = 1,4
      READ(7,*)I1,TEMP(I),STIFF(1,I),STIFF(2,I),STIFF(3,I),STIFF(4,I),
     +STIFF(5,I)
 155  CONTINUE
      READ(7,95)TEXT
      READ(7,95)TEXT
      READ(7,*)ESAL_Y
      READ(7,95)TEXT
      READ(7,95)TEXT
      READ(7,*)TAGF
      READ(7,95)TEXT
      READ(7,95)TEXT
      READ(7,*)LAY
      READ(7,95)TEXT
      READ(7,95)TEXT
      READ(7,95)TEXT
        DO 200 I = 1,4
        READ(7,*)ID,TEMP(I),PHI(LAY,I),ZHI(LAY,I),VOID(LAY,I)
 200    CONTINUE
       read(7,95)text
```

```
      READ(7,95)TEXT
      READ(7,*)A_RT(1),A_RT(2),A_RT(3),A_RT(4),A_RT(5),A_RT(6)
      READ(7,*)B_RT(1),B_RT(2),B_RT(3),B_RT(4),B_RT(5),B_RT(6)
      read(7,95)text
      READ(7,95)TEXT
      read(7,*)lay_inc,inc
      READ(7,95)TEXT
      READ(7,95)TEXT
      read(7,*)calibration
      READ(7,95)TEXT
      READ(7,95)TEXT
      read(7,*)DES_LIFE,DES_ESALS,RUT_LIM
     CLOSE(7)
     RETURN
     END
C*********************************************************************
      subroutine calfactor(H,CALIBRATION,calib_fact,lay_inc,inc)

      COMMON /PD1/ID_LAY1,ID_LAY2,ID_LAY3,ID_LAY4,ID_LAY5
      integer ID(5),ID_LAY1,ID_LAY2,ID_LAY3,ID_LAY4,ID_LAY5,LAY_INC
      INTEGER ILL/0/
      REAL*8 h(4),cal_tot/0./,lime_1/0./,sectype/0./,rtacbs,
     +calib_fact,cal(5),INC,CALIBRATION
      data cal(1)/0./,cal(2)/0./,cal(3)/0./,cal(4)/0./,cal(5)/0./

      ILL=ILL+1
      IF(ILL .GE. 2)THEN
       H(lay_inc)=H(lay_inc)+inc
      ENDIF

C     WRITE(8,115)ID_LAY1,ID_LAY2,ID_LAY3,ID_LAY4,ID_LAY5
C     WRITE(*,115)ID_LAY1,ID_LAY2,ID_LAY3,ID_LAY4,ID_LAY5
C     write(8,116)h(1),h(2),H(3),H(4)
C     write(*,116)h(1),h(2),H(3),H(4)

C115  FORMAT('LAYER id    ->'4X,I1,7X,I1,7X,I1,7X,I1,11X,I1)
C116  FORMAT('LAYER THICK ->'2X,F6.3,2X,F6.3,2X,F6.3,2X,F6.3,2X,'
C    +SEMI-INFIN')


      id(1)=id_lay1
      id(2)=id_lay2
      id(3)=id_lay3
      id(4)=id_lay4
      id(5)=id_lay5

      IF (ID(1) .EQ. 1) cal(1)=h(1)*(-65.099)
      IF (ID(2) .EQ. 2) cal(2)=h(2)*(-65.099)
      IF (ID(2) .EQ. 3) cal(3)=h(3)*(-0.477)
      IF (ID(3) .EQ. 4) cal(3)=h(3)*(-0.477)
      IF (ID(3) .EQ. 5) cal(3)=h(3)*(-0.477)
      do 118 i=3,5
      IF (ID(I) .EQ. 6) cal(4)=h(4)*7.158
      IF (ID(I) .EQ. 7) cal(4)=h(4)*7.158
      IF (ID(I) .EQ. 8) cal(4)=0.0
      if (id(i) .eq. 6) lime_1=0
      if (id(i) .eq. 7) lime_1=1.0
      if (id(i) .eq. 8) lime_1=-1.0
  118 continue
      if (id(2) .eq. 3) sectype=-1.0
      if (id(3) .eq. 3) sectype=-1.0
      if (id(2) .eq. 4) sectype=1.0
      if (id(3) .eq. 4) sectype=1.0

      cal_tot=0.0
```

```
      do 120 i=1,4
      cal_tot=cal_tot+cal(i)
120   continue
      if(id(2).eq.2) then
      rtacbs=((h(1)+h(2))/h(3))
      else
      rtacbs=((h(1))/h(2))
      endif

C     write(*,*)cal(1),cal(2),cal(3),cal(4),cal_tot,rtacbs,lime_1,sectype

      calib_fact=197.154+cal_tot-32.948*lime_1
     ++77.861*sectype+166.008*rtacbs

      IF (SECTYPE .EQ. 1.0 .AND. CALIB_FACT .LE. 150.0)THEN
        CALIB_FACT =150.0
      ELSEIF(SECTYPE .EQ. -1.0 .AND. CALIB_FACT .LE. 15.0)THEN
        CALIB_FACT=15.0
      ENDIF

      IF (CALIBRATION .GT. 0.0) CALIB_FACT = CALIBRATION


C       write(*,*)calib_fact
C        read(*,*)ijj
C       if(ijj .eq. 10)then
C        read(*,*)calib_fact
C       endif
       end

c**********************************************************************
      subroutine TRAFIC(DES_LIFE)
      COMMON /traf/ESAL_Y,TAGF,ESALF,ESALR,CSESAL,CYESAL

      INTEGER ESAL_Y,ESALF(35,4),ESALR(35),DES_LIFE
      REAL*8 TAGF,CSESAL(35,4),CYESAL(35)
      REAL*8 CFE/0./,CRE/0./
        DO 150 J=1,(DES_LIFE+10)
         ESALR(J)=0.6*ESAL_Y+0.4*12*30*24*60
         CRE= CRE+ REAL(ESALR(J))
         CYESAL(J)=CRE
           DO 152 I=1,4
              ESALF(J,I) = (ESAL_Y/4)
                ESALF(J,I)=0.6*ESALF(J,I)+0.4*3*30*24*60
                CFE=CFE+REAL(ESALF(J,I))
                CSESAL(J,I)=CFE
C             WRITE(*,151)ESALF(J,I)
C151          FORMAT(1X,I6,\)
 152        CONTINUE

          ESAL_Y = ESAL_Y+(ESAL_Y*(REAL(TAGF)/100.00))
 150     CONTINUE

C145  FORMAT(I6)
C146  FORMAT(I2)

        END
c**********************************************************************
      SUBROUTINE FATIG(STIFF,calib_fact,DES_LIFE,FAT_LIFE,FAT_ESAL)
      COMMON /WESP/STRAINY,STRESSZ,STRAINZ
      COMMON /FAT/ VOID,PHI,ZHI,LAY
      COMMON /traf/ESAL_Y,TAGF,ESALF,ESALR,CSESAL,CYESAL
      COMMON /STRUCT/P_TYPE,TEMP,N_SEAS
      COMMON /DIST/SDAMG,RD
```

```
      REAL*8 RD(35),TEMP(4)
      INTEGER P_TYPE,N_SEAS,DES_LIFE
      REAL*8 STIFF(5,5),TAGF,CSESAL(35,4),CYESAL(35),FAT_ESAL
      INTEGER ESAL_Y,ESALF(35,4),ESALR(35),LAY
      REAL*8 STRAINY(15,15),STRESSZ(15,15),STRAINZ(15,15)
      REAL*8 PHI(4,4),ZHI(4,4),VOID(4,4),T(4)
      REAL*8 STR(15,15),DAMG/0./,SDAMG(35,4)
      REAL*8 M, NFL_1(4),NFL_2(4),NF(4)
      REAL*8 calibration,calib_fact
      REAL*8 R_LIME1,RTACBS,THICBS,THICAC,SECTYPE
      INTEGER J,I_COUNT /1/,I_EQN /1/,FAT_LIFE
      REAL*8 EPS_TH,CORR_ST,EPS_REF /0.00018/,REF_STIFF /600032./
C*********************************************************************
C     write(*,*)'LAYER TO BE FATIGUED:',LAY
C     write(8,*)'LAYER TO BE FATIGUED:',LAY

C     write(8,*)'FATIGUE EQN:',I_EQN
C     WRITE(*,*)'-------------------------------------------------'
C     WRITE(8,*)'-------------------------------------------------'
C     write(8,*)'CALIBRATION :',CALIB_fact
      write(*,*)'CALIBRATION :',CALIB_fact
C     WRITE(*,*)'-------------------------------------------------'
C     WRITE(8,*)'-------------------------------------------------'

      write(*,*)' SEASON    MODULI     STRAIN     # OF CYCLES'
C     write(8,*)' SEASON    MODULI     STRAIN     # OF CYCLES'
C     WRITE(*,*)'-------------------------------------------------'
C     WRITE(8,*)'-------------------------------------------------'
      DO 200 K = 1,4
      STR(LAY,K)=ABS(STRAINY(LAY,K))
      M = SIN(PHI(LAY,K)*3.142/180)

      NFL_1(K)=(-5.078+(0.101*VOID(LAY,K))
     ++(-0.046*TEMP(K))
     ++(1.363*LOG(ZHI(LAY,K)))
     ++(-4.813*LOG(STR(LAY,k)))
     ++(-1.837*LOG(STIFF(LAY,K)))
     ++(-0.902*LOG(M)))
      NF(K) = exp(NFL_1(K))*CALIB_fact

      write(*,199)K,STIFF(LAY,K),STR(LAY,K),NF(K)
C     write(8,199)K,STIFF(LAY,K),STR(LAY,K),NF(K)

 199  FORMAT(3X,I1,4X,E10.4,4X,E10.4,4X,E10.2)

 200  CONTINUE
C************************************
      WRITE(*,*)'  FATIGUE LIFE ESTIMATION - MODIFIED SHELL METHOD'
      WRITE(*,*)' -----------------------------------------------'
C     WRITE(8,*)'  FATIGUE LIFE ESTIMATION - MODIFIED SHELL METHOD'
C     WRITE(8,*)' -----------------------------------------------'
      WRITE(*,*)'  YEAR  SEASON  CSESAL   DAMAGE'
C     WRITE(8,*)'  YEAR  SEASON  CSESAL   DAMAGE'
C     WRITE(8,*)' --------------------------------'
      damg=0.0
      sdamg=0.0
      I_COUNT=1
      DO 400 J = 1,(DES_LIFE+1)
        DO 395 I = 1,4
           DAMG=DAMG+((REAL(ESALF(J,I)))/(NF(I)))
        SDAMG(J,I)=DAMG
C****************************************
      WRITE(*,391)J,I,CSESAL(J,I),DAMG
C     WRITE(8,391)J,I,CSESAL(J,I),DAMG
 391  FORMAT(3X,I2,8X,I1,3X,E7.2,3X,E10.4)
```

```
C*******************************************
      IF(DAMG .GT. 1.0) GOTO 450
      I_COUNT = I_COUNT + 1
 395    CONTINUE
 400  CONTINUE
         WRITE(*,*)'----------------------------------------'
C        WRITE(8,*)'----------------------------------------'
C
 450     WRITE(*,*)
C        WRITE(*,475)I_COUNT*3
C451     WRITE(8,475)I_COUNT*3
 475     FORMAT(' FATIGUE CRITERIA: PAVMT FAILS IN   ',I3'  MONTHS')

C480     WRITE(*,490)CSESAL(J,I)
C481     WRITE(8,490)CSESAL(J,I)
 490  FORMAT(' FATIGUE CRITERIA: PAVMT FAILS AFTER ',F11.2)
C     WRITE(*,*)' CORRECTED ESALS'
C     WRITE(8,*)' CORRECTED ESALS'
         WRITE(*,*)'----------------------------------------'
C        WRITE(8,*)'----------------------------------------'
      FAT_LIFE=I_COUNT*3
      FAT_ESAL=CSESAL(J,I)

 500  CONTINUE
 600     RETURN
      END
C*************************************************************************
      SUBROUTINE ACRUT(H,CYESAL,RUT_LIM,DES_LIFE,DES_ESALS,RUT_LIFE,
     +RUT_ESAL,RUT_AMT,A_RT,B_RT)
      COMMON /PD1/ID_LAY1,ID_LAY2,ID_LAY3,ID_LAY4,ID_LAY5
      COMMON /DIST/SDAMG,RD

      INTEGER RUT_LIFE,DES_LIFE
      REAL*8 D(6),A(6),A_RT(6),B_RT(6),H(5),RD(35),RD_1,RUT_ESAL
      REAL*8 CYESAL(35),mul(6),RUT_LIM,RUT_AMT,DES_ESALS
      REAL*8 SDAMG(35,4)
      DATA A(1)/1.5/,A(2)/1.0/,A(3)/1.0/,A(4)/1.0/,A(5)/1.0/,A(6)/1.0/
      DATA D(1)/0./,D(2)/0./,D(3)/0./,D(4)/0./,D(5)/.0/,D(6)/.0/

      if(ID_LAY1 .eq. 1 .and. H(1) .le. 2.0) then
       mul(1)=1.0
       mul(2)=0.0
       D(1)=H(1)
       D(2)=0.0
       else if (ID_LAY1 .eq. 1 .and. H(1) .gt. 2.0) then
        mul(1)=1.0
        mul(2)=1.0
        D(1)=2.0
        D(2)=H(1)-2.0
        end if

        if(ID_LAY2 .eq. 2 .and. (H(1)+H(2)) .le. 5.0) then
        mul(3)=1.0
        mul(4)=0.0
        D(3)=5.0-H(1)
        D(4)=0.0
        else if(ID_LAY2 .eq. 2 .and. (H(1)+H(2)) .gt. 5.0) then
        mul(3)=1.0
        mul(4)=1.0
        D(3)=5.0-H(1)
        D(4)=(H(1)+H(2))-5.0
        end if

        if(ID_LAY3 .eq. 3 .and. (H(1)+H(2)+H(3)) .le. 5.0) then
        mul(5)=1.0
```

```
        mul(6)=0.0
        D(5)=5.0-(h(1)+h(2))
        D(6)=0.0
        else if(ID_LAY3 .eq. 3 .and. (H(1)+H(2)+H(3)) .gt. 5.0) then
        mul(5)=1.0
        mul(6)=1.0
        D(6)=5.0-(H(1)+H(2))
        D(6)=(H(1)+H(2)+H(3))-5.0
        endif

C     WRITE(*,*)'RUT DEPTH PREDICTIONS - AC LAYER ONLY'
C     WRITE(8,*)'RUT DEPTH PREDICTIONS - AC LAYER ONLY'
C     WRITE(8,*)'*****************************************'
      WRITE(*,*)'YEAR      CYESAL     RUTDEPTH (in)'
C     WRITE(8,*)'YEAR      CYESAL     RUTDEPTH (in)'
C     WRITE(*,*)'-----------------------------------'
C     WRITE(8,*)'-----------------------------------'

      DO 700 J = 1,DES_LIFE
           RD(J) = 0.0
           DO 712 ip=1,6
           RD_1=MUL(ip)*(A(ip)*A_RT(ip)*(CYESAL(J)**B_RT(ip))*D(IP))
           RD(J) = RD(J) + RD_1
 712    CONTINUE
C***************************************
      WRITE(*,699)J,CYESAL(J),RD(J)
C     WRITE(8,699)J,CYESAL(J),RD(J)
 699  FORMAT(1X,I3,4X,E10.4,4X,F5.2)
      IF (RD(J) .gt. RUT_LIM) GOTO 710

 700  CONTINUE
      IF (RD(DES_LIFE) .LE. RUT_LIM)THEN
       RUT_LIFE=DES_LIFE
       RUT_ESAL=CYESAL(DES_LIFE)
       RUT_AMT=RD(DES_LIFE)
      RETURN
      ENDIF
 710   WRITE(*,*)'-----------------------------------'
C       WRITE(8,*)'-----------------------------------'
        WRITE(*,715)J
C       WRITE(8,715)J
 715    FORMAT(' RUTTING  CRITERIA: PAVMT FAILS IN',I2'  YEARS')

        WRITE(*,720)CYESAL(J)
C       WRITE(8,720)CYESAL(J)
 720  FORMAT(' FATIGUE CRITERIA: PAVMT FAILS AFTER ',F11.2)
C     WRITE(*,*)' CORRECTED ESALS'
C     WRITE(8,*)' CORRECTED ESALS'
       WRITE(*,*)'-----------------------------------'
C      WRITE(8,*)'-----------------------------------'

      RUT_LIFE=J
      RUT_ESAL=CYESAL(J)
      RUT_AMT=RD(J)


 750  RETURN
      END

c*********************************************************************
      subroutine out_life

      common /out/depth,fat_period,fat_traf,rut_period,rut_traf,np,
     +RUT_MEAS
      COMMON /PD1/ID_LAY1,ID_LAY2,ID_LAY3,ID_LAY4,ID_LAY5
```

```
      integer fat_period(50),rut_period(50),np,ID_LAY1,ID_LAY2,
     +ID_LAY3,ID_LAY4,ID_LAY5
      real*8  fat_traf(50),rut_traf(50),depth(4,50),RUT_MEAS(50)

      write(8,175)ID_LAY1,ID_LAY2,ID_LAY3,ID_LAY4
  175 FORMAT(1X,'LAYER ID-->',1X,I1,1X,I1,1X,I1,1X,I1)
      write(8,180)
  180 format(3x,'H1',4x,'H2',4x,'H3',4X,'H4',3X,'FAT.LIFE(MONTHS)',
     +2X,'ESALS TO FAT.',/,60('-'))

      do 200 i=1,np
      write(8,190)depth(1,i),depth(2,i),depth(3,i),depth(4,i),
     +fat_period(i),fat_traf(i)
  190  format(1x,f5.2,1x,f5.2,1x,f5.2,1x,f5.2,4x,i3,12X,e10.2)

  200  CONTINUE

      WRITE(8,210)
  210  format(3x,'H1',4x,'H2',4x,'H3',4X,'H4',3X,'RUT LIFE',2X,
     +'ESALS TO RUT',2X,'MAX. RUT',/,60('-'))
      DO 300 I=1,NP
      write(8,225)depth(1,i),depth(2,i),depth(3,i),depth(4,i),
     +rut_period(i),rut_traf(i),RUT_MEAS(I)
  225  format(1x,f5.2,1x,f5.2,1x,f5.2,1x,f5.2,4x,i3,5x,e10.2,3X,F5.2)
  300  continue
      return
      end
```

```
    THIS PROGRAM - RELPAV.FOR -IS WRITTEN IN MICROSOFT FORTRAN.
    THE PROGRAM NEEDS TO BE COMPILED ALONG WITH WES.FOR
    INPUT INFORMATION IS PROVIDED WITHIN THE MAIN PROGRAM
    PROGRAM DEVELOPED BY SATISH SANKARAN**************

    THIS PROGRAM WAS USED FOR THE VARIABILITY ANALYSIS USED IN CHAPTER 7
    THIS PROGRAM IS ONLY AN ANALYSIS TOOL TO CALCULATE
    RELIABILITY BASED ESTIMATES OF STRAIN AND FATIGUE OF AC LAYER

C**********INITIALISATION OF VARIABLES**************
      CHARACTER*72 FILE
      CHARACTER*1 CMDCHAR
      COMMON NF,var(25,25)
      REAL*8 STIFF(5,5),des(3,25)
      REAL*8 TEMP(4),MOIST(4),H(4),U(5),LA(4)
      REAL*8 PHI,ZHI,VOID,strain,NF,mod
      INTEGER L,L1,LS(50),IRQST,layr,n,ik1,ik2,i_end,i_var(300,15)
      COMMON PROV(50,1,9),RES(50,1,9)
      REAL*8 J1(20),RESULTS(50,1,19)
      REAL*8 A(20),P(20),LOAD(20),XC(20),YC(20)
      REAL*8 XS(50),YS(50),ZS(50)
      real*8 E1(3),E2(3),E3(3),E4(3),E5(3)
      real*8 T1(3),T2(3),T3(3),T4(3)
      REAL*8 STR_MEAN,STR_SIG,SUM,SSQ,nf_mean,nf_sig,nf_sum,nf_ssq
      INTEGER I_NUMB

C*********DATA FOR ELASTIC LAYER ANALYSIS**********
      DATA A(1) /4.00/,LOAD(1) /4500./,P(1) /90./
      DATA A(2) /4.00/,LOAD(2) /4500./,P(2) /90./
      DATA XC(1) /0.0/,YC(1) /0.0/
      DATA XC(2) /13.5/,YC(2) /0.0/
      DATA L /2/,L1 /6/,LS(1) /1/,LS(2) /2/,LS(3) /3/
      DATA LS(4) /4/,LS(5) /1/,LS(6) /1/,IRQST /1/
      DATA LA(1) /1./,LA(2) /1./,LA(3) /1./

      DATA XS(1) /6.75/,XS(2) /6.75/,XS(3) /6.75/,XS(4) /6.75/
      DATA XS(5) /2.0/,XS(6) /6.75/
      DATA YS(1) /0./,YS(2) /0./,YS(3) /0./,YS(4) /0./,YS(5) /0./
      DATA YS(6) /0./

      DATA STR_SUM/0./,STR_SSQ/0./I_NUMB/0/,nf_sum /0./,nf_sq /0./

C********STIFFNESS AND THICKNESS DATA ALONG WITH THEIR VARIABILITY***
      data des(1,1) /209330./,des(2,1) /36170.0/
      data des(1,2) /3.5/,des(2,2) /.25/
      data des(1,3) /13730./,des(2,3) /2680.0/
      data des(1,4) /12.0/,des(2,4) /.25/
      data des(1,5) /10000./,des(2,5) /500.0/
      data des(1,6) /0./,des(2,6) /0.0/
      data des(1,7) /10000./,des(2,7) /500.0/
      data des(1,8) /0./,des(2,8) /0.0/
      data des(1,9) /3430./,des(2,9) /1330.0/
      DATA U(1)/0.35/,U(2)/0.35/,U(3)/0.45/,U(4)/0.45/,U(5)/0.45/

      data kk=0

C***********CREATES OUTPUT FILE********
       call begin
C*******************************
      des(3,1)=des(1,1)
      des(3,2)=des(1,2)
      des(3,3)=des(1,3)
      des(3,4)=des(1,4)
```

```
      des(3,5)=des(1,5)
      des(3,6)=des(1,6)
      des(3,7)=des(1,7)
      des(3,8)=des(1,8)
      des(3,9)=des(1,9)
      write(*,*)'layer to be fatigued'
      read(*,*)layr
      WRITE(*,*)'number of variables in pem'
      read(*,*)n
      i_end=2**n

c************SETS UP FOR POINT ESTIMATE METHOD********
      call PEM(n,i_var)

       do 250 ik1=1,i_end
          do 225 ik2 = 1,n
         WRITE(*,*)I_VAR(IK1,IK2)
       if (i_var(ik1,ik2) .eq. 1) then
      des(3,ik2)=des(1,ik2)+des(2,ik2)
       else
       des(3,ik2)=des(1,ik2)-des(2,ik2)
       ENDIF
  225     continue

      ZS(1)=des(3,2)
      ZS(2)=des(3,4)+ZS(1)
      ZS(3)=des(3,6)+ZS(2)
      ZS(4)=des(3,8)+ZS(3)
      ZS(5)=ZS(1)
      ZS(6)=ZS(1)
      WRITE(*,*)des(3,1),des(3,2),des(3,3),des(3,4),des(3,5),
     +des(3,6),des(3,7),des(3,8),des(3,9),ZS(1),ZS(2),ZS(3),
     +ZS(4),ZS(5),ZS(6)
c**********CALLS WES.EXE FOR DETERMINING LAYER STRAINS******
       CALL WES(des(3,1),des(3,3),des(3,5),des(3,7),des(3,9),
     +des(3,2),des(3,4),des(3,6),des(3,8),
     +U(1),U(2),U(3),U(4),U(5),LA(1),LA(2),
     +LA(3),L,P,A,XC,YC,L1,LS,XS,YS,ZS,RESULTS,IRQST)
       write(*,*)'*******************************'

       WRITE(*,*)RESULTS(1,1,17),RESULTS(4,1,3)

       I_NUMB=I_NUMB+1
       strain = abs(results(layr,1,17))
       STR_SUM = STR_SUM + ABS(STRAIN)
       STR_SSQ = STR_SSQ + ABS(STRAIN)**2

       if (layr .eq. 1) then
           mod = DES(3,1)
       else if (layr .eq. 2) then
           mod = DES(3,3)
       else if (layr .eq. 3) then
         mod = DES(3,5)
       endif
         write(*,*)'mod===',mod

       write(8,333)des(3,1),des(3,2),des(3,3),des(3,4),des(3,5),
      +des(3,6),des(3,7),des(3,8),des(3,9),
      +STRAIN,RESULTS(4,1,3),NF
       nf_SUM = nf_SUM + nf
       nf_SSQ = nf_SSQ + nf**2

  333  format(F9.0,',',F6.2,',',F9.0,',',F6.2,',',F9.0,',',
     +F6.2,',',F9.0,',',F6.2,',',F9.0,',',E10.4,',',F4.2,',',E10.4)
```

```
 250  continue
      write(*,*)kk
      WRITE(*,*)'STR_MEAN,STR_SIG'
      STR_MEAN=STR_SUM/REAL(I_NUMB)
      STR_SIG= ((STR_SSQ - (STR_SUM**2/REAL(I_NUMB)))/
     +(REAL(I_NUMB)-1))**0.5
      nf_MEAN=nf_SUM/REAL(I_NUMB)
      nf_SIG= ((nf_SSQ - (nf_SUM**2/REAL(I_NUMB)))/
     +(REAL(I_NUMB)-1))**0.5

      WRITE(*,*)STR_MEAN,STR_SIG
      WRITE(8,252)STR_MEAN,STR_SIG
      WRITE(*,*)nf_MEAN,nf_SIG
      WRITE(8,252)nf_MEAN,nf_SIG
 252  FORMAT(E10.4,E10.4)

C********FATIGUE MODULE************
      call fatig1(STR_mean,STR_sig,mod)
      end

C*****SUBROUTINES - BEGIN, PEM & FATIG1 ARE GIVEN BELOW **********

      SUBROUTINE BEGIN
      CHARACTER*72 INFILE,OUTFILE
   1  FORMAT(A)
 949  WRITE(6,'(1X,A,\)')'ENTER OUTPUT DATA FILENAME = '
      READ(5,1)OUTFILE
      OPEN(8,ERR=950,FILE=OUTFILE,STATUS='NEW')
      GO TO 980
 950  WRITE(6,'(1X,A,\)')'OUTPUT FILE ALREADY EXISTS!!!  TRY AGAIN!'
      GO TO 949
 980  RETURN
      END
C*************************************************************
      subroutine PEM(n,i_var)
      logical MTC
      DIMENSION IN(15)

      integer n,i_var(300,15)
      DATA NLAST/0/

      I_end= 2**N
      do 200 ik1=1,I_end
  10  if(N .EQ. NLAST) GO to 15
  20  M=0
      MTC=.TRUE.
      DO 21 I=1,N
  21  IN(I)=0
      NCARD=0
      NLAST=N
      GO TO 100
  15  IF (.NOT. MTC) GO TO 20
  30  M=M+1
      M1=M
      J=0
  39  J=J+1
  40  IF(MOD(M1,2) .EQ. 1) GO TO 60
  50  M1=M1/2
      GO TO 39
  60  L=IN(J)
      IN(J) = 1-L
      NCARD=NCARD+1-2*L
      MTC=NCARD.NE.1.OR.IN(N).EQ.0
 100  do 150 ik2=1,n
      i_var(ik1,ik2)=in(ik2)
```

```
 150  continue
 200  continue
      return
      END
C*******************************************************
      subroutine fatig1(STR_mean,STR_sig,STIFF)
      COMMON NF
      REAL*8 VOID /6./,PHI /25./,ZHI /0.36/,T /42./,STIFF
      REAL*8 STRAIN,STR,DAMG /0.0/,rel
      REAL*8 M, NFL_1,NF,ESAL_TOT /0./
      REAL*8 FUDGE /100.0/,STR_mean,STR_sig
      INTEGER ESAL(35,4),J,I_COUNT /1/,layr

      WRITE (*,*)'FATIG EQN: NF = f(VOID,STIFF,TEMP,PHASE-ANGLE,
     +ZHI,STRAIN)'

      write(*,*)'stiffness =',stiff

      do 1000 rel=3,-3.2,-0.2
      STRAIN = STR_mean+(rel*str_sig)

      STR =ABS(STRAIN)
      M = SIN(PHI*3.142/180)

      IF (I_EQN .EQ. 1)  THEN

      NFL_1=(-5.078+(0.101*VOID)
     ++(-0.046*T)
     ++(1.363*LOG(ZHI))
     ++(-4.813*LOG(STR))
     ++(-1.837*LOG(STIFF))
     ++(-0.902*LOG(M)))
      NF = exp(NFL_1)*FUDGE

      WRITE(*,*)rel,strain,nf
      WRITE(8,*)rel,strain,nf

 1000 continue
      return
      end
```